



Swansea University  
Prifysgol Abertawe



## Swansea University E-Theses

---

# Audio plant condition monitoring.

**Blakeley, Bruce**

How to cite:

---

Blakeley, Bruce (2001) *Audio plant condition monitoring..* thesis, Swansea University.  
<http://cronfa.swan.ac.uk/Record/cronfa42239>

Use policy:

---

This item is brought to you by Swansea University. Any person downloading material is agreeing to abide by the terms of the repository licence: copies of full text items may be used or reproduced in any format or medium, without prior permission for personal research or study, educational or non-commercial purposes only. The copyright for any work remains with the original author unless otherwise specified. The full-text must not be sold in any format or medium without the formal permission of the copyright holder. Permission for multiple reproductions should be obtained from the original author.

Authors are personally responsible for adhering to copyright and publisher restrictions when uploading content to the repository.

Please link to the metadata record in the Swansea University repository, Cronfa (link given in the citation reference above.)

<http://www.swansea.ac.uk/library/researchsupport/ris-support/>

EPSRC Engineering Doctorate  
Engineering and Environment Theme Group

# **Audio Plant Condition Monitoring**

BRUCE BLAKELEY

Thesis submitted to the University of Wales  
for the degree of Engineering Doctorate

Department of Mechanical Engineering  
University of Wales - Swansea  
September 2001

ProQuest Number: 10797947

All rights reserved

INFORMATION TO ALL USERS

The quality of this reproduction is dependent upon the quality of the copy submitted.

In the unlikely event that the author did not send a complete manuscript and there are missing pages, these will be noted. Also, if material had to be removed, a note will indicate the deletion.



ProQuest 10797947

Published by ProQuest LLC (2018). Copyright of the Dissertation is held by the Author.

All rights reserved.

This work is protected against unauthorized copying under Title 17, United States Code  
Microform Edition © ProQuest LLC.

ProQuest LLC.  
789 East Eisenhower Parkway  
P.O. Box 1346  
Ann Arbor, MI 48106 – 1346



## *Synopsis*

Accelerometers are widely used in plant condition monitoring (PCM) to diagnose faults in rotating machinery. This can be expensive, and is typically only used to monitor the condition of critical machines. The objective of this project is to develop a system, using microphones, that could screen less critical machines for faults. Microphones are non-contact sensors that can be placed away from the machines, to avoid damage. If the data gathered by the microphone is reduced to a single parameter, that increases with wear, then analysis would be greatly simplified.

This system could be used to provide basic PCM screening for equipment not considered important enough for routine vibration monitoring. To achieve this objective, a test-rig was designed and constructed, consisting of a motor, gearbox and load. Various faults were introduced into the test-rig, and a microphone used to record the sound. These results were then compared to accelerometer readings.

Time synchronous averaging (TSA) was employed to increase the signal to noise ratio. It was proven that Kurtosis and crestfactor of a microphone signal both increase, if used with a high pass filter, when an impacting fault such as a broken gearbox tooth was introduced into the test-rig. It proved harder to reduce the sound of other non-impacting faults, such as misalignment, into a single parameter. The technique was tested in an industrial environment with a 100 dB background noise level. It was shown that the technique was capable of detecting faults even with a signal to noise ratio of -15 dB.

A one dimensional FEA model was created, with six degrees of freedom, modelling the test-rig's vibrational behaviour. This was used to investigate the affect of a broken tooth, and to explain the increase in noise as the tooth passing frequency coincided with a resonance.

## ***Declaration***

This work has not previously been accepted in substance for any degree and is not being concurrently submitted in candidature for any degree.

Signed ..... (candidate)

Date 4.4.02 .....

### STATEMENT 1

This thesis is the result of my own investigations, except where otherwise stated.

Other sources are acknowledged by footnotes giving explicit references.

Signed ..... (candidate)

Date 4.4.02 .....

### STATEMENT 2

I hereby give consent for my thesis, if accepted, to be available for photocopying and for inter-library loan, and for the title and summary to be made available to outside organisations.

Signed ..... (candidate)

Date 4.4.02 .....

## *Acknowledgements*

The author would like to thank the Engineering and Physical Sciences Research Council (EPSRC), Corus UK and the University of Wales - Swansea for their generous support of this project. The advice and help of Dr. Barrie Lewis, Prof. Arthur W. Lees, Mr. John Howells, Mr. Dennis George, Mr. Brian A. Woods, Mr Steve Price and all the staff of the Welsh Technology Centre is also very much appreciated.

## *Nomenclature*

The following acronyms and abbreviations are used regularly throughout this thesis. Other symbols and acronyms are used, such as in equations, but these are defined in the text.

PCM	Plant condition monitoring
TSA	Time synchronous averaging
FEA	Finite element analysis
EPSRC	Engineering and physical sciences research council
SPL	Sound pressure level
FFT	Fast Fourier transform
RMS	Root mean square
RPM	Revolutions per minute
RPS	Revolutions per second
CPS	Cycles per second
TPF	Tooth passing frequency
GM	Gear meshing (frequency)
AM	Amplitude modulation
FM	Frequency modulation
IM	Inter-modulation
dB	Decibel
ordf	Outer race defect frequency
irdf	Inner race defect frequency
cgdf	Cage defect frequency
redf	Rolling element defect frequency



# *Table of Contents*

	page
<b>Synopsis</b>	
<b>Declaration</b>	
<b>Acknowledgements</b>	
<b>Nomenclature</b>	
<b>Table of contents</b>	
<b>1 Introduction</b>	<b>1</b>
<b>2 Literature review</b>	<b>6</b>
2.1 Introduction	6
2.2 The time domain signal	14
2.2.1 <i>Root mean square</i>	14
2.2.2 <i>Crestfactor</i>	15
2.2.3 <i>Kurtosis</i>	15
2.3 The frequency domain	16
2.3.1 <i>The Fourier transform</i>	17
2.3.2 <i>Windows and filtering</i>	18
2.3.3 <i>Bearing faults</i>	20
2.3.4 <i>Common fault frequencies</i>	23
2.3.5 <i>Cepstrums and gear tooth faults</i>	25
2.4 Time synchronous averaging	27
2.5 Enveloping	29
2.6 Conclusion	32
<b>3 Sound and vibration experiments</b>	<b>33</b>
3.1 Introduction	33
3.2 The test-rig	34
3.2.1 <i>Design and construction</i>	34
3.2.2 <i>Bearings</i>	35
3.2.3 <i>Problems with the test-rig</i>	36
3.3 Experiments in the workshop	37

3.3.1	<i>Manufacturing and assembly errors</i>	37
3.3.2	<i>Misalignment</i>	40
3.3.3	<i>Broken Tooth</i>	42
3.3.4	<i>Displace shaft</i>	44
3.3.5	<i>Tooth lubrication failure</i>	46
3.3.6	<i>Worn teeth</i>	48
3.3.7	<i>Cage fault</i>	50
3.3.8	<i>Partial rotor rub</i>	52
3.4	Plant trials	55
3.4.1	<i>Introduction</i>	55
3.4.2	<i>Analysis of background noise</i>	55
3.4.3	<i>Broken tooth</i>	58
3.4.4	<i>Displaced shaft</i>	62
3.5	Figures of experimental work	66
<b>4</b>	<b>Mathematical modelling</b>	<b>126</b>
4.1	Introduction	126
4.2	Methodology	127
4.2.1	<i>Stiffness matrix for the bar element</i>	129
4.2.2	<i>Mass matrix for the bar element</i>	130
4.2.3	<i>Element mass matrix for discs</i>	130
4.2.4	<i>Simple model of bearings</i>	131
4.2.5	<i>The rubber coupling</i>	132
4.2.6	<i>Eigenvalues and eigenvectors</i>	133
4.2.7	<i>Validation</i>	133
4.2.8	<i>The model of the test-rig</i>	133
4.2.9	<i>Bearing stiffness</i>	134
4.2.10	<i>Coupling the gearwheels</i>	135
4.2.11	<i>Modelling a partially broken tooth</i>	136
4.3	Results of mathematical model	138
4.4	Figures of mathematical work	141
<b>5</b>	<b>Discussion</b>	<b>155</b>
5.1	Discussion of mathematical model	155

5.2	Discussion of experimental work	158
<b>6</b>	<b>Conclusions</b>	<b>160</b>
<b>7</b>	<b>References</b>	<b>162</b>
<b>8</b>	<b>Appendix</b>	<b>165</b>
8.1	Plates	166
8.2	Spectrograms	168
8.3	Record of training	170
8.4	Table of course results	173

# *1 Introduction*

There are three maintenance policies used by engineers. The first is the 'breakdown' maintenance policy, where items of plant are only replaced after they have failed. The second is the 'scheduled' maintenance policy where items are replaced after a certain number of hours service or mileage. The third policy is the 'condition based' or 'reliability based' maintenance policy where the condition of the item is monitored, using non destructive testing, and is only replaced when unacceptable wear has occurred. Which of the three maintenance policies is used largely depends on the criticality of the machine, and the cost of monitoring. A reliability based maintenance policy has the advantage over the schedule maintenance policy, in that the component is not replaced until it is required. This saves money. The scheduled maintenance policy can also cause problems if the item of plant fails unexpectedly. The disadvantage of the reliability based policy is the cost of monitoring. This is why it is typically reserved for critical machines, whose continued operation is vital to the plant's profitability and safety. For example, Corus' Port Talbot Cold Mill loses £M 1.1 per day in lost production alone, if one of its critical machines fails. Plant Condition Monitoring (PCM) consists of various non destructive observations that can be used to monitor the condition of the plant as part of a reliability based maintenance policy.

These non destructive tests include vibration analysis, thermography, motor current monitoring, oil and grease analysis and many others. Vibration analysis is often used, as it is capable of detecting mechanical problems many months before failure. However, it can be capital and/or labour intensive. The collection of vibration data can be achieved with either hardwired systems, with many accelerometers permanently attached to the machine, or with hand held accelerometers that are placed onto the machine by hand with a magnet. The vibration data is then recorded onto a hand held data logger. The data must then be analysed by highly trained personnel. Both methods of vibration data collection are prohibitively expensive for

indiscriminate use. It can therefore, be understood why vibration analysis is reserved for critical machines only.

The objective of this project was to reduce the cost of monitoring by using airborne sound and microphones, rather than vibration and accelerometers. The reduction in cost of monitoring would make it possible to monitor less critical machines for faults. The sound and microphones or 'Audio PCM' technique would not replace vibration monitoring. Vibration analysis would still be used for monitoring the most critical machines, and for confirming diagnosis in less critical machines.

Audio PCM would be used to provide a cheaper, less sophisticated monitoring system. It would not provide the same level of protection or give such an early warning as vibration monitoring, but would have the advantage of considerably lower monitoring costs.

There are several reasons why an Audio PCM monitoring system would be less expensive to implement and maintain than vibration analysis. Sound is 'global'; sound information, generated by each part of a machine, can be picked up by one microphone. An accelerometer must be placed on *each* bearing house in three orientations. This is because some faults will only generate 'local' vibration fault frequencies with high attenuation rates, that can not be picked up with just one accelerometer alone. This point can be extended - one microphone may be capable of monitoring more than one machine, replacing dozens of hardwired accelerometers. This would make the initial implementation costs significantly lower.

The cost of maintaining such a system would also be significantly lower, as there would be fewer sensors to maintain. The non-contact microphone could be placed away from the machinery, where it would be less likely to be damaged than a contact sensor such as an accelerometer. Hardwired accelerometers are prone to being dislodged by maintenance personnel, and wires are easily broken or disconnected.

Once the data had been gathered there would be considerably less data to analyse, again reducing costs. Ideally the systems would be automated by reducing the microphone data down into just a few parameters, such as Sound Pressure Level (SPL). These parameters could be trended, and alarm levels set.

The objective of this project is to investigate the possibility of using an Audio PCM system in an industrial setting. The requirements of such a PCM system are:

- To separate the sound of each machine from the background noise.
- To reduce the data to give parameters that increase with wear.
- To provide a limited level of protection, below that provided by vibration monitoring, with a shorter lead time to failure.
- To give the initial detection of a fault, so that vibration analysis could then be used to diagnose and confirm the presence of the fault.

In short, audio PCM would be used to provide a cost effective screening service. The following steps were taken to achieve this objective:

- A comprehensive literature survey was conducted.
- A test-rig with motor, gearbox and load was built.
- Initial experiments were performed in a relatively quiet workshop (76 dB).
- Plant trials were performed in a descaling fluid pump house (100 dB).
- Finite Element Analysis (FEA) of the test-rig was used to support the experimental work and improve the understanding of the measured data.

The thesis is split into three main sections – the literature review, experimental work and mathematical modelling. Figures are presented at the back of each chapter while small diagrams are presented in the text. A selection of photographs of the test-rig can be found in the appendix.

The literature review concentrated on three areas of investigation: general vibration analysis of rotating machinery, the use of sound in PCM and techniques to isolate the

sounds. The most successful technique for separating out the sounds of the individual machines was Time Synchronous Averaging (TSA). It has been shown that this technique can separate out the sounds of individual machines even with a -15 dB signal to noise ratio. The literature review also describes the parameters known as 'crestfactor' and 'Kurtosis'. These parameters reduce a sound or vibration signal down into a single number that increases with machine wear, if used correctly with a high pass filter.

This thesis shows that by combining these techniques, and applying them to a microphone signal, it is possible to isolate and identify impacting faults in an industrial environment, with a background noise level in excess of 100 dB. It was shown that the use of a high pass filter could remove the low frequency sounds, generated by the machines, leaving the higher frequency impact harmonics created by such faults as gear teeth failure. Double differentiation of the microphone signal emphasised these higher frequency harmonics. As the impacts are synchronous with the shaft speed, time synchronous averaging could be used to isolate them from the background noise produced by other machines. Kurtosis and crestfactor were used to identify and measure the size of these impacts in relation to the remainder of the sound signal, and were used as the parameters to measure the severity of the fault. As the techniques described in this thesis worked well for impacts, they were the logical choice to use.

To carry out this investigation a purpose built test-rig was designed and constructed. Photographs of the test-rig can be seen in the appendix. The test-rig consists of a drive motor, gearbox and brake motor which acts as a load. A shaft encoder was placed on the output shaft of the gearbox for accurate measurement of running speed and for time synchronous averaging. The accelerometer and microphone were used to record baselines before introducing deliberate faults, such as a broken tooth, into the rig. New recordings of sound and vibration were then made and compared to the baseline.

These initial experiments were conducted in a relatively quiet workshop (76 dB on average) with no sound proof enclosure. These experiments provided useful results, comparing the differences in sound and vibration of the various faults. Once it was proven that a microphone could be used in this manner, the test-rig was moved to a noisier environment - the descaling fluid pump house, this was to show that the sound of the rig could be separated from the sound of the large industrial machinery.

Before the initial trials at the pump house commenced, the sound of the background noise was recorded and analysed. This background noise was produced by four large motors, gearbox and pump arrangements. These pumps provide descaling fluid to the mill's hot mill. Once the background noise of the descaling fluid pumps had been analysed and understood the experiments conducted in the quiet workshop were repeated. It was demonstrated that the sound of the descaling fluid pumps could be used to identify potential faults by studying the harmonics of the pump's vane passing frequency. Time synchronous averaging was used to separate the sounds of the rig and the descaling pumps. The results of these experiments are detailed in the 'experimental work' section of this thesis.

The final section of this thesis details the mathematical modelling work. A one dimensional mathematical modelling model was created to investigate the vibrational properties of the test-rig. Mass, stiffness and damping matrices were generated and solved to find the eigenvalues and vectors. Forcing functions were added to simulate vibrations caused by a broken tooth. This model was used to enhance the understanding of the experimental results.



## **2 Literature Review**

### **2.1 Introduction**

The concept of using microphones to monitor the condition of rotating machines has been developed over a number of years. The work in this field falls into a number of different applications:

- Assessing the condition of refurbished gearboxes [1].
- Reducing the noise of gearboxes [2,3].
- Monitoring emergency generators [4].
- Pattern recognition systems applied to the sound of cutting and machining during the manufacturing process [5,6,7].
- Plant Condition Monitoring (PCM) [1,6,8,9,10].

The majority of work using a microphone in PCM has involved the study of gearbox noise in the laboratory. None of the authors have attempted to test their techniques in a noisy industrial environment. Many of the authors have used sound proof enclosures and Time Synchronous Averaging (TSA) to reduce the background noise.

Badi et al. [8] used such a test-rig to compare the use of microphones, stress wave sensors and accelerometers to diagnose two intentional faults. These two faults were 'shaved teeth' and 'weld blip'. The shaved tooth was created by using an angle grinder to score the surface of one tooth, which simulated damage to the tooth profile. The second fault was created by welding a small amount of metal to one tooth. This simulated the affect of 'scuffing' or 'scoring', which is the welding together of surfaces. The stress wave sensor and accelerometer were placed on the gearbox bearing house, while the microphone was placed very close to the gearbox casing. The close proximity of the microphone to the casing is likely to have caused near field errors. The near field is the area close to the machine in which readings of Sound Pressure Level (SPL) are inaccurate [11].

Badi's paper demonstrates the ability of microphones to detect the tooth passing frequency, but little else. This may be due to the poor resolution of the Fast Fourier Transform (FFT), used by the author. The microphone also performed poorly in the low frequency regions below 50 Hz. The microphone was not very successful in diagnosing the two faults in the frequency domain; the only major change in the signal was a rise in SPL. Little or no digital signal processing was performed on the signals from the stress wave sensor, accelerometer and microphone. RMS and SPL of the unfiltered signals were compared at different running speeds in the time domain. A low resolution FFT was used to examine the signals in the frequency domain, but analysis of the FFT was restricted to the low frequency regions below the tooth passing frequency.

There are several techniques used to study impacts in the high frequency regions including enveloping [12,13,14,15], Kurtosis [12,15,16], wavelets [17,18,19], crestfactor [12,13,15] and spectrograms [17]. Maynard [12] has shown that the higher frequency resonances are often excited by impacts, but has not used any of these techniques to study the impacts in detail. A higher resolution FFT may have been able to resolve the sideband pattern around the tooth passing frequency created by the impacts [20].

It is interesting to note that Badi chose to run the gearbox without any lubricating oil in the gearbox casing. Only the bearings were lubricated. Badi et al. continued their research by investigating the difference in lubrication condition [10]. The previous experiments, involving a weld blip and shaved gear, were repeated using the same three sensors but with the gearbox run in it's lubricated and non lubricated state. Higher resolution FFTs were used, as were cross-spectrums and Cepstrums [15,20,21,22]. The author defines the cross-spectrum as the multiplication of two spectra, one from each sensor, claiming that this will enhance any points of agreement between any two sensors.

The conclusion of this paper is that lubrication can attenuate noise and vibration. This damping effect may reduce the effect of faults, making it harder to make a

correct diagnosis. Badi et al. recommends that gearboxes should be only lightly lubricated when taking vibration readings. This is unlikely to be practicable in an industrial environment. Badi also concludes that the Cepstrum is a reliable technique in diagnosing gear faults.

The FFTs used by Badi [10], are of a higher resolution and more advanced techniques have been used, such as the cross-spectrum and Cepstrum, but no examination of the higher frequency regions was demonstrated.

The objective of this project is to develop a system using microphones to assess the condition of rotating machines, in particular gearboxes. This would replace the subjective assessment of gearbox condition made by plant personnel listening to the sound produced. The work of Johnson and Trmal [1] had a similar objective: to replace the subjective opinion of inspectors who assessed the condition of rebuilt gearboxes. To achieve this objective, Johnson and Trmal constructed a test-rig with a drive motor, gearbox and load. A shaft encoder was attached to the shaft to provide 256 pulses per revolution. A microphone was placed in the near field to record the sound of the gearbox, using time synchronous averaging to improve the signal to noise ratio. The authors demonstrated that for 'n' revolutions of the shaft the signal to noise ratio was improved by  $\sqrt{n}$  as expected.

The sound signal was then assessed in the time domain by using kurtosis and shaft order analysis [2]. Unfortunately, the authors do not explain how they obtained high resolution FFTs from a 256 point signal. Time synchronous averaged signals are typically short in length. A signal with relatively few samples will give a low resolution FFT. Faults such as worn teeth, manufacturing errors and cracked teeth were diagnosed using this method. The use of digital filtering in the frequency domain is also used to filter out mechanical resonances from the signal. Cepstrum analysis of the signals was used to identify faults without using time synchronous averaging.

The authors have proved that this technique works well for diagnosing tooth faults, but does not work for bearing faults. The reason for this is that the exact bearing fault frequencies cannot be determined as the bearing dimensions cannot be measured precisely enough and the bearings rarely have 0% slip. This is less of a problem when identifying bearing fault frequencies in a FFT, but does become a problem when using time synchronous averaging, as a far greater degree of accuracy is required for this technique to work. The exact time period for *each individual* rotation of a component must be known precisely over several hundred revolutions for time synchronous averaging to work adequately.

This paper also explains how tooth faults generate noise. Johnson and Trmal [1] show that the variation of contact forces in gears and bearings causes vibration, which is transmitted into the gearbox casing and radiated as noise. The variation of forces can result in forced vibration or in a pulse excited vibration at one of the natural frequencies which can decay before the pulse is repeated. The radiated noise is dependent on the nature of the excitation forces, the response characteristics and radiating efficiency of the gearbox casing. The defects in gearboxes which are responsible for the noise generation can be divided into gear and bearing related defects.

When power is transmitted from one gear tooth to another, the line of action of contact force is deformed due to tooth deflection. Spiral bevel gears are subjected to varying contact forces because of this deflection. Sliding action on either side of the pitch line causes wear during the normal operation of a gear and changes the tooth profile. Errors in the profile can also arise in manufacturing. Errors of the tooth profile results in noise with a significant proportion at the tooth meshing frequency and its harmonics, or at system resonance.

The tooth contact between the gears can be lost for an instant due to errors in the tooth profile. When contact is re-established there is a velocity difference between the teeth which causes impact. Such impacts will excite the natural frequencies of the gearbox [1].

Maynard [12] built a similar test-rig to examine vibration signals of damaged gearboxes. However, the work did not incorporate deliberate faults. Instead, a healthy gearbox was run at excessive loads until the gearbox failed. The majority of failures were broken teeth, however, some gearboxes failed when their output shafts broke. A band pass filter was used to filter out all vibrations except the noise between the third and fourth tooth passing frequency. The results showed that, as the teeth failed, the impacts generated excited resonances in this area of the spectrum. Kurtosis, crestfactor and RMS all increased as the damage spread throughout the gears. Envelope analysis was used to identify the failure mechanism. Maynard claims that the best frequency range is between the third and fourth tooth passing frequency, but gives no justification for this. The frequency response must depend upon the system.

It was also demonstrated that this technique was an accurate indicator of gear tooth health and was not affected by changes in load. Results could be trended, or in the case of kurtosis could be used as a single measurement.

There are two points in this paper that are of relevance to this project:

1. The first is that the majority of dramatic gearbox failures are due to cracked and broken teeth.
2. Kurtosis, crestfactor and RMS in the high frequency band pass area are reliable indicators of tooth damage.

If the time synchronous average of a sound signal, described by Johnson and Trmal, could be combined with this method it may be possible to determine the basic condition of a gearbox in a noisy industrial environment by using a single microphone and shaft encoder. Time synchronous averaging would increase the signal to noise ratio of the sound signal above the background noise and the use of Kurtosis, crestfactor and SPL in the higher frequency regions may provide indications of machine condition.

Middleton and Rumble [2], describe some of the problems of using a microphone to measure the sound from a gearbox. The microphone will record sound directly from the gearbox, but will also record the sound reflected off surfaces, such as the floor. The resultant signal will be a summation of the two. If the two signals are in phase they will be larger than expected; if they are out of phase, partial cancellation will take place. This means that the SPL will not decrease linearly with distance from the source, but may fluctuate. This fluctuation will also occur if the microphone is moved from side to side. The wavelength of the signal will effect this phenomena, as will air temperature.

Middleton and Rumble recommend spatial averaging to reduce this effect. Several recordings of sound are taken from various points around the sound source and then averaged in the frequency domain. Unfortunately, this method is impractical to use with time synchronous averaging, as the short signal lengths give poor resolution in the frequency domain [23]. Much of the work done with time synchronous averaging signals is performed in the time domain, such as spectrograms, wavelets, Kurtosis etc. These techniques cannot be used if the phase information is lost by spatial averaging.

Middleton and Rumble [2] also highlight the problem of speed and load. If the excitation frequency generated by the gearbox coincides with a resonance of the gearbox casing, the SPL will increase. If the loading changes then the tooth deflection will change, causing the tooth profile to alter. Both speed and load have an effect on the gearbox noise. This information is particularly relevant to the project, highlighting the need for consistency. Ideally the gearbox should be running at the same speed and load from one recording of sound to the next. Constructive/destructive interference of the direct and reflected sound is less important as the exact SPL is of no interest, trending of the signal is predominantly used. Unfortunately, time synchronous averaging does not remove these effects.

The effect of air temperature and changes in building acoustic properties is beyond control, however, the effect of these two parameters should be minor if the impacts

are studied in the high frequency range. Impacts consist of a wide range of frequencies, some of which may be slightly increased or decreased with change in air temperature or building acoustics, but the overall effect will not change dramatically. However, reflection of the sound impulses created by the impacts (echoes) may decrease Kurtosis and crestfactor.

Time synchronous averaging is not the only way to increase signal to noise ratio. Heng and Mohd [9] compared traditional sound signals with air particle acceleration, using two microphones spaced a fixed distance apart. This arrangement, known as a microphone pair or microphone probe, is normally used to measure sound intensity [24]. However, air particle acceleration is a derivative of sound intensity [9], both having a vector nature. The highly directional property of air particle acceleration can be used to improve the signal to noise ratio in a noisy environment.

Heng and Mohd [9] also used time synchronous averaging and a sound proof enclosure when investigating rolling element bearing faults. They attempted to use time synchronous averaging to improve the signal to noise ratio further, but were only able to do this when the bearing was loaded at only 2% of its rated load and turned at only 100 RPM. This was required to maintain its ideal behaviour. At any other load or speed, the bearings would slip. This slipping action makes it impossible to use time synchronous averaging, as the precise speed of the bearing cannot be determined. Even with these unrealistic conditions they were only able to calculate a time synchronous average signal from eight revolutions of the shaft. This demonstrates the difficulty of using time synchronous averaging with microphones and bearings.

Heng and Mohd claim that air particle acceleration was better at detecting bearing faults in the higher frequency region at higher speeds. Only basic analysis was undertaken in the time domain (kurtosis, crestfactor and SPL) and in the frequency domain (bearing defect frequencies [15]). No filtering or more advanced techniques were applied.

A directional microphone, such as the microphone probe, might be useful for this project, but an omni directional microphone is required if more than one machine is to be monitored with a single microphone. It may also be possible to attach the directional microphone to a motorised base, which could be moved to point the microphone at the relevant machine. However, this would add an extra degree of complexity, and would dramatically increase the cost of the system. The movement of the microphone may also introduce inconsistencies, as previously discussed.

Sumita et al. [4] have developed a full audio and visual remote monitoring system to monitor the condition of an office block emergency generator. Pictures from a camera and sound from a microphone are transmitted through the Internet to a central location. However, this system is very basic in terms of PCM. No background noise suppression technique was used, and no attempt was made to identify faults in the frequency domain [25]. Only one potential fault was investigated - a restriction in the fuel supply. The results showed a drop in SPL above 15 kHz.

This paper is of little relevance to the project technically, but does demonstrate that an audio PCM system would be a valuable addition to plant condition monitoring.



## 2.2 The Time Domain Signal

The purpose of this section is to highlight some of the techniques used to evaluate sound and vibration signals recorded from rotating machines in order to diagnose faults. The function  $x(t)$  represents the output signal from the sensor and hardware, collectively known as the 'front end', it may have the units of acceleration, velocity, displacement, or in the case of sound, sound pressure.

### 2.2.1 Root Mean Square

The most basic indicator of machine condition is the Root Mean Square (RMS) of the signal. In the case of sound, the same parameter is known as the sound pressure level (SPL).

$$RMS = \left\{ \overline{x^2} \right\}^{\frac{1}{2}}$$

where

$$\overline{x^2} = \lim_{T \rightarrow \infty} \frac{1}{T} \int_0^T x^2 dt$$

**equation 2.1**

$x$  = signal in the time domain

The lower the value of RMS, the better the condition of the machine [15].

### 2.2.2 Crestfactor

When a fault, such as a pit on a bearing, comes into contact with another component a sharp impulse will be created [12,15]. Crestfactor is defined as: -

$$\text{crest factor} = \frac{\text{peak value of } |x(t)|}{\text{RMS value of } x(t)}$$

**equation 2.2**

### 2.2.3 Kurtosis

Kurtosis is the fourth statistical moment after mean, standard deviation and skew. It is defined as [15,12]:

$$\text{Kurtosis} = \overline{\{x^4\}} - \{\bar{x}\}^4$$

**equation 2.3**

Where  $x$  is a normalised signal in the time domain. A completely random signal will have a Kurtosis value of 3, however, a signal with some periodicity in time will have a higher value. If a single pit is created in the outer race of a bearing, the signal generated will contain a regular feature, produced as each roller passes over the defect. This periodicity will increase the value of Kurtosis. However, as the damage spreads to the rollers and to the rest of the bearing, this periodicity will be lost, and the signal will become random once more. When this happens the value of Kurtosis falls back to 3.

Both the values of Kurtosis and crestfactor will increase with damage as a bearing develops a fault, but will decrease as the damage spreads. Diagram 2.1 demonstrates how Kurtosis increases, then decreases in value with increasing damage. This highlights the danger of using such methods in the time domain alone. A variety of techniques in the time and frequency domain should be used to effectively monitor faults in rotating machinery.

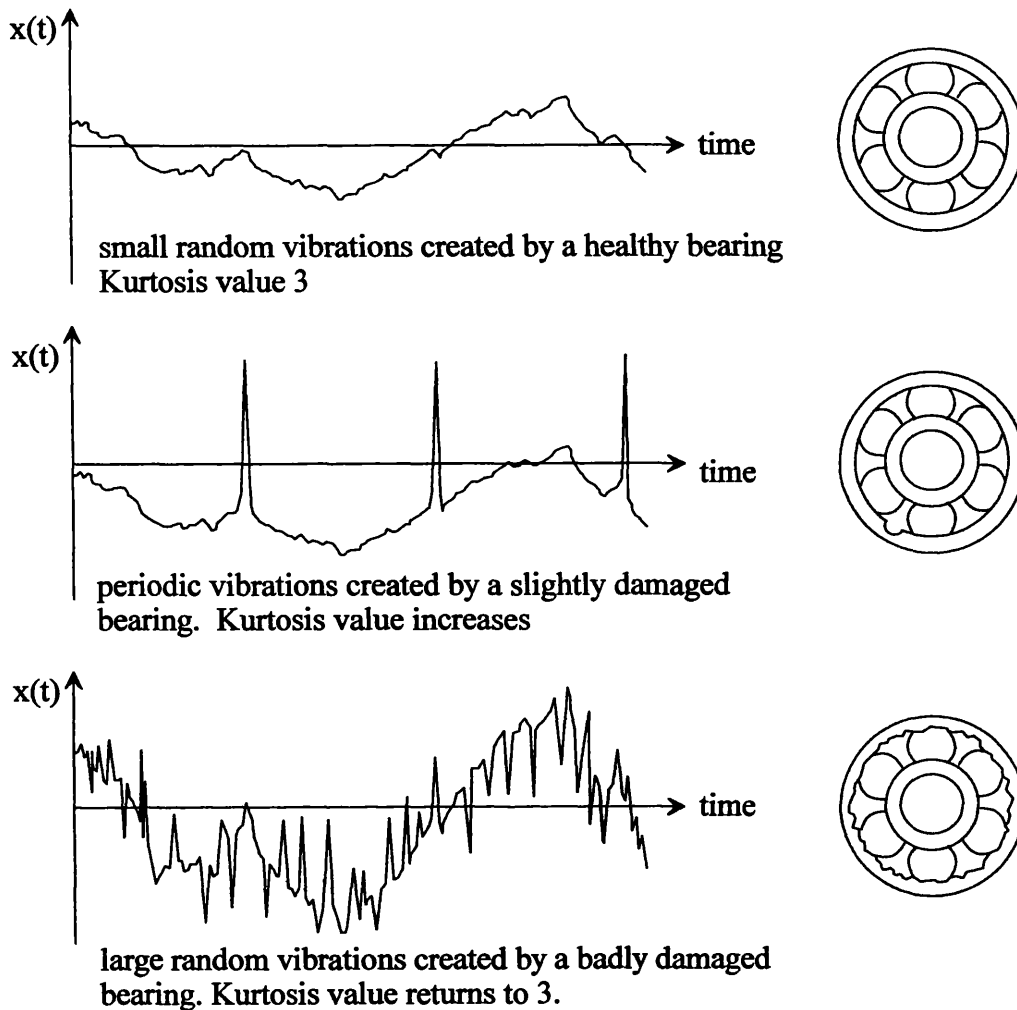


**diagram 2.1**

### 2.3 The Frequency Domain

Trending is one of the principal techniques used by condition monitors [26,27]. Using this technique, the deterioration of a component can be monitored over a period of time, until it is finally deemed unfit for service, and replaced or repaired. Simple trending can be done by measuring and recording an overall vibration parameter such as RMS, crestfactor or Kurtosis. If any of these single parameters reaches an upper limit then the component is replaced. The setting of these upper limits, or 'alarms', is either set by using vibration standards or empirically by experienced staff, based on the past history of the particular machine [25,28,29,30].

The problem with using such a simple method is that it gives very little lead time to failure; the time between warning of a breakdown and actual breakdown of the component may be too short to be of any practical use. Studying the vibration signal in the frequency domain will reveal more information regarding the precise fault. This is essential if a more detailed diagnosis is required, or if individual faults need to be trended over time.

### 2.3.1 *The Fourier Transform*

The standard spectrum used is the Fourier Transform. The Fast Fourier Transform (FFT) is an efficient algorithm for calculating the Fourier transform. The Fourier transform is defined as [15]:

$$\mathfrak{F}(f) = \int_{-\infty}^{\infty} x(t)e^{-i2\pi ft} dt$$

**equation 2.4**

t = time

f = frequency (Hz)

x(t) = signal in the time domain

Other spectra include the cross spectrum [15]:

$$S_{xy} = \mathfrak{F}_x(f) \cdot \mathfrak{F}_y(f)^*$$

**equation 2.5**

$\mathfrak{F}_x(f)$  = Fourier transform of signal x(t).

$\mathfrak{F}_y(f)^*$  = complex conjugate of the Fourier transform of signal y(t).

and the auto cross spectrum [15]:

$$S_{xx} = \mathfrak{F}_x(f) \cdot \mathfrak{F}_x(f)^*$$

**equation 2.6**

### 2.3.2 Windows and Filtering

If the signal corresponds to exactly one revolution of the shaft no window is required. Time synchronous averaged signals require no windowing function [31]. All other signals used in this project have been evaluated using the Hanning window [23]. Aliasing has been avoided by sampling at greater than two times the maximum frequency of the signal.

Two types of digital filter were used during the course of this project, the Butterworth filter and the Fourier filter. The Fourier filter has the advantage of precision and accuracy, but can only be used if the signal to be filtered corresponds exactly to an integer number of shaft rotations. In all other cases the Butterworth filter was employed. A Butterworth filter can be used even when the signal does not contain an integer number of shaft revolutions. It is created by the 'moving average' technique [23].

The Butterworth filters, used in this project were created in the programming language 'Matlab'. Pass frequency, stop frequency, allowable ripple and attenuation are entered into the program to create a zero phase filter of order 'N'. N is calculated by Matlab to achieve the filter specified by the input arguments. See diagram 2.2.

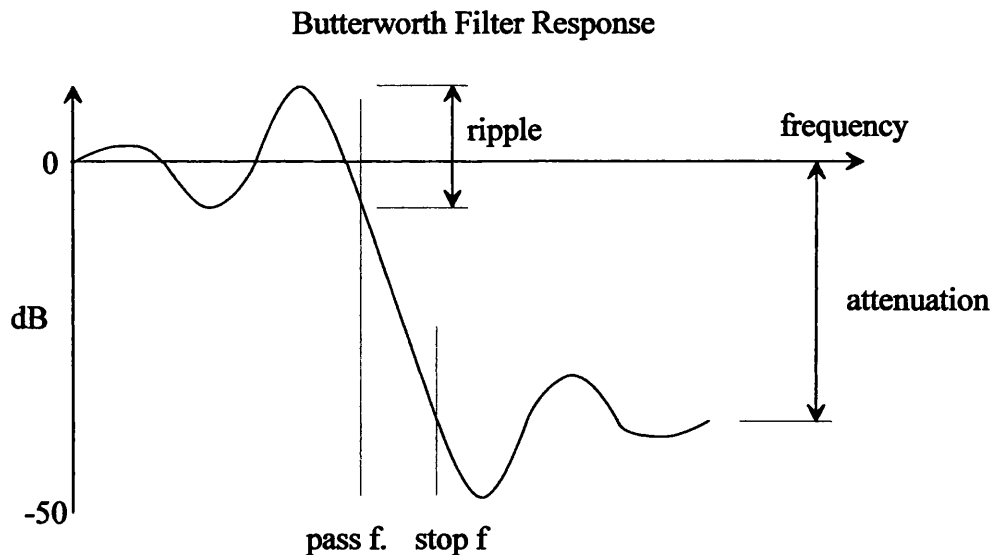
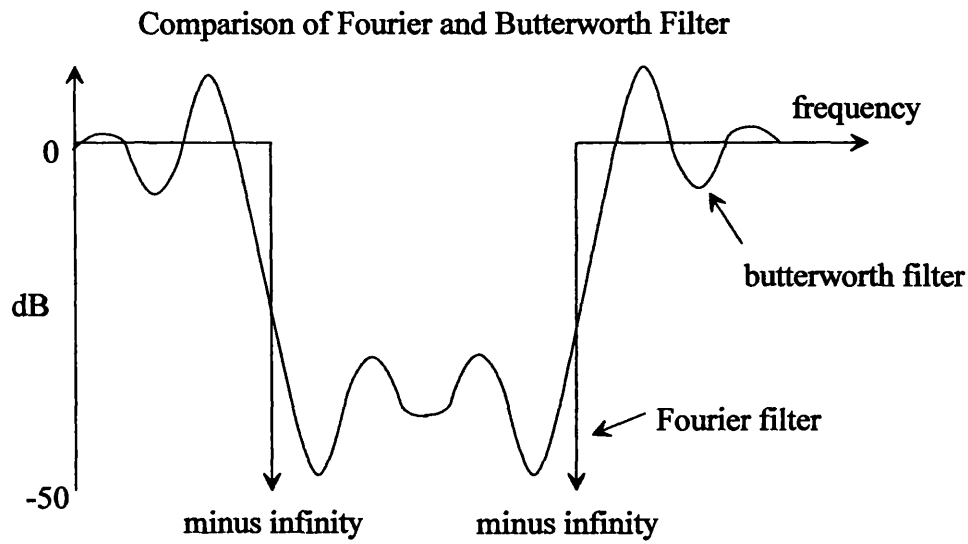


diagram 2.2

The Fourier filter is created by calculating the FFT of the signal, with no windowing function. The frequencies to be removed are set to zero in the real and complex plane, then an inverse Fourier transform is used to calculate the filtered signal [1]. Diagram 2.3 compares the frequency response of a Fourier and a Butterworth Band stop filter.



**diagram 2.3**

### ***2.3.3 Bearing Faults***

The condition of bearings is one of the main concerns of the condition monitor, and can be determined using several techniques and sensors from the most basic, such as RMS, Kurtosis and crestfactor of an accelerometer signal, to the more sophisticated techniques and sensors such as stress waves and acoustic emission sensors [32]. The more sophisticated techniques and sensors are more sensitive, and will give a longer lead time to failure.

Data is typically trended over a period of time. A sharp rise in the 'bearing fault frequencies' is indicative of a developing fault within a rolling element bearing. Other bearing types exist, but were not examined in this project, as the gearboxes used contained rolling element bearings only.

#### ***The Bearing Fault Frequencies***

As a bearing defect, such as a pit in the outer race of a rolling element bearing, comes into contact with another component of the bearing, an impulse will be generated. The rate at which these impulses are generated is described by the bearing defect or bearing fault frequencies. Impacts occur over a wide range of frequencies. When these impacts are repeated at a uniform rate the Fourier transform will show harmonics of the bearing defect frequencies up into the higher range of the spectrum.

These bearing defect frequencies are calculated from the bearing defect equations [14], see diagram 2.4 and equation 2.7.

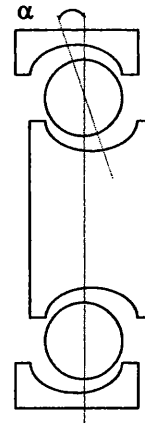
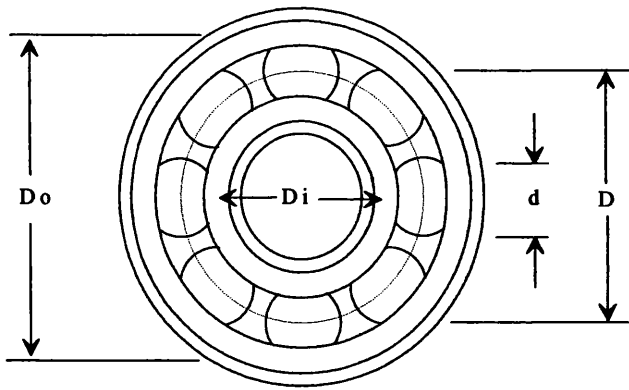


**diagram 2.4**

- D<sub>o</sub>** outer diameter.
- D<sub>i</sub>** Inner diameter.
- d** rolling element diameter
- α** contact angle (degrees).
- n** number of rolling elements.
- f** shaft speed.
- cgdf** cage defect frequency.
- irdf** inner race defect frequency.
- ordf** outer race defect frequency.
- redf** rolling element defect frequency.

$$D = \frac{D_o + D_i}{2}$$

$$cgdf = \frac{f}{2} \left( 1 - \frac{d}{D} \cos \alpha \right)$$

$$irdf = f \frac{n}{2} \left( 1 + \frac{d}{D} \cos \alpha \right)$$

$$ordf = f \frac{n}{2} \left( 1 - \frac{d}{D} \cos^2 \alpha \right)$$

$$redf = \frac{fD}{2d} \left( 1 - \frac{d^2}{D^2} \cos^2 \alpha \right)$$

**equation 2.7**

When the manufacturer quotes the bearing frequency, the contact angle  $\alpha$  is always assumed to be  $0^\circ$ . If this is not the case for the bearing in question, the fault



frequencies will not be accurate; e.g. a deep groove ball bearing placed under axial loading. There may also be a degree of slip between the rollers and the race that will decrease the fault frequencies slightly [9].

Once the fault frequencies are known, they can be identified in the spectrum and trended. If any of the fault frequencies reaches an upper limit, or alarm, the bearing should be scheduled for replacement.

### **2.3.4 Common Fault Frequencies**

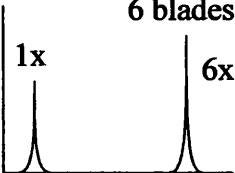
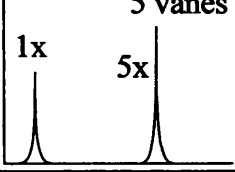
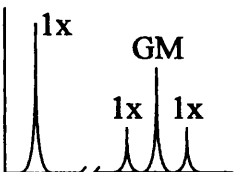
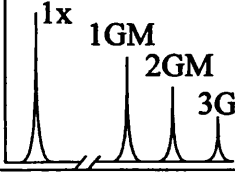
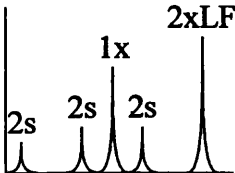
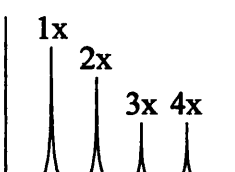
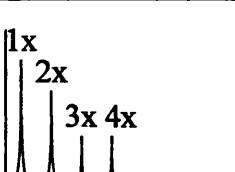
Bearing faults are not the only faults that can be diagnosed by condition monitoring techniques. Other faults can be diagnosed by vibration analysis such as misalignment, imbalance, gear tooth faults, rotor rub and electrical motor faults. This section is not intended to be an exhaustive description of the many faults that can be diagnosed by vibration analysis, but illustrates some of the faults that have been studied during the course of this project.

All the faults discussed in this section are diagnosed from an FFT of a vibration signal recorded from a bearing house in the axial, vertical and horizontal plane. It is assumed that the exact speed of the shaft is known and that some detailed information regarding the machine in question is also known. Such information includes:

- Number of vanes on fans, including the motor cooling fans.
- Number of teeth on gear wheels.
- Number of poles on motor.
- Type of coupling employed.
- The line frequency (typically 50 Hz).
- General description of machine, e.g. pump, blower, reciprocating machine.

The diagnostic information described in this section has been supplied by the PCM department of Corus Strip Products by private communication, but is readily available from any of the major PCM companies. The format of this information is typically in tables, such as table 1. It should be noted that:

- '1x', or 'one times', means one times the shaft speed.
- The tooth passing frequency (TPF) or gear meshing frequency (GM) is the number of teeth on the gear wheel times the shaft speed.
- The blade passing frequency is the number of vanes on a fan times the shaft speed.

<i>Probable Cause</i>	<i>Other Characteristics</i>	<i>Visual Description of FFT</i>	<i>Possible Action to Confirm Fault</i>
Fan blades	Inherent vibration  Only problem if level is high	6 blades 	Check clearance  Check looseness of blades
Pump impeller	Inherent vibration  Only problem if level is high	5 vanes 	Check clearance  Check looseness of blades
Gear	Problem if gear mesh has 1x RPM sidebands, equal to 50% of GM		Check gear teeth
	Problem if 2xGM and 3xGM appear (misalignment is a common problem)		Check alignment
Motor faults	'LF' is line frequency (50 Hz) 's' is slip frequency		Cut power: Vibration disappears almost instantly
Shaft coupling misalignment	High 2x, 3x or 4x.		Check alignment
Impacts	machine involving impacts will show harmonics of shaft speed		Check for impacts

**Table 1**

Once these fault frequencies have been identified, in the frequency domain, the diagnostic engineer is able to recommend a possible course of action to repair the fault or to confirm the severity of the fault. Trending of the fault frequencies over a period of time will provide a lead time to failure or help the maintenance engineer plan their maintenance priorities.

### 2.3.5 Cepstrum And Gear Tooth Faults

A Cepstrum can be thought of as a Fourier transform of a Fourier transform, although in reality it is slightly more complex than that. It is used to reveal the modulating frequency of sidebands in the frequency domain. Many faults in a rotating machine will produce modulating sidebands or harmonics of the shaft speed. The Cepstrum emphasises harmonic structure of a FFT [20]. Each peak of the Cepstrum can be thought of as representing a group of sidebands from an FFT. The height of the peaks is dependent upon the height and number of the sidebands.

The Cepstrum is defined as [20]:

$$C(q) = \mathfrak{F}_x^{-1}[\log_{10}\{\mathfrak{F}_{xx}(f)\}]$$

where

$$\mathfrak{F}_{xx}(f) = |\mathfrak{F}(f_x(t))|^2$$

equation 2.8

- t = time
- $\mathfrak{F}_x(f)$  = Fourier transform
- $\mathfrak{F}_x(f)^{-1}$  = inverse Fourier transform
- C(q) = Cepstrum
- q = quefrequency
- $f_x(t)$  = signal in time domain

The Cepstrum is similar to the auto correlation function, but the transmission path of vibration through the gearbox is reported to be less important [20]. If a fault exists,

such as a gear tooth fault, it will create an Amplitude Modulation (AM) of the tooth passing frequency (TPF) and the shaft speed.

This gives rise to a varying tooth contact pressure causing a Frequency Modulation (FM) of the tooth passing frequency and the shaft speed. This mixture of AM and FM is known as an Inter-Modulation (IM), an FFT of an inter-modulation results in a sloping distribution of sidebands; the direction of slope depends upon the phase relationship [21].

In general, an AM is due to a change in load and the response function of the casing, while an FM signal is due to a change in torque. The two usually appear together, resulting in an inter-modulation (IM). A Cepstrum will typically show several 'rharmonics', similar to harmonics in an FFT; the rharmonics contain little additional diagnostic information [20].

#### *Toothmesh Harmonics*

These harmonics are produced by deviations from the ideal tooth profile of teeth entering and leaving the mesh. In theory, the perfect tooth profile for a given load and speed should produce no harmonics; in practice, however, this cannot be achieved, as the teeth will deflect under load [2]. As wear increases, the tooth passing frequency (TPF) harmonics will increase [20].

For trending Cepstrums, it is reported that the load must be even, and the teeth must be in permanent contact. If the load is constant, any wear will be highlighted by an increase of TPF and harmonics [20].

## 2.4 Time Synchronous Averaging

Measuring sound provides global information from every component of the machine plus background noise from neighbouring machines. Time synchronous averaging (TSA) is used to suppress the background noise and separate out the sounds from shafts running at different speeds [1]. The sound generated from each shaft in the machine is cyclo-stationary [33] - the same sound is produced each time the shaft turns through one revolution. By using a shaft encoder the precise time period of *each individual* rotation of the shaft can be measured. This information is used to divide the sound signal into sections; each section corresponds *exactly* to one revolution of the shaft. The time periods for each revolution will vary slightly, so each section will contain a different number of samples. The sections are individually resampled, using Matlab's 'resample' command, so that they contain the same number of samples. An average value of the individual sections is calculated. The resulting signal is the cyclo-stationary sound produced as that particular shaft turns through 360°. Any sound that is not synchronous with the shaft is reduced. Johnson and Trmal [1] demonstrated that for a shaft turning through 'n' revolutions the signal to noise ratio is improved by a factor of  $\sqrt{n}$ . Time synchronous averaging has been used successfully by many of the authors studying the sound of gearboxes, and also be used in an identical manner for vibration [34].

The advantage of using time synchronous averaging is that the signal to noise ratio is improved, and the sound of each individual shaft can be isolated from the background noise. No windowing function is required when transforming a TSA signal into the frequency domain, and the more precise Fourier filter can be used [1]. The disadvantage is that the resulting short signal gives poor resolution when transformed into the frequency domain [23]. TSA signals are usually evaluated in the time domain [34] or using frequency/time domain techniques, such as the spectrogram [17] or wavelet [18,19] because of this.

Another disadvantage of using the TSA technique, is that not every fault is entirely synchronous with the shaft speed. Bearings rarely have 0% slip [9] and motor faults often exhibit 2x line frequency (100 Hz) fault frequencies.

## 2.5 Enveloping

Enveloping [15] is used to demodulate an AM signal. See diagram 2.5. The signal contains some small impacts and some low frequency components. The small impacts excite high frequency resonances. The purpose of enveloping is to remove the low frequency components and demodulate the impact frequency and the resonant frequency.

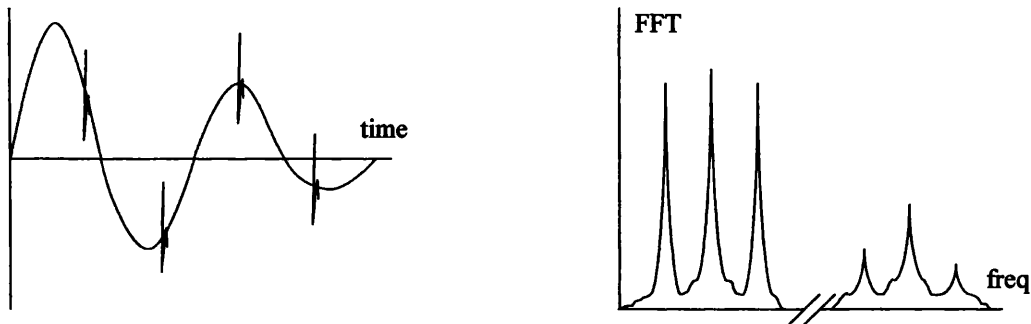


diagram 2.5

To do this the signal is passed through a high pass, or band pass, filter. See diagram 2.6.

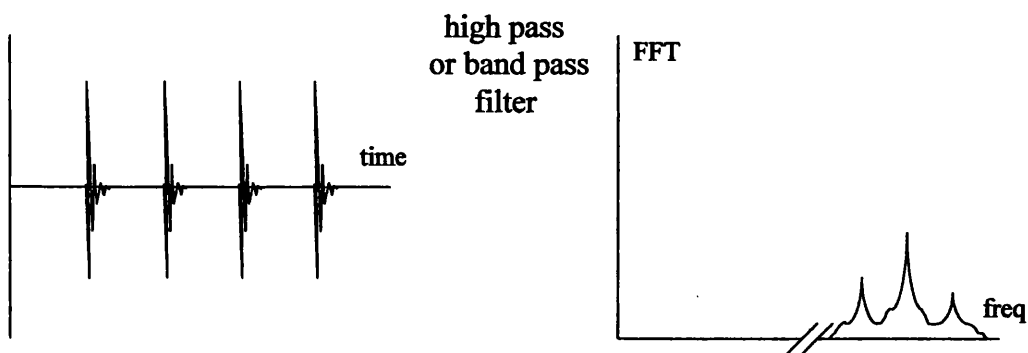
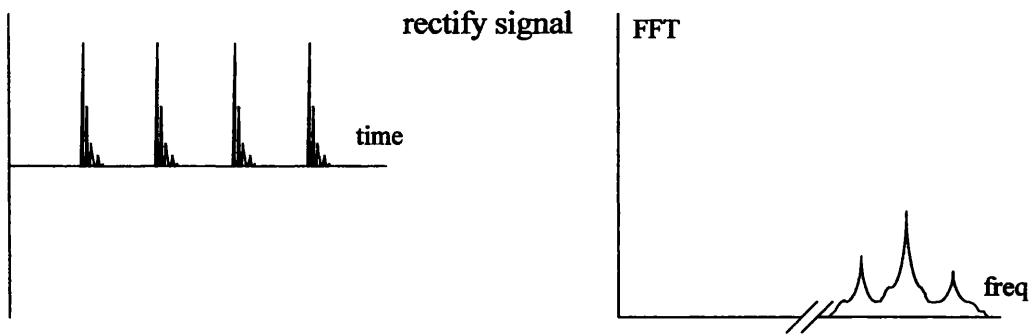


diagram 2.6



The signal is then rectified. See diagram 2.7.



**diagram 2.7**

The final stage employs a low pass filter, or 'smoothing capacitor', to remove the high frequency resonance. See diagram 2.8.

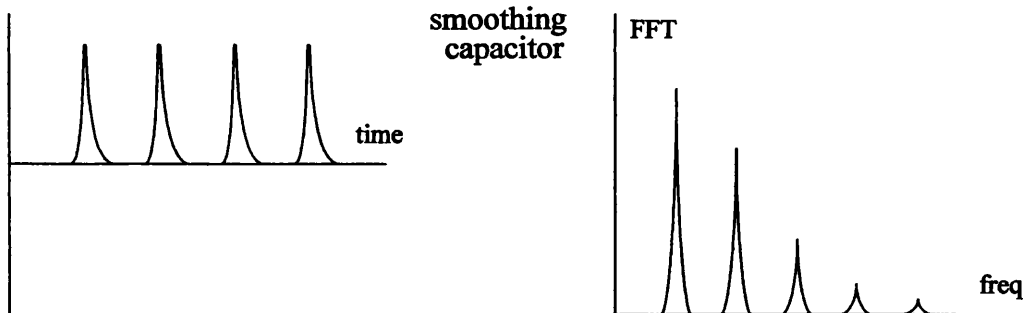


**diagram 2.8**

In summary, the signal is passed through either a high pass filter to filter out the lower frequencies, or a band pass filter to concentrate on a specific area of the spectrum, i.e. a resonance. The signal is then rectified and smoothed by a smoothing capacitor or its digital equivalent. An FFT of the output signal reveals the low frequency characteristic of the high frequency signal. Diagram 2.9 demonstrates the importance of setting the 'roll off rate' of the smoothing capacitor correctly.

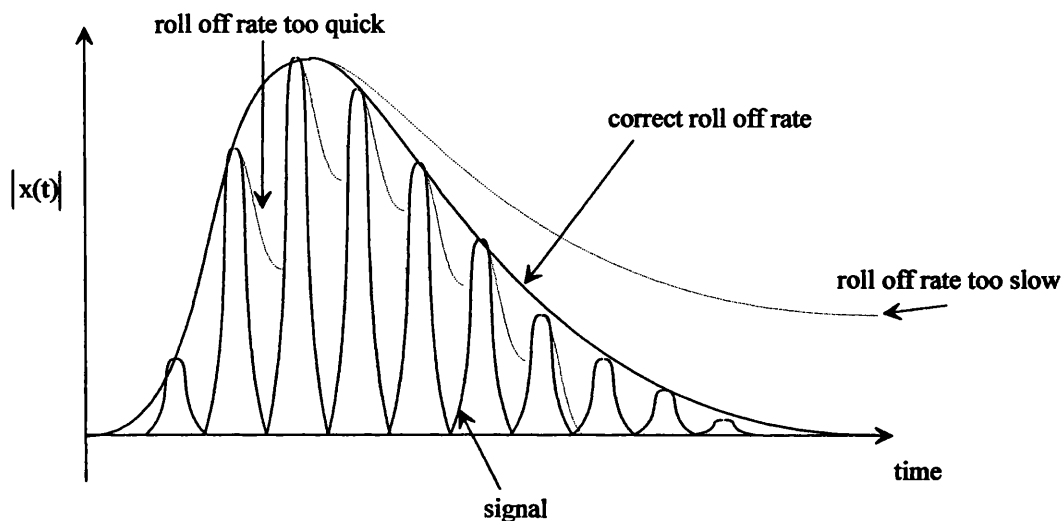


**diagram 2.9**

## 2.6 Conclusion

Johnson and Trmal [1] have shown that time synchronous averaging can be used to increase the signal to noise ratio by a factor of  $\sqrt{n}$ , for  $n$  revolutions of a shaft. They have also demonstrated that the time synchronous averaged signal can be used to diagnose gearbox faults. Time synchronous averaging was the only technique that was found during the literature survey that was capable of separating out the sound of individual components from a high background noise, without the use of a sound proof enclosure. Time synchronous averaging can be used if a shaft encoder is attached to one shaft of the machine in question. Shaft encoders are common place, and it would not be unrealistic to fit shaft encoders to the machines to be monitored. This would be the only sensor in contact with the machine. Johnson and Trmal [1] and Badi et al. [10] have both proved that sound can be used to monitor the condition of gearboxes.

Maynard [12] has shown that the impacts arising from gear tooth faults can be reliably diagnosed by applying Kurtosis, crestfactor and RMS after filtering out the lower shaft orders, tooth passing frequency and harmonics.

The objective of this project is to combine the work of these authors and to develop a system of microphones and shaft encoders capable of diagnosing gearbox faults. This will be done by using time synchronous averaging of sound to isolate the sound of the individual gearbox shafts from the background noise. A high pass filter will be employed to remove the lower shaft orders, tooth passing frequency and harmonics. The final signal will be evaluated using Kurtosis, crestfactor and SPL.

The gearbox to be investigated will be attached to a purpose built test-rig. After initial investigation in a relatively quiet workshop, a realistic background noise will be provided by the descaling fluid pumps at Corus's Port Talbot plant.

### **3     *Sound and Vibration Experiments***

#### **3.1   Introduction**

The objective of this project was to develop a technique, using microphones, that is capable of screening a number of machines for faults. A test-rig composed of drive motor, gearbox, flywheel and brake motor was built as part of this purpose. The test-rig was used to study the sound and vibration characteristics of several faults such as broken and worn teeth, rotor rub and misalignment. This was done in two stages, the first was to place the rig in a relatively quiet workshop. The sound and vibration characteristics of the fault were compared to the baseline sound and vibration to ensure that the microphone signal could be used in a similar manner to the accelerometer in diagnosing faults. Once this stage was complete, the rig was moved to the descaling pump house at Corus's steel plant in Port Talbot. The background noise level of this location varied between 96 to 100 dB. Some of the experiments conducted in the workshop were repeated, using time synchronous averaging as a background noise suppression technique, to establish whether if the techniques developed from the workshop could be used in a noisy environment.

## 3.2 The Test-rig

### 3.2.1 Design and Construction

Diagram 3.1 is a diagram of the test rig. Plates 1 to 4, in the appendix, show the construction of the test-rig.

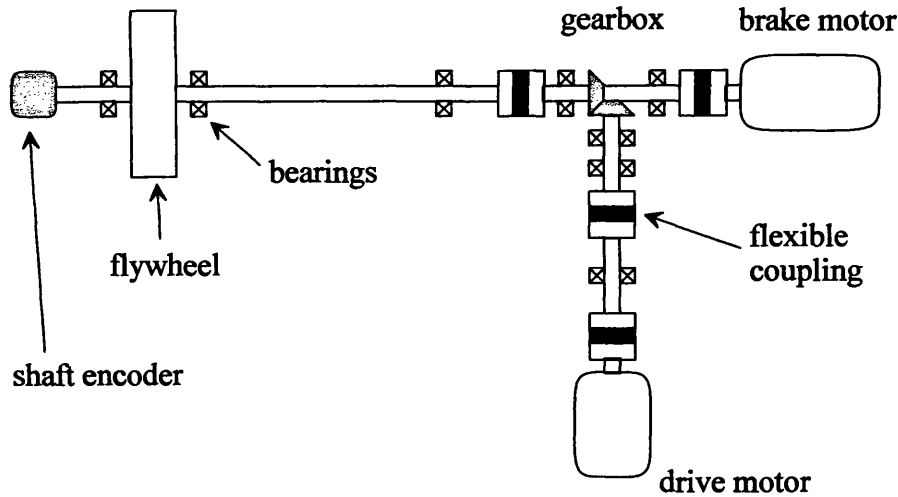


**diagram 3.1**

The drive motor was a 350 W, 2 pole, 3 phase induction motor. The speed controller was a 3 phase inverter, capable of running the motor at 10 to 40 cps (600 to 2400 rpm). The gearbox (plates 2 & 3) was a spiral toothed bevel gearbox with a reduction ratio of 2:1. The input gear wheel had 12 teeth, whilst the output had 24 teeth. The brake motor was a 1.6 kW permanent magnet DC motor with a regenerative absorption drive. This system placed a 1 Nm braking torque on the output shaft of the gearbox. The flywheel was a 200 mm diameter steel disc, 80 mm in width. Two brake pads surrounded the disc, see plate 4, and were used to create a rotor rub effect as one of the faults (see section 3.3.8). The brake pads were not used as a load, as the precise braking torque could not be measured, unlike the braking motor, and was only used for the rotor rub experiment. The flexible couplings were 3-jaw Essex couples with a rubber torque disc that damped torsional vibrations and prevented lateral vibrations passing from one component to the next through the

shafts. A shaft encoder (see plate 4) was attached to the output shaft. This provided 1 or 1000 pulses per revolution. The 1 pulse per revolution was used for time synchronous averaging and the 1000 pulse per revolution signal was passed into a frequency/voltage converter, which converted the pulses into a DC signal, whose magnitude varied linearly with the rotational speed of the output shaft.

The test-rig was supported on a table made of a 10 mm thick steel plate on a 40 mm box section steel frame. Unfortunately, this structure suffered from lightly damped resonances (see section 3.2.3).

### 3.2.2 The Bearings

The following bearings were used in the test-rig. All of them were deep groove ball bearings.

Location	Gearbox	Motor	Pedestal
Manufacturer	SKF	NSK	RHP
Serial No.	6003	07M-6202V	1025-25G
ordf	4.08	3.066	3.585
irdf	5.92	4.9338	5.415
cgdf	0.41	0.3834	0.3984
redf	5.28	2.025	2.3574

Outer race defect frequency (Hz) = ordf x shaft speed (cps).

Inner race defect frequency (Hz) = irdf x shaft speed (cps).

Cage defect frequency (Hz) = cgdf x shaft speed (cps).

Rolling element defect frequency (Hz) = redf x shaft speed (cps).

### **3.2.3 Problems With the Test-rig**

The test-rig, used in these experiments, suffered from several problems. The most serious problems being low frequency resonance. Plate 1, in the appendix, is a picture of the test-rig. The support structure, below the motor, gearbox and load, caused resonance that greatly increased the RMS levels to unrealistically high levels. It would have been more appropriate to place the rig directly on the floor, bolted to ensure correct mechanical grounding. This would have also prevented the vibrations of one component passing through the support table to the next component. This problem made it difficult to locate the source of some of the fault frequencies.

In order to identify the frequency of the table support structure, a rubber headed mallet was used to strike the rig. The resulting vibration was measured with an accelerometer. Figures 1 to 3, at the end of the experimental work chapter, show the results of these experiments. 'x' is axial to output shaft, 'y' is horizontal and 'z' is vertical. It is interesting to note that the resonance appears to 'drift' as the vibration decays away. It is assumed that this is due to a non-linear effect.

The gearbox also had a problem with resonances, between 300 and 500 Hz. This is studied in more detail by the mathematical modelling. Unfortunately, the tooth passing frequency, at 2400 RPM, coincided with this resonance, causing increased values of RMS.

Other problems occurred with the drive motor and speed control. This was of the open loop variety. Once the fault had been introduced into the gearbox, the gearbox efficiency would decrease, causing the rig to turn at a slightly slower speed. This made the comparison of fault and baseline vibration more complicated. The final problem was overheating of the drive motor at low speeds. The motor had a coolant fan attached to its shaft. At speed, the fan would cool the motor, but at low speeds the motor would overheat. When this happened the controller would shut down the motor completely. This hampered the experiments.

### **3.3 Experiments in the Workshop**

#### **3.3.1 Manufacturing and Assembly Errors**

##### *Introduction*

The objective of this part of the project is to compare the sound and vibration of a healthy machine (baseline) against the sound and vibration of a damaged machine with a specific fault. The gearbox chosen for these experiments is a right angled spiral bevel gearbox with a reduction ratio of 2:1, manufactured by Fenner Power Transmission Ltd. Several gearboxes were required for the project; one for each fault. One of the main criteria for choosing this particular type of gearbox was cost. The project had limited resources, so the destruction of several expensive gearboxes was deemed unacceptable, and therefore, a lower quality, cheaper gearbox was chosen. These low cost gearboxes were of a sufficient quality for the project, but did contain some manufacturing faults, such as miss-aligned teeth and ghost frequencies.

Once the sound and vibration baseline of the supposedly 'healthy' gearbox was taken, the baseline was examined for faults before adding the deliberate fault under investigation. In order to introduce the fault the gearbox had to be removed from the test-rig and dismantled. The fault, such as a broken tooth, was then added and the gearbox reassembled and fitted back on the rig. It was important to establish whether the process of dismantling and re-assembling would introduce larger errors and faults than the intended fault. To investigate this possible source of error, a baseline of a healthy gearbox was taken. The gearbox was then removed and dismantled. No intentional fault was introduced before reassembling the gearbox and fitting it back on the rig. The sound and vibration readings were then repeated and the results examined for manufacturing and reassembly errors.



## *Methodology*

To record the vibration produced by the rig, an accelerometer was placed on one of the bearing houses. The output from the accelerometer/charge amplifier was then logged on a two channel data logger. The second channel of the data logger recorded the speed of the rig via the frequency/voltage converter. The variable speed drive was set to turn the drive motor over at 40 cycles per second (40 cps). The rig was run at this speed for a few seconds before dropping the speed to 35 cps. This was repeated until the drive motor was running at 10 cps.

The accelerometer was then moved to the next position and the process repeated. This was done until vibration readings had been taken from each bearing house on the rig in the axial, vertical and horizontal directions. Vibration readings from the test-rig structure were also taken in three orthogonal directions.

The process was repeated one last time with the microphone. The microphone was placed one metre above the gearbox and two metres to one side. This position was maintained for all the workshop experiments.

## *Results*

Figure 4 is a waterfall plot of the vibration readings taken from the gearbox in the vertical direction. The baseline is black, while the results from the reassembled gearbox is red. The yellow lines indicate the tooth passing frequency and harmonics. A structural resonance between 200 and 600 Hz mechanically amplifies the tooth passing frequency when the output shaft is running at a speed greater than 12 cps. An examination of the side band structure around the tooth passing frequency reveals unevenly distributed tooth faults on both the input and output gear wheels. The presence of the tooth passing frequency harmonics indicates an error in tooth profile [20]. The side band structure around the reassembled gearbox tooth passing frequency has been reduced after reassembly, as has the tooth passing frequency harmonics. This suggests that careful reassembly of the gearbox has improved the

alignment of the teeth, indicating less than perfect manufacturing techniques for the alignment of the input and output shafts in the factory.

A smaller peak can be seen at 100 Hz. This is caused by a mechanical resonance of the test-rig structure which is excited by a 2 x LF fault (two times the line frequency of 50 Hz). This fault relates to the drive motor.

The final manufacturing fault can be seen at less than 100 Hz on the baseline. Figure 5 is a zoom waterfall plot of this area. The yellow lines indicate the shaft orders. The fault frequencies, at approximately 3.2 times indicated by the blue dashed line, increases with shaft speed, but does not correspond with any shaft order, bearing fault frequency or any other fault frequency. It is believed to be a ghost frequency [20]. Figure 6 is a waterfall plot taken from the same accelerometer position, but the brake torque has been varied rather than the shaft speed. The shaft orders are indicated by the dashed black lines, whilst the ghost is indicated by the dashed red line. The magnitude of the ghost frequency does not vary with load. This confirms it is a ghost frequency [20].

### *Discussion*

A ghost frequency is generated by an imperfect tooth profile. This is caused by a fault on the machine used to cut the teeth during the gearbox manufacturing process. Its frequency increases linearly with shaft speed, but does not correspond with the shaft orders, and does not vary with load [20].

The fact that the side band structure around the tooth passing frequency and harmonics decrease with careful reassembly suggests a less than perfect manufacturing process [20].

The unduly high tooth passing frequency is a property caused by a resonance which mechanically amplifies any forcing frequency between 200 and 600 Hz. This

increases the RMS level, but is not a problem for this project, as all the results are comparative.

The fault frequency at 100 Hz is due to the drive motor not the gearbox. This fault frequency is amplified by a resonance and is passed through the test-rig support structure into the gearbox.

### *Conclusions*

1. Reassembly does not introduce unacceptably high errors.
2. Resonance amplifies all frequencies between 200 and 600 Hz.
3. A ghost frequency is present.
4. Vibration generated by the motor has been transmitted through the structure.
5. No other fault frequencies, such as bearing fault frequencies, were large enough to cause concern.

### *3.3.2 Misalignment*

Shaft coupling misalignment is one of the more common faults associated with rotating machinery. A fault frequency of 2x may indicate a misaligned shaft of a motor, gearbox or load [25]. The aim of this experiment is to deliberately misalign the brake motor, and investigate the change in sound and vibration in an attempt to diagnose this fault using the microphone.

### *Methodology*

The baseline sound and vibration from the reassembled gearbox #1 had already been recorded. The brake motor was misaligned by 1.35°, 0.47 mm in the horizontal plane. Waterfall plots of sound and vibration were recorded in an identical manner to the baseline.

## *Results*

The misaligned shaft had little effect upon the frequencies greater than 60 Hz. This is because misalignment does not cause high frequency impacts or harmonics, and it's expected fault frequency is 2x. Figure 7 is a waterfall plot taken from the gearbox in the horizontal direction. The 3x has increased dramatically. The peak at 28 Hz, 9.5 cps is due to a structural resonance.

Figure 8 was taken from the axial direction, and shows a near identical result, as does the vertical direction.

Figure 9 is a waterfall plot of sound. The shaft orders cannot be distinguished; the signals appear to be composed almost entirely of resonances. These resonances can be clearly seen at 36 and 55 Hz.

## *Discussion*

For this particular machine a rise in the 3x indicates misalignment. It is interesting to note that the misaligned coupling was a 3-jaw Essex coupling. It would be interesting to repeat the experiment with a two or four jaw coupling to see if the 2x or 4x increased.

The results of sound shows little correlation with the results from vibration. Sound has a much lower attenuation rate from the fault source to the sensor, compared with vibration. This means that the microphone receives signals from each part of the test-rig including the surfaces of guards and electrical cabinet surfaces. The surfaces have many unknown low frequency undamped resonances, and are believed to be the source of the low frequency sound. If the 3x fault frequency does produce a 3x sound signal it has been masked by these low frequency sounds.

## *Conclusions*

- Misalignment causes a rise in the 3x vibration signal, possibly due to the three jaw Essex coupling.
- The microphone could not detect this fault.

### **3.3.3 Broken Tooth**

#### *Introduction*

The objective of this experiment is to determine the ability of the microphone to detect a broken tooth. A severely damaged tooth will increase the sideband structure around the tooth passing frequency and harmonics along with an increased 1x and harmonics. The gearbox in question has a 2:1 reduction ratio, so if a tooth on the input shaft is broken an inter-modulation of the tooth passing frequency and input shaft speed will occur. The input shaft speed is twice that of the output shaft. A local fault impact will create sidebands spanning a wide frequency band.

#### *Methodology*

Gearbox #1 was removed from the test-rig and carefully dismantled. A small angle grinder was used to remove most of one tooth from the input shaft. The shaft was then cleaned of debris, greased, and the gearbox reassembled and fitted back on the test-rig. Waterfall plots of sound and vibration were then generated in the usual manner and compared with the sound and vibration waterfall plots of the reassembled gearbox #1 baseline.

#### *Results*

Figure 10 is a waterfall plot of vibration taken from the horizontal position of the gearbox input shaft. The shaft speed is that of the output shaft. It is a zoom plot, focusing on the tooth passing frequencies of the gearbox rotating between 10 and 17

cps; the tooth passing frequency is indicated by the yellow line. The sidebands around the tooth passing frequency have also increased. These sidebands are most notable when the gearbox output shaft is running at 17 cps. At this speed the tooth passing frequency is at 400 Hz, which is a resonant frequency of the gearbox. The resonance mechanically amplifies the tooth passing frequency and sidebands. This would normally be considered a design flaw, but is useful for these experiments as it provides an excellent signal to noise ratio for the fault frequencies under investigation.

Figure 11 is a Fourier transform of the baseline and broken tooth experiment from the gearbox running at 17 cps as mentioned above. The x-axis is in shaft orders rather than Hz; shaft order 1 equals 17 Hz, shaft order 2 equals 34 Hz, etc. The tooth passing frequency is the 24<sup>th</sup> shaft order as there are 24 teeth on the output shaft. The increased tooth passing frequency and the modulated sidebands are clearly visible. NB: the modulating frequency is the input shaft speed which is twice that of the output shaft. The sidebands extend over a wide frequency band, which is consistent with a localised impact of a severely damaged single tooth.

Figure 12 is an identical shaft order plot to figure 11, but compares the microphone signals. It has very similar properties to the vibration readings, in that the tooth passing frequency has increased, as have the size and number of the sidebands modulated with the input shaft speed.

### *Discussion*

Figure 12 proves that the microphone can detect the broken tooth fault; in fact the results are clearer than the accelerometer signal. It should be noted however, that this experiment was conducted in a relatively quiet workshop with a background SPL of 70 dB. The SPL of the fault was approximately 84 dB. The high signal to noise ratio means that time synchronous averaging was not required. This would be very different on plant. These fault frequencies are higher than the low frequency

resonances of the guards and cabinet surfaces, enabling the microphone to detect them without being masked by noise.

### *Conclusions*

- The microphone had no problem in detecting a badly damaged single tooth in a relatively quiet workshop.
- Both microphone and accelerometer signals agree with the standard theory for sound and vibration of a broken tooth.

### *3.3.4 Displaced Shaft*

#### *Introduction*

Misalignment of the shafts within the gearbox will increase the magnitude of the tooth passing frequency and harmonics [20]. In this case axial misalignment of the shafts causes the teeth to impact upon one another. These impacts produce harmonics of the tooth passing frequency.

#### *Methodology*

The output shaft is held in place, within the gearbox, by two oil seals mounted on screw threads. These oil seals can be screwed in or out to adjust the lateral alignment of the output shaft. This was used to displace the output shaft by approximately 1 mm, without effecting the angular alignment.

A baseline of gearbox #2 was taken in the normal manner before introducing the internal misalignment. The shaft was then displaced in the manner described above, and the new readings of sound and vibration were recorded.

## *Results*

Figure 13 is a waterfall plot of vibration, comparing the baseline with the vibration caused by axial misalignment of the displaced output shaft. As predicted, the tooth passing frequency increases, as does the harmonics of the tooth passing frequency. These were caused by the teeth impacting upon one another.

Figure 14 is a zoom of figure 13, showing a clearer picture of the localised sideband activity. Figure 15 is a Cepstrum comparing the vibration caused by the displaced shaft against the baseline. The peaks occur at a time period equal to that of the time period of the input shaft (approximately 60 ms) and the output shaft (approximately 120 ms). This proves that the size and number of the sidebands has increased [20].

Figure 16 is a waterfall plot of sound. This plot shows the same result as figure 13 for vibration. This experiment differs from normal misalignment, in that the axial misalignment affect the tooth passing frequency, rather than the two or three times.



## *Discussion*

The fault frequencies generated by the displaced shaft agree with the theoretical fault frequencies, and can be detected using both the accelerometer and the microphone.

The increased sideband activity around the tooth passing frequency may be caused by small variations in the tooth profile from tooth to tooth. The vibrations produced by these small variations is increased significantly by the tooth impacts.

These fault frequencies are higher than the low frequency resonances of the guards and cabinet surfaces, enabling the microphone to detect them without being masked by noise.

## *Conclusions*

- The microphone can detect internal misalignment within the gearbox.

### **3.3.5 *Tooth Lubrication Failure***

#### *Introduction*

This experiment investigated the situation of lubrication failure within the gearbox. The gearbox bearings were not affected as they have separate lubrication and oil seals. Badi [10] has investigated the effect of lubrication failure and has found that lubrication reduces the tooth passing frequency, sidebands and harmonics. An incorrectly lubricated gearbox should have more pronounced tooth passing frequency, sidebands and tooth passing frequency harmonics.

## *Methodology*

Gearbox #2 was dismantled and thoroughly cleaned of all lubricating oil. It was then re-assembled. In theory, the results of this experiment should be very similar to the results of the previous experiment, a misaligned shaft, so great care was taken in re-assembling the gearbox to avoid any misalignment errors.

## *Results*

Figure 17 is a waterfall plot of vibration. As predicted the tooth passing frequency harmonics have increased substantially. Figure 18 is a zoom plot of the tooth passing frequency and sidebands. The tooth passing frequency has increased dramatically while the sidebands have increased. Figure 19 plots the change in RMS, Kurtosis and crestfactor against shaft speed for the lubricated and unlubricated conditions. The change in crestfactor and Kurtosis is disappointingly slight, but the RMS level is approximately double for the unlubricated gearbox compared to the lubricated gearbox.

Figure 20 and 21 are waterfall plots of sound. As expected the results of sound shows a close correlation to the vibration results. The tooth passing frequency, sidebands and harmonics have all increased substantially.

## *Discussion*

The sound and vibration results agree with the expected fault frequencies. It is interesting to note that the input shaft appears to be most strongly affected, particularly when the rig is running at its highest speed. Crestfactor and Kurtosis does not appear to be affected by the lubrication condition, but RMS is. This may be due to the fact that the sampling frequency, used in the experiments was too low. If the sampling frequency were higher, a high pass filter could have been employed to filter out the tooth passing frequency harmonics, this may have increased the difference in crestfactor and Kurtosis.

## *Conclusions*

- RMS was strongly affected by lubrication condition, crestfactor and Kurtosis were not, probably because a high pass filter was not used.
- A microphone can be used to identify the lubrication condition.
- The results match the predicted fault frequencies.

### **3.3.6 Worn Teeth**

#### *Introduction*

After prolonged service the teeth will become worn, and the tooth profile will deviate from normal, this may create a modulation of the tooth passing frequency and the shaft speed [25]. The gearbox in question has a 2:1 reduction ratio. The output shaft turns at half the speed of the input shaft. As both the input and output gear wheels are worn, both modulations should occur. The tooth passing frequency harmonics will increase [20], due to the poor tooth profile.

#### *Methodology*

In the previous experiment gearbox #2 was cleaned of lubricating oil and the sound and vibration recorded. Gathering this data took at least one hour of running the gearbox. Running a dry gearbox for this length of time is likely to damage the teeth in the manner required for the worn teeth experiment. It was decided to use this gearbox for the worn teeth experiment, rather than a new unused gearbox. The gearbox was dismantled, and a small angle grinder used to further damage the tooth profile of the teeth on both the input and output shaft.

After cleaning, the newly damaged gearbox was reassembled and lubricated with a grease recommended by the manufacturer. The gearbox was refitted to the test-rig and recordings of sound and vibration were taken in the normal manner.

## *Results*

Figure 22, is a waterfall plot of vibration, comparing the worn teeth's vibration with the baseline. The tooth passing frequency harmonics have increased, as expected. Figure 23 is a zoom of figure 22. The increased tooth passing frequency and sidebands are clearly visible. The sidebands around the tooth passing frequency have also increased, indicating the spread of damage was not as evenly distributed across the teeth. Figure 24 is a waterfall plot of sound, which shows that many of the tooth passing frequency harmonics have increased. Figure 25, the zoom plot of sound, also shows more sideband increases than were anticipated. There appears to be resonances at approximately 240, 440 and 590 Hz. Apart from these discrepancies the rest of the plot is comparable to the vibration results.

Figure 26 is a Cepstrum of sound of the worn teeth compared with the baseline. The time period of the output shaft is approximately 60 ms (1000/shaft speed). The rharmonics have increased due to the increase in size and number of sidebands [20]. Figure 27 is a plot of SPL, crestfactor and Kurtosis. It shows that the fault sound is approximately twice as loud as the baseline, but crestfactor and Kurtosis are unaffected, due to the low sampling rate as described in the previous experiment.

## *Discussion*

The vibration waterfall plot agrees with the predicted fault frequencies, whilst the sound waterfall contains more sideband activity than expected, but is otherwise similar. The Cepstrum of sound confirms the increased size and number of sidebands. The sidebands around the tooth passing frequency indicate non uniform ware of the teeth. These irregularities were probably introduced by the use of the small angle grinder which was used to score the surface of the teeth. It is interesting to note that the drive motor did not have a closed loop speed control between itself and the motor speed controller. As the gearbox becomes less efficient, due to the damage, the speed of the test-rig decreases. This can be seen on all the Cepstrums and waterfall plots discussed to date. The crestfactor and Kurtosis values appear to

be largely unaffected by the worn teeth, due to the absence of a high pass filter. A second possible explanation for this, is that the damage is so severe that both values have increased to a maximum value, and have then decreased. This is a normal property of both crestfactor and Kurtosis. Once the damage has become evenly distributed, the sound and vibration signal becomes more random in nature, causing deceptively low readings of crestfactor and Kurtosis.

### *Conclusions*

- A microphone can be used to diagnose tooth damage.
- The Cepstrum confirms the increase in size and number of the modulated sidebands.
- The fault sound is approximately twice as loud as the baseline.
- Crestfactor and Kurtosis are deceptively low.

### *3.3.7 Cage Fault*

#### *Introduction*

Rolling element bearing faults are one of the foremost problems facing the maintenance engineer. The vast majority of condition monitoring techniques focus on this one area alone. The purpose of this experiment was to determine whether a microphone was capable of detecting a bearing fault, Bearing faults produce small impacts which occur at the bearing fault frequency, see section 2.3.3 [14,35]. For this experiment it was decided to introduce a damaged cage, as this is the easiest component of the bearing to damage, the inner and outer race are treated to make them very hard and, therefore, could not be easily drilled, cut or scratched. The rolling elements cannot be affected without damaging the cage in the process.

## *Methodology*

Gearbox #3 was attached to the test-rig and a baseline of sound and vibration taken as normal. The gearbox was then removed and dismantled. The oil seal on one of the output shaft bearings was then removed and the lubricating grease cleaned out. A small angle grinder was then used to cut a small groove through the cage. The grease and oil seal were replaced and the gearbox reassembled and refitted to the test-rig. The sound and vibration were then recorded and compared to the baseline.

## *Results*

Figure 28 is a shaft order analysis of the vibration produced by the broken cage compared with the baseline. The vertical yellow lines indicate the cage defect frequency ( $0.41 \times$  shaft speed). The first twelve cage defect frequency harmonics have increased dramatically, but there is little difference in the higher orders. Kurtosis, crestfactor and RMS varied little.

Figure 29, the results of sound showed very little difference from the results of vibration.

## *Discussion*

As previously mentioned low frequency sound reveals little diagnostic information as it becomes masked by resonances. Enveloping the sound signal did little to improve the quality of the information, as the cage defect signal has been too highly attenuated in the higher frequencies. Time synchronous averaging also proved to be of little help, as the cage speed could not be determined accurately enough to provide a synchronous signal. In theory, the cage should rotate at half the speed of the shaft, but in reality slips by a few percent.

## Conclusions

- The cage defect frequency was easily detected using the accelerometer, but could not be detected using the microphone.

### 3.3.8 Partial Rotor Rub

#### Introduction

The test-rig consists of a drive motor, gearbox, brake motor and load - see plate 4. The flywheel is a steel disc, 200 mm in diameter and 80 mm thick. Originally a mechanical brake was fitted to the rig instead of the brake motor. Brake pads pressing against the side of the flywheel provided the braking action. See diagram 3.2.

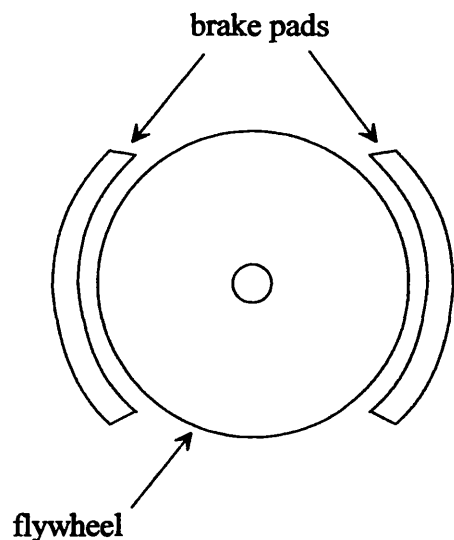


**diagram 3.2**

Unfortunately, the precise braking torque could not be calculated from this mechanical device, and it was replaced by a brake motor. It was also found that the flywheel was slightly eccentric, creating an uneven braking torque. It was decided to

use this eccentricity to generate a partial rotor rub, and then investigate the change in sound and vibration.

### *Methodology*

One brake pad was fitted and adjusted to provide a light intermittent partial rotor rub, so that the flywheel would be in contact with the brake pad for approximately 90° of its rotation. For the remaining 270° of the rotation the flywheel would not be in contact. Readings of sound and vibration were recorded and compared to the baseline. The eccentricity of the flywheel was measured using a dial gauge, taking readings every 10° of rotation.

### *Results*

Figure 30 is a plot of eccentricity of the flywheel. Figure 31 is an exaggerated representation of the eccentricity. The red circle represents the ideal profile, with its centre shown in green, while the blue circle is taken from the data in figure 30. This clearly shows the flywheel is off centre. This eccentricity is very small, and makes little difference to the test-rig operation. Any major out of balance forces would create a large 1x [25], but the 1x is typically small. However, it is large enough to create a partial rotor rub as it comes into contact with the brake pad.

Figure 32 is a shaft order analysis of vibration compared to the baseline. The accelerometer was placed on the flywheel support bearing in the horizontal direction. The 1x to 5x has increased due to the once per revolution impact, but the most significant change is the tooth passing frequency and sidebands. These vibrations are generated by the teeth in the gearbox, and are then transmitted through the test-rig structure to the accelerometer.

Figure 33 is a spectrogram view of the same vibration signal. An explanation of the spectrogram is given in the appendix. Resonances exist between 200 and 600 Hz which amplify the tooth passing frequency and harmonics. As the eccentric flywheel



rubs against the brake pad the load on the gearbox teeth increases. This increases the size of the tooth passing frequency. The sidebands also increase as the shaft is slowed down by the increasing torque required to overcome the friction of the rub. Envelope analysis confirms this. Figure 34 is a comparison of enveloped signals from the rotor rub and the baseline. This was created by enveloping the signals after filtering through a band pass filter based on 400 Hz with a band width of 400 Hz. One fifth times harmonics have also been created by the rub. This is consistent with rotor rub theory.

Figure 35 is a comparison of Kurtosis, crestfactor and RMS.

Figure 36 is a comparison of enveloped sound signals. A band pass filter of  $400 \pm 200$  Hz shows little change, but a wider band pass of  $800 \pm 1200$  Hz, shows increased one times to eight times frequencies, due to the nature of the impacts. The one fifth times orders are also present.

### *Discussion*

The sound produced by the fault is complex, and may be due to the change in sound of the gearbox as the load fluctuates within each revolution. A subjective assessment, by the operator, would suggest that the sound of the gearbox is far greater than the sound of the partial rub, so it is not surprising that the sound signal is mostly affected by the change in load of the gearbox. It is interesting to note that sound is often used to monitor the condition of gearboxes, but is rarely used for monitoring other faults. This experiment is a good demonstration of why this is the case.

The values of Kurtosis and crestfactor vary little. Both these parameters are most strongly affected by sudden knocks or impacts. In the case of the partial rotor rub, the impact of the flywheel against the brake pad is less than that of a partially broken tooth entering and leaving the mesh. This may explain why the parameters do not change as much as expected.

## *Conclusions*

- The sound signal changes dramatically, but appears to be more affected by the change in load of the gearbox.

### **3.4 Plant Trials**

#### **3.4.1 Introduction**

The objective of the plant trials was to verify that the background noise suppression techniques can be used successfully in a typical industrial environment. This must be done without losing diagnostic information. To this end the test-rig was moved into the descaling fluid pump house. The noise level in this part of the plant varies between 95 and 100 dB. Johnson [1] has shown that the signal to noise ratio is improved by  $\sqrt{n}$ , when using time synchronous averaging, where 'n' is the number of shaft revolutions. Maynard [12] has shown that Kurtosis and crestfactor increases in the high frequency ranges as the gearbox fails. The plant trials attempted to combine these two techniques.

#### **3.4.2 Analysis of Background Noise**

##### *Introduction*

The hot mill descaling pump house contains four pumps which deliver descaling fluid to the hot rolling mill. This descaling fluid is used to remove oxides from the steel slabs before rolling. Each pump comprises a four pole motor, a gearbox and impeller pump with seven vanes. The gearbox has 87 teeth on the input gear wheel and either 76 or 43 teeth on the output. A fluid clutch automatically shifts the gears to the correct ratio depending on the fluid flow requirements of the hot mill. The objective of this analysis is to record the sound of these pumps and relate the frequency components to the expected fault frequencies. No background noise

suppression technique is required as there are no other machines housed in the descaling pump house.

### *Methodology*

The microphone was left in its standard position, just above the test-rig gearbox, to ensure consistency. The test-rig was stopped and isolated so that only the descaling pumps could be heard. The sound of the descaling pumps was recorded at a high sampling rate of 50 kHz for 10 seconds.

### *Results*

Figure 37 is a Cepstrum of the descaling pump sound, which shows that rharmonics of 40.60 ms are clearly visible. From this, a shaft speed of 24.63 cps can be deduced. This is consistent with a four pole motor connected to a 50 Hz supply with a slip frequency of 1.5 %. It is assumed that the shaft turning at 24.63 cps is the input shaft.

Once the input shaft speed is known, the two possible output shaft speeds of 28.19 cps (35.47 ms) or 49.83 cps (20.07 ms) can be calculated. Neither the 36 nor the 20 ms rharmonic can be identified in the Cepstrum, however, sideband analysis of the tooth passing frequency revealed that the 76 toothed gearwheel was engaged.

Figure 38 is an FFT of the pump noise. The vertical green dashed lines indicate the shaft orders. The 1x, 3x, 4x, 6x, 7x and 8x are all high in relation to the rest of the signal.

Figure 39 is a similar plot, but with the tooth passing frequency and the first harmonic indicated. There is little sideband activity around the tooth passing frequency and harmonics.

Figure 40 highlights the pump vane passing frequency and harmonics. These are not unduly high relative to the other fault frequencies.

Figure 41 is a zoom FFT of the pump sound with the cage defect frequencies indicated. This shows that there is a potential bearing fault on the output shaft.

### *Discussion*

The Cepstrum clearly shows rharmonics relating to the input shaft speed. This suggests that components driven by this shaft create the most sound. Figure 38 shows that the first few shaft orders are present, which indicate mechanical looseness.

The high 1x, tooth passing frequency and the second harmonic, shown on figure 39 are typical of misalignment within the gearbox, or uniform deviation from the ideal tooth profile [20]. Figure 40 shows that while the vane passing frequencies are present, they are not unduly high and have no sidebands, suggesting the pump itself is healthy. Figure 41 indicates a bearing fault on the output shaft.

### *Conclusions*

- Some component on the input shaft is loose, causing an impact once per revolution.
- The motor and gearbox may be incorrectly aligned or mechanically loose.
- The gearbox may be internally misaligned, or the teeth worn.
- The majority of sound is created from the components revolving with the input shaft.
- There is a bearing fault on the output shaft.
- The gearbox may have some slight internal misalignment, or the teeth may be slightly worn.

### 3.4.3 Broken Tooth

#### Introduction

A serious failure, such as a broken tooth, will lead to a catastrophic breakdown. The objective of this project is to screen machines for such faults using a microphone. The problem with using a microphone is that the machine in question is likely to be operating in a high background noise environment. The objective of this experiment is to determine whether it is possible to use a microphone to detect such a fault in a high background noise environment. In order to do this the test-rig was moved into the descaling pump house as discussed in the previous chapter. The background noise level in the pump house varies between 96 to 100 dB. Time synchronous averaging was used to reduce the background noise level.

Much of the information regarding the impact of a broken tooth can be found in the higher frequency regions of the spectrum, beyond the tooth passing frequency harmonics [12]. This high frequency information can be uncovered by filtering out the low frequencies or by differentiating. Differentiating has the effect of weighting the higher frequencies. See equation 3.1.

$$x(t) = Ae^{i2\pi ft}$$
$$\frac{\partial x(t)}{\partial t} = i2\pi fAe^{i2\pi ft} = i2\pi fx(t)$$

**equation 3.1**

t	time
x(t)	displacement signal in the time domain
dx(t)/dt	velocity signal in the time domain
A	constant
f	frequency

Differentiating increases the higher frequency components, but also changes the phase of the signal. Fortunately, the phase of the signal is unimportant in the following analysis.

A broken tooth will create an impact once per revolution of the shaft. In theory, this will increase the modulation sidebands of the tooth passing frequency and shaft speed, and will also increase the first few shaft orders. The impacts will also excite the higher frequency resonances, which in turn will increase the SPL, RMS, crestfactor and Kurtosis in the higher frequency range [12].

### *Methodology*

Gearbox #5 was fitted to the test-rig in the descaling fluid pump house. Readings of sound and vibration were taken in the normal manner to establish a baseline. The gearbox was then removed and dismantled. A small angle grinder was used to remove most of one tooth from the input gear wheel. The grease was replaced and the gearbox re-assembled and fitted back on the test-rig. The new values of sound and vibration were then recorded. Time synchronous averaging was used to suppress the background noise. Approximately 300 rotations of the output shaft were used in compiling the time synchronous averaged signal. A once per revolution pulse, generated by the shaft encoder, was used to calculate each individual time period of the output shaft.

### *Results*

Figure 42 is a vibration waterfall plot of the broken tooth compared to the baseline. As expected, the tooth passing frequency and modulated sidebands have increased significantly. The yellow diagonal lines indicate the tooth passing frequency. The increase in the tooth passing frequency is likely to have been caused by secondary damage to the other teeth, due to the broken tooth.

Figure 43 is a Cepstrum of the same data. The 60 ms rharmonics have increased, which corresponds to a worsening of the input gear wheel condition, as expected.

Figure 44 is a time domain plot of vibration caused by the broken tooth. A high pass filter has been used to filter out the lower shaft orders, tooth passing frequency, sidebands and harmonics. It should be noted that the gearbox has a reduction ratio of 2:1, as the output shaft turns through one revolution, the input shaft, with the broken tooth, will turn through two rotations creating the two impacts shown.

Figure 45 is a spectrogram view of the vibration caused by the broken tooth. Again, two impacts per revolution of the output shaft can be seen. The vibration signal was differentiated to highlight the higher frequency components. Figure 46 is the same signal after time synchronous averaging has been applied. Time synchronous averaging has increased the signal to noise ratio, providing clearer results.

Figure 47 is a comparison of statistics for the broken tooth and baseline after filtering through the high pass filter. The value of crestfactor and Kurtosis have increased dramatically in this high frequency region, due to the impact created by the broken tooth. It is interesting to note that the values of crestfactor and Kurtosis varied little if the signals are not filtered prior to calculating these parameters. The impacts that excite the higher frequency resonances are small in comparison with the tooth passing frequency sidebands and lower shaft orders. These lower order faults do not give rise to a higher value of crestfactor and Kurtosis as in the higher frequency regions [12]. The frequency range used to calculate crestfactor and Kurtosis should always be considered when dealing with these parameters.

All the figures discussed in this section so far relate to the vibration caused by a broken tooth entering and leaving the mesh. The next set of figures relate to the sound created by the broken tooth. All of these sound signals were created using the time synchronous averaging technique to reduce the background noise generated by the descaling pumps. Approximately 300 ensembles were used for each signal. Figure 48 is the unfiltered time synchronous averaged sound of the broken tooth. The SPL is 84.6 dB, the crestfactor and Kurtosis are only 2.91 and 2.78 respectively.

Figure 49 is the same signal after the implementation of a 5 kHz high pass filter. The two impacts are clearly visible and the crestfactor and kurtosis are 8.18 and 11.52 respectively. This demonstrates the need to filter the signal before calculating these parameters as discussed earlier. The SPL has dropped from 84.6 to 61.4 dB.

Figure 50 is the baseline sound averaged and filtered in an identical manner to figure 49. The SPL is 58 dB, crestfactor and Kurtosis are 3.51 and 3.41 respectively.

Figure 51 confirms that crestfactor and Kurtosis rise dramatically, in the high frequency range, for the broken tooth compared to the baseline sound.

Figure 52 and 53 are spectrogram views of the differentiated baseline and broken tooth sounds.

### *Discussion*

The result of this experiment confirms that a microphone can be used to detect serious tooth damage on a gearbox, even with a -15 dB signal to noise ratio, using the time synchronous averaging technique.

For ease of interpretation the differentiated spectrogram view can be used to view the time/frequency history as the shaft turns through one revolution.

Crestfactor and Kurtosis of a high pass filtered signal rise dramatically with fault severity and could be used to provide a basic value of machine condition if the system were to be automated. This would negate the need for complex interpretation by experienced personnel.

### *Conclusions*

- The vibration pattern produced by the broken tooth agrees with accepted theory.



- Time synchronous averaging of the sound produces similar results with a signal to noise ratio of -15 dB.
- The differentiated spectral view provides a convenient method of analysing the time/frequency history of the signals.
- Crestfactor and Kurtosis both rise dramatically with fault severity after filtering out the lower fault frequencies, and could be used to provide a basic value of machine condition if used in an automated system.

#### ***3.4.4 Displaced Shaft***

##### *Introduction*

The analysis of the descaling fluid pump noise, discussed in chapter 3.4.2, concluded that there may be some problem with the pump's gearbox, possibly internal misalignment. Internal misalignment of the input and output shaft within a gearbox is a common fault. Incorrect alignment of the gear wheels may produce harmonics of the tooth passing frequency [20]. If the gearwheels are badly misaligned the teeth entering and leaving the mesh may momentarily lose contact. When the teeth regain contact, the impact will generate tooth passing frequency harmonics, which will also excite structural resonances.

The purpose of this experiment is to determine whether the microphone can record the sound of an internally misaligned gearbox with a high background noise content.

##### *Methodology*

Gearbox #6 was fitted to the test-rig and a baseline of sound and vibration was established. The gearbox was then removed, and the output shaft axially misaligned in an identical manner to chapter 3.3.4. The gearbox was refitted to the rig and new readings of sound and vibration recorded, in the same way as the previous experiments.

## *Results*

Figure 54 compares the vibration of the displaced shaft with the baseline. As predicted the tooth passing frequency has increased along with the tooth passing frequency harmonics. Note: shaft order 24 represents the tooth passing frequency, as there are 24 teeth on the output shaft. The first harmonic of the tooth passing frequency has been mechanically amplified by a resonant frequency.

Figure 55 compares values of RMS crestfactor and Kurtosis for the displaced shaft and the baseline vibration. As mentioned in the previous chapter, the values of crestfactor and Kurtosis should be calculated after passing the signal through a high pass filter to remove the lower shaft orders, tooth passing frequency and harmonics. The values of crestfactor and Kurtosis increase as the shaft is displaced. This increase is caused by impacts of the teeth as they lose and regain contact in the mesh.

Figure 56 is an envelope of the displaced shaft vibration created by using a  $3.5 \pm 1.5$  kHz band pass filter. The 24<sup>th</sup> shaft order has increased dramatically. This relates to the tooth passing frequency, and confirms that 24 impacts per revolution of the output shaft occur. Harmonics of the tooth passing frequency are also produced, which is consistent with periodic impacts. The baseline, enveloped in an identical manner, is also shown on this plot in green. No tooth passing frequency and harmonics are visible, proving that no impacts were occurring before the output shaft was displaced. Figure 57 is a spectrogram view of the displaced shaft vibration pattern. It has been differentiated to highlight the higher frequencies. Twenty four impacts are clearly visible in the upper frequency range, as the output shaft turns through one rotation.

Figure 58 relates to the sound of the tooth impacts, created by the displaced shaft, after being treated by time synchronous averaging to suppress the background noise of the descaling fluid pumps. The signal has been filtered to remove the lower frequencies, leaving only the smaller tooth impact vibrations. Again twenty four impacts can be seen.

Figure 59 compares SPL, crestfactor and Kurtosis of the sound of the displaced shaft and the baseline, filtered to remove frequencies below 3 kHz. All three parameters increase dramatically, except at rotational speeds above 12.7 cps. At this speed the impact sounds do not have enough time to decay away before the next impact occurs. The impact sounds blend into one another creating a near random signal with a Kurtosis value close to three.

Figure 60 is a spectrogram view of the time synchronous averaged sound of the displaced shaft. It has been differentiated twice to emphasise the impact sounds in the higher frequencies. As before 24 impacts can be seen, relating to 24 teeth.

### *Discussion*

If figure 60 is compared to figure 57, the spectrogram of the vibration signal, it can be seen that the duration of the impact sounds is longer than that of the vibration impacts. This may be due to reverberation of the sound being reflected off various surfaces before finally being absorbed. As the speed of the machine increases these impacts become closer together until eventually they merge into one another. This decreases the value of crestfactor and Kurtosis as previously mentioned. It is also interesting to note that the 'sharper' vibration signal produces higher values of crestfactor and Kurtosis than the sound, even though both signals were treated in an identical manner. This problem of reverberation may mark an upper limit on the use of this technique as a condition monitoring tool. If the machine speed is too high reverberation effects reduces the value of crestfactor and Kurtosis. It may be possible to avoid this affect by using higher frequency microphones, with a higher frequency high pass filter.

Generally, the microphone has successfully picked up on the impact sounds created by the teeth losing and regaining contact, particularly if the sound signal has been doubly differentiated, to emphasise the higher harmonics. The values of crestfactor and Kurtosis have increased sufficiently for them to be useful indicator of gearbox

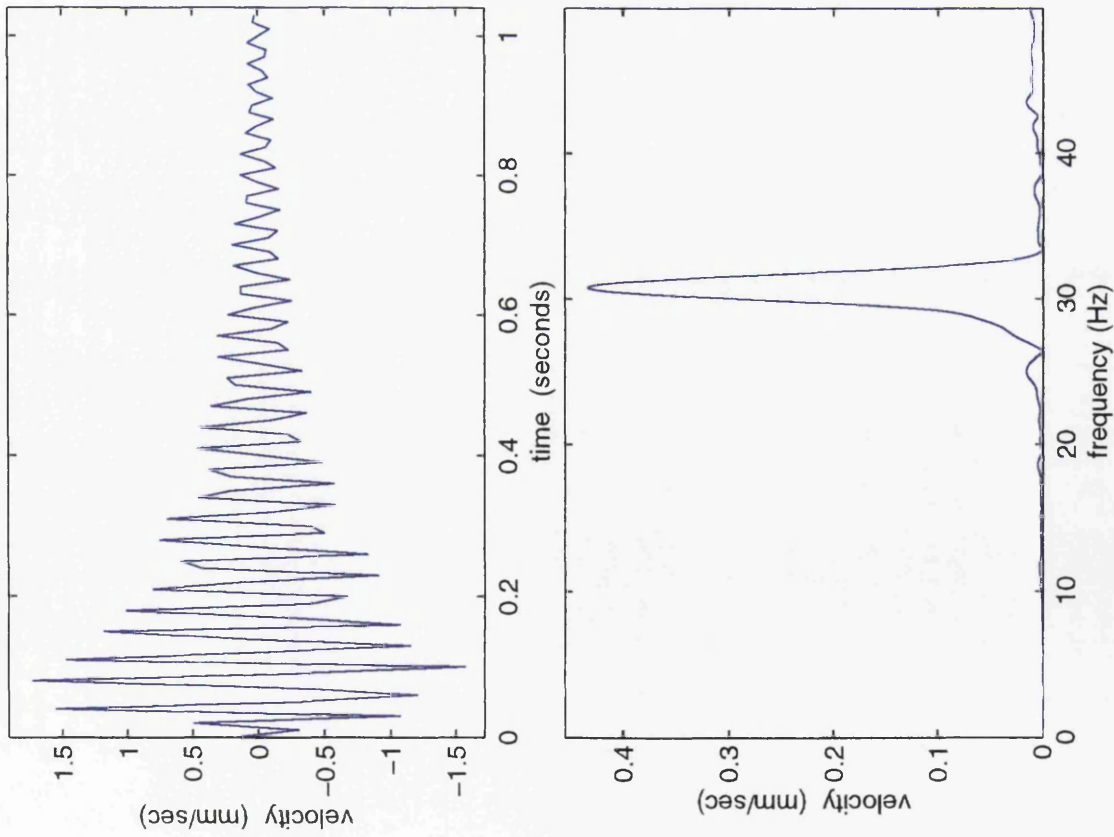
condition. A more detailed analysis of the sound using the spectrogram view reveals more detailed information regarding the fault. Many other faults occur in gearboxes. If more time was available another experiment would have been performed, that of worn teeth. The results of the two previous experiments and the work of Maynard [12], suggest that this fault would also be detected by the microphone, although this has not been proven.

### *Conclusions*

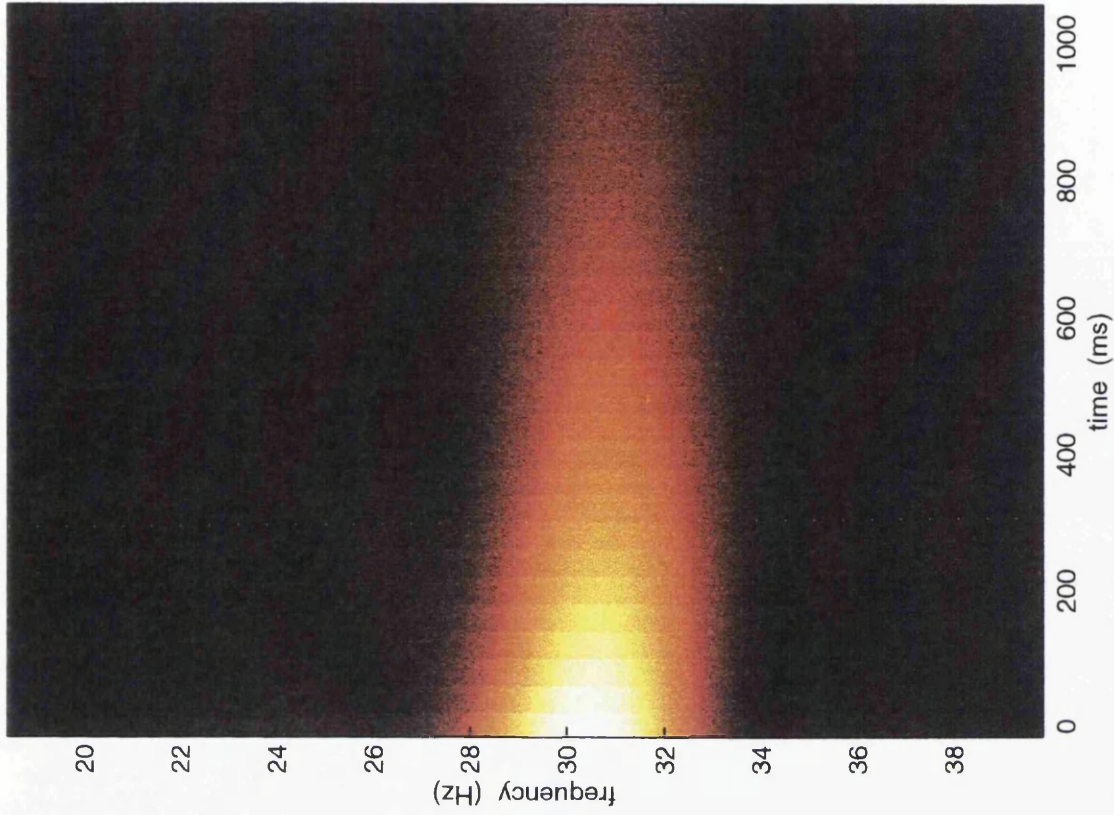
- The microphone can detect the sound of impacting teeth generated by internal misalignment within the gearbox.
- The spectrogram view can be used to gain a more detailed 'picture' of the fault.
- Crestfactor and Kurtosis can be used as a basic parameter of 'health', although problems with reverberation may hamper efforts to diagnose faster machines. This may be solved with the use of a higher frequency microphone.
- Double differentiating the sound signal emphasises the higher frequencies.

The final discussion and conclusions to the experimental and the mathematical modelling work can be found in chapters five and six respectively.

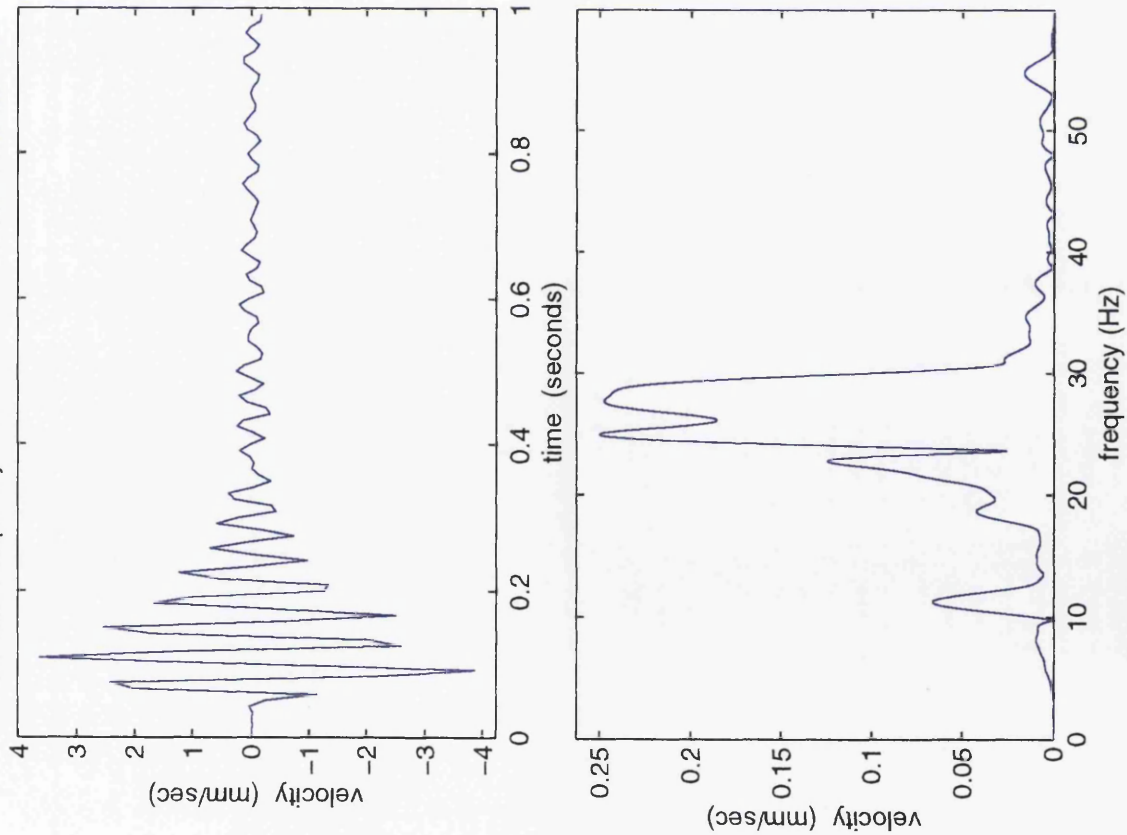
Time and Frequency Domain Plot of Table Resonance: Z



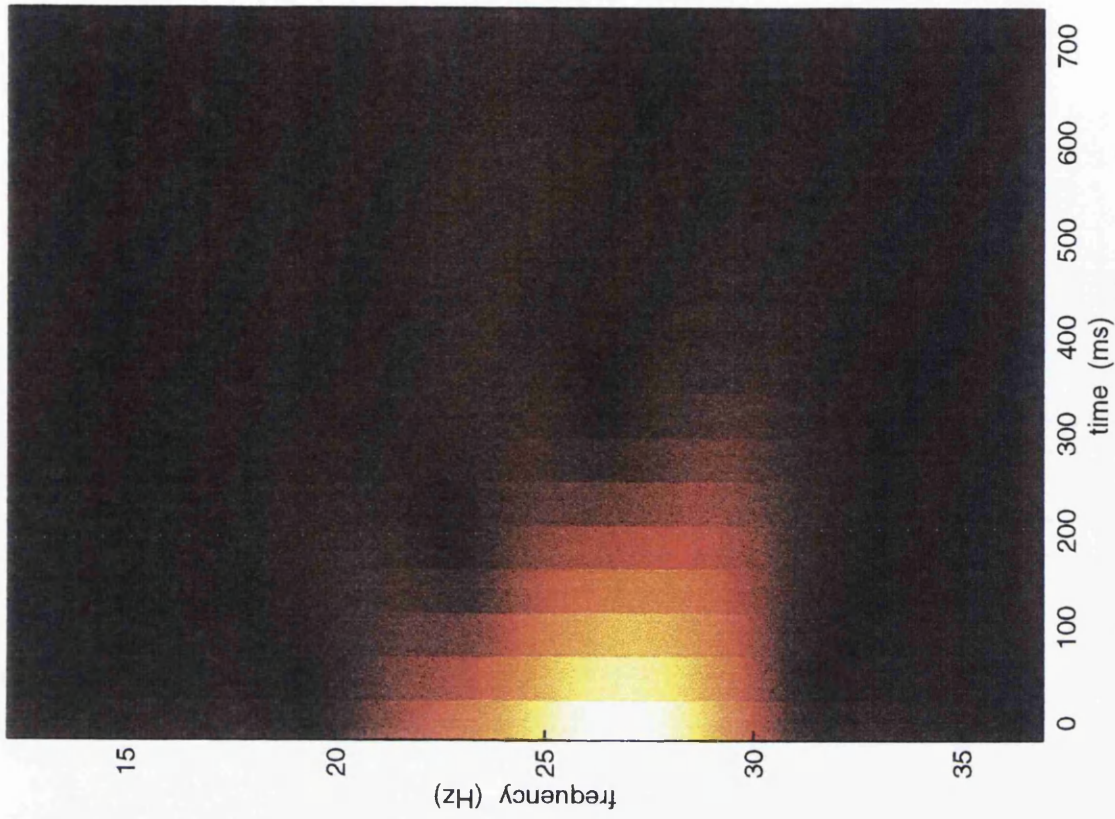
Spectrogram of Table Resonance: Z



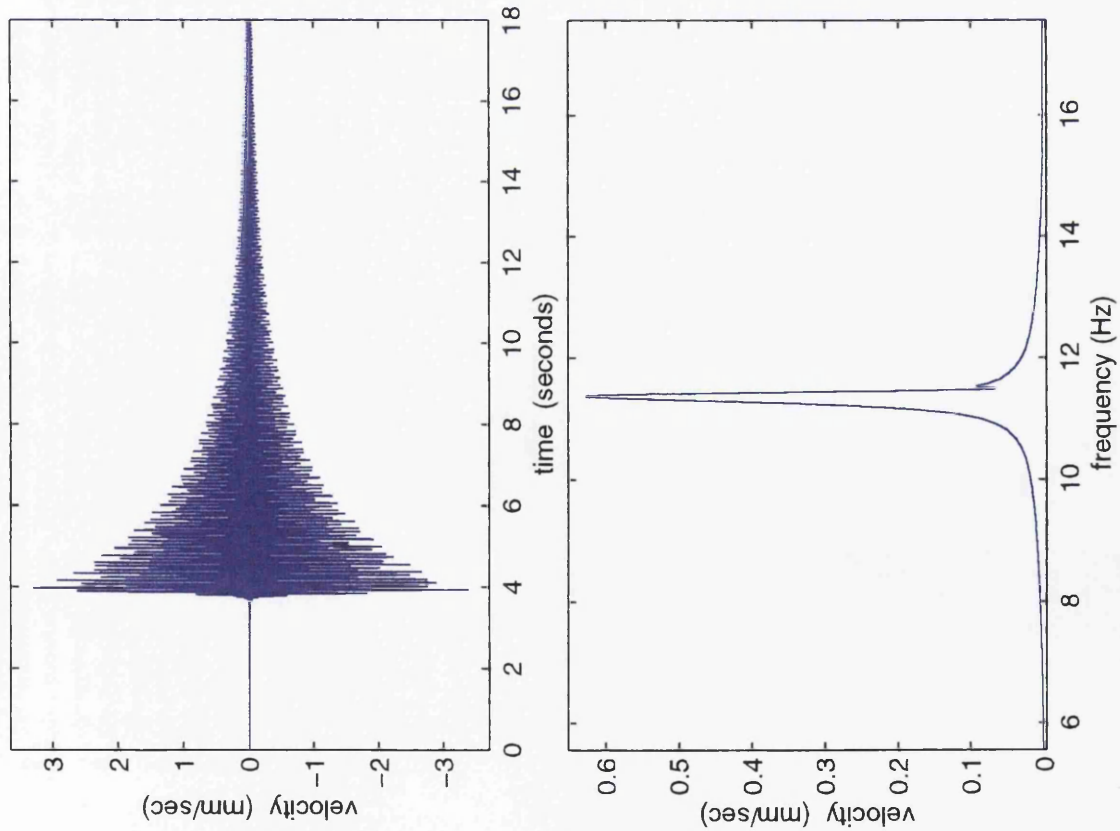
Time and Frequency Domain Plot of Table Resonance: Y



Spectrogram of Table Resonance: Y



Time and Frequency Domain Plot of Table Resonance: X



Spectrogram of Table Resonance: X

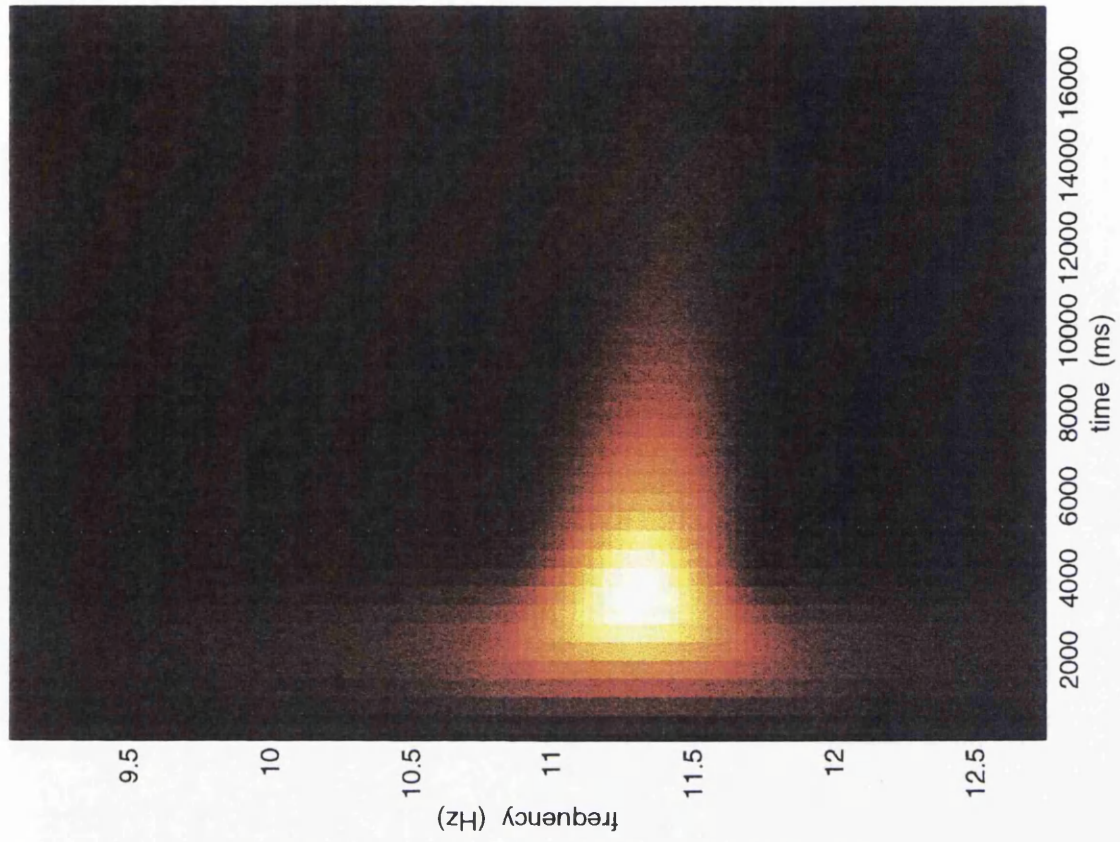
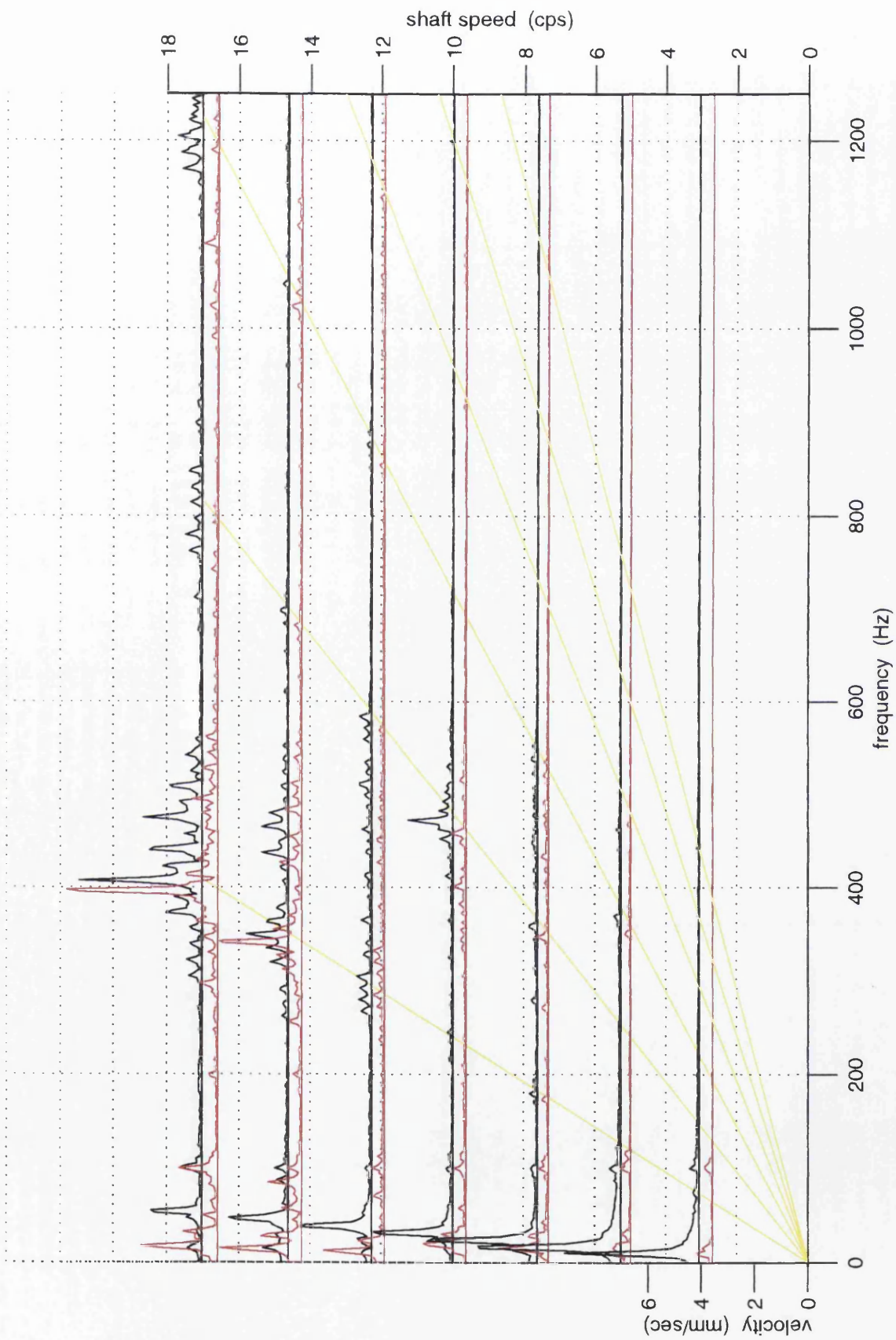


figure 3

Comparison of Gearbox One Baseline (black) and Reassembled Gearbox (red)





Comparison of Gearbox One Baseline (black) and Reassembled Gearbox (red)

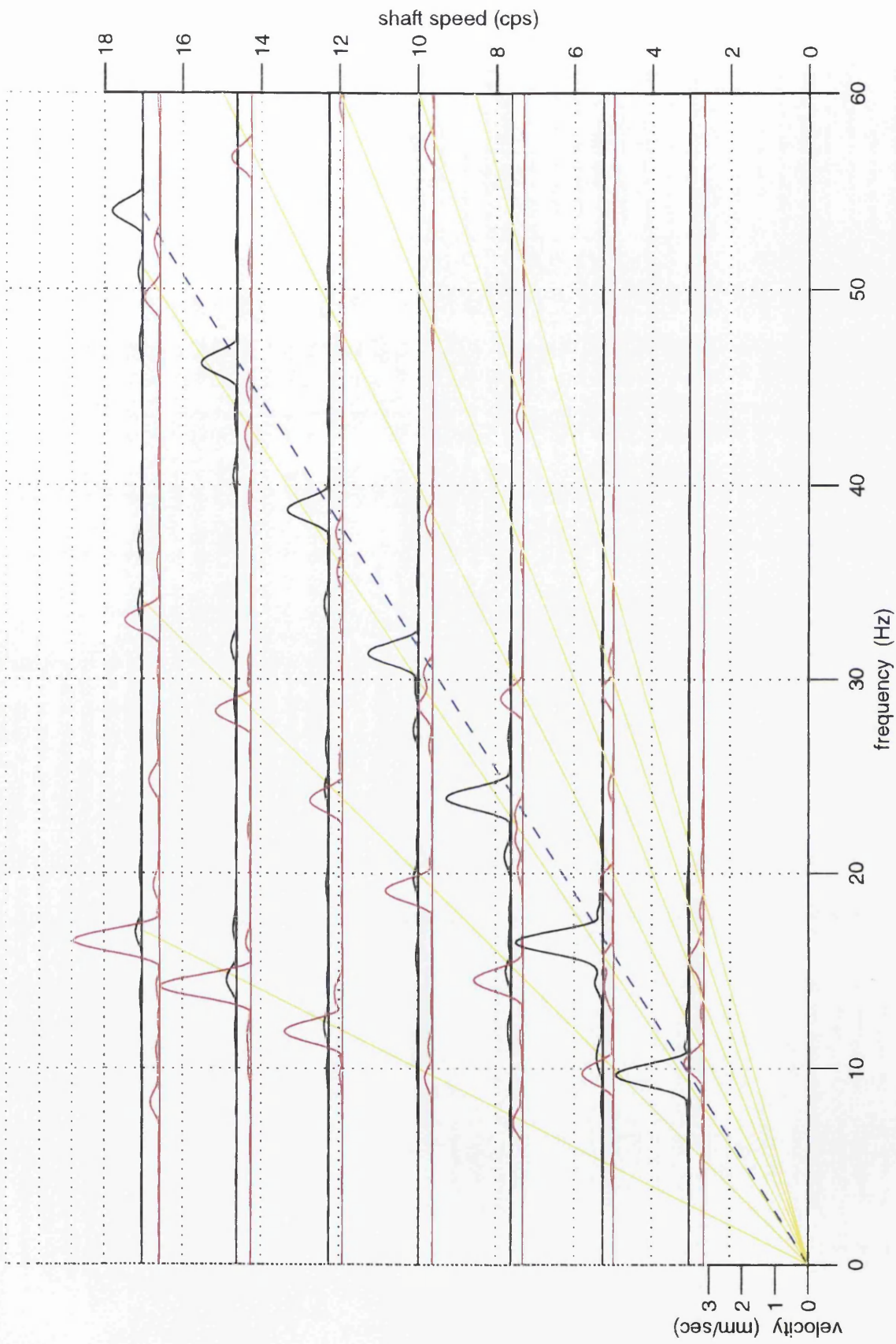


figure 5

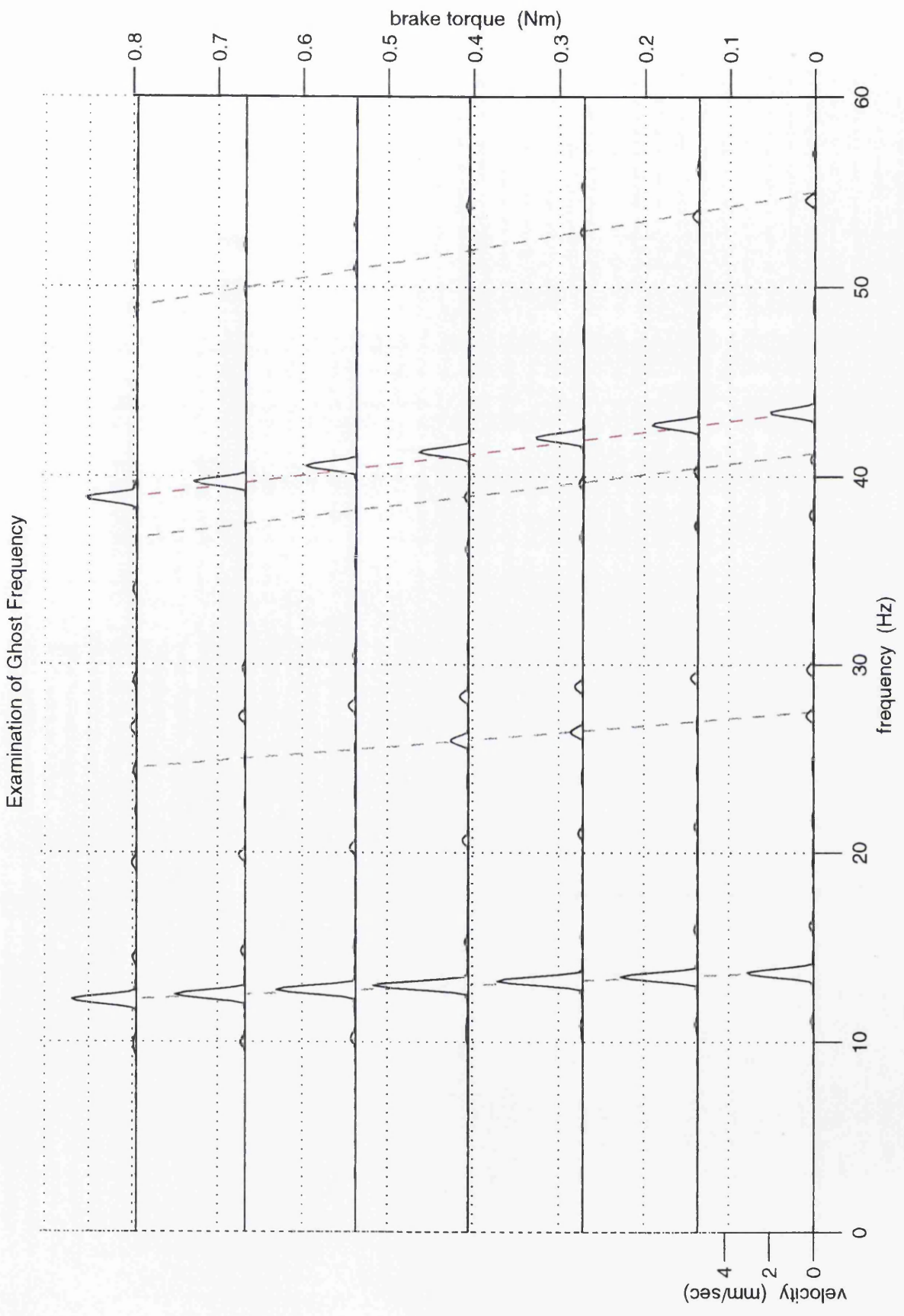
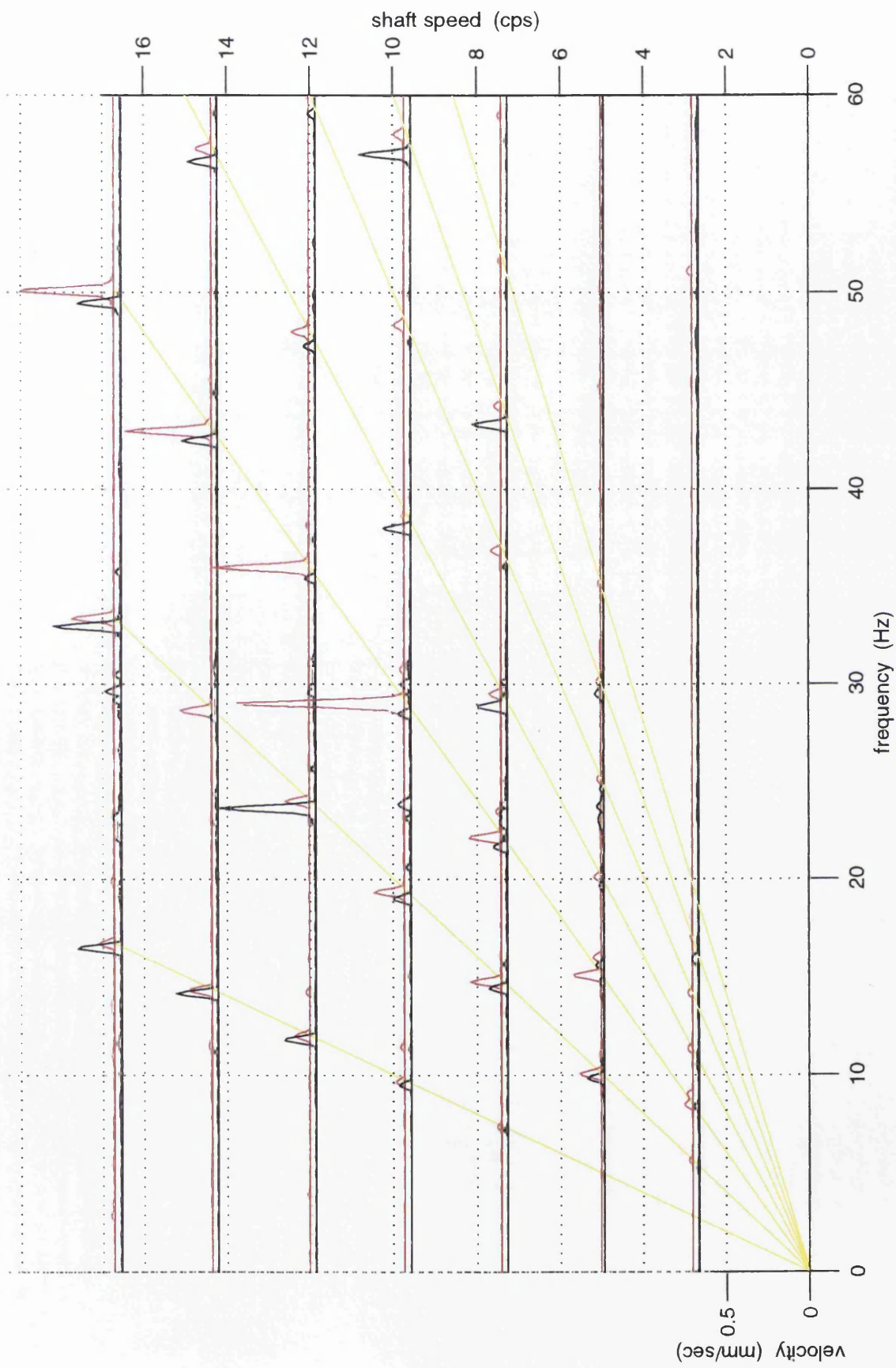


figure 6

Comparison of Gearbox One Reassembled (black) and Misalignment (red): Horizontal



Comparison of Gearbox One Reassembled (black) and Misalignment (red): Axial

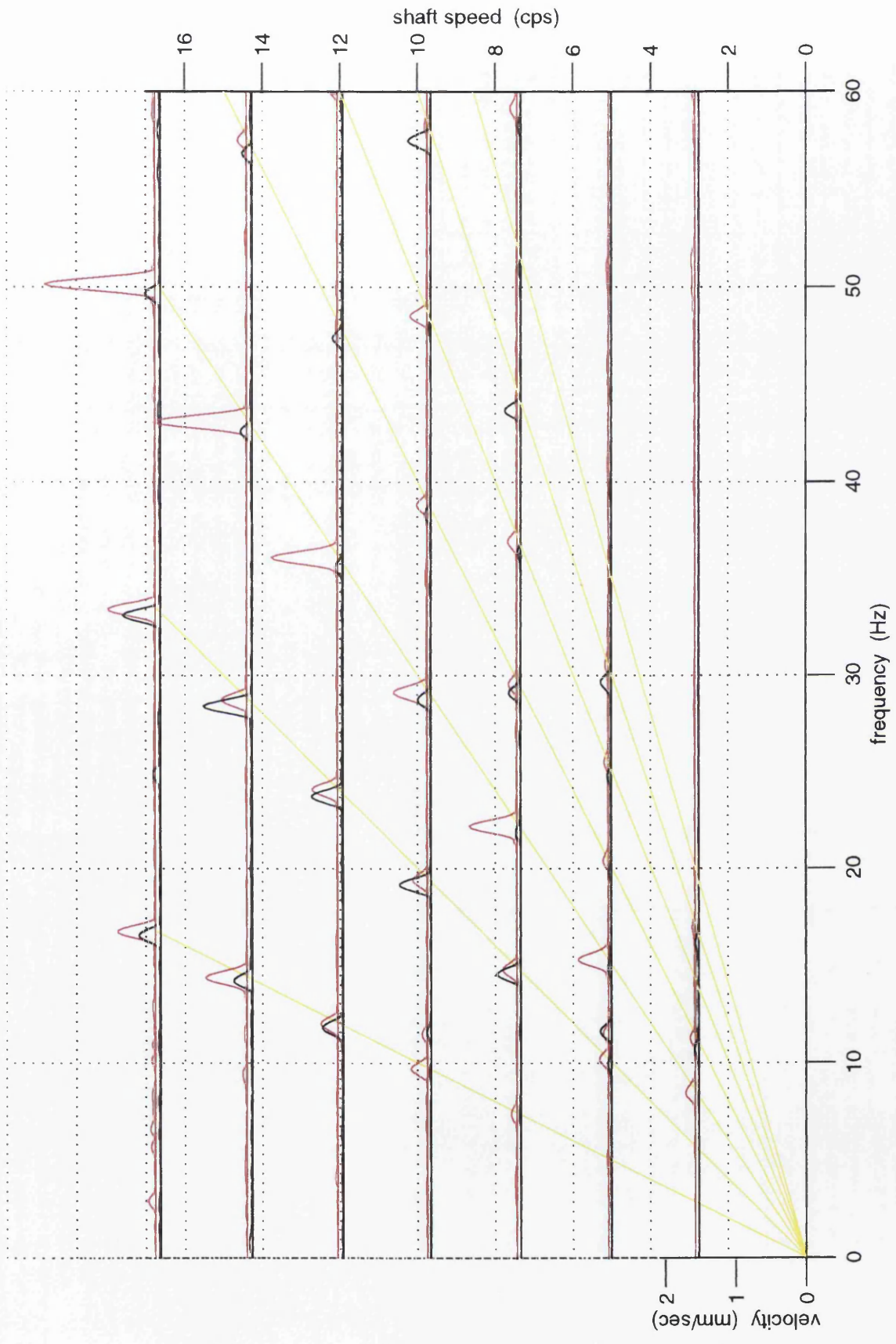


figure 8

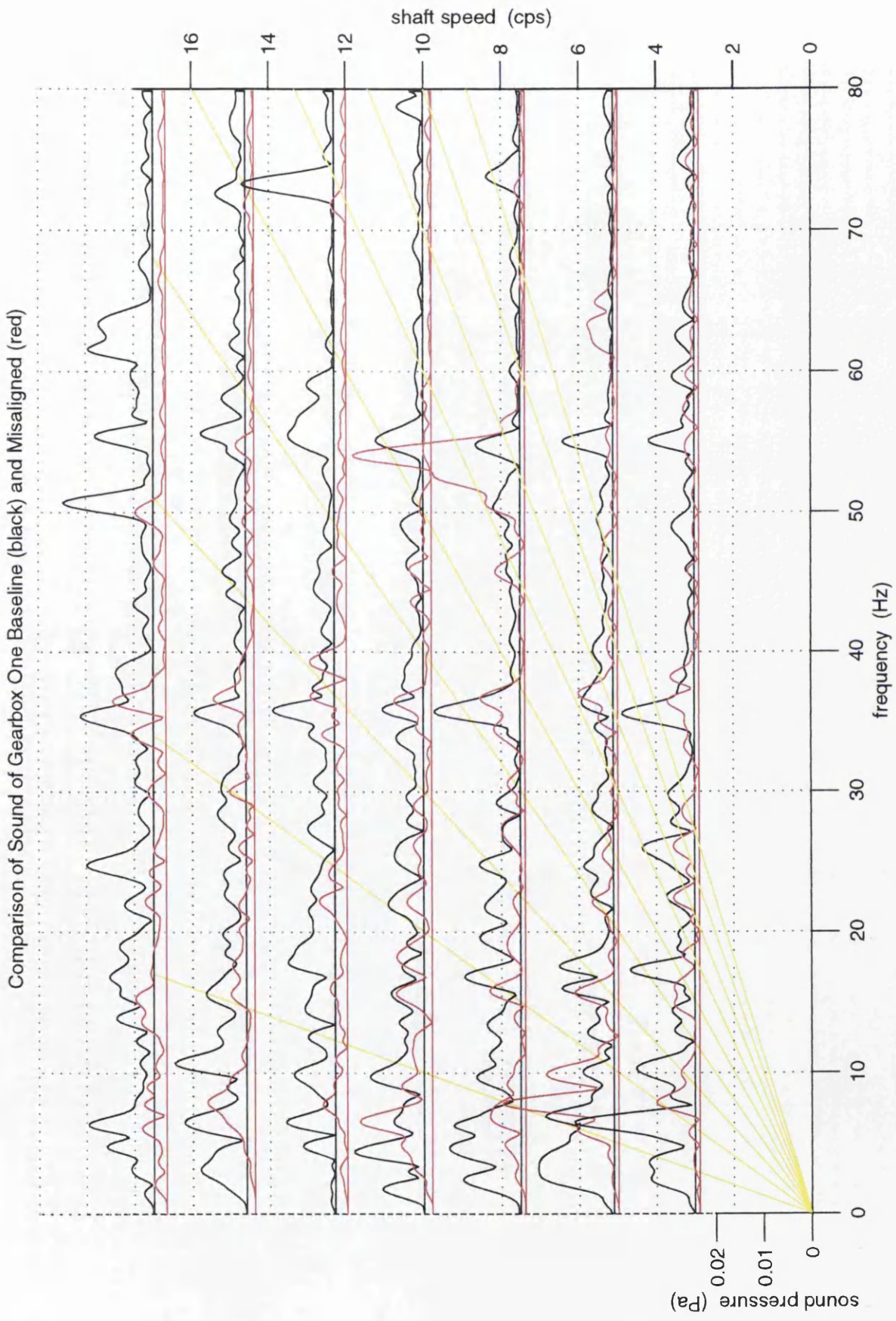
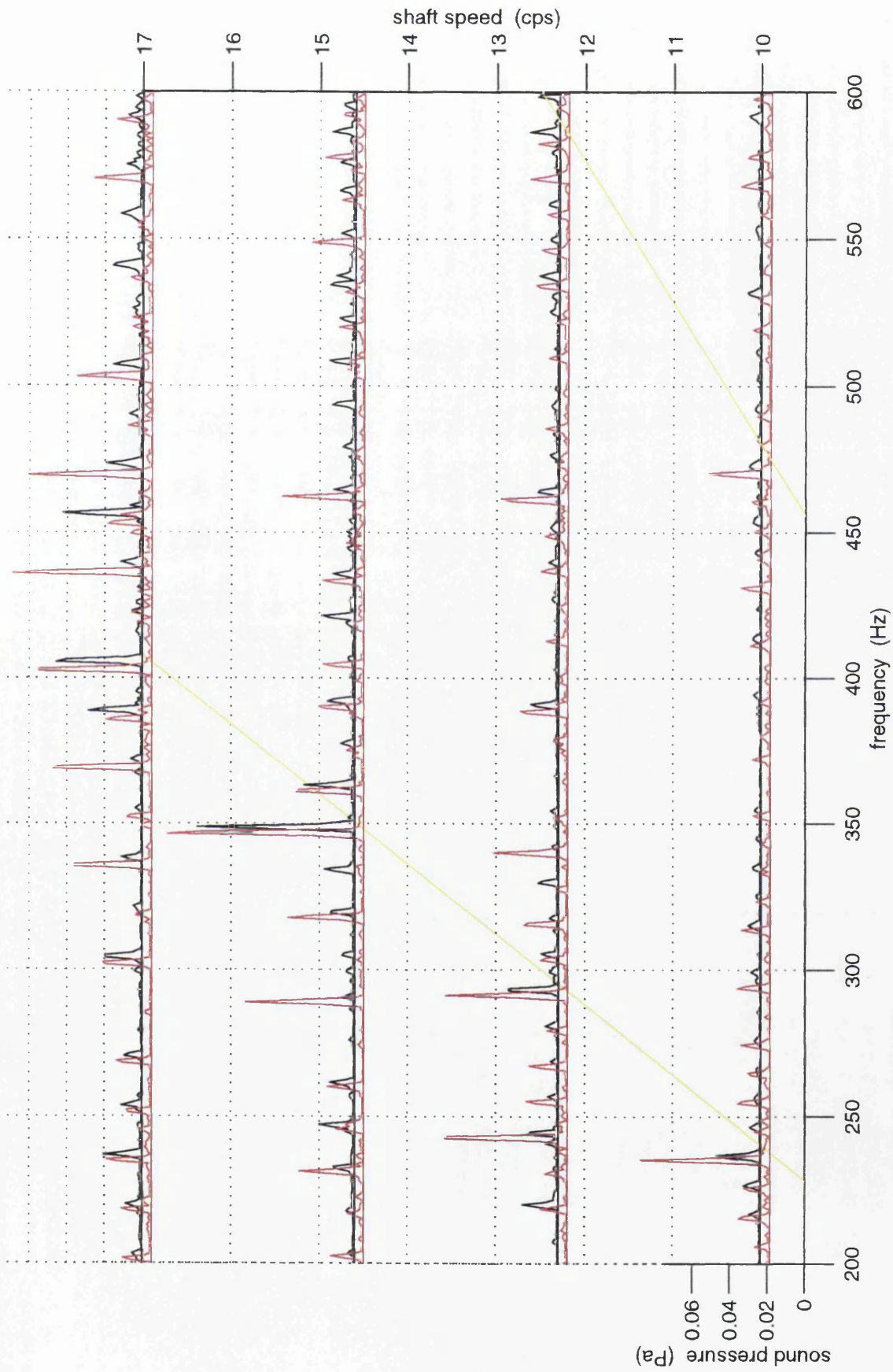


figure 9

Comparison of Sound of Gearbox One Baseline (black) and Broken Tooth (red)



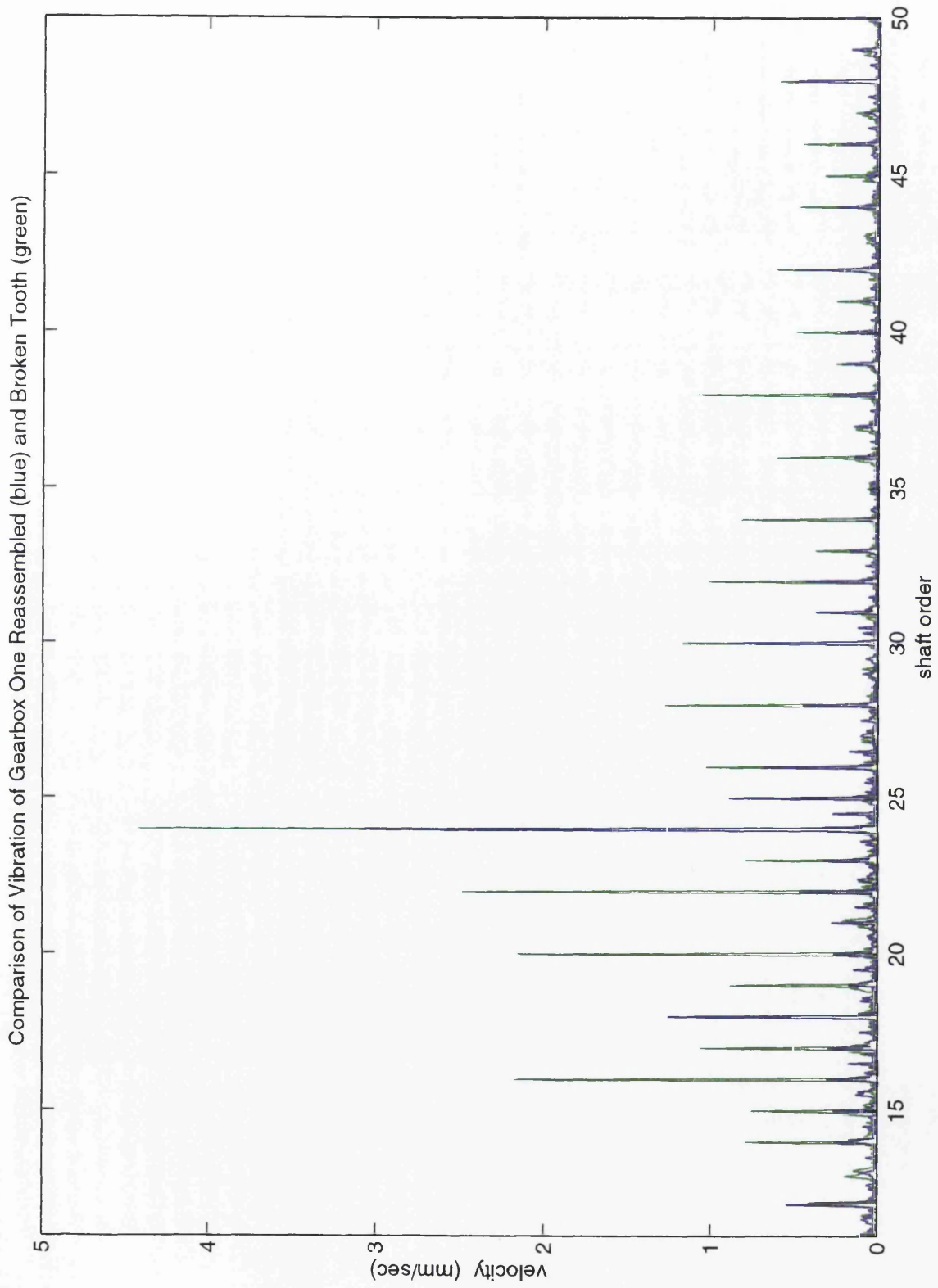


figure 11

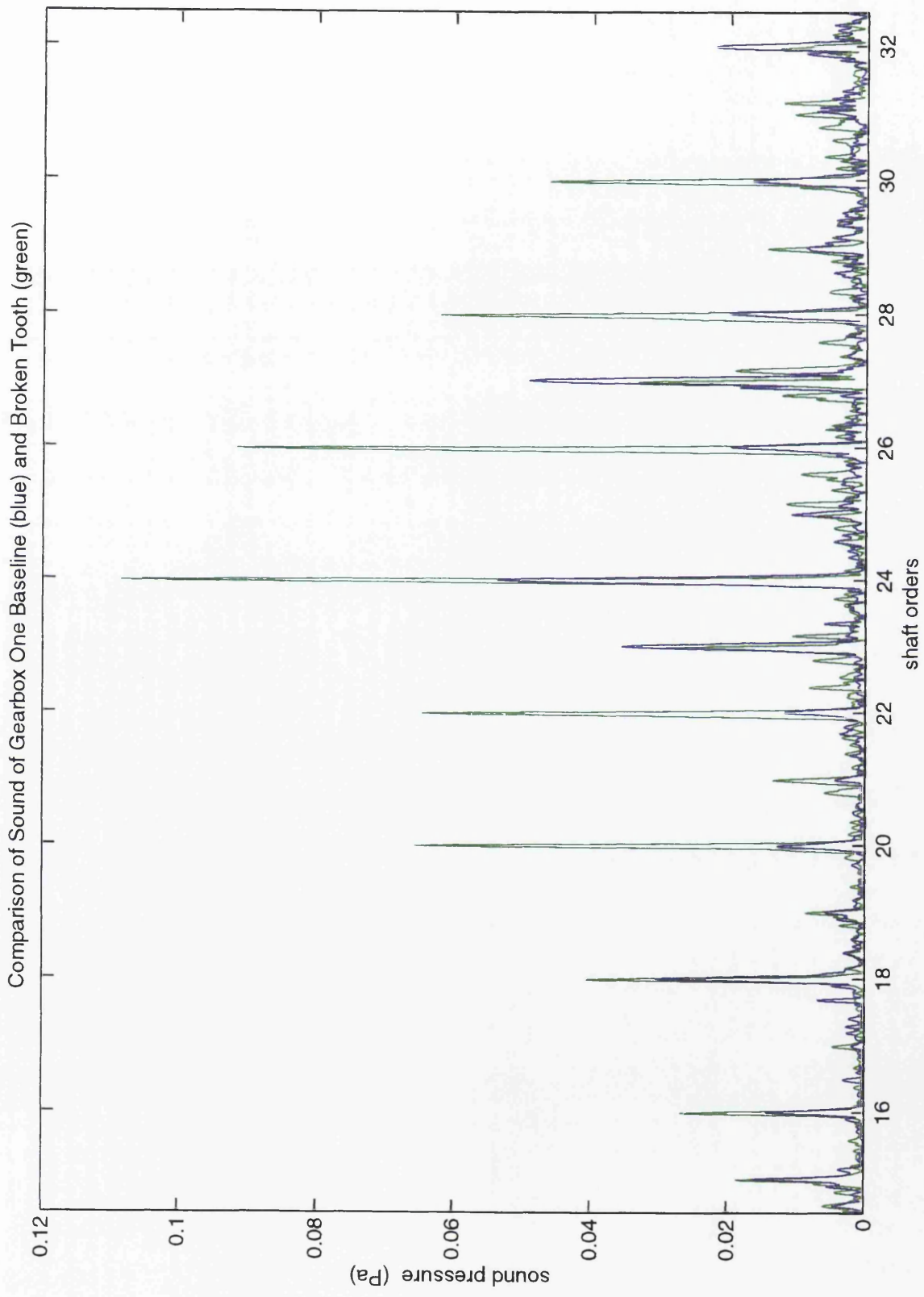


figure 12



Comparison of Vibration of Gearbox Two Baseline (black) and Displaced Shaft (red): Horizontal

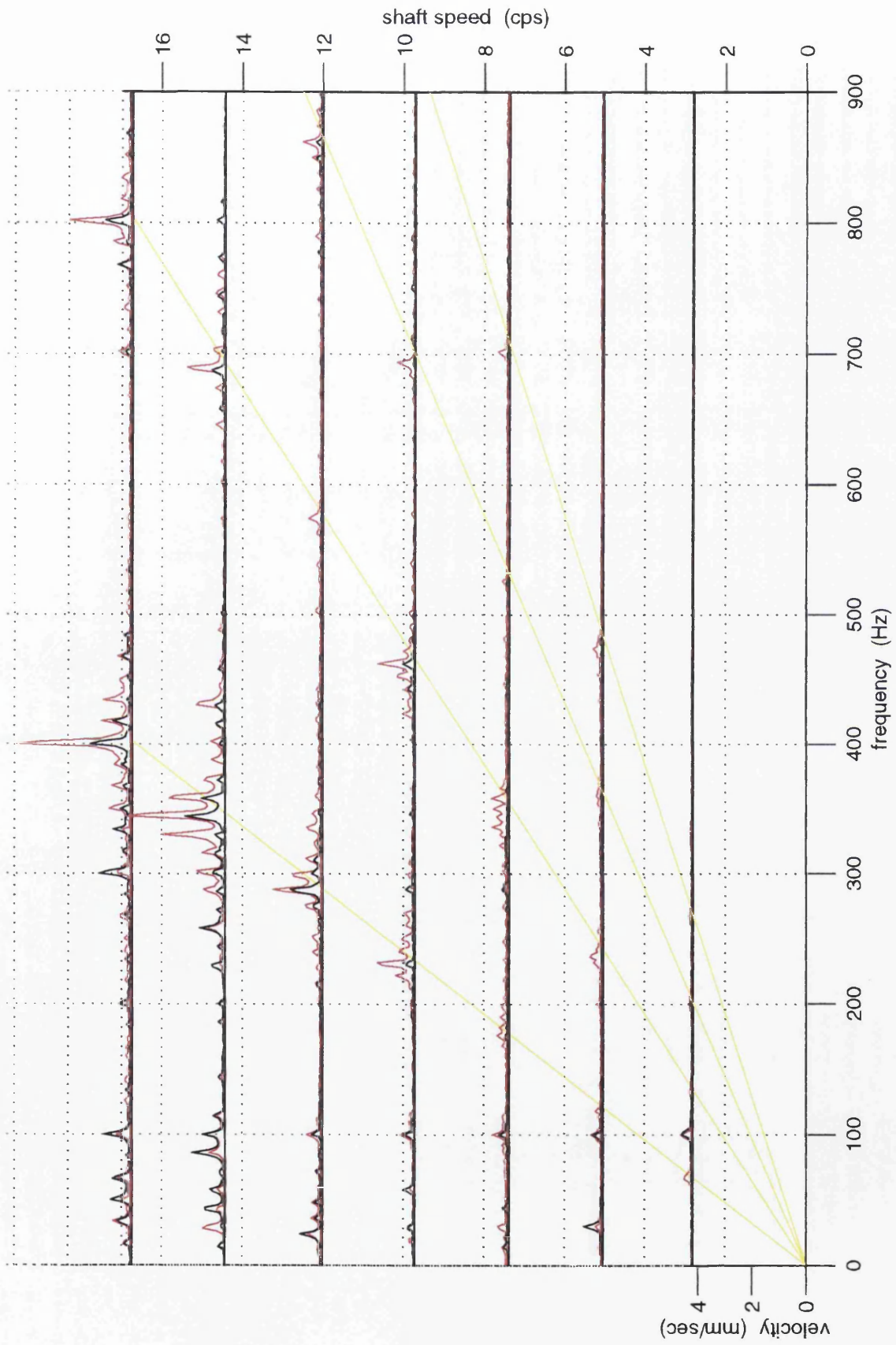


figure 13

Comparison of Vibration of Gearbox Two Baseline (black) and Displaced Shaft (red): Horizontal

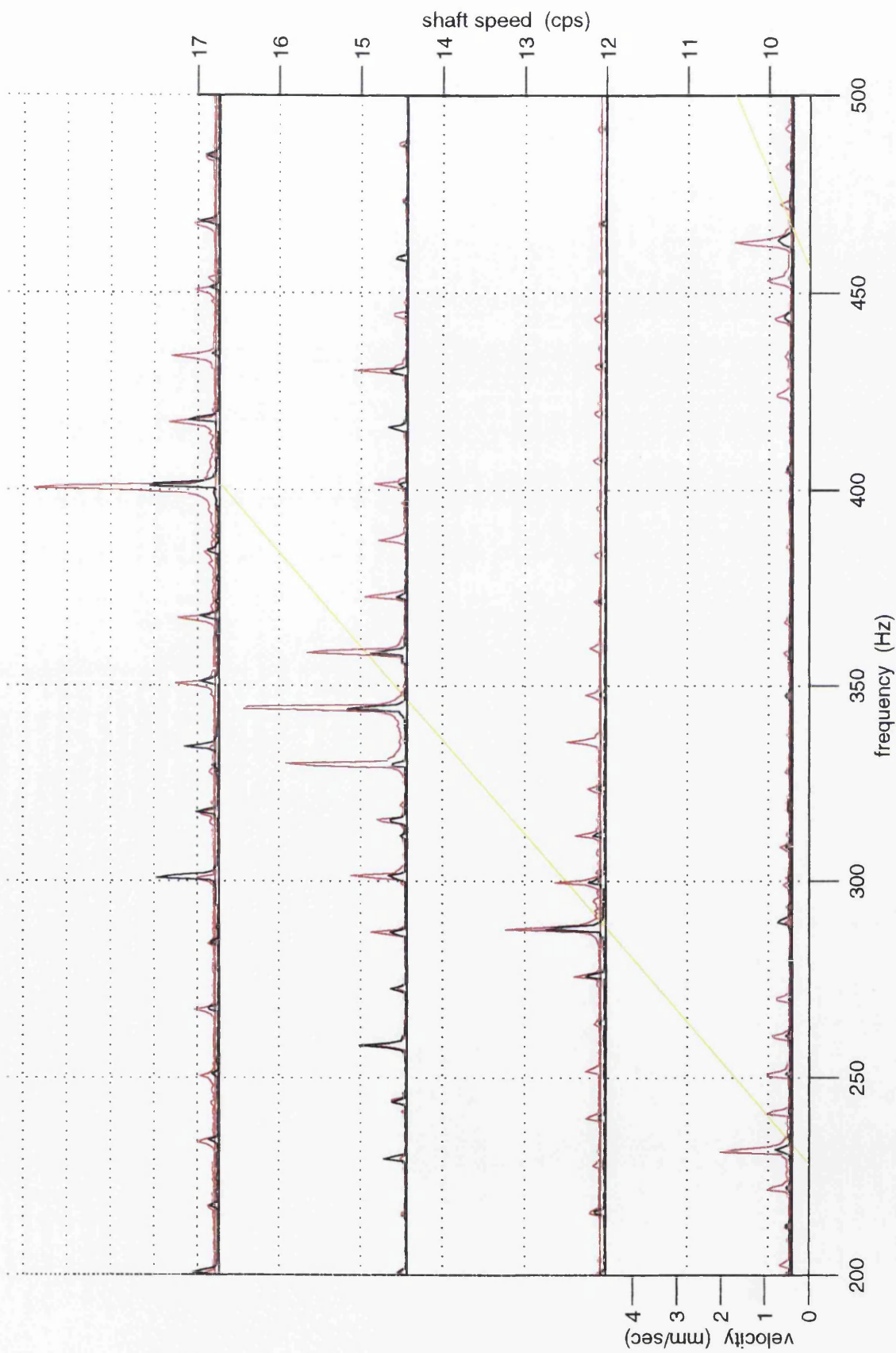


figure 14

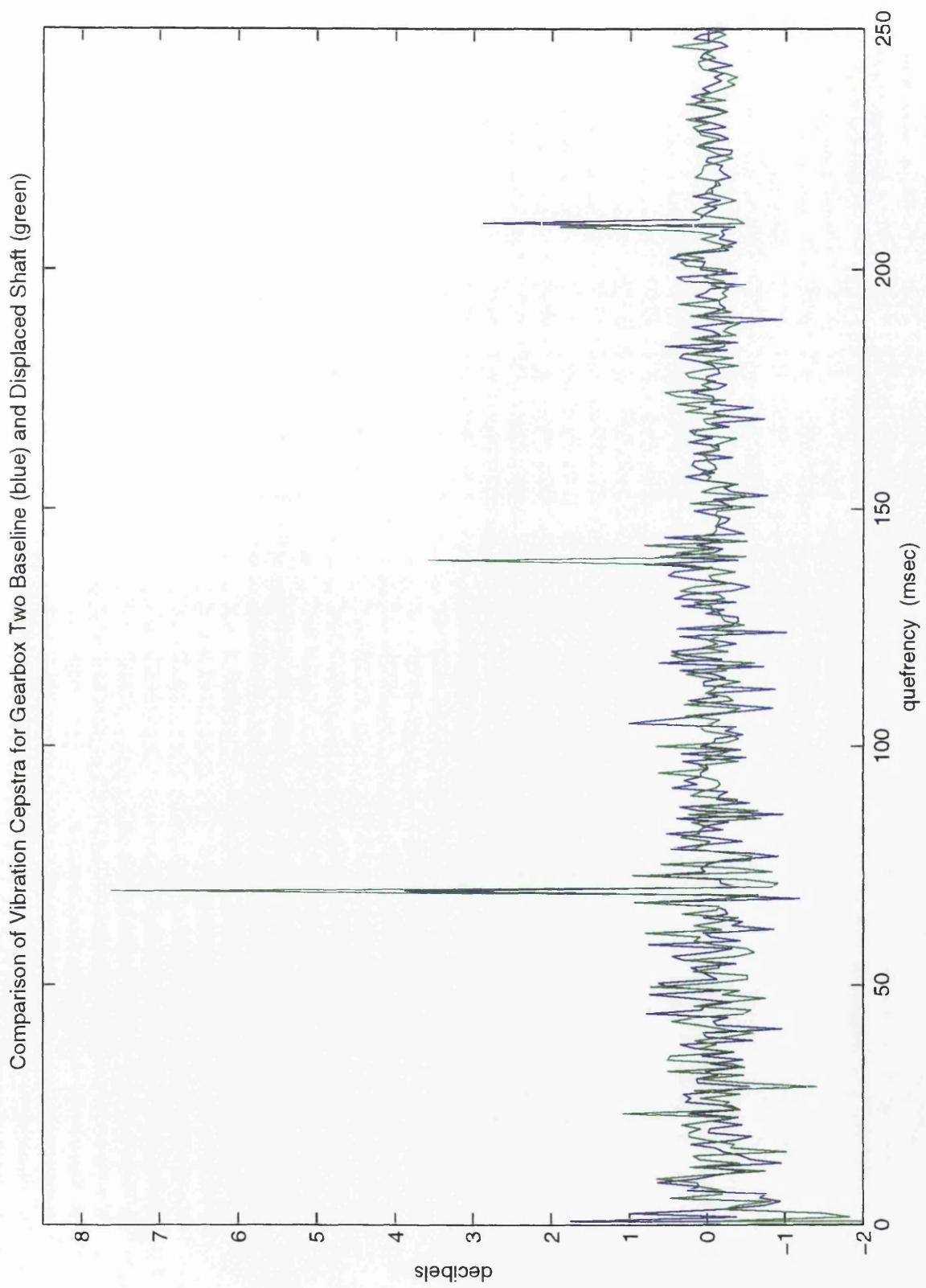


figure 15

Comparison of Sound for Gearbox Two Baseline (black) and Displaced Shaft (red)

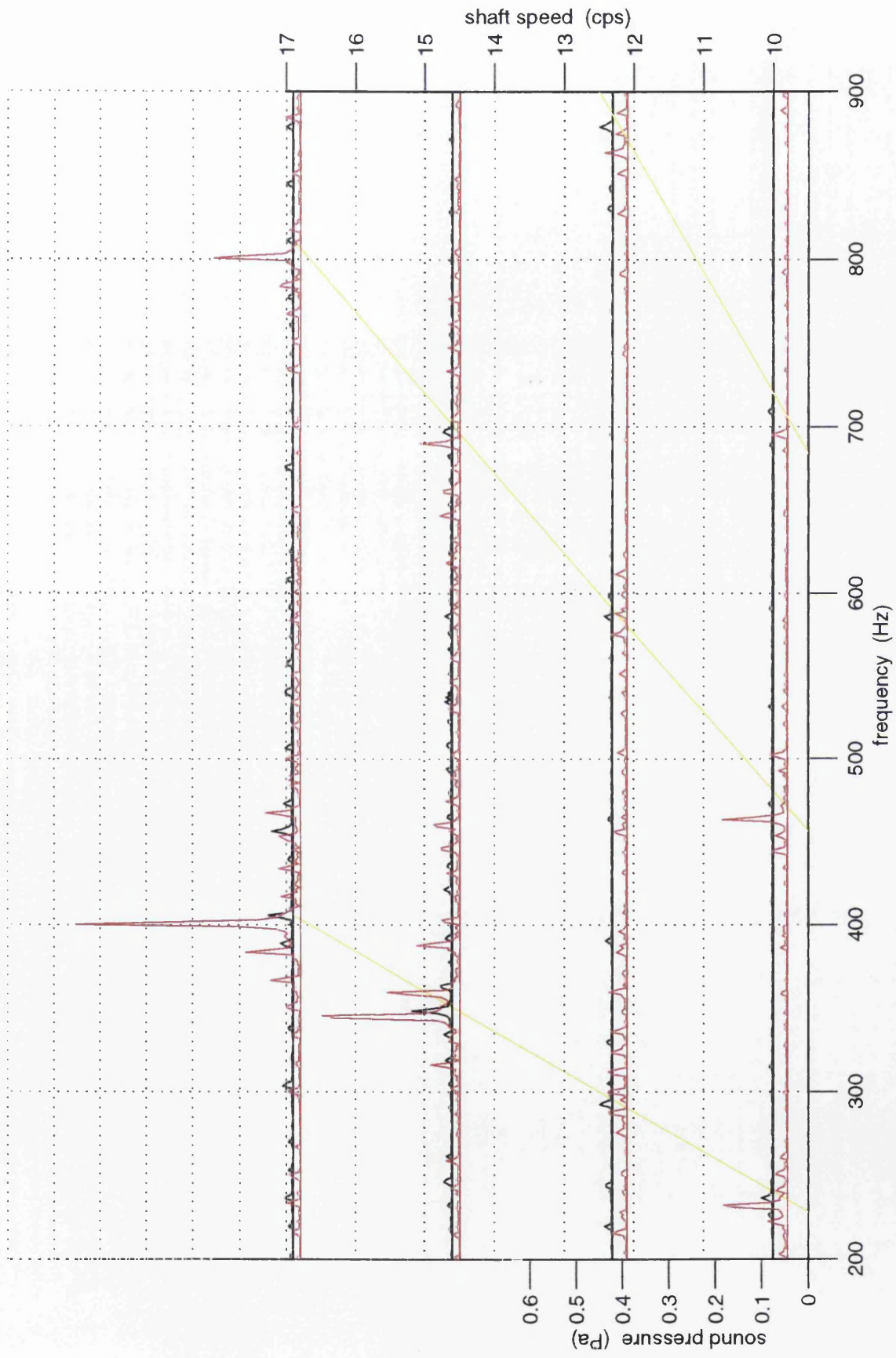
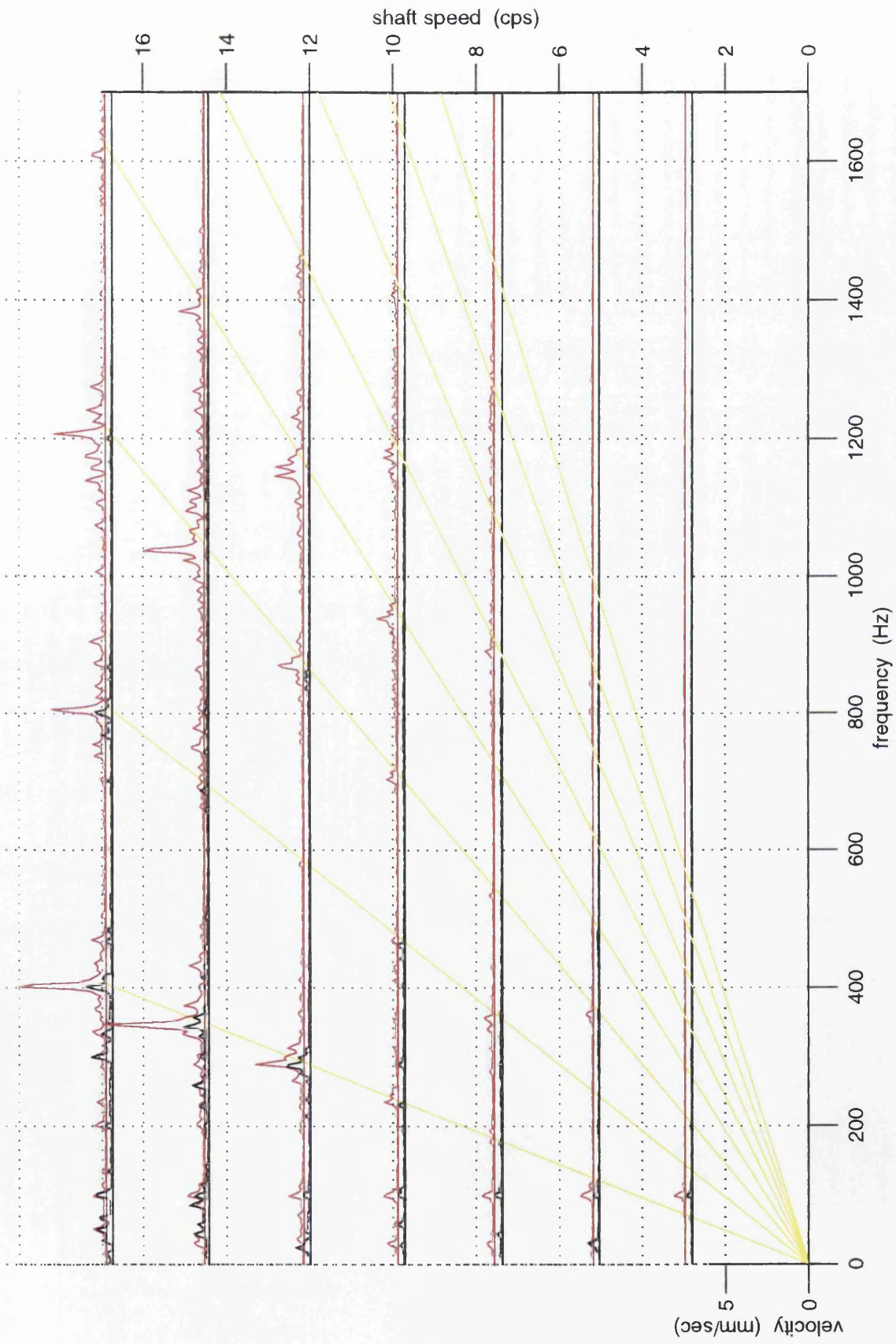


figure 16

Comparison of Vibration of Gearbox Two Baseline (black) and Tooth Lubrication Failure (red): Horizontal



Comparison of Vibration of Gearbox Two Baseline (black) and Tooth Lubrication Failure (red): Horizontal

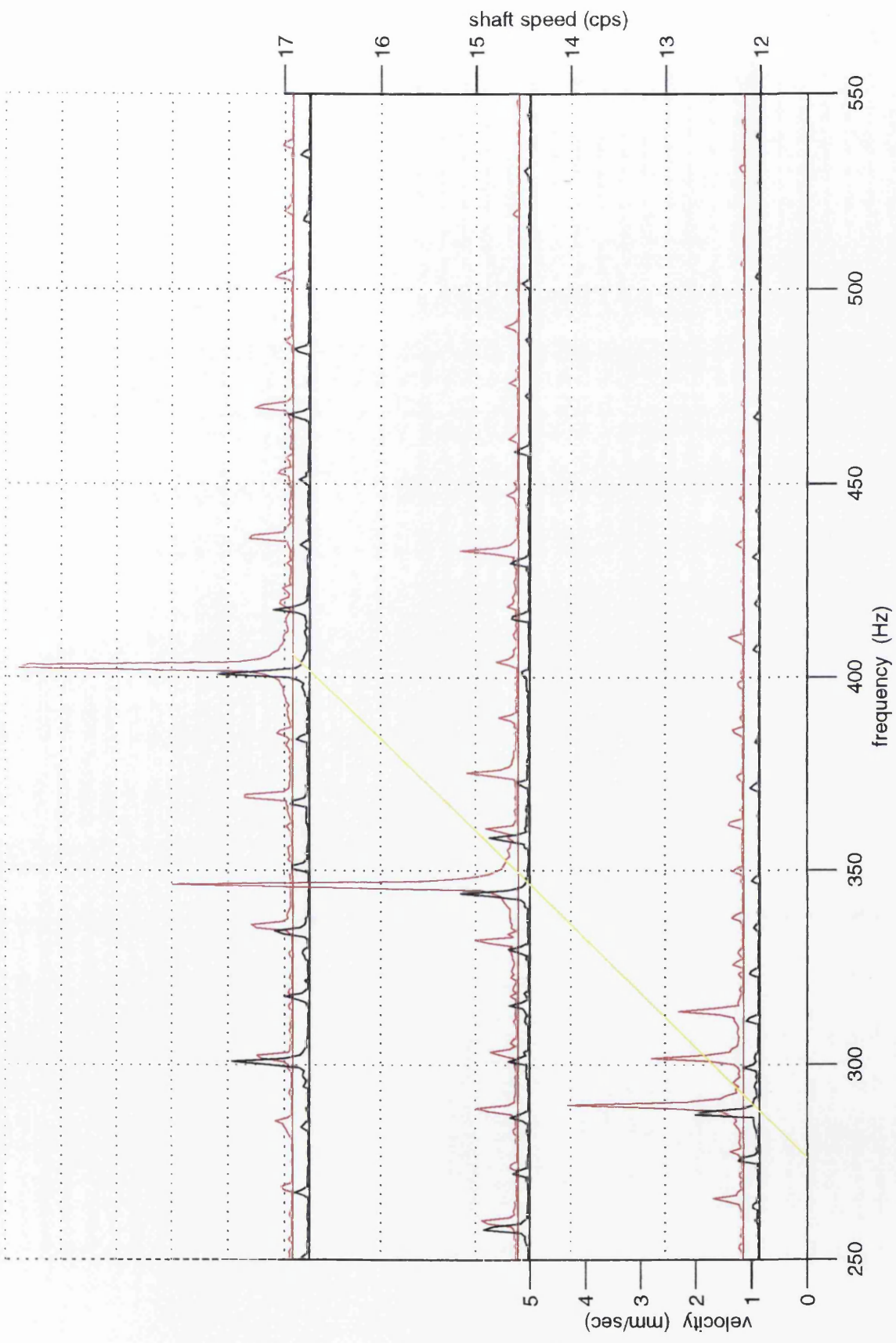


figure 18

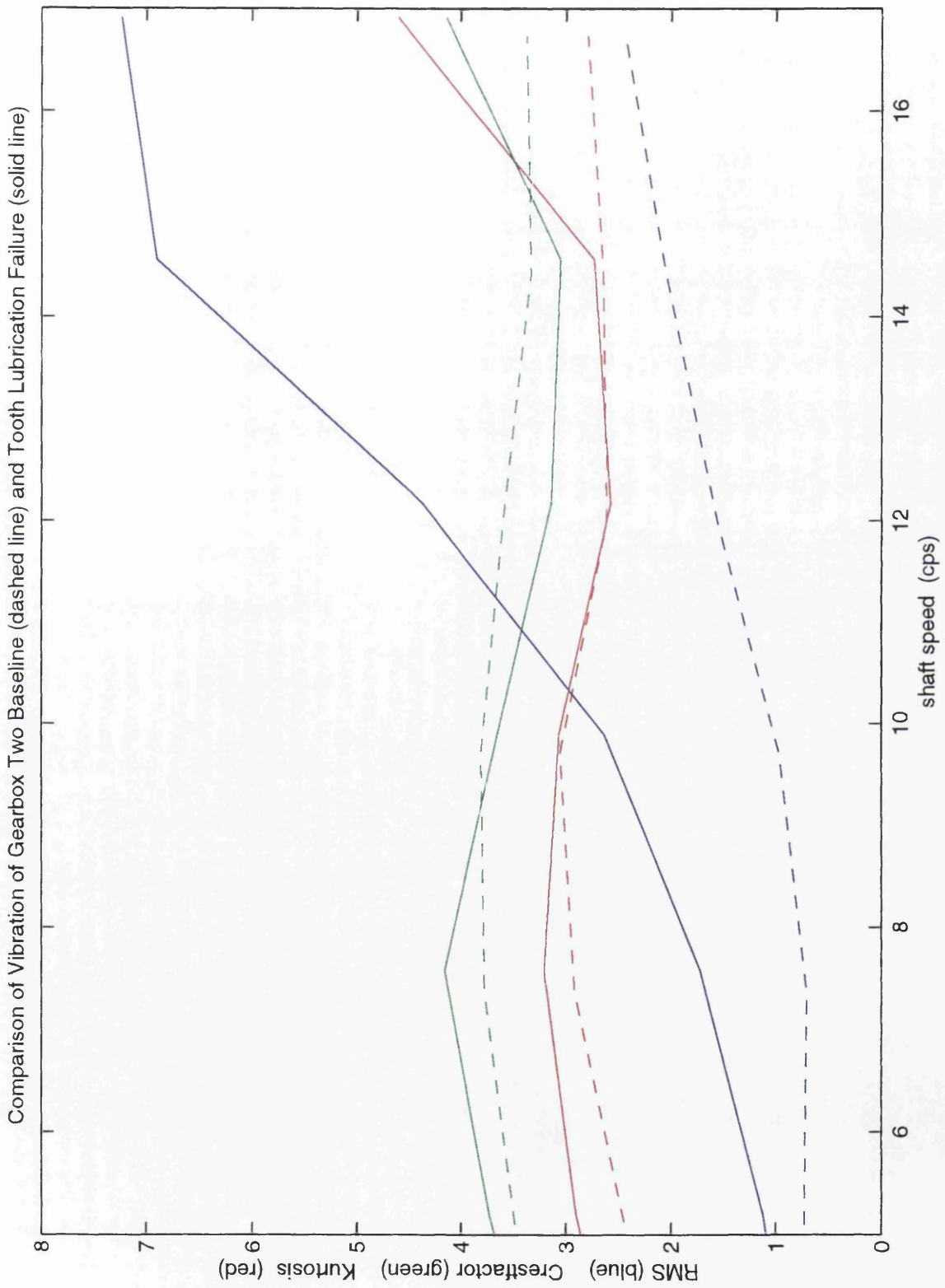
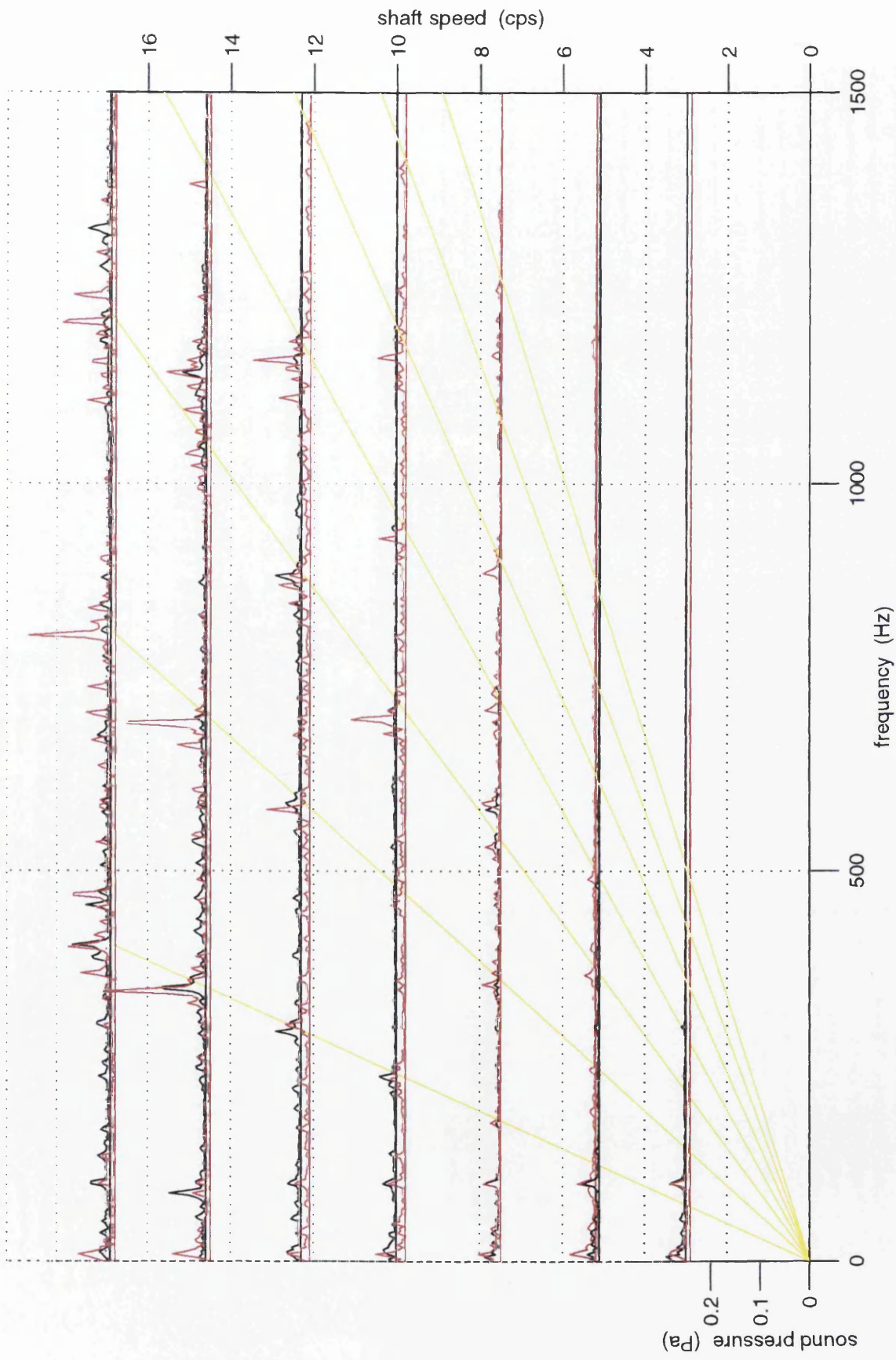


figure 19

Comparison of Sound of Gearbox Two Baseline (black) and Tooth Lubrication Failure (red)





Comparison of Sound of Gearbox Two Baseline (black) and Tooth Lubrication Failure (red)

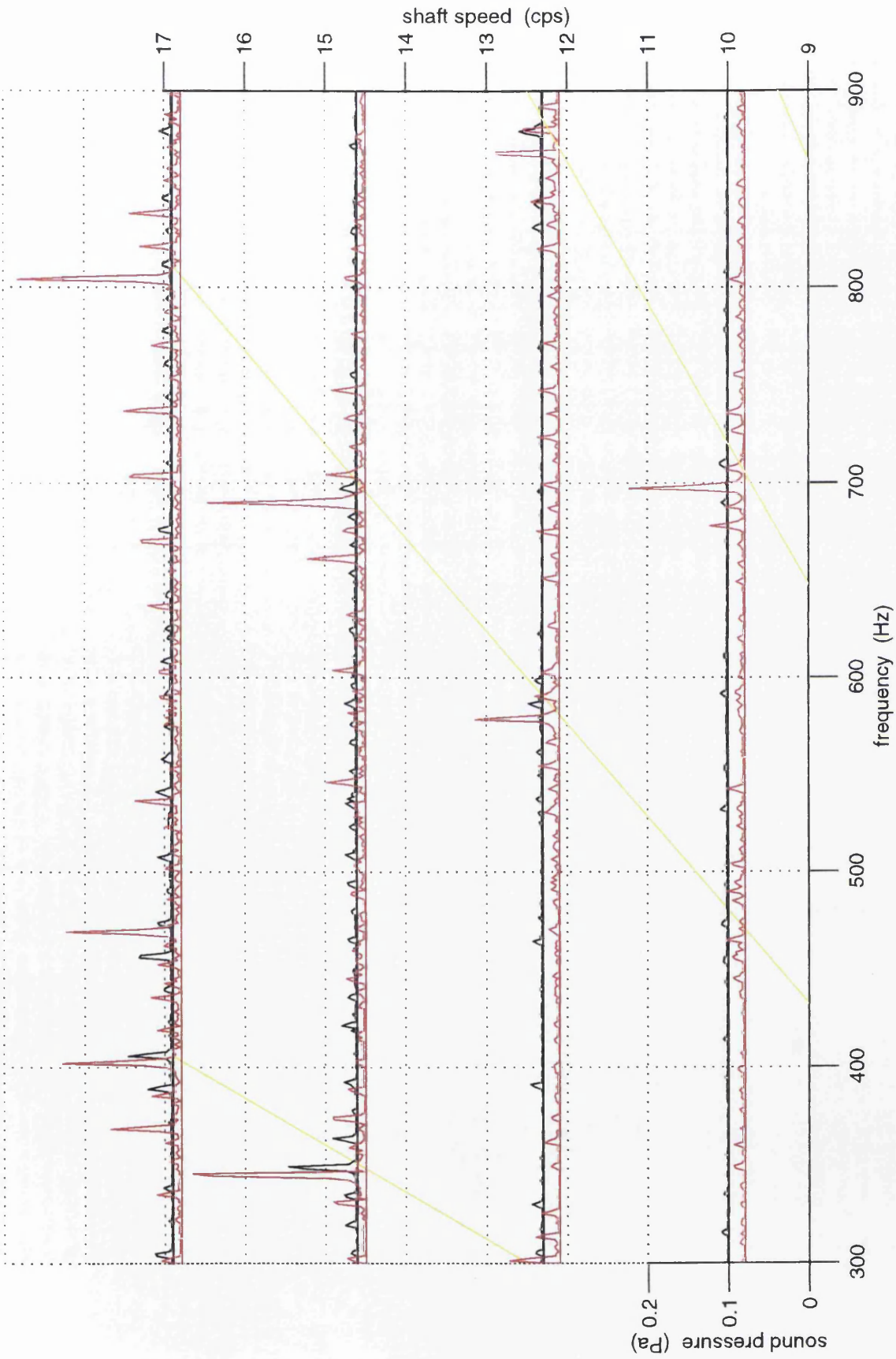


figure 21

Comparison of Vibration of Gearbox Two Baseline (black) and Worn Teeth (red): Horizontal

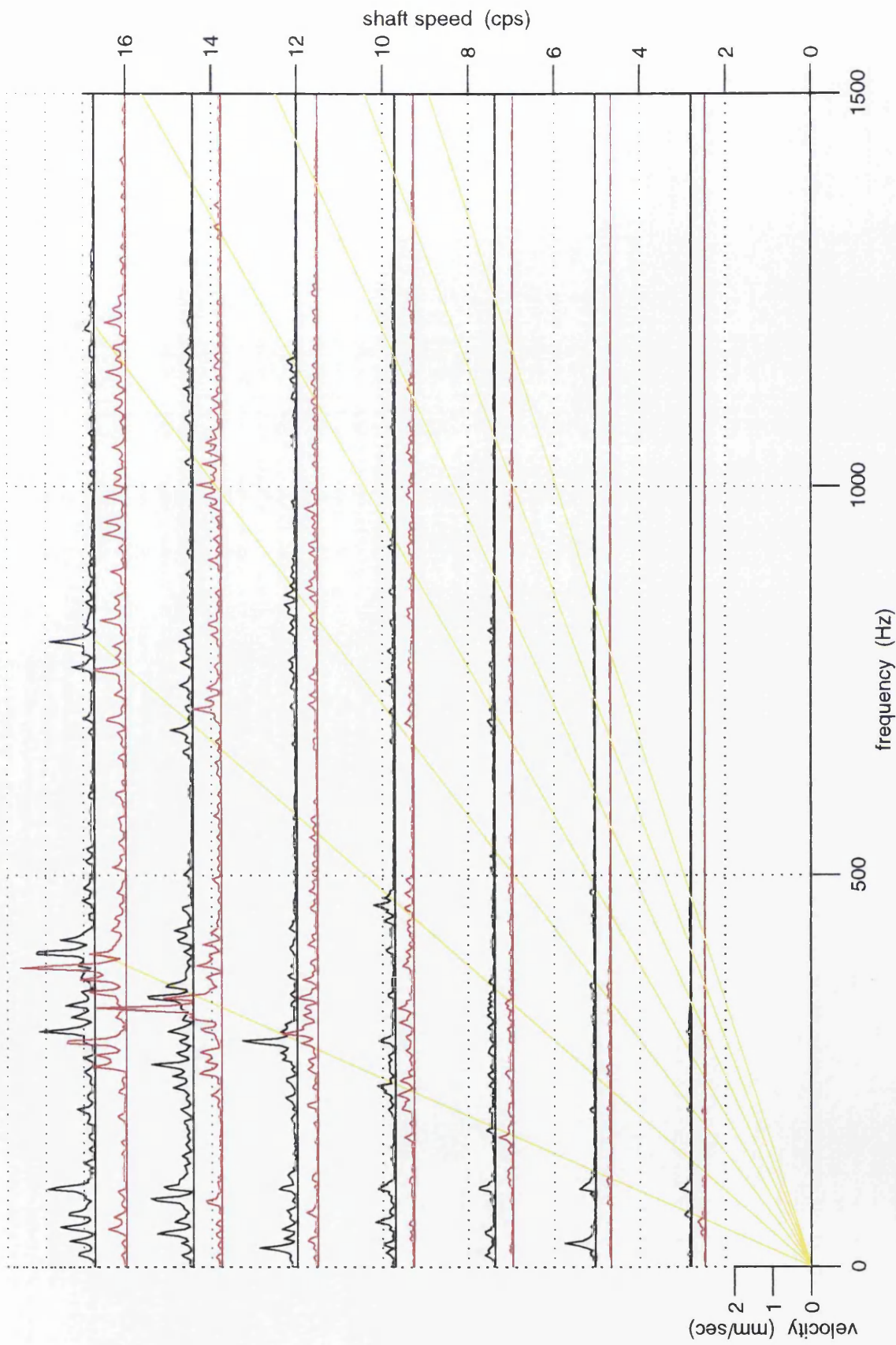
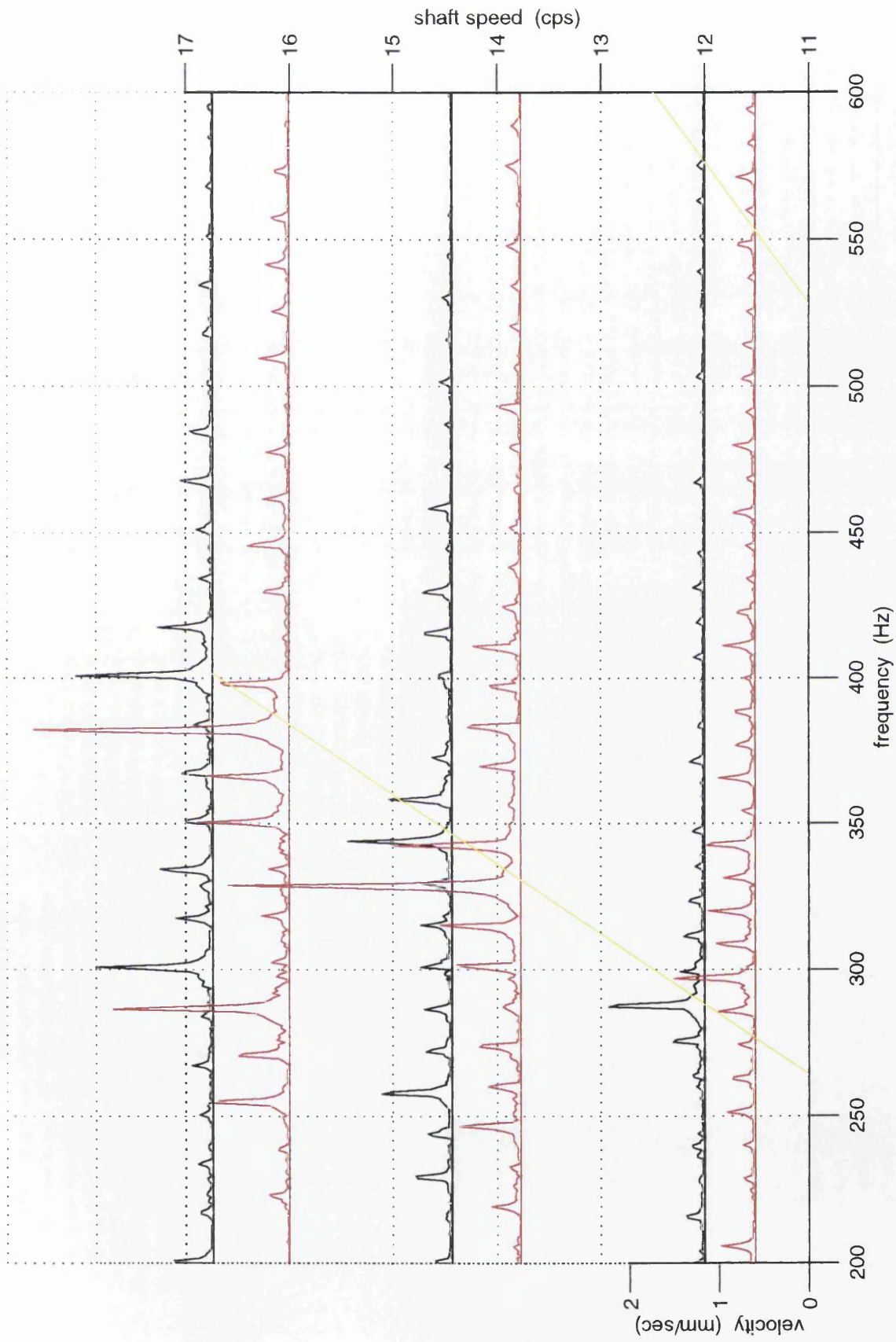
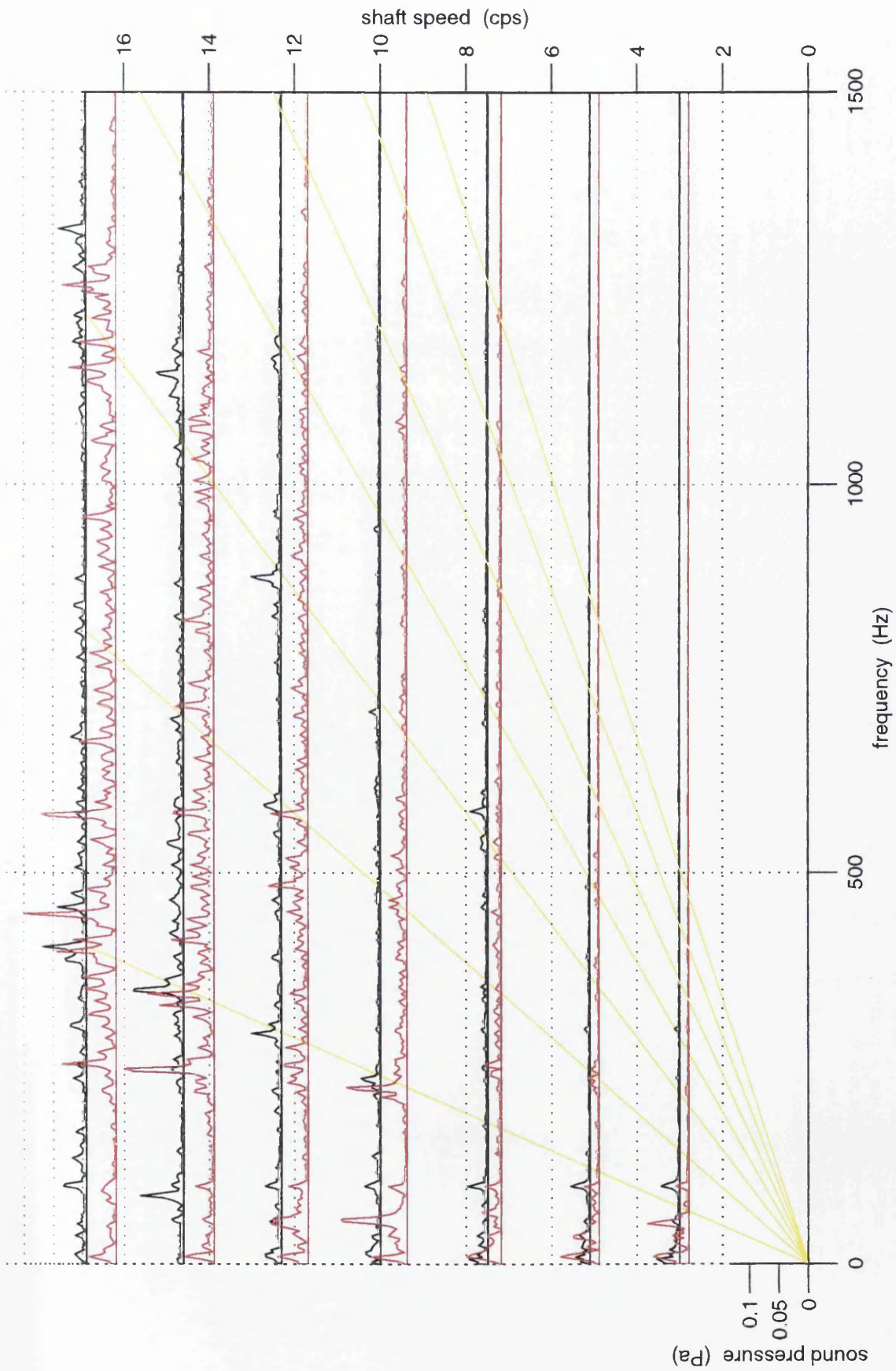


figure 22

Comparison of Vibration of Gearbox Two Baseline (black) and Worn Teeth (red): Horizontal



Comparison of Sound of Gearbox Two Baseline (black) and Worn Teeth (red)



Comparison of Sound of Gearbox Two Baseline (black) and Worn Teeth (red)

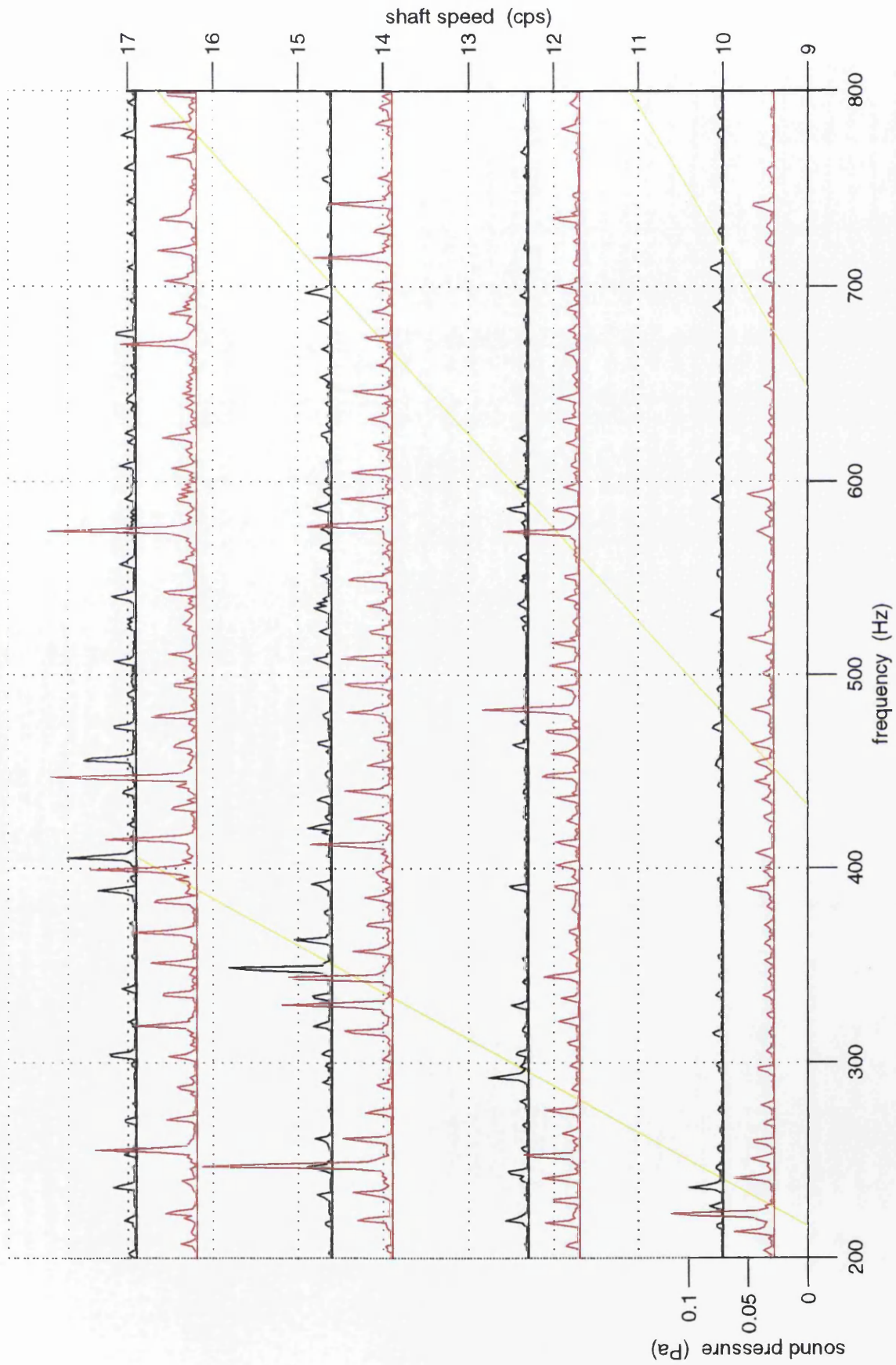


figure 25

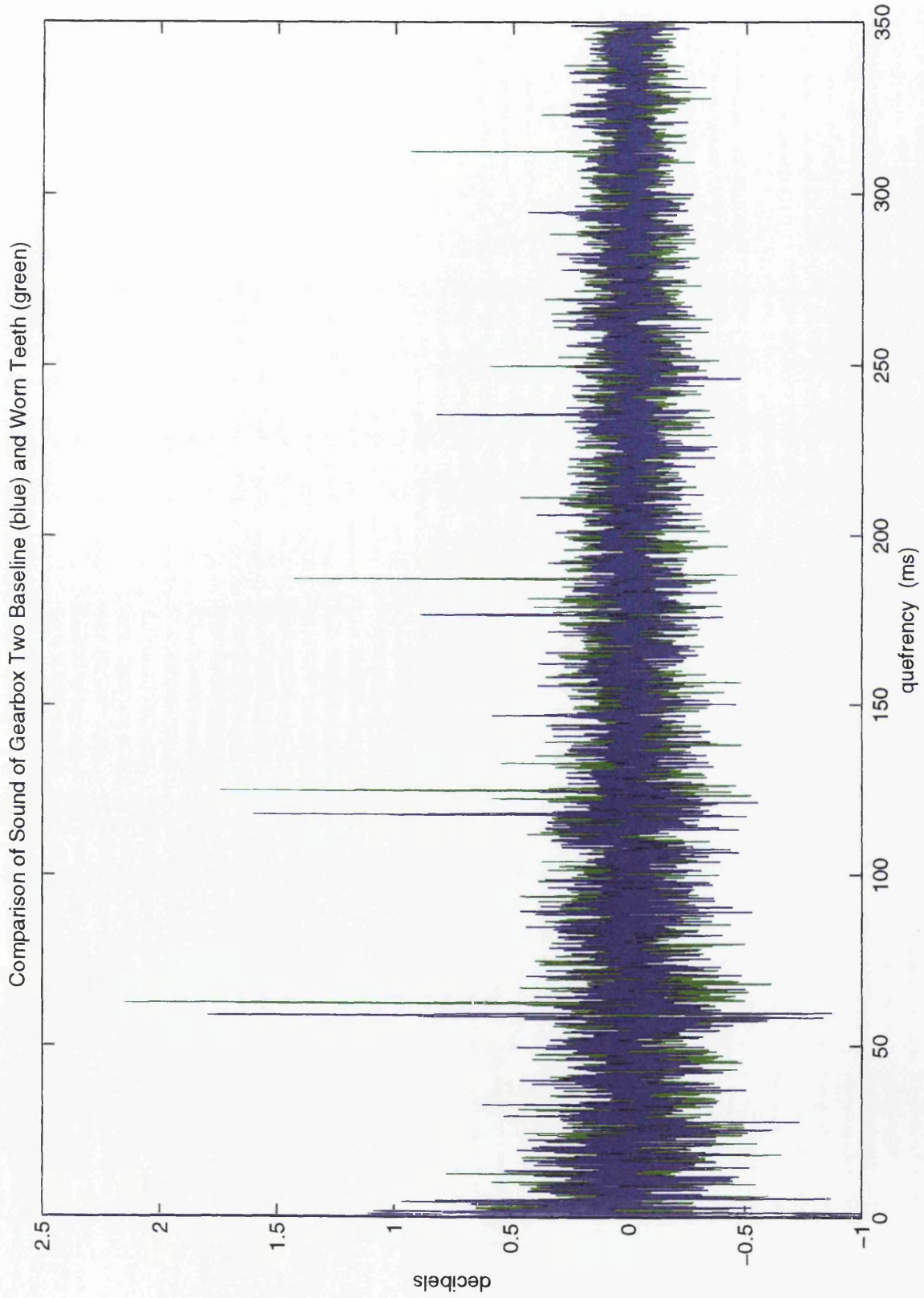


figure 26

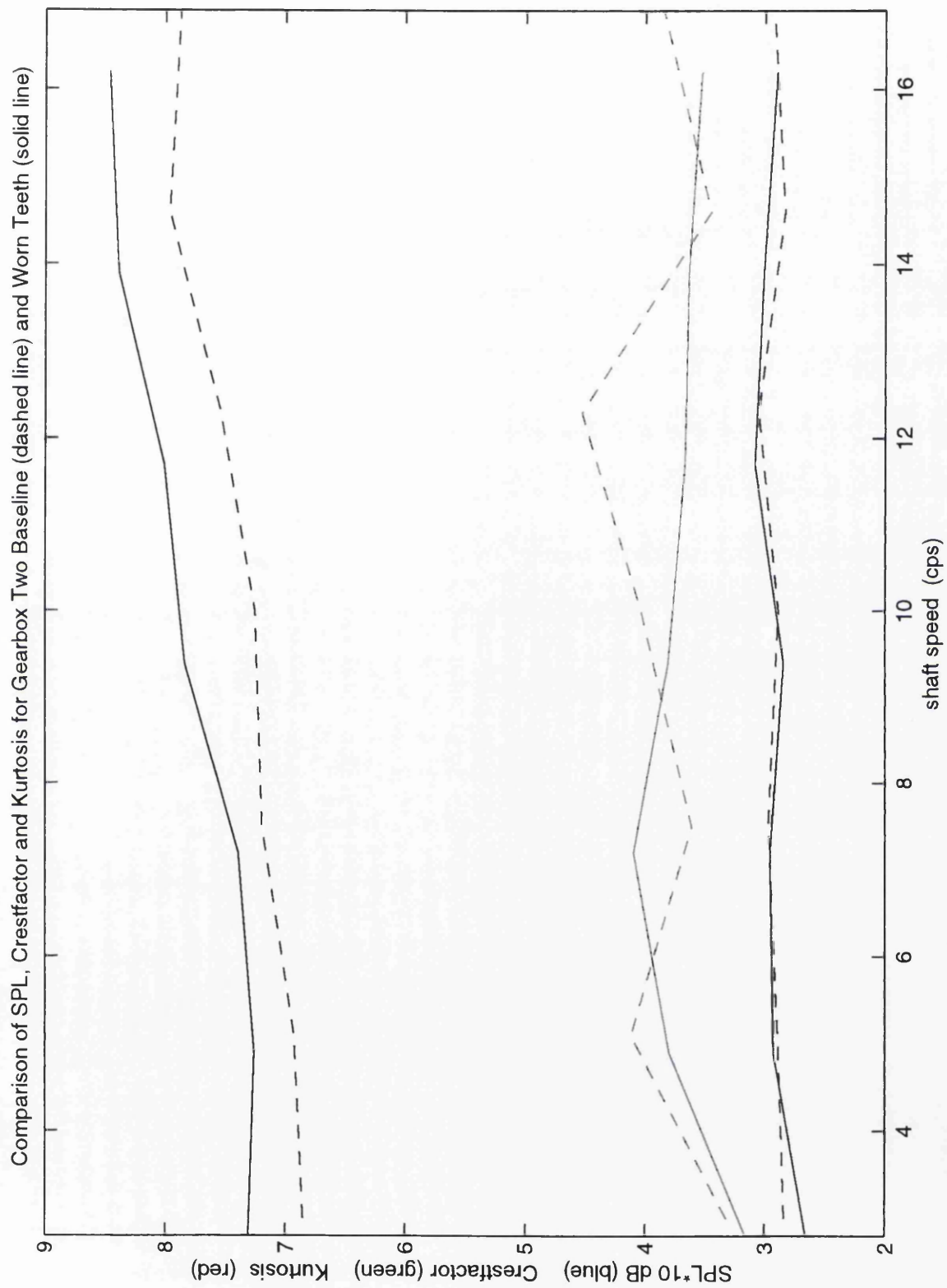
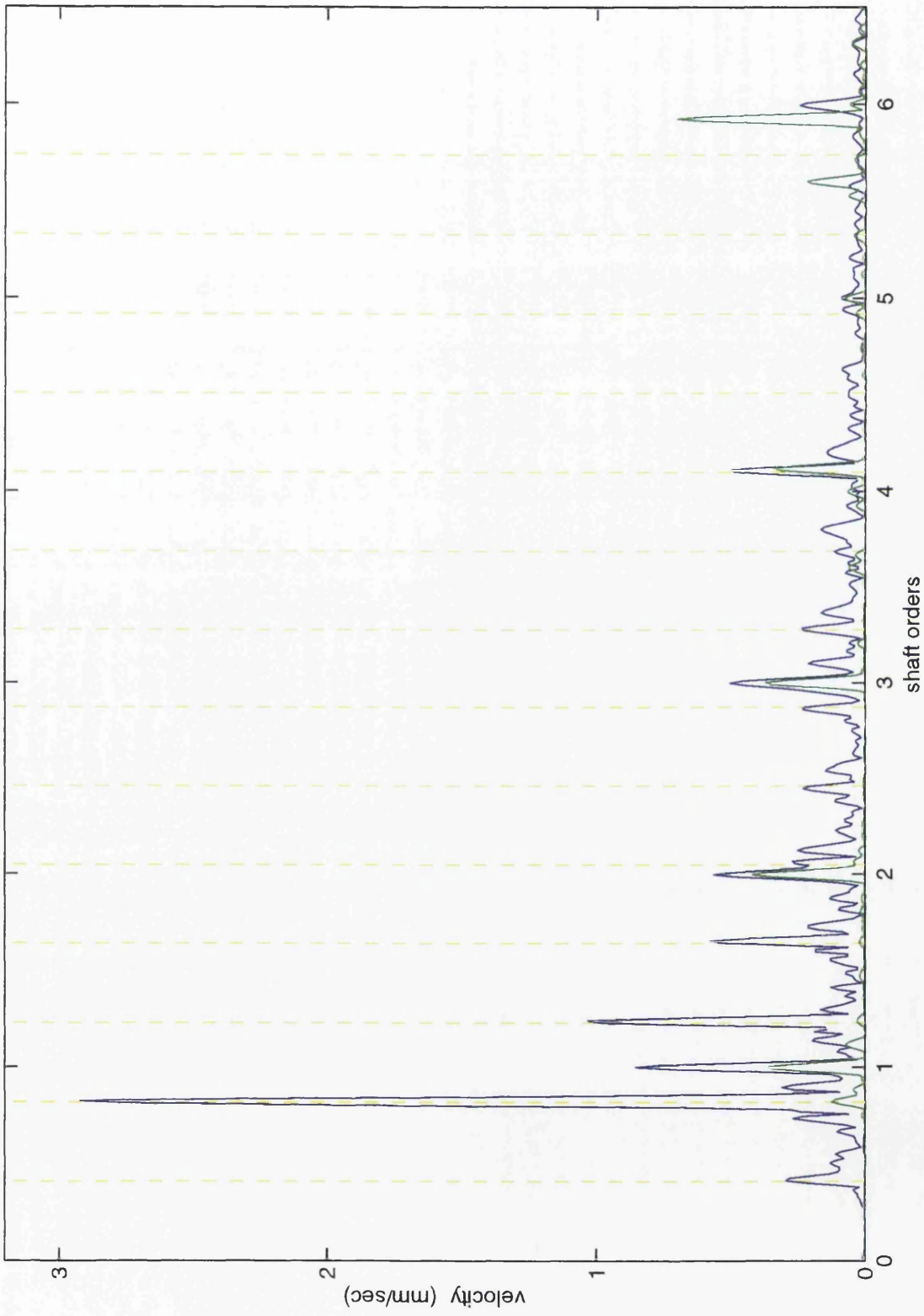


figure 27

Comparison of Vibration of Gearbox Three Baseline (green) and Cage Fault (blue)





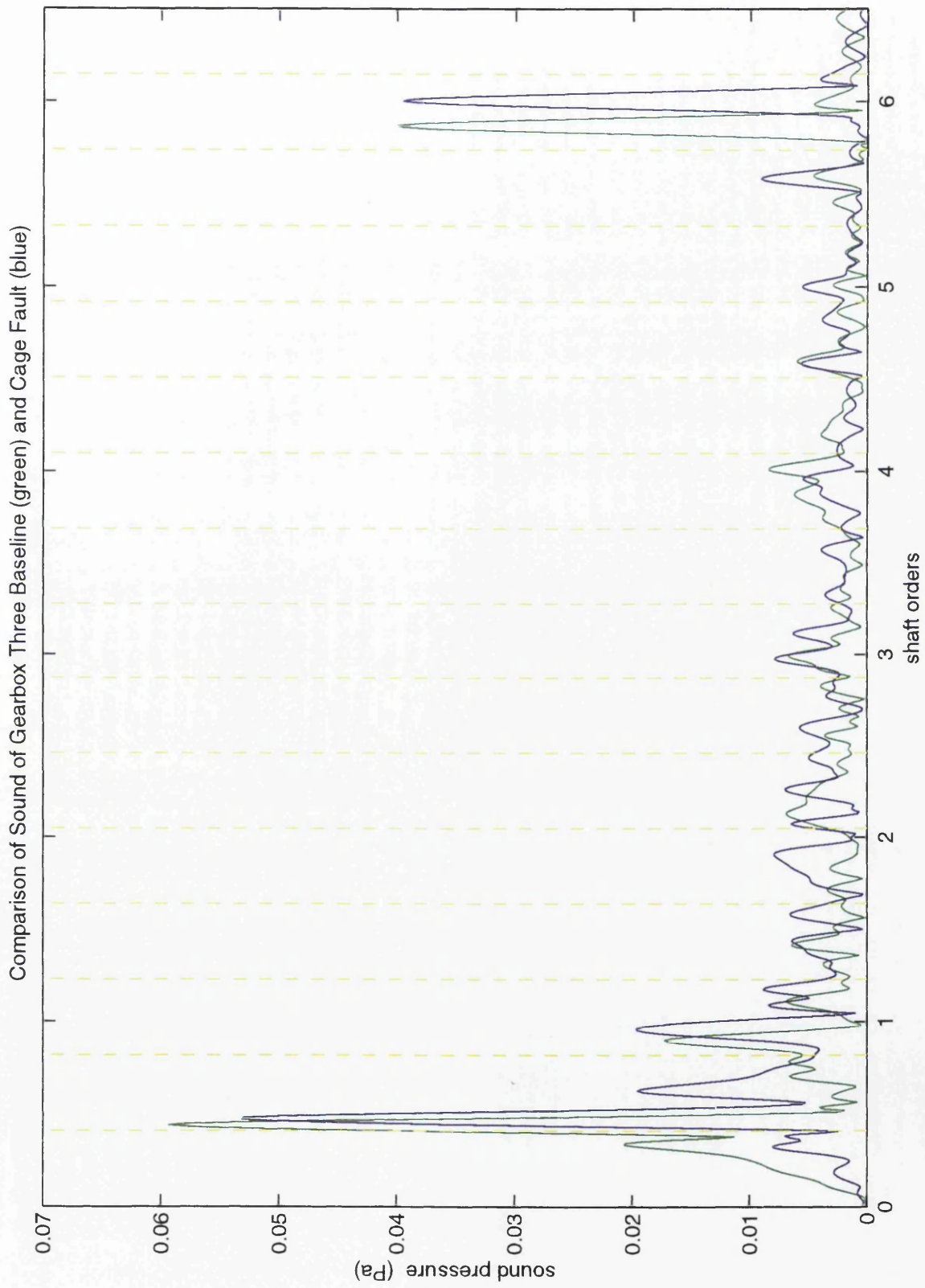


figure 29

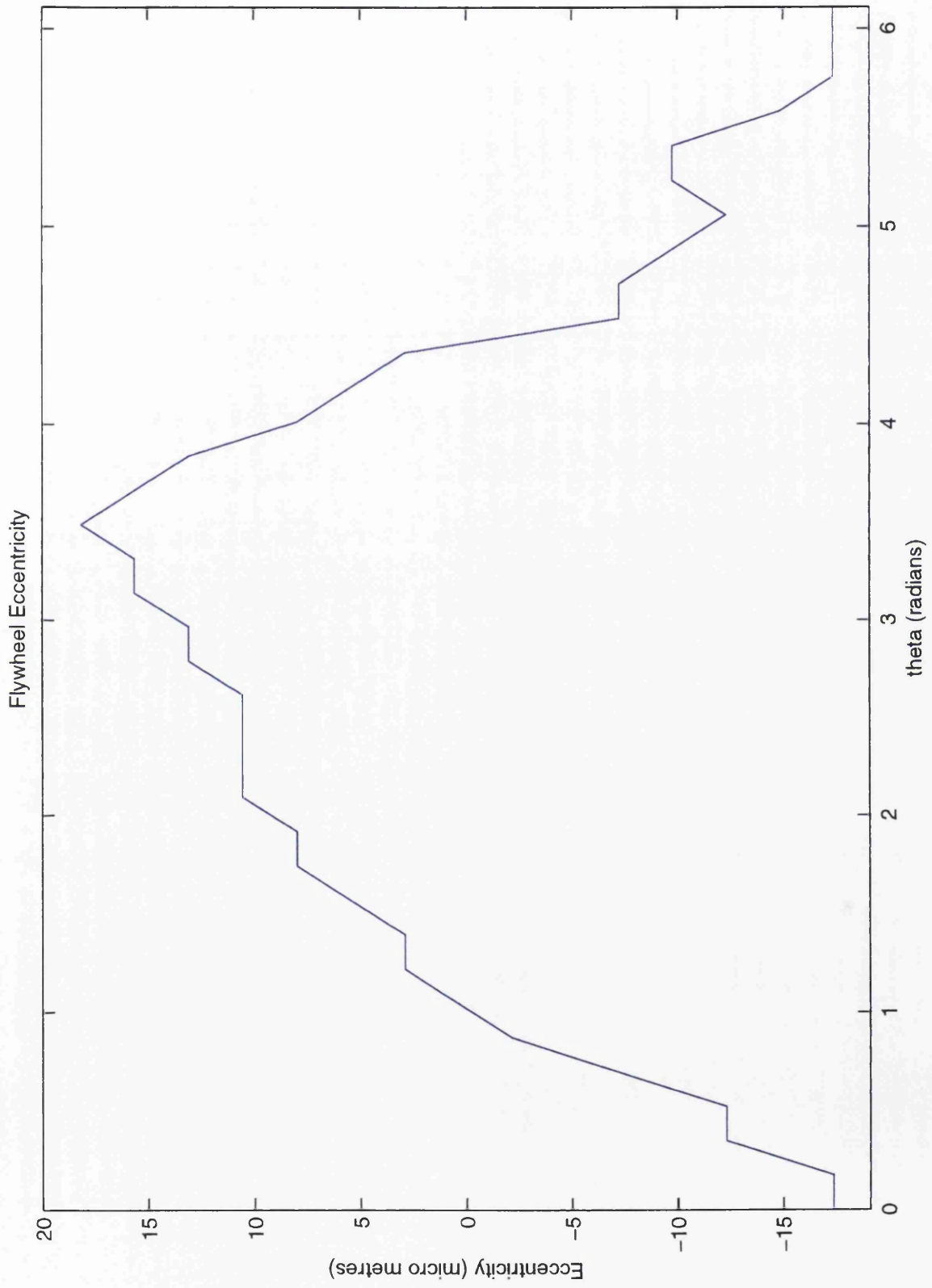
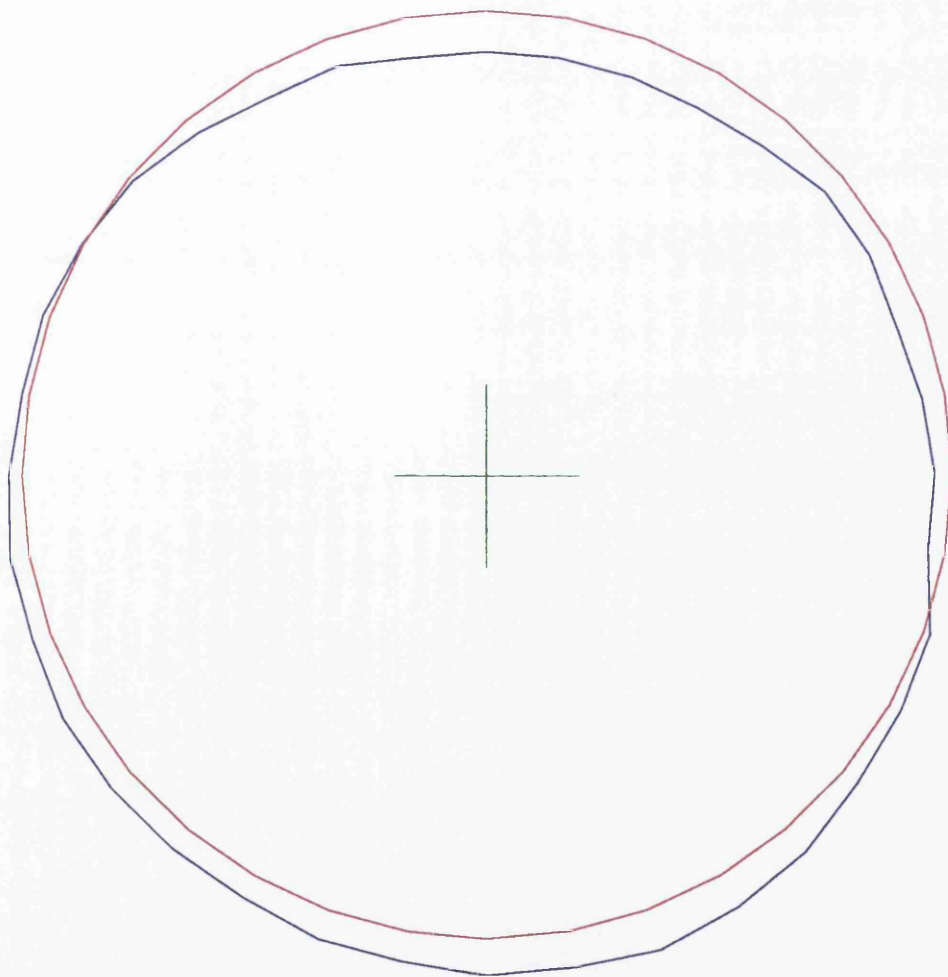


figure 30

Representation of Flywheel Eccentricity



*figure 31*

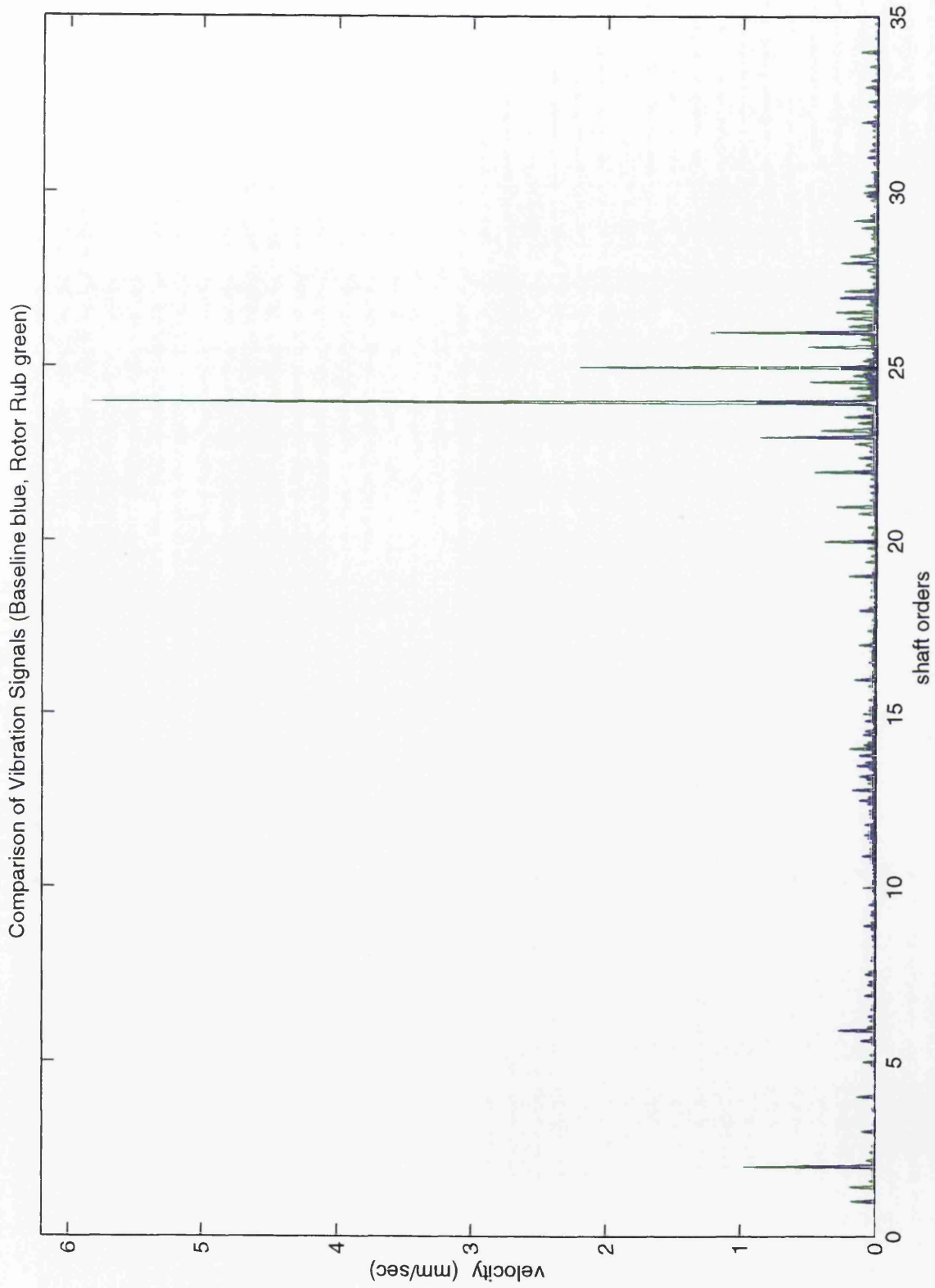


figure 32

Spectrogram View of Vibration Generated By Partial Rotor Rub

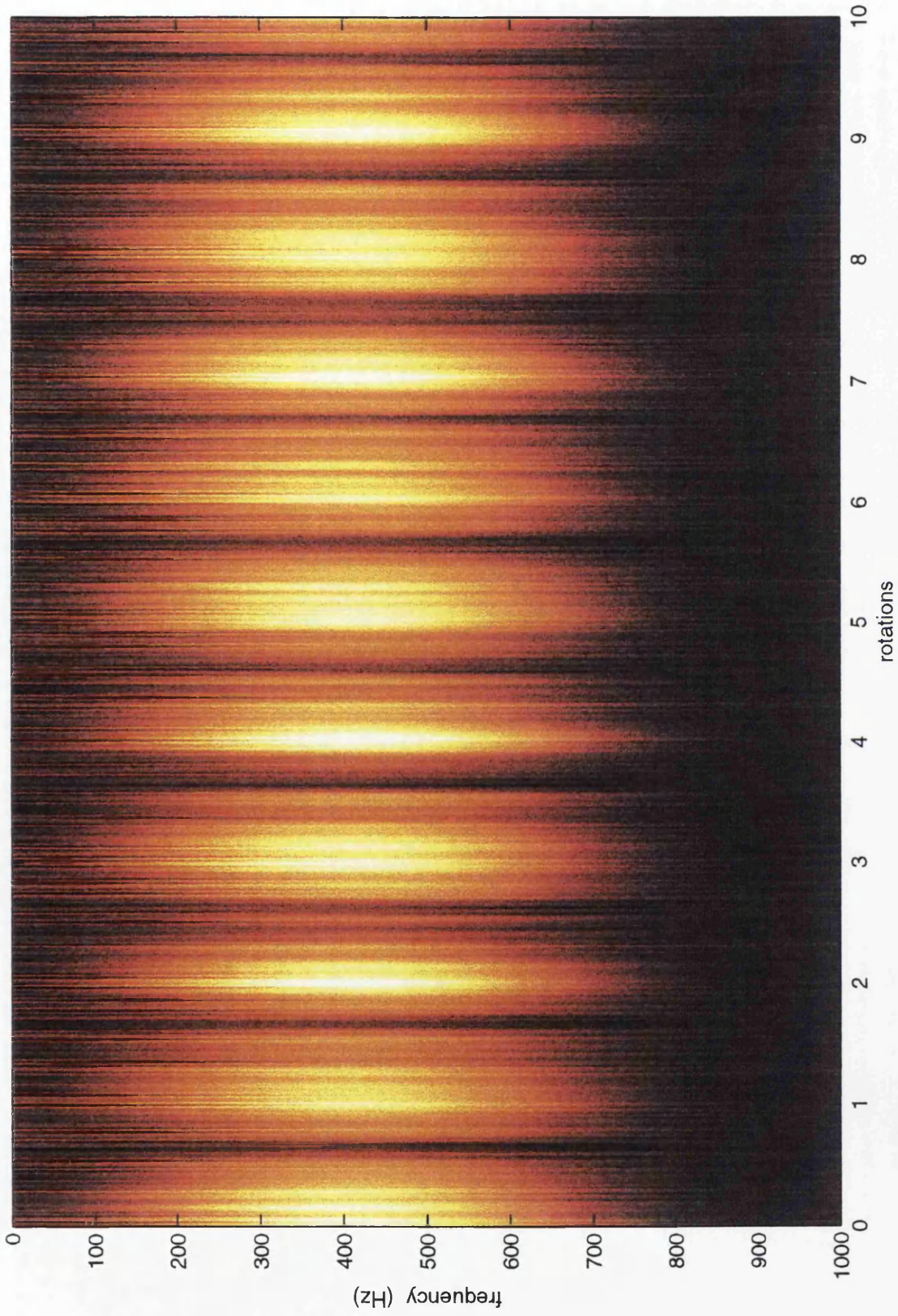


figure 33

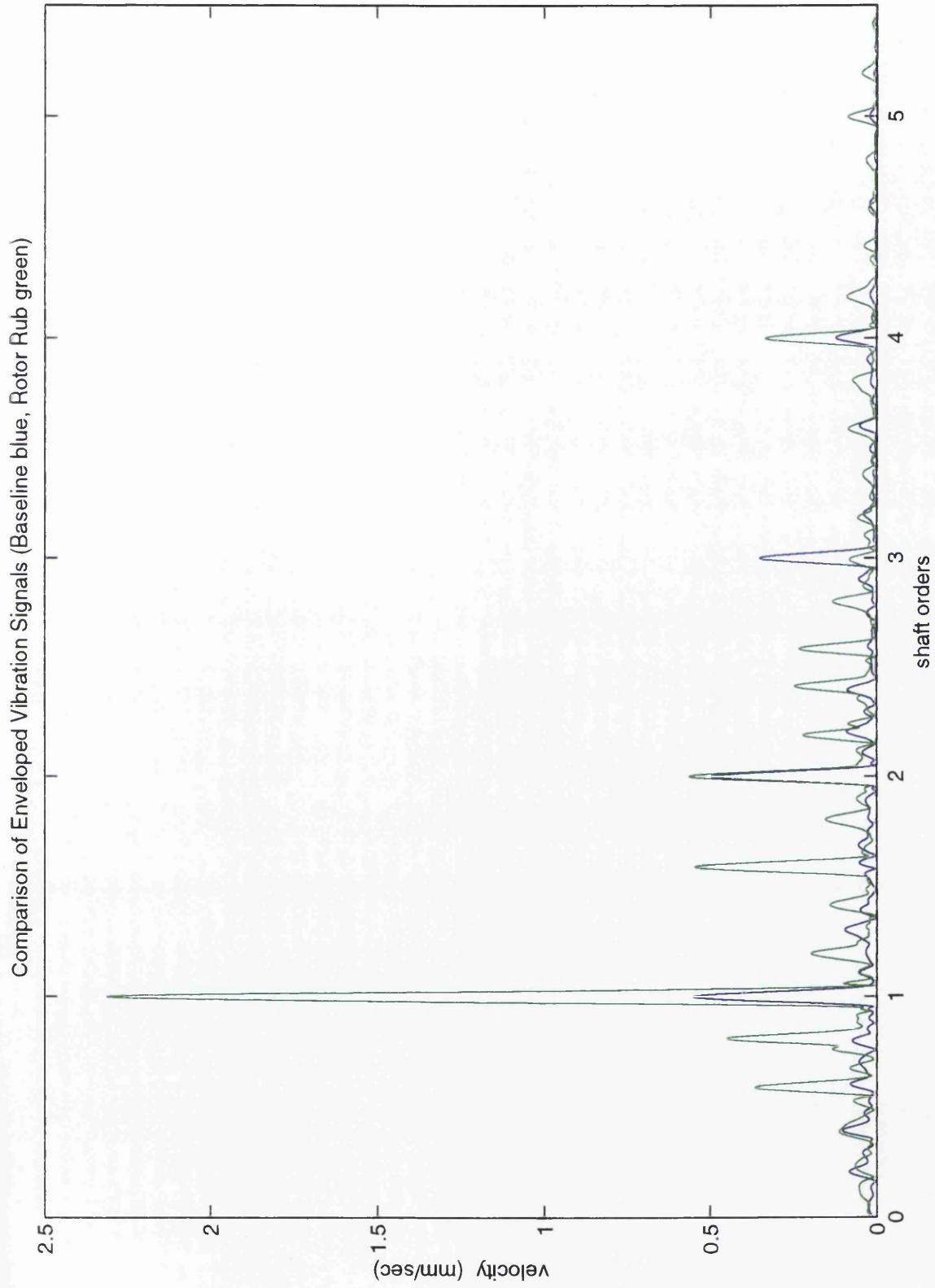


figure 34

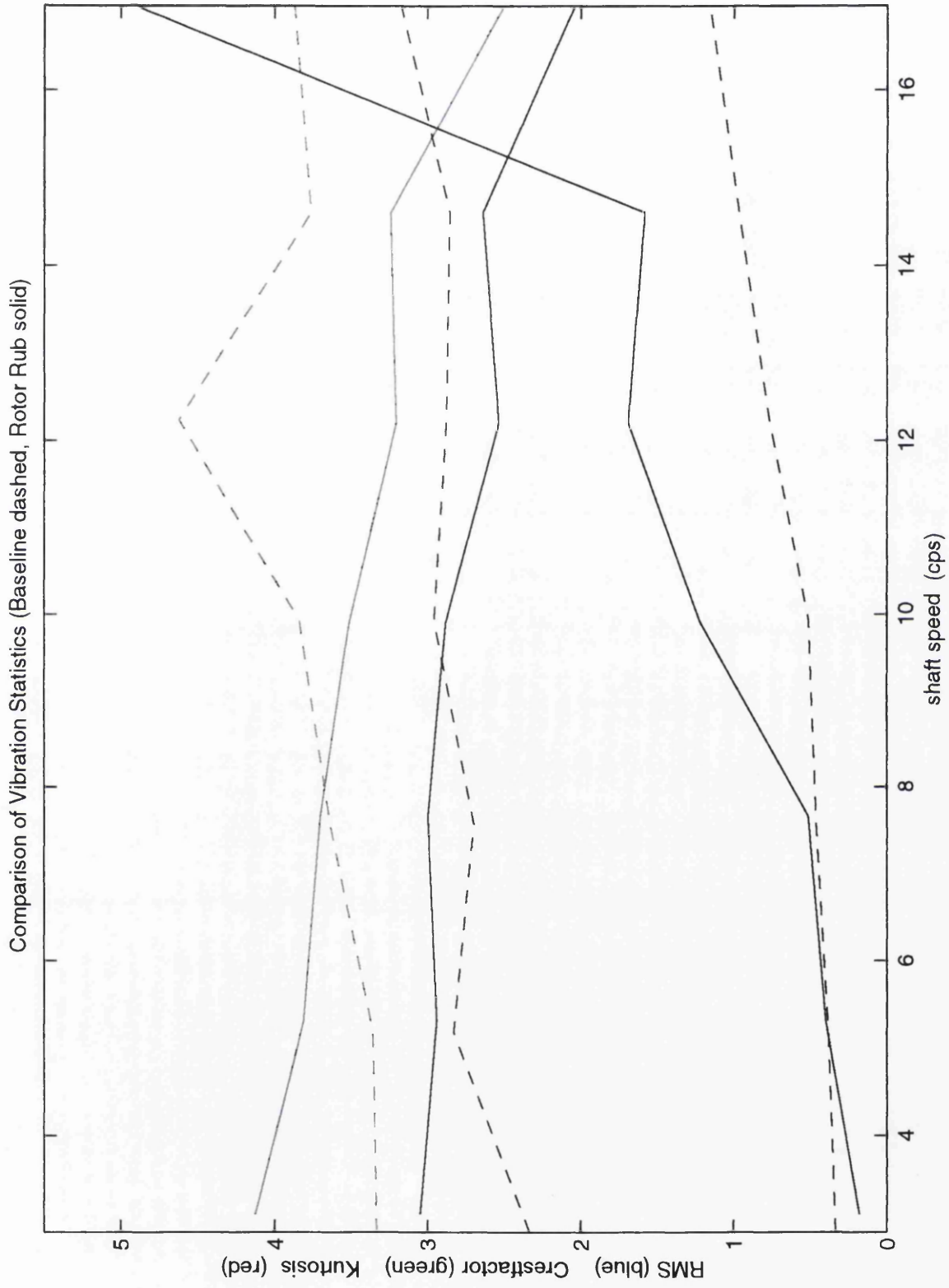


figure 35

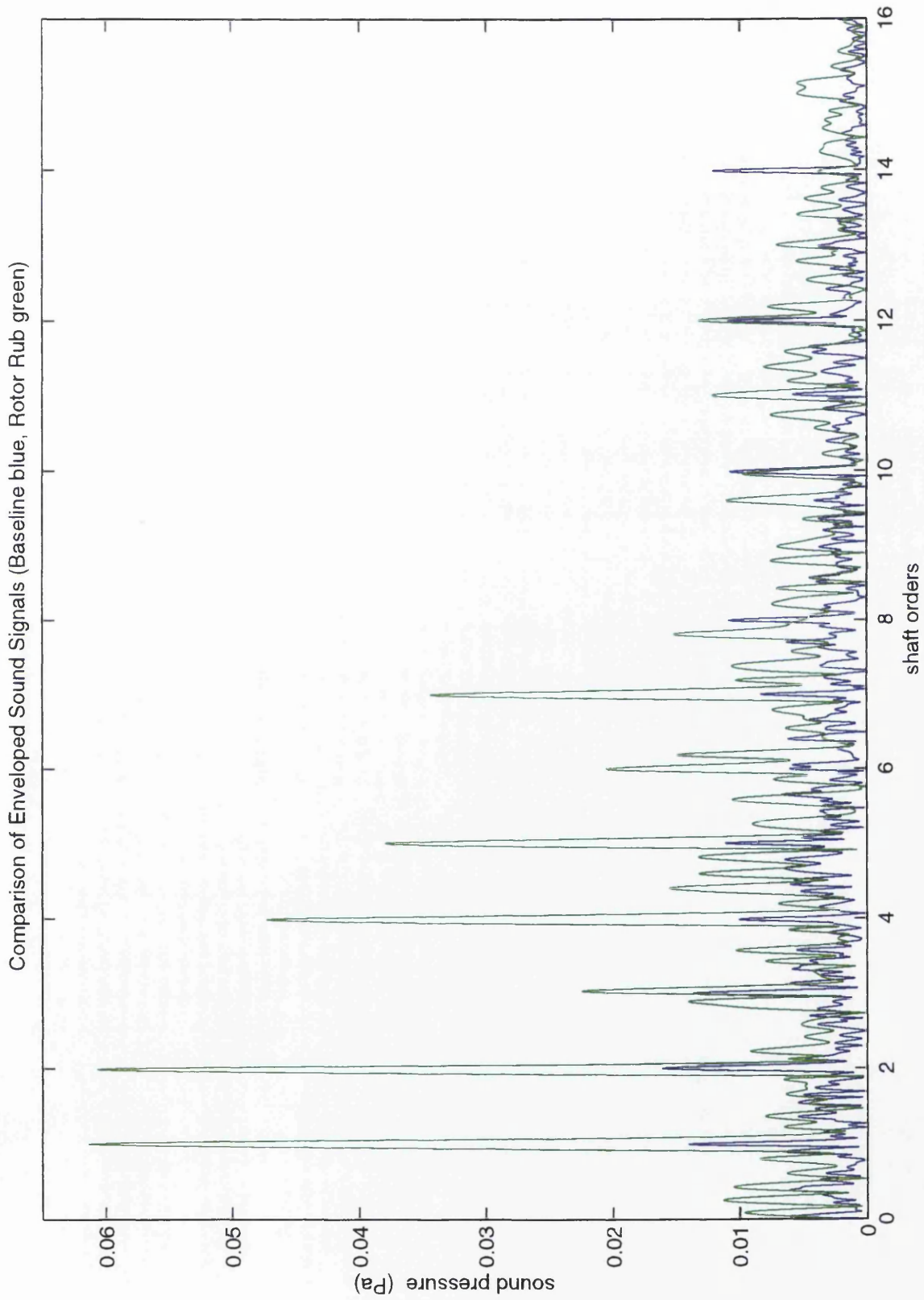


figure 36





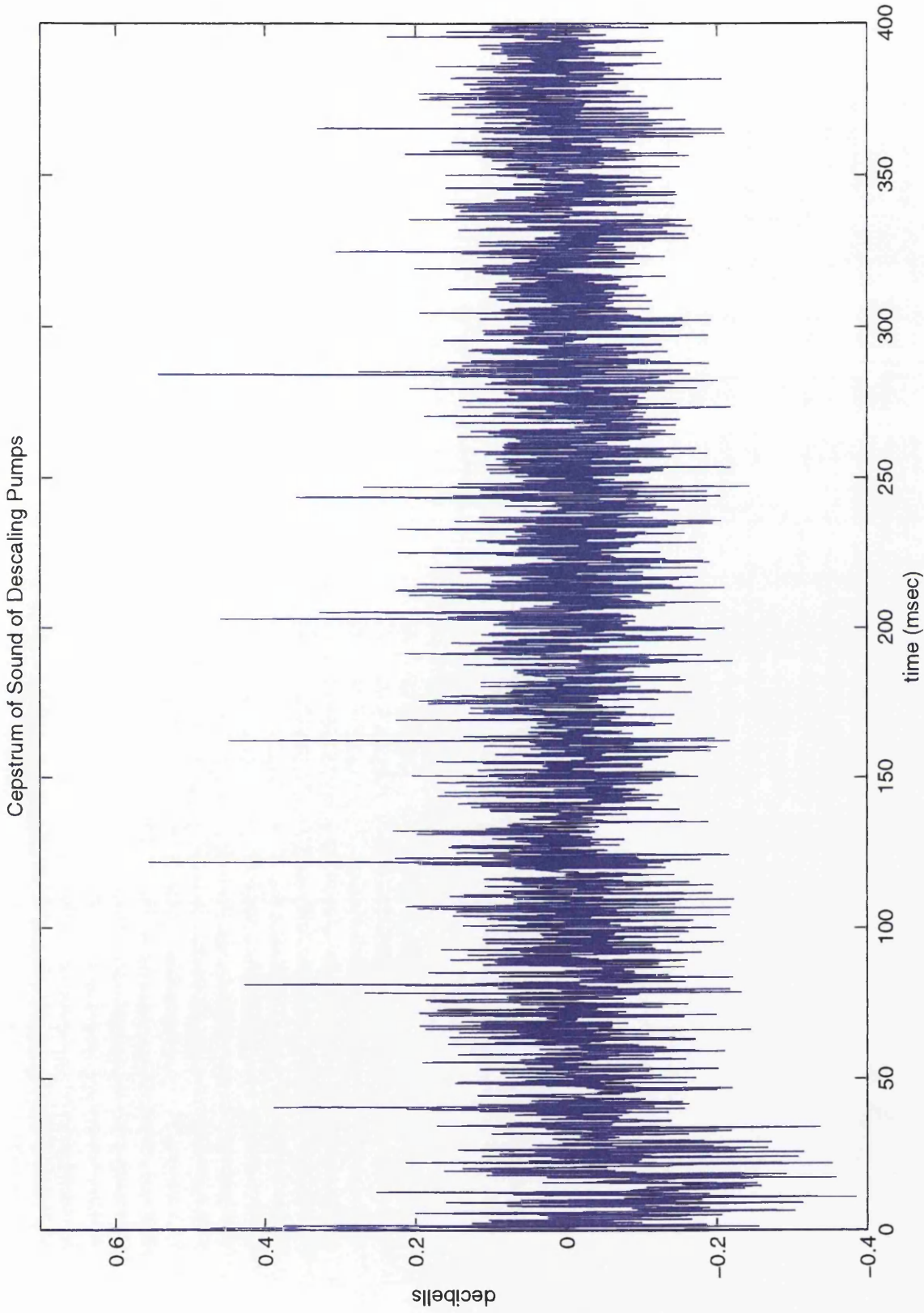


figure 37

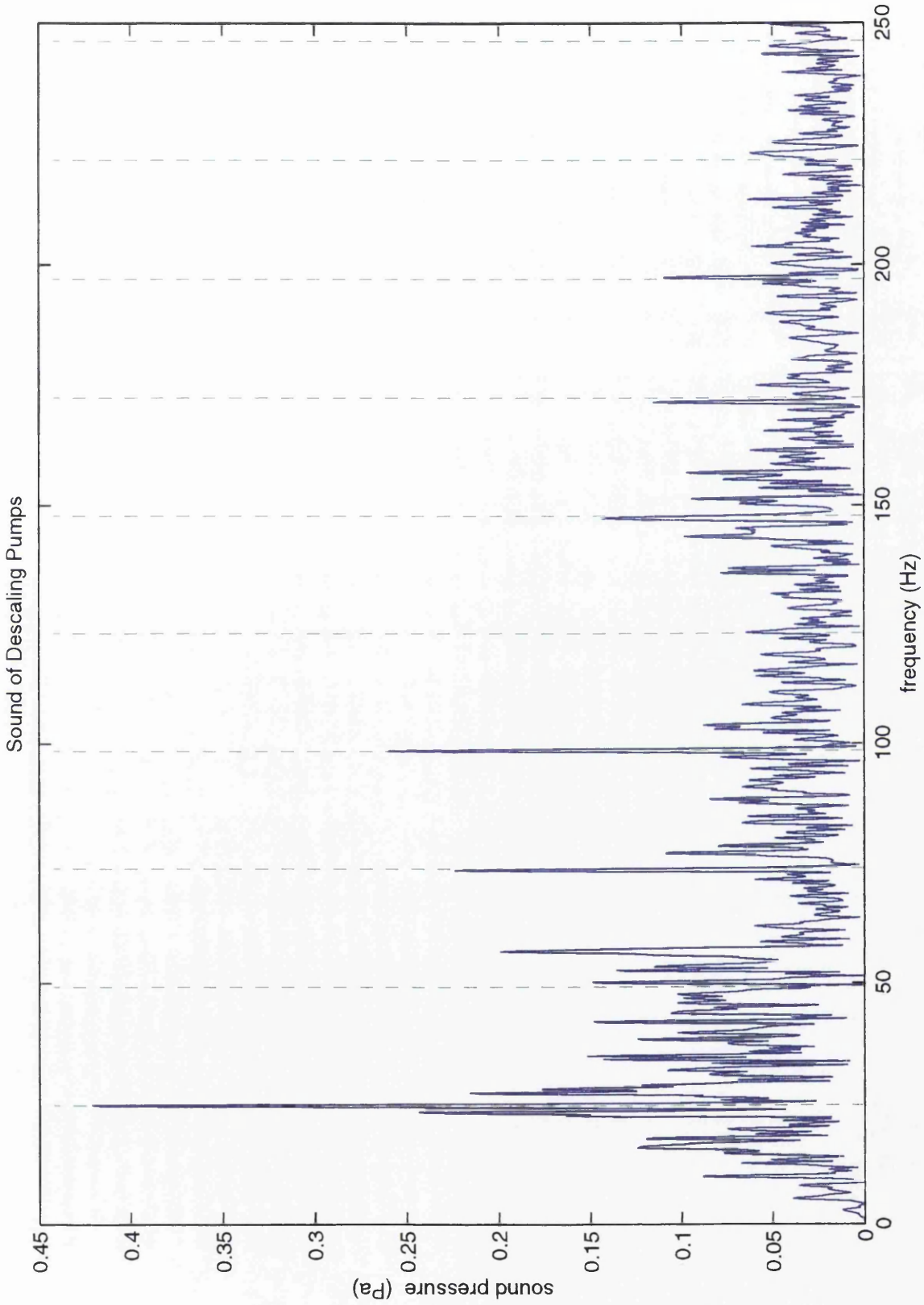


figure 38

Sound of Descaling Pumps With TPF and Second Harmonic Indicated

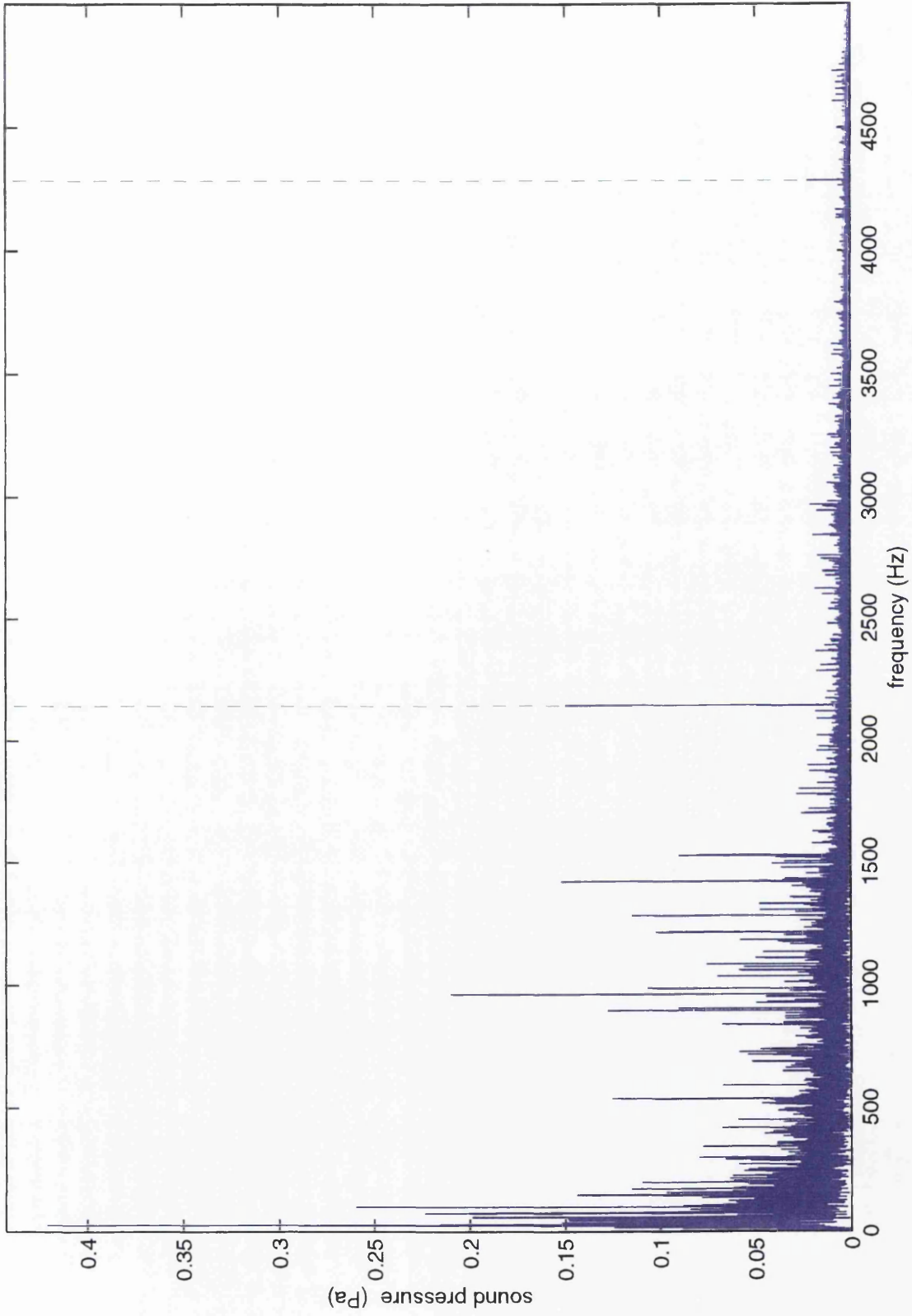


figure 39

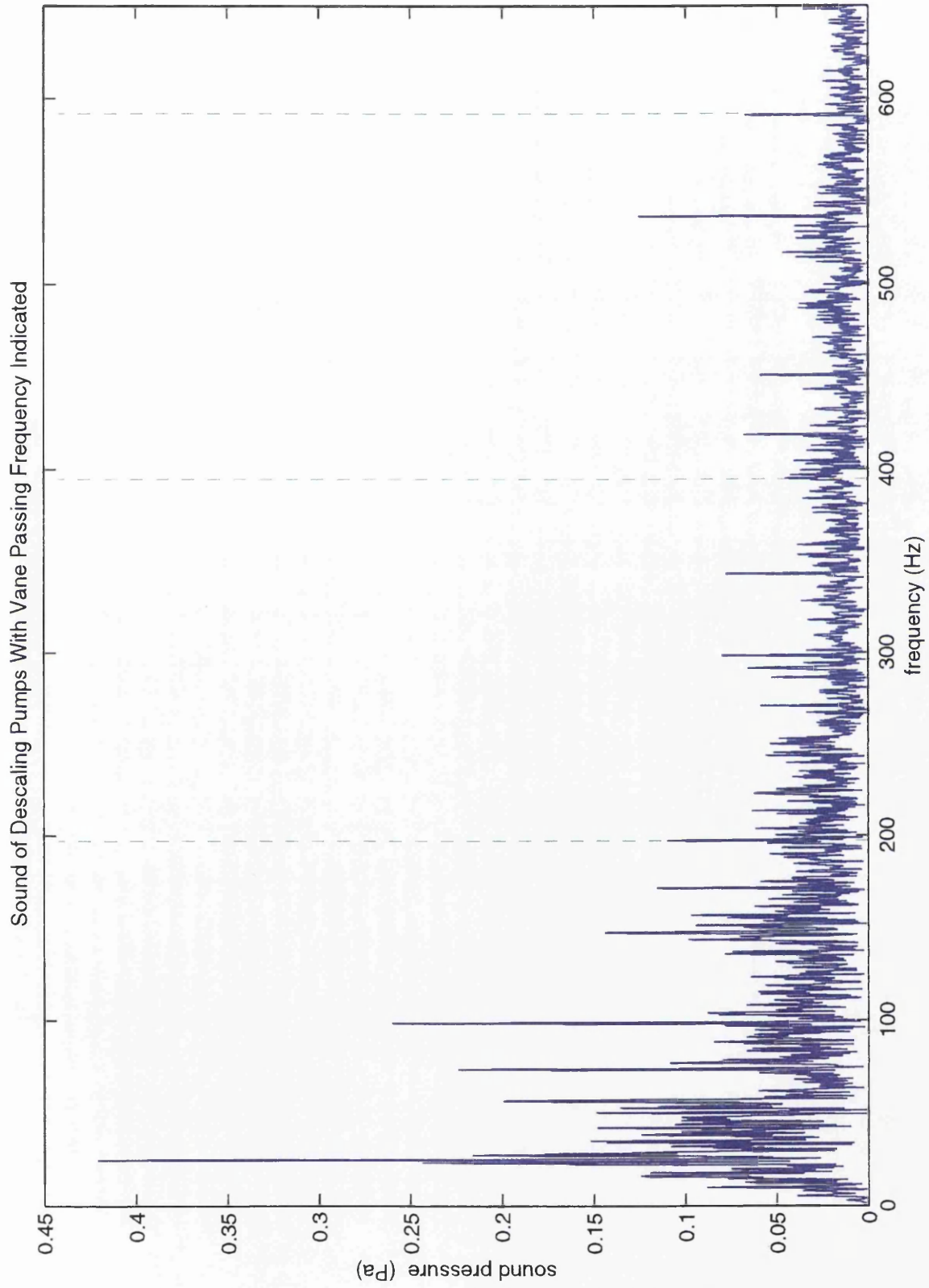


figure 40

FFT of Descaling Pump Sound With Cage Defect Frequency Indicated

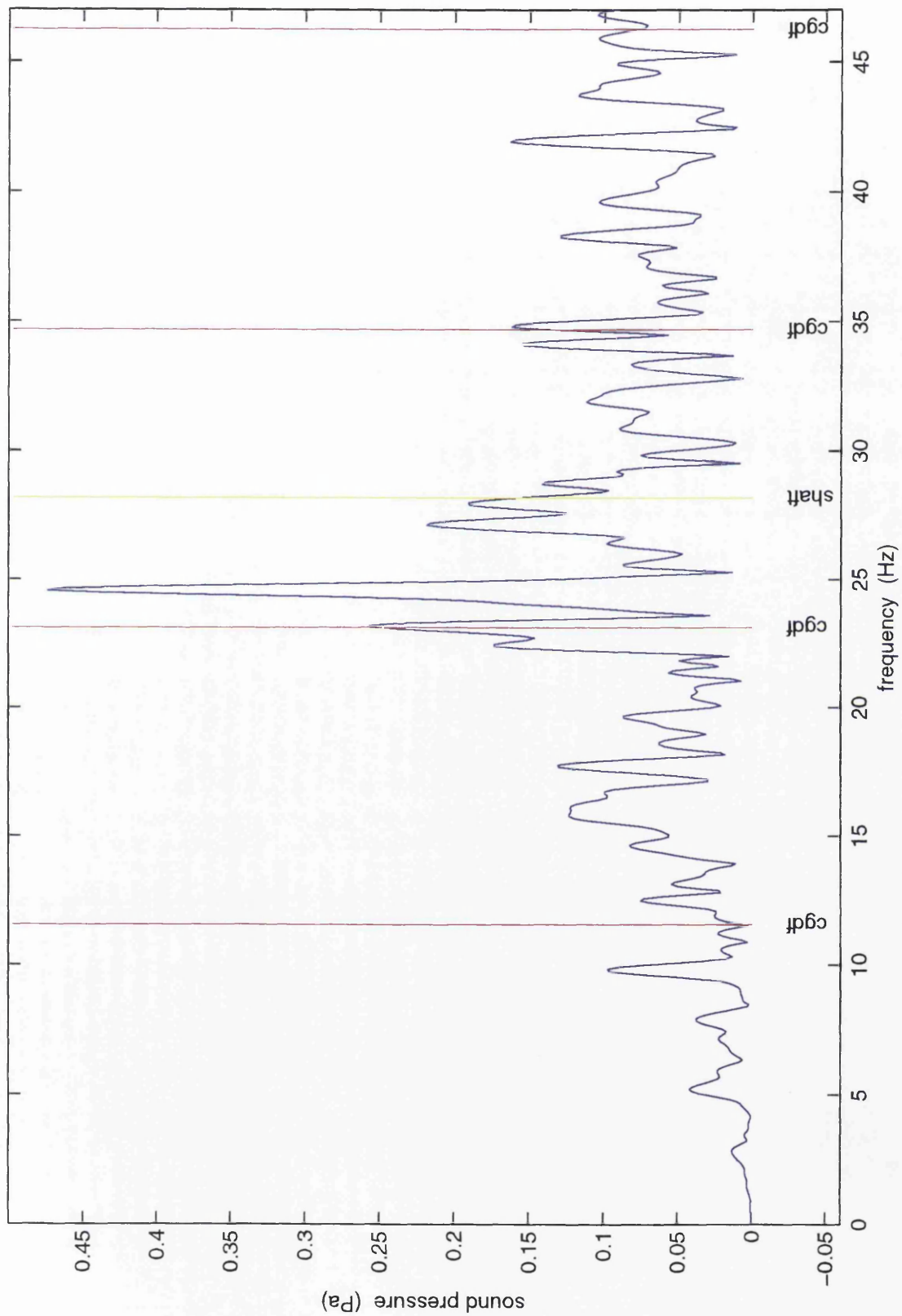
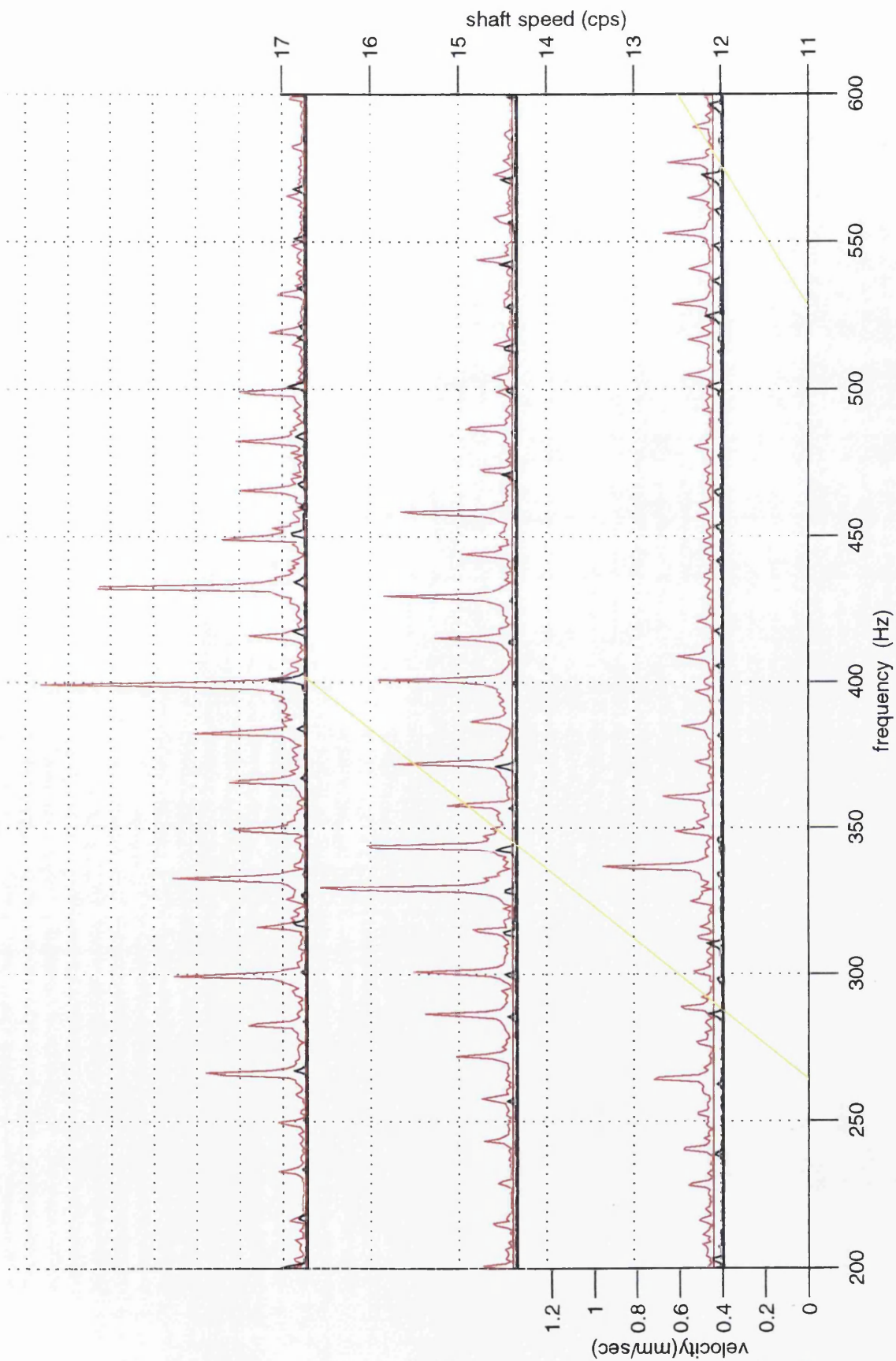


figure 41

Comparison of Vibration of Gearbox Five Baseline (black) and Broken Tooth (red): Vertical



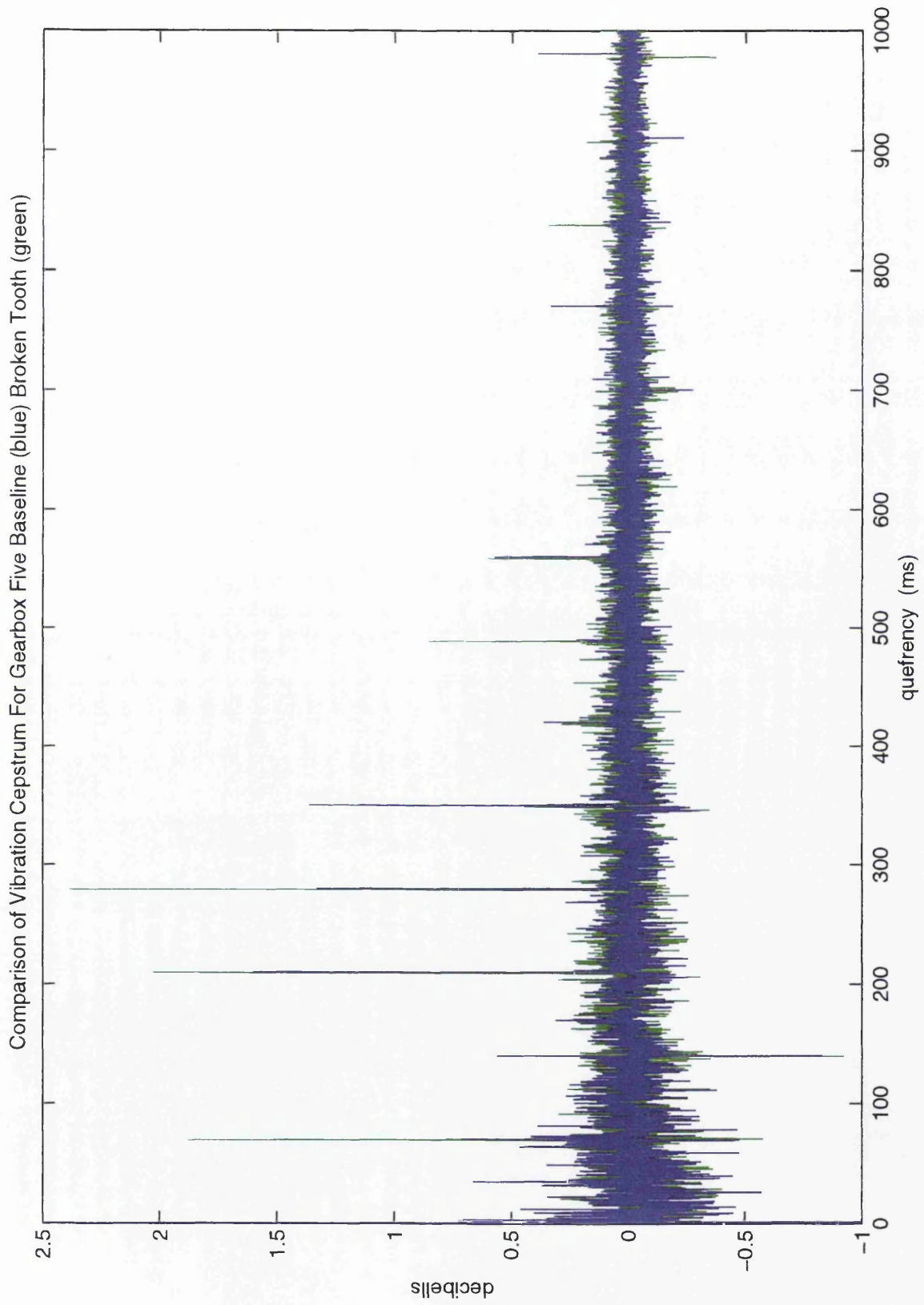


figure 43

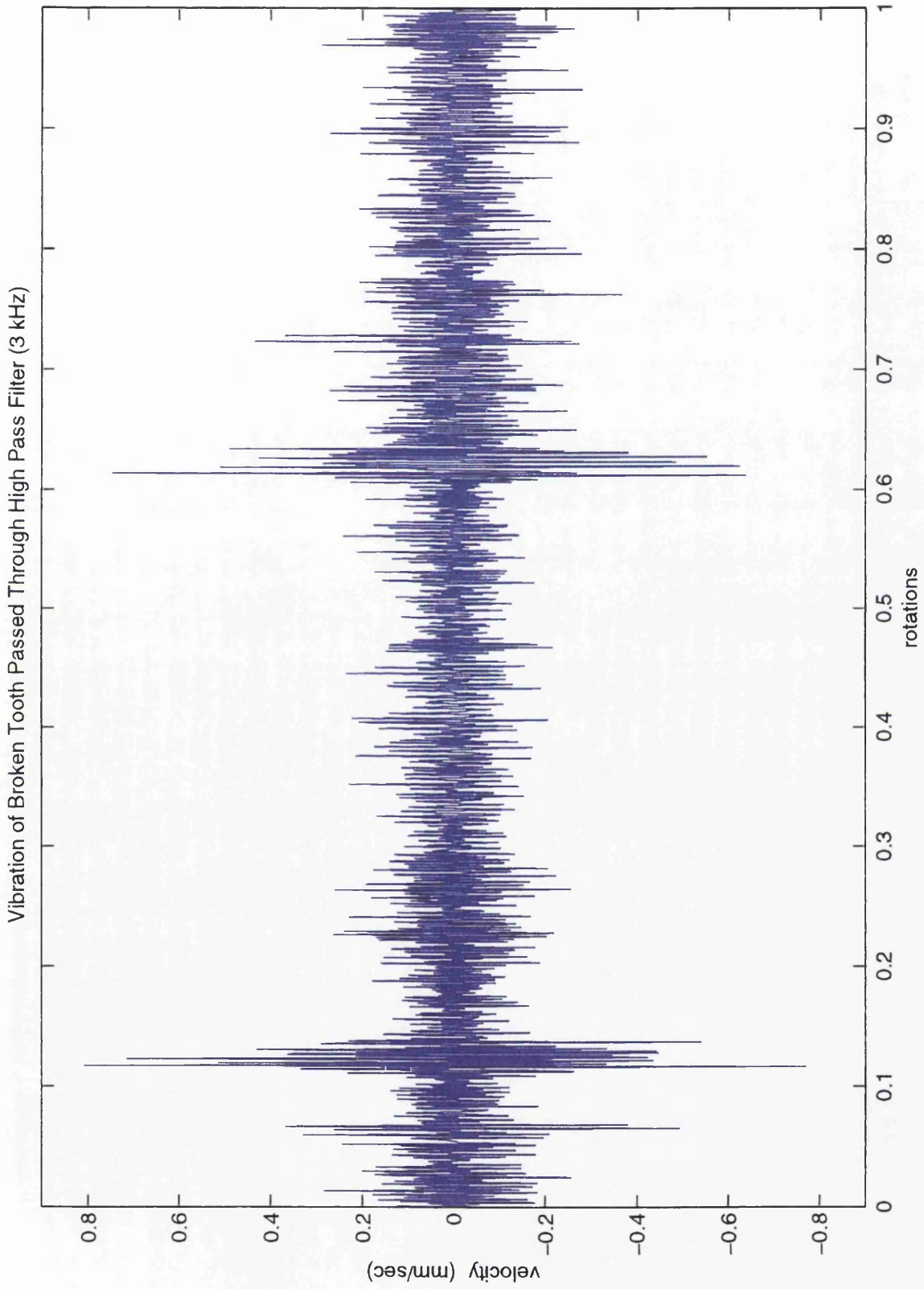


figure 44



Spectrogram View of Vibration of Broken Tooth

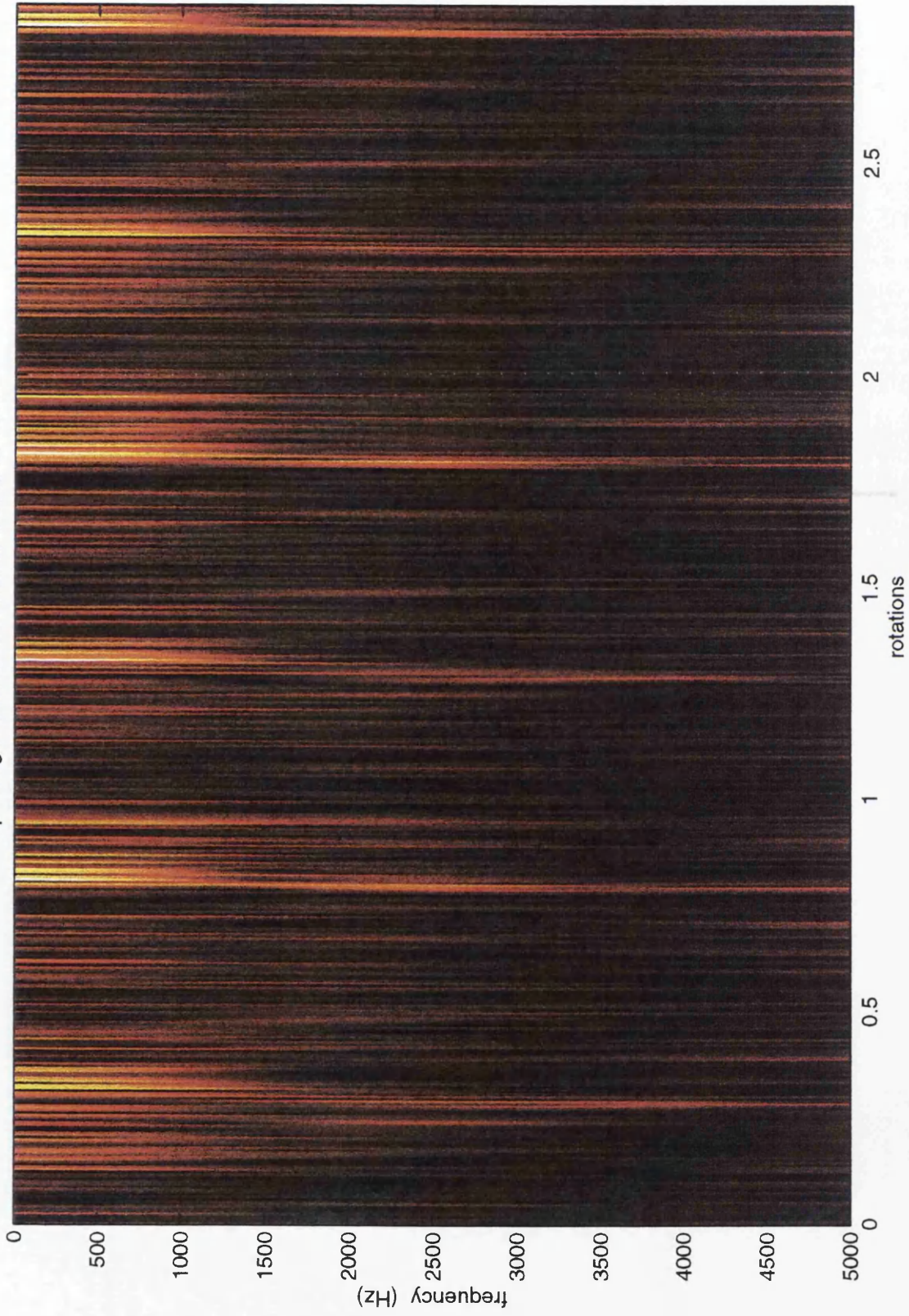


figure 45

Spectrogram View of TSA Vibration of Broken Tooth

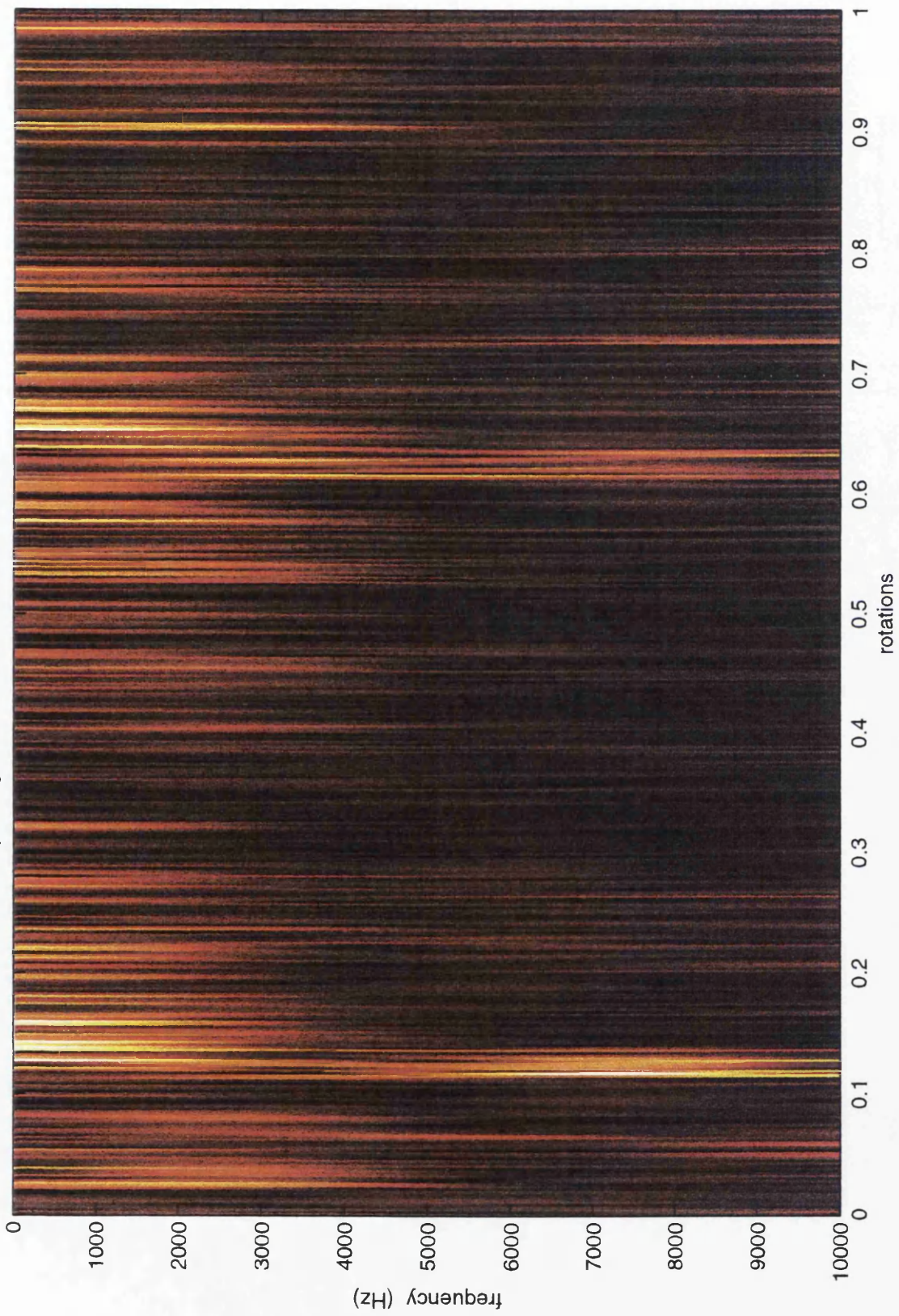


figure 46

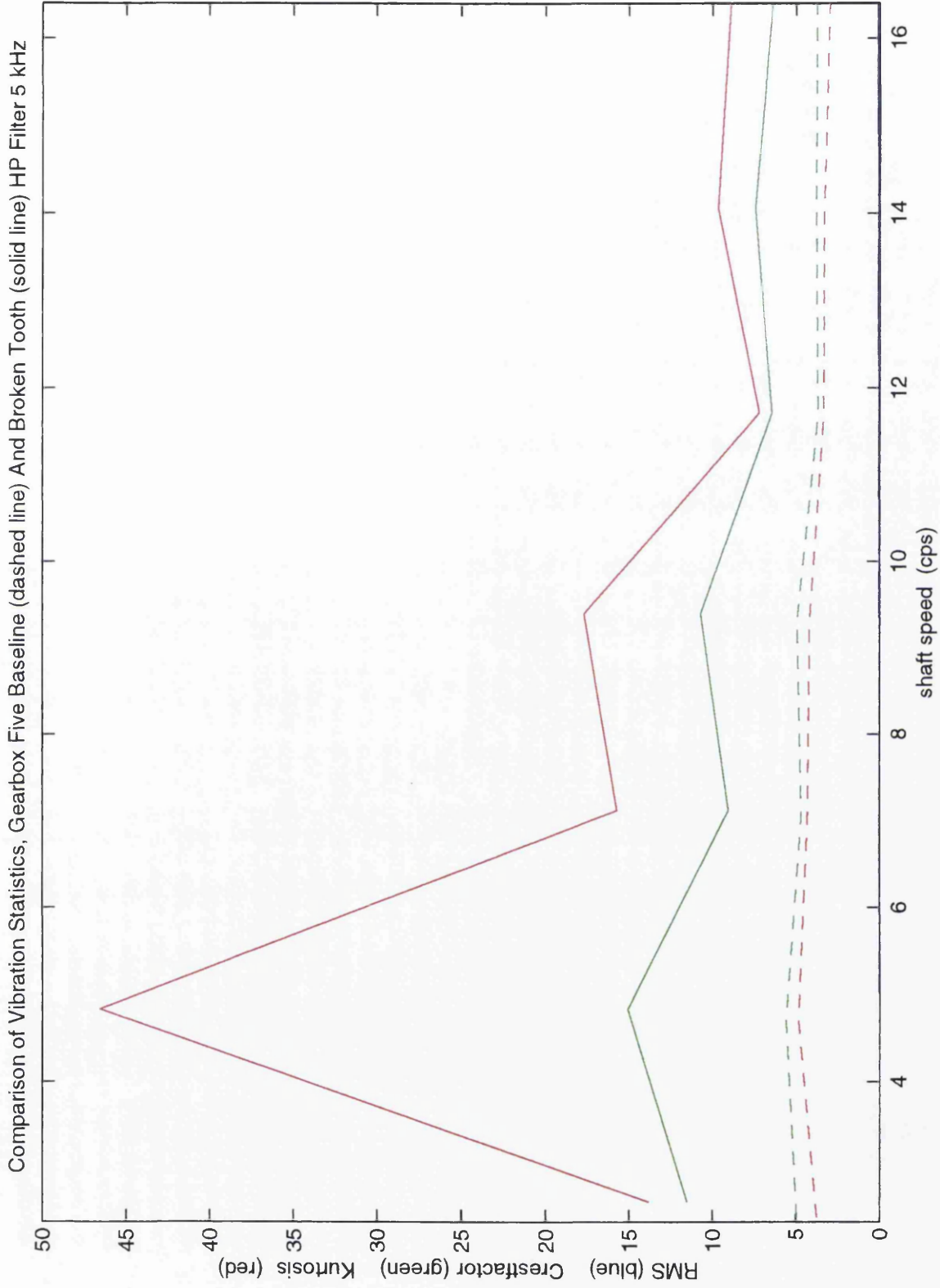


figure 47

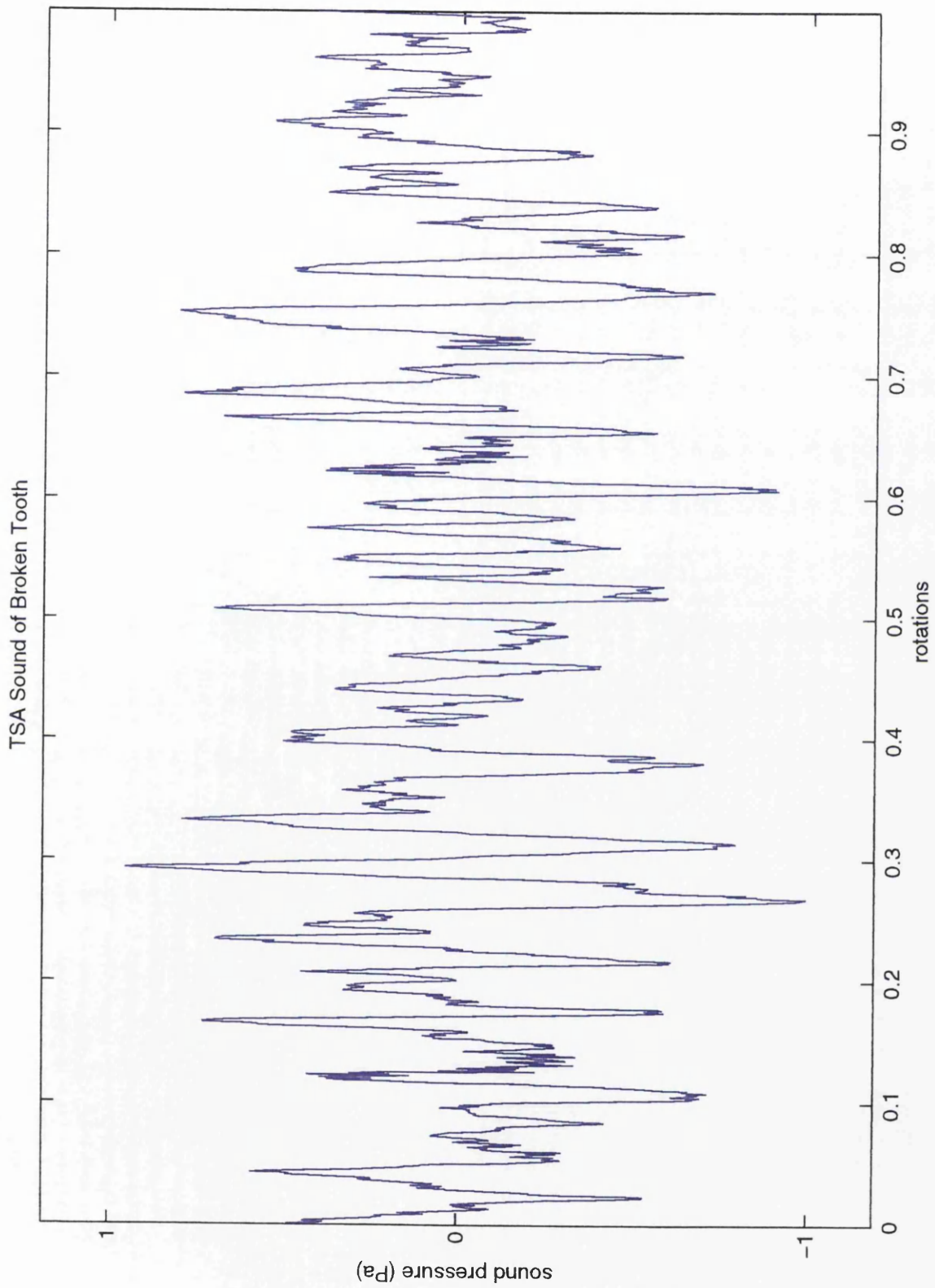


figure 48

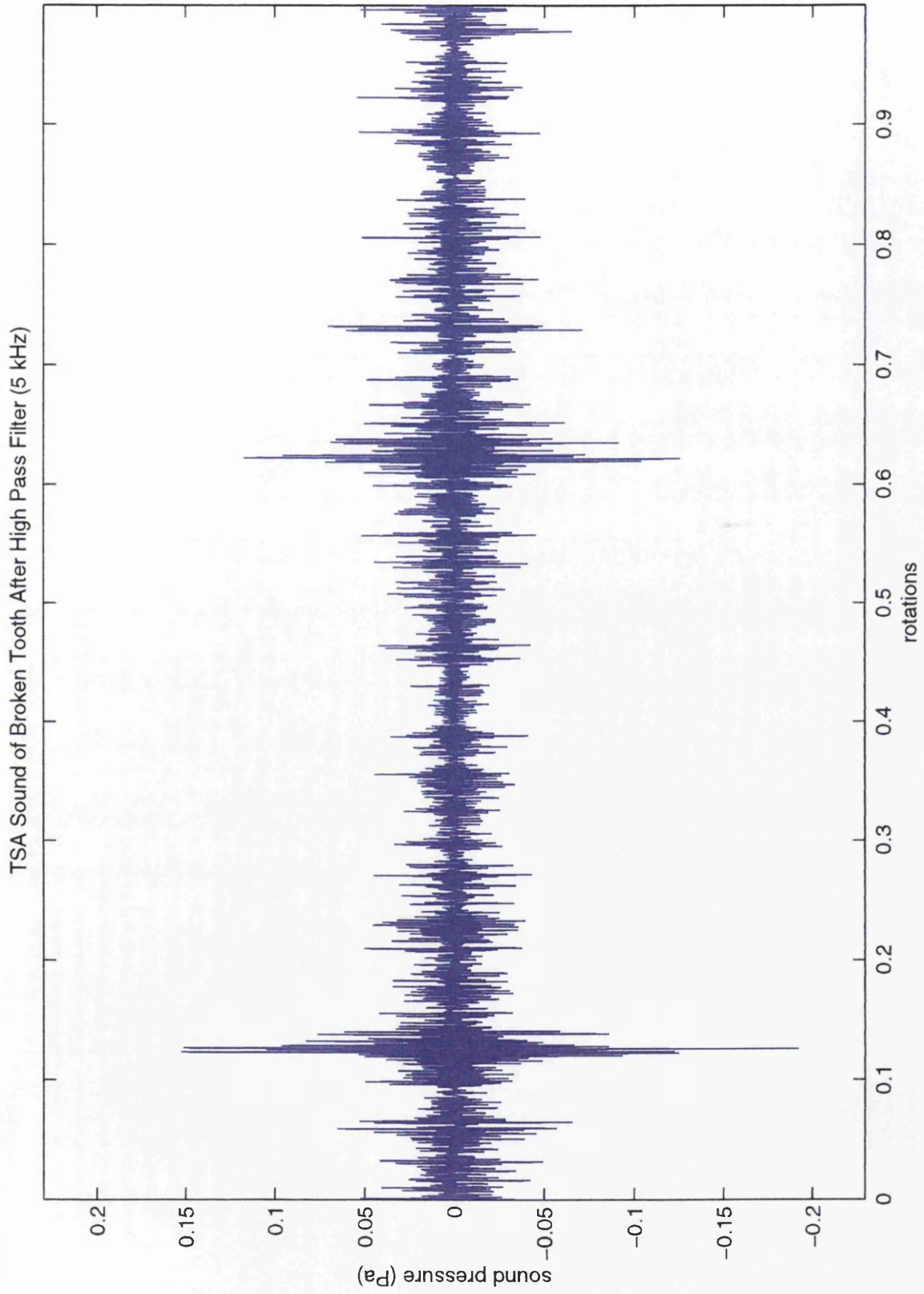


figure 49

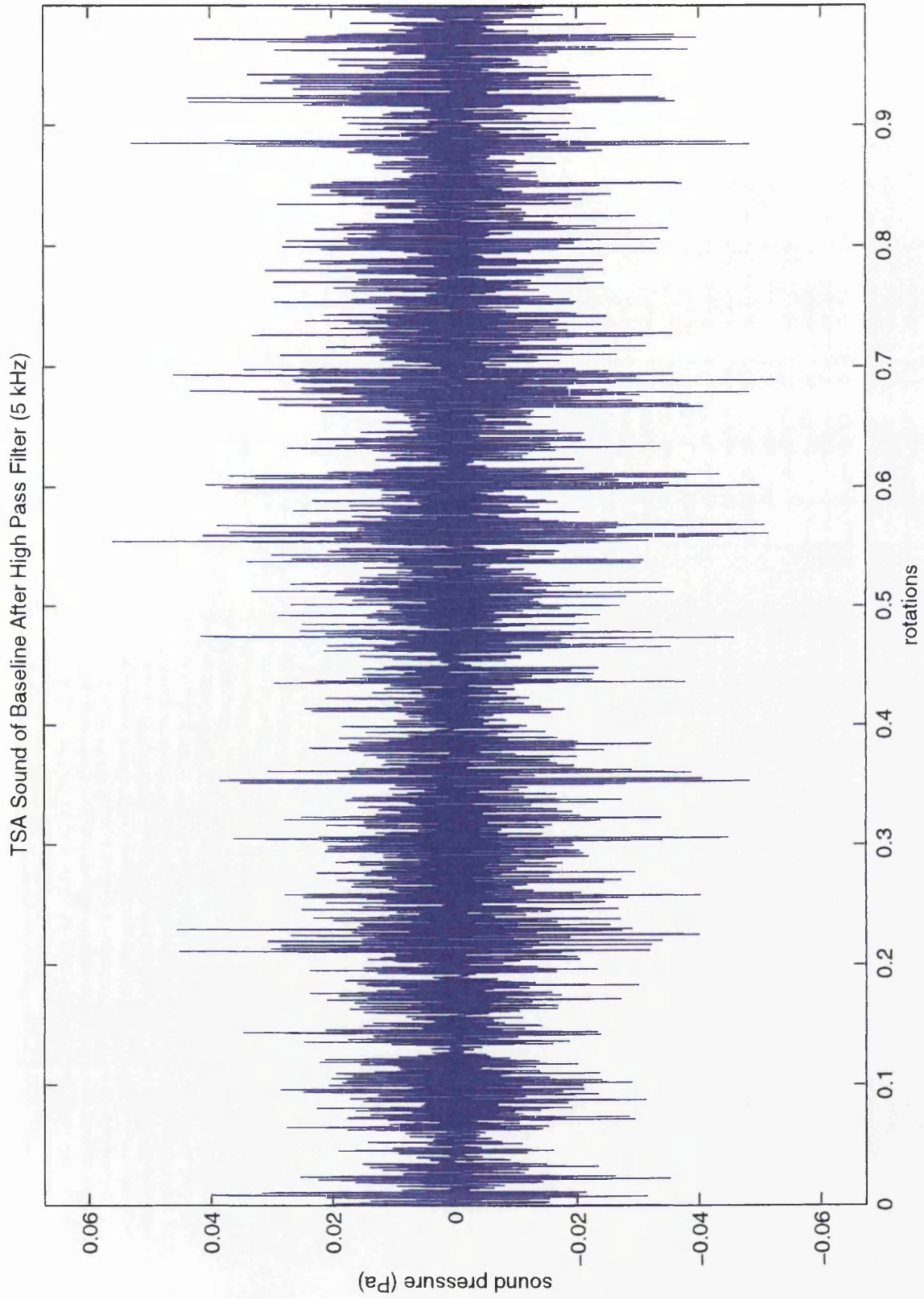


figure 50

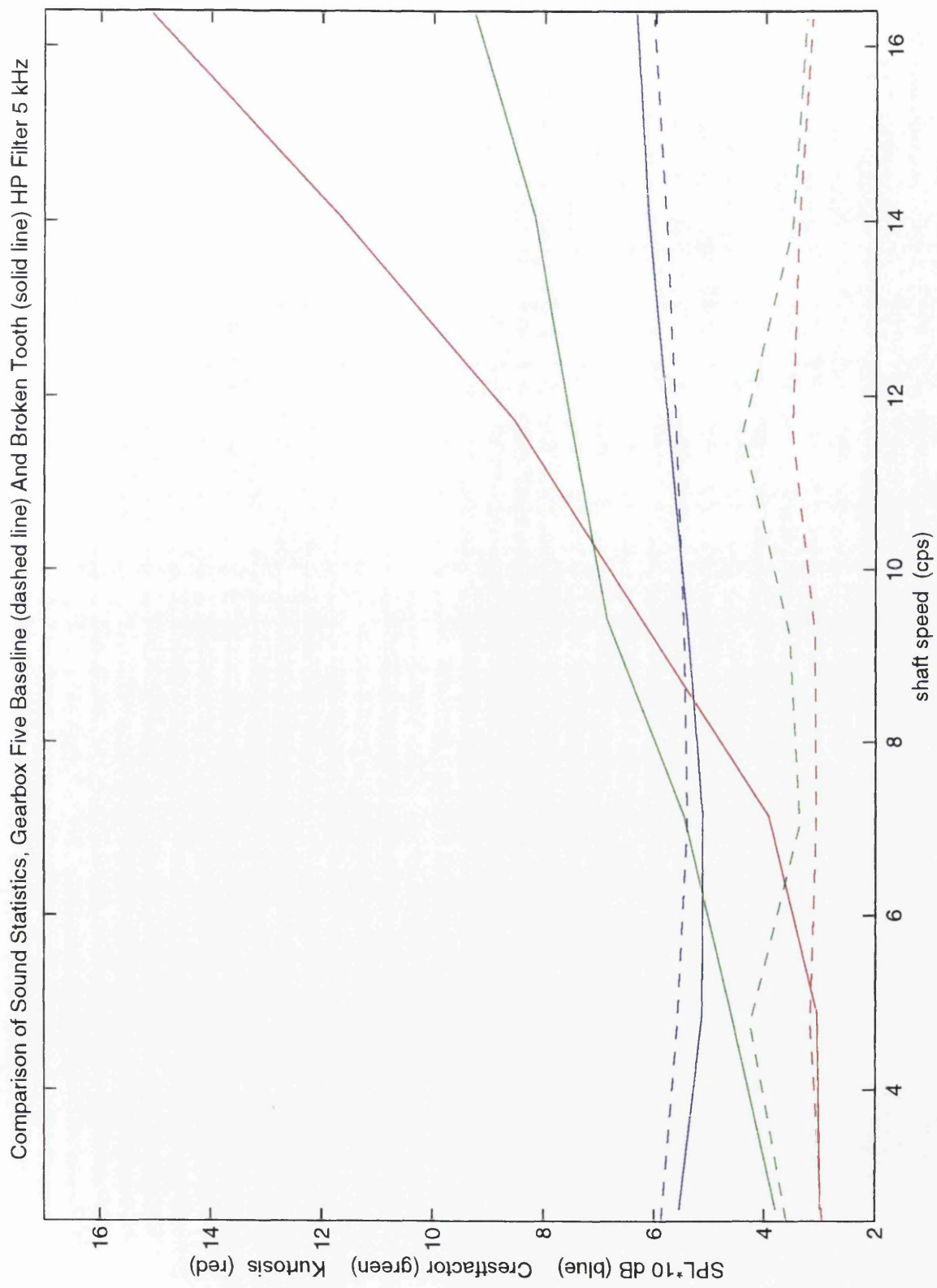


figure 51

Spectrogram View of TSA Sound of Baseline (differentiated)

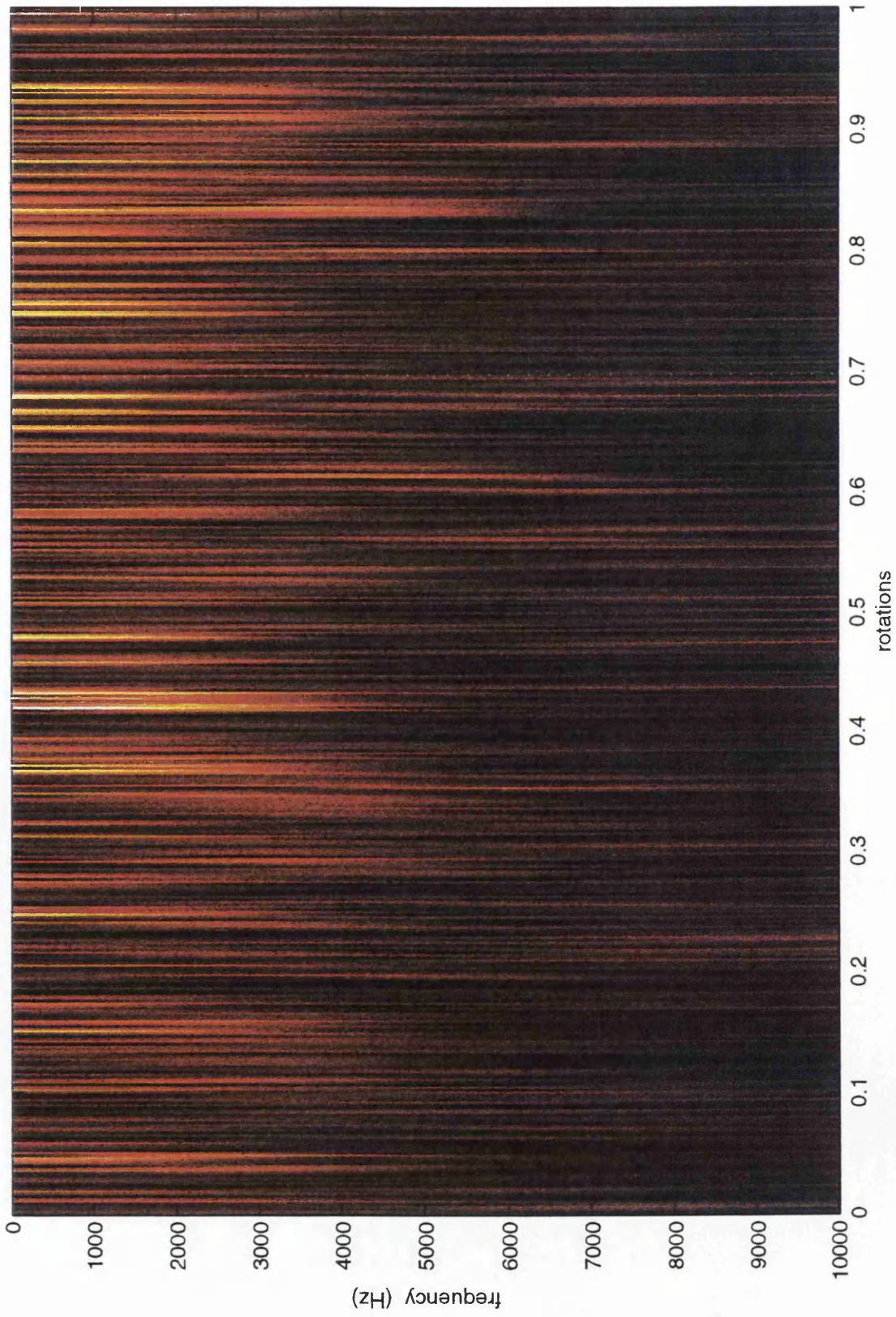


figure 52



Spectrogram View of TSA Sound of Broken Tooth (differentiated)

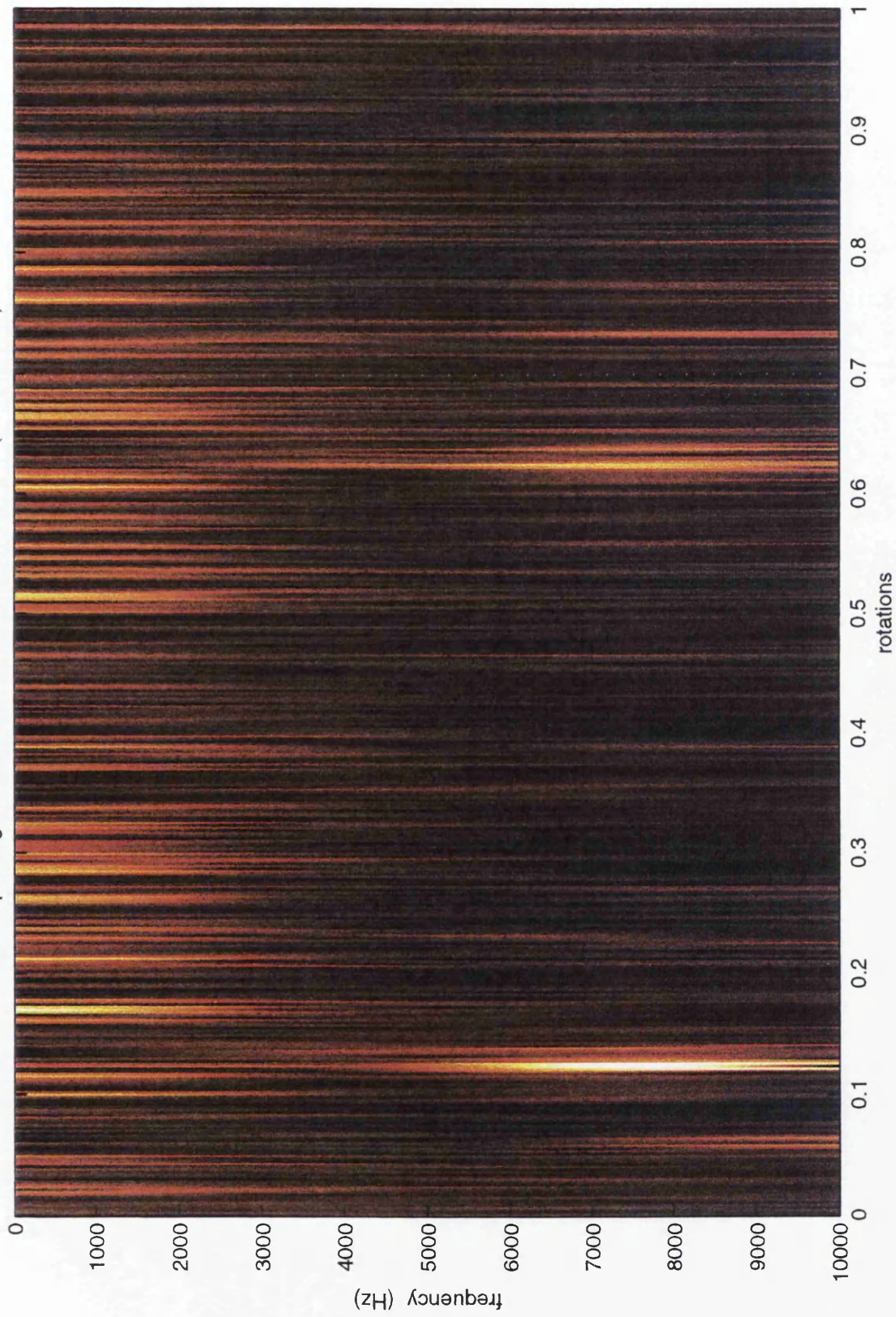


figure 53

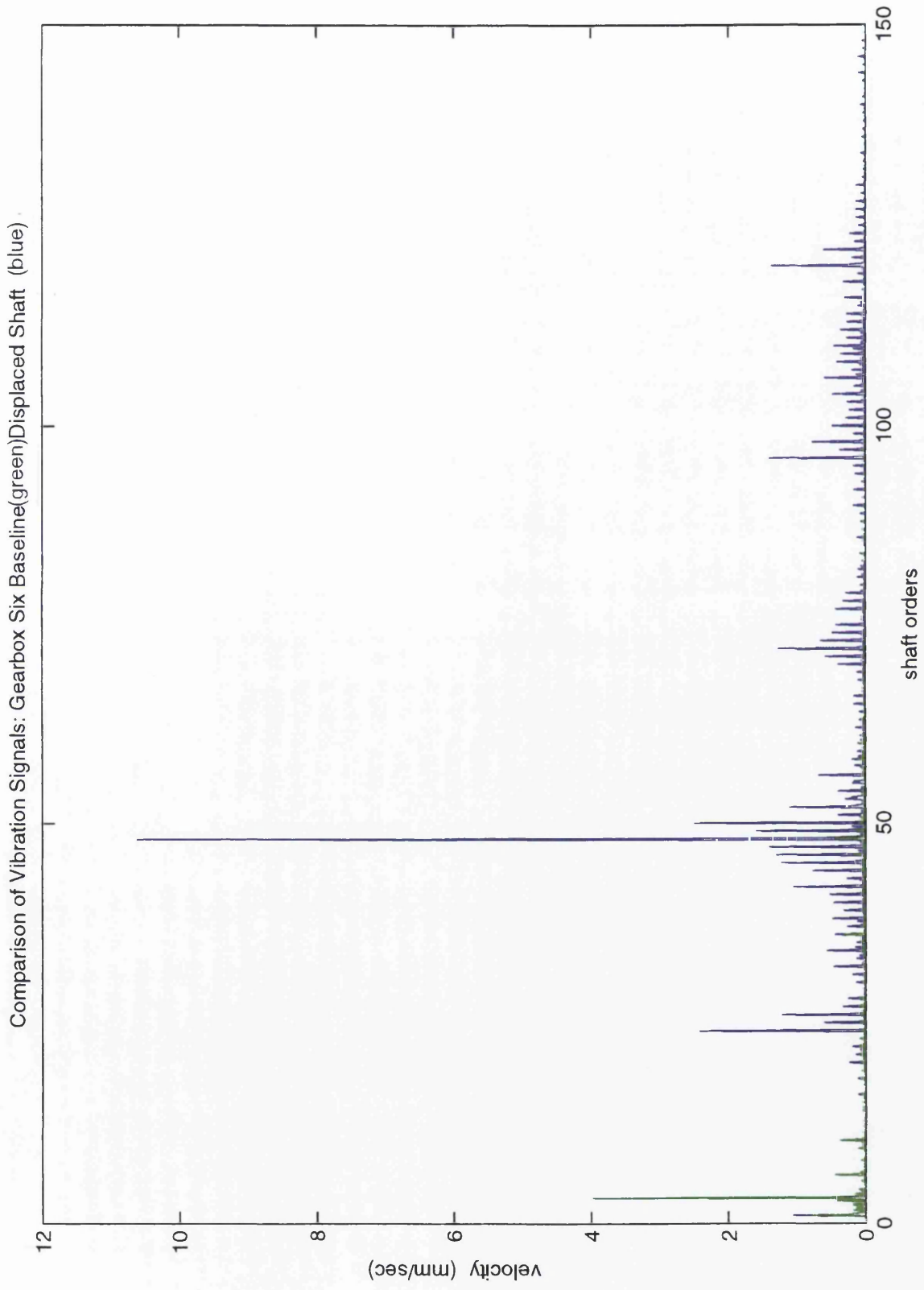


figure 54

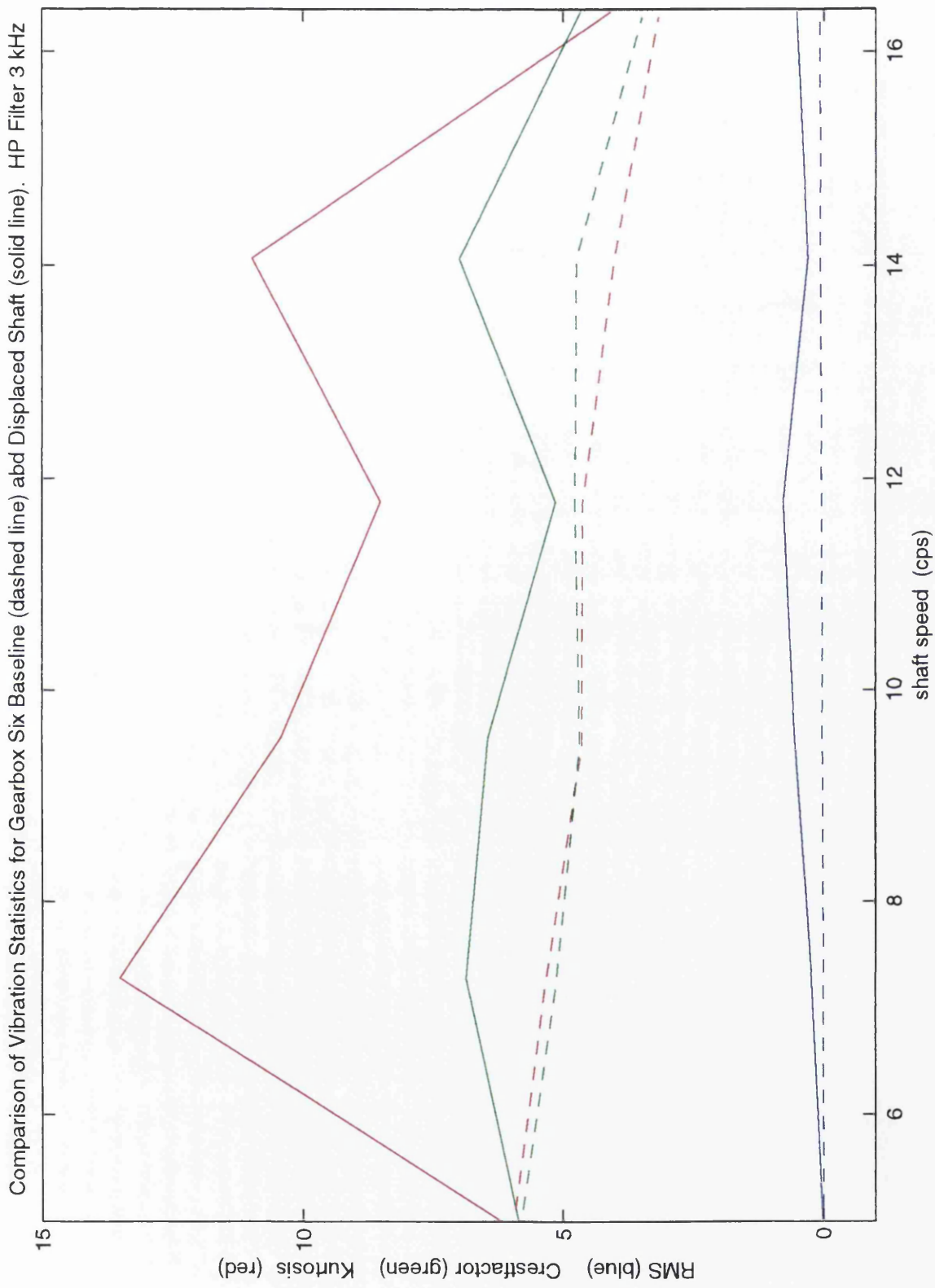


figure 55

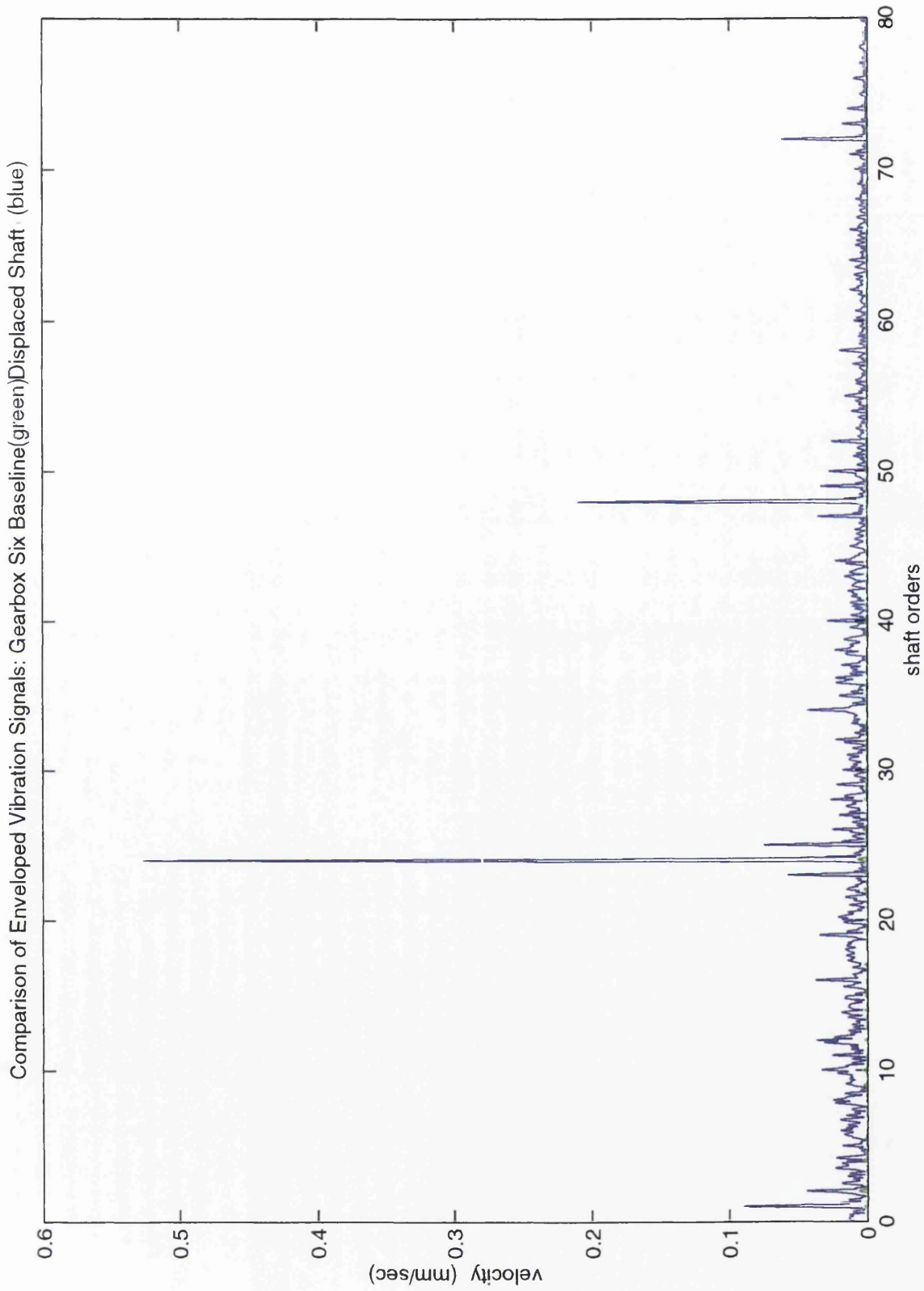


figure 56

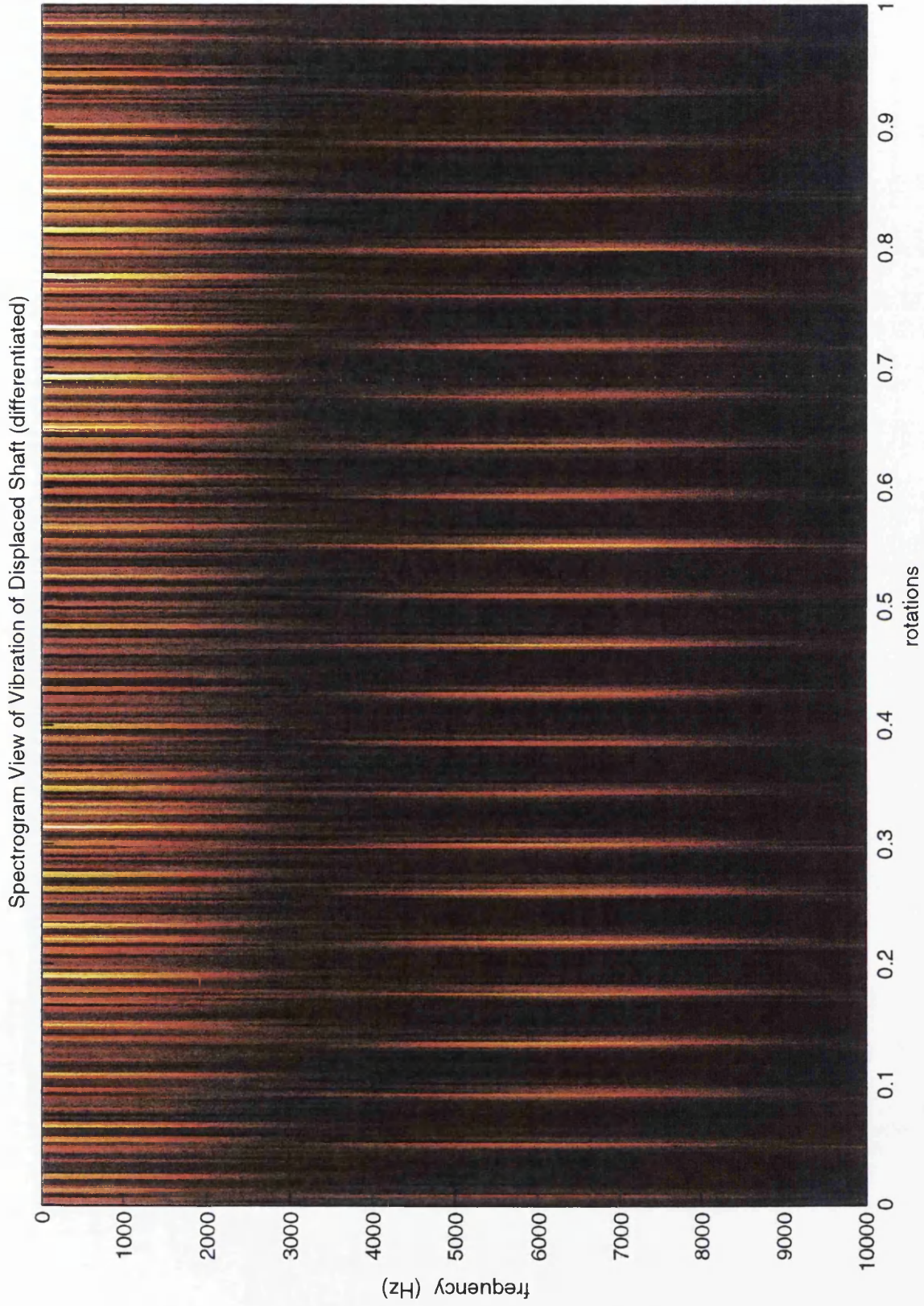


figure 57

Sound of Displaced Shaft. HP Filter 3 kHz

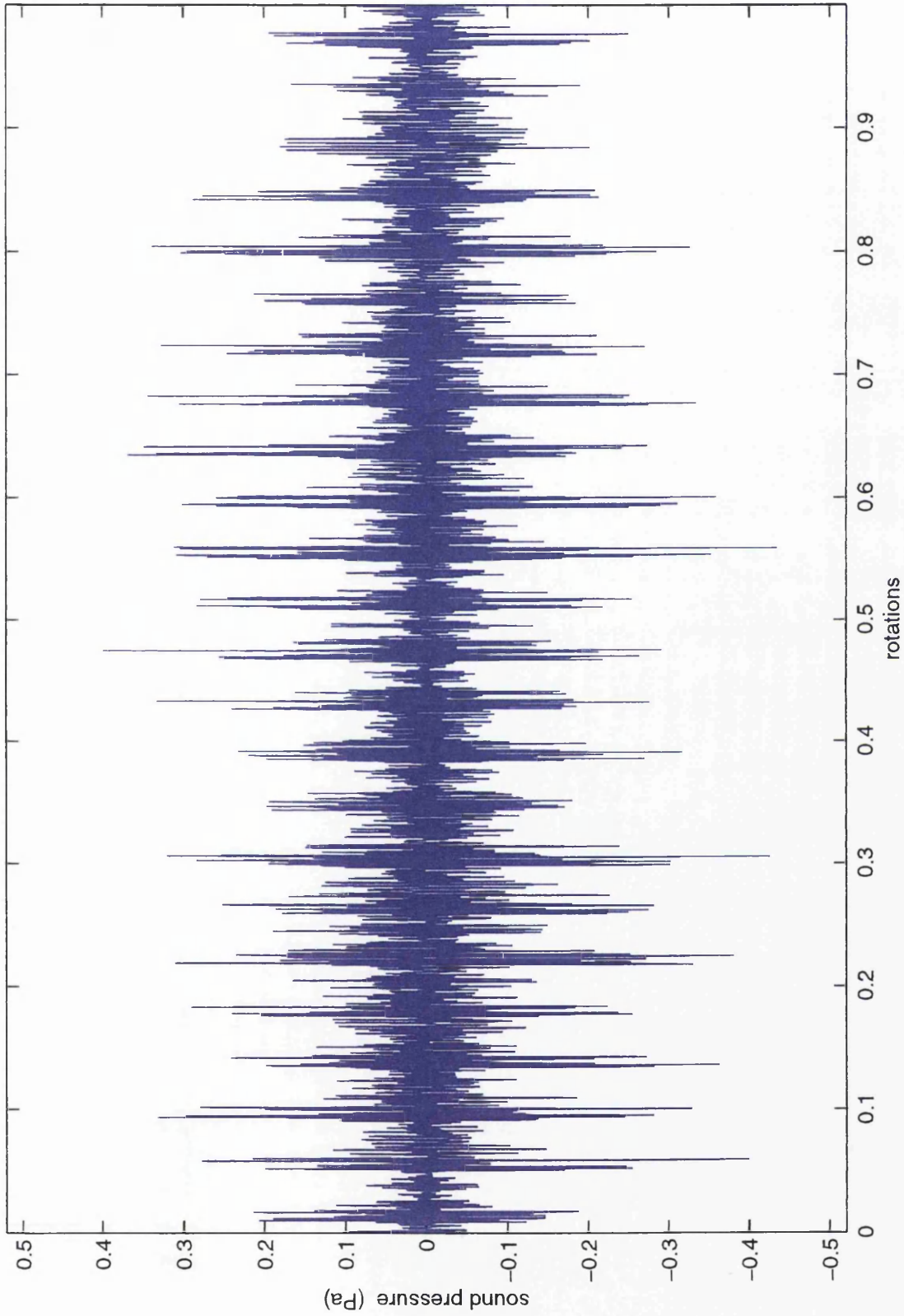


figure 58

Comparison of Sound Statistics for Gearbox Six Baseline (dashed line) and Displaced Shaft (solid line). HP Filter 3 kHz

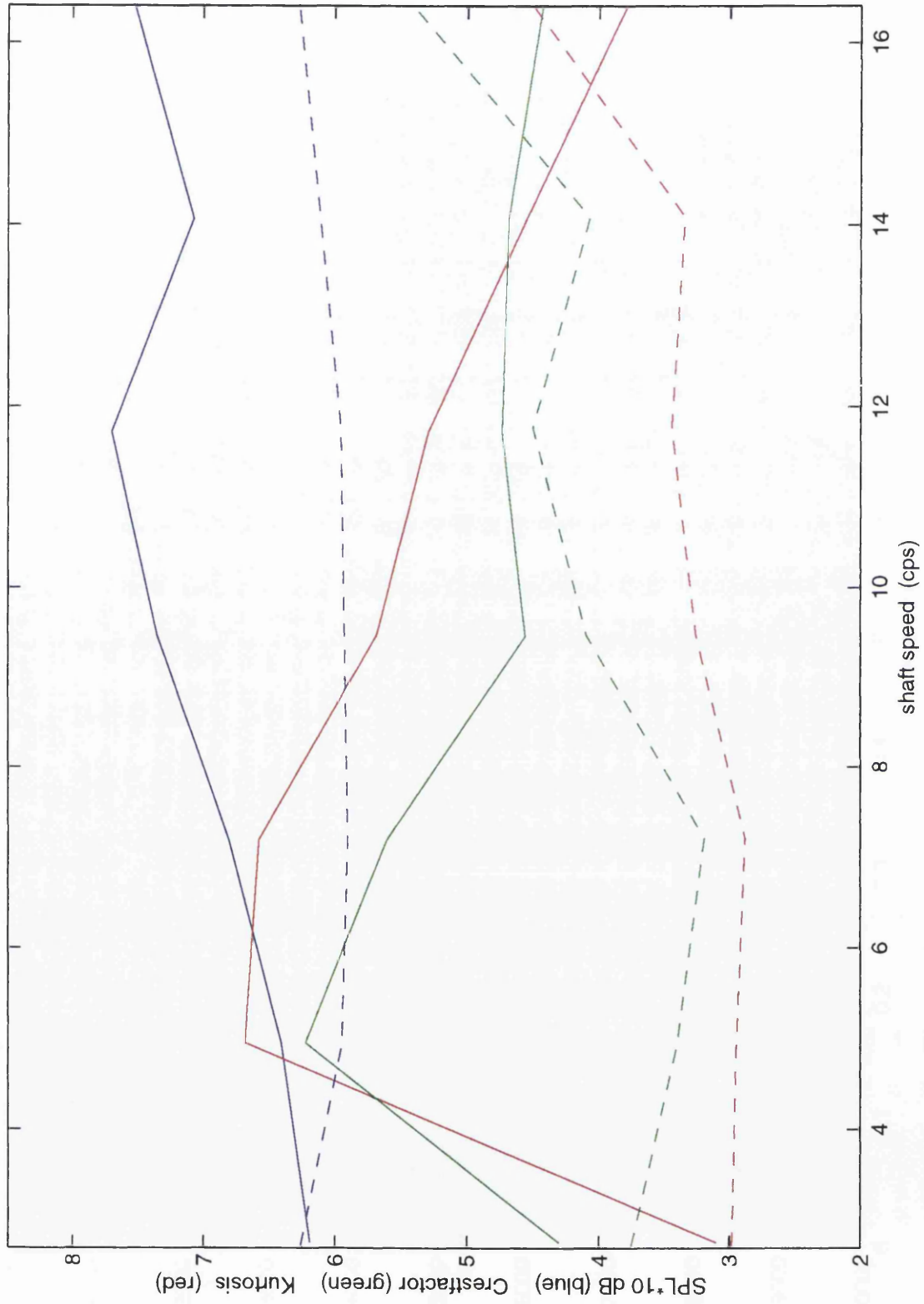


figure 59

Spectrogram View of TSA Sound of Displaced Shaft (double differentiation)

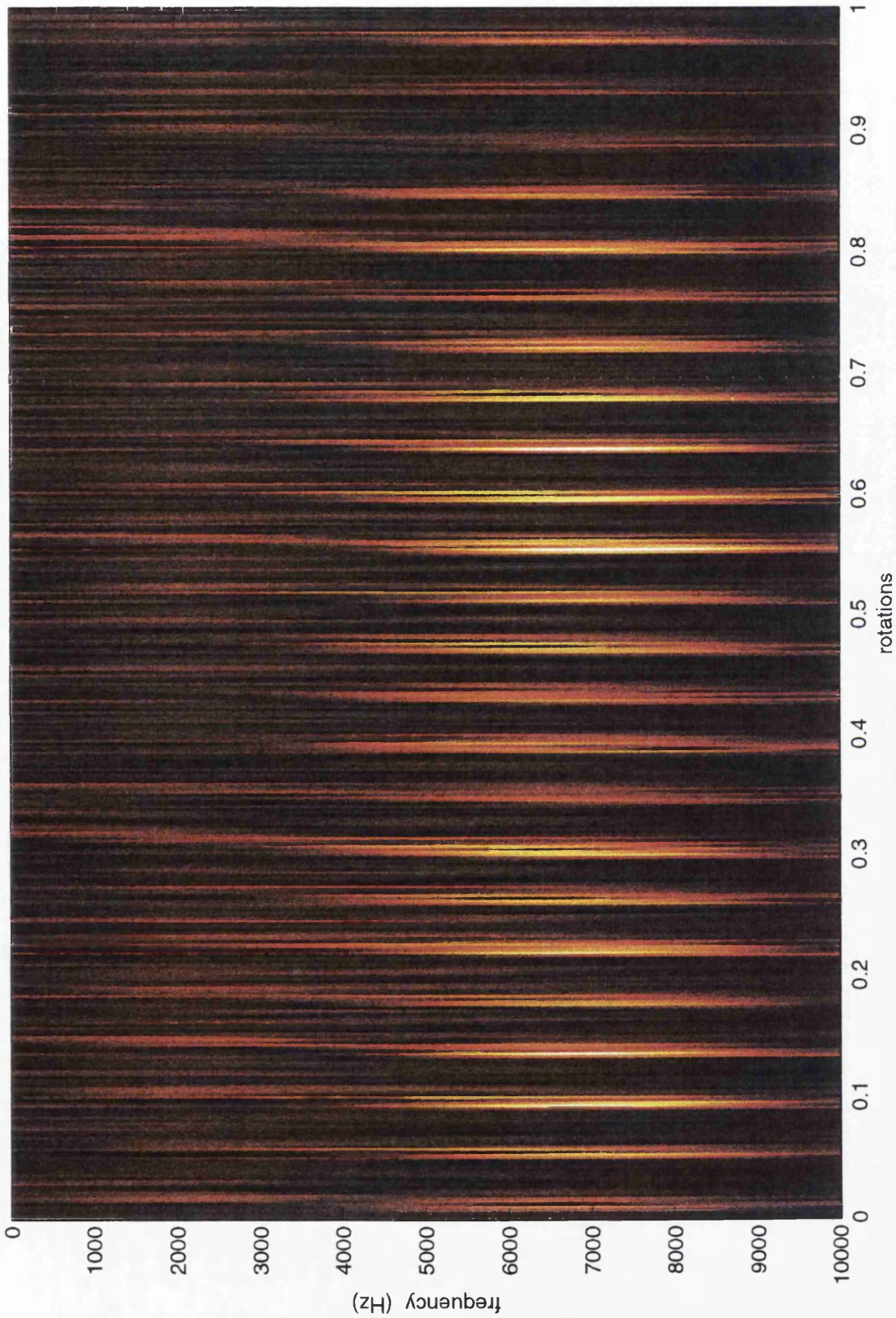


figure 60



## **4 Mathematical Modelling**

### **4.1 Introduction**

In order to gain a more detailed understanding of vibrations within the rig, a Finite Element Analysis (FEA) model was created. This model was written from first principles in the programming language 'Matlab'. The model was one dimensional consisting of bar elements with a single node at each end of the elements. Each node had four degrees of freedom, allowing the nodes to move in the vertical and horizontal axis, and to twist around the vertical and horizontal axis - see diagram 4.1. However, the nodes could not move axially, nor could they rotate (twist around the axial axis). The model was adapted to include these extra degrees of freedom, this was to allow the shafts to rotate and extend.

Matrices for stiffness 'K', mass 'M' and damping 'C' were generated and the eigenmodes and eigenfrequencies were calculated [36]. A forcing function 'F' was then added to investigate the model's behaviour, when subjected to sinusoidal forces, in accordance with traditional vibration theory.

The original plan was to adapt the four degree of freedom model to a six degree of freedom model, add bearings to connect the shafts to ground and then couple the input and output shafts at the gearwheels to complete the final model. Fault subroutines would then model the forces created by mechanical faults, such as misalignment and worn teeth.

This information was then be used to locate the principle sources of vibration within the rig, excited by faults. Sound generated by a machine is caused by these vibrations exciting the resonant frequencies of the machine's casing. The 'plates', making up the machine's casing, then act as loud speakers which radiate sound energy into the surrounding atmosphere.

## 4.2 Methodology - The FEA Model

In order to gain a more detailed knowledge of vibrations within the rig, a Finite Element Analysis (FEA) model was created. A detailed explanation of FEA will not be given in this report.

The FEA models consist of simple beam and bar elements with six degrees of freedom per node. This gives each node the ability to move in any direction ( $u, v$  &  $w$ ) and have any orientation ( $u', v'$  and  $w'$ ), see diagram 4.1.

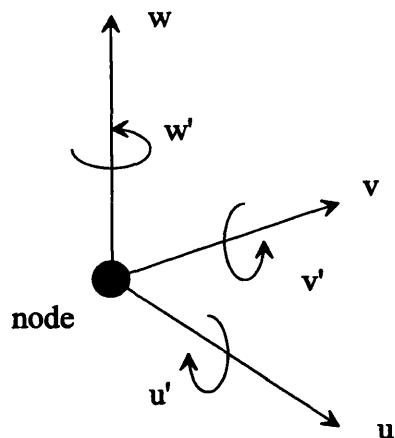


**diagram 4.1**

v	vertical axis
u	horizontal axis
w	axial axis
v'	rotation around vertical axis
u'	rotation around horizontal axis
w'	rotation around axial axis

Each element of the model consists of a one dimensional bar element containing two nodes, see diagram 4.2.

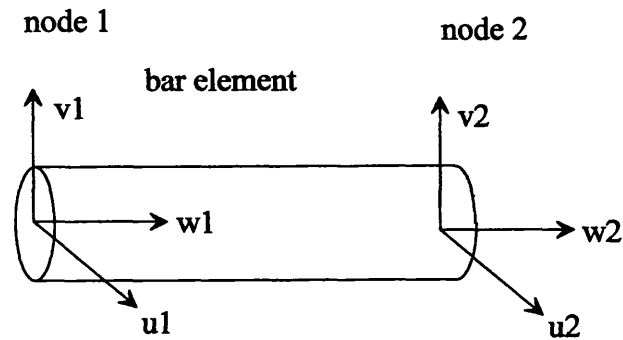


**diagram 4.2**

Several elements are placed in sequence to represent the shafts of a rotating machine. The rotors are represented as rigid masses placed on the appropriate nodes. A stiffness, mass, damping and gyroscopic matrix are generated for each element. No derivation of these matrices will be given in this report [37].

### 4.2.1 Stiffness Matrix for Bar Element

The stiffness matrix for the beams were generated from the following equations [37]. Without derivation the equations of motion are as follows.

$$\begin{Bmatrix} T_{w1} \\ T_{w2} \end{Bmatrix} = \frac{GI_p}{l} \begin{bmatrix} 1 & -1 \\ -1 & 1 \end{bmatrix} \begin{Bmatrix} w'_1 \\ w'_2 \end{Bmatrix}$$

equation 4.1

$$\begin{Bmatrix} F_{v1} \\ T_{u1} \\ F_{v2} \\ T_{u2} \end{Bmatrix} = \frac{2I_d E}{\beta} \begin{bmatrix} 6 & -3l & -6 & -3l \\ -3l & 2l^2 & 3l & l^2 \\ -6 & 3l & 6 & 3l \\ -3l & l^2 & 3l & 2l^2 \end{bmatrix} \begin{Bmatrix} v_1 \\ u'_1 \\ v_2 \\ u'_2 \end{Bmatrix}$$

equation 4.2

$$\begin{Bmatrix} F_{u1} \\ T_{v1} \\ F_{u2} \\ T_{v2} \end{Bmatrix} = \frac{2I_d E}{\beta} \begin{bmatrix} 6 & 3l & -6 & 3l \\ 3l & 2l^2 & -3l & l^2 \\ -6 & -3l & 6 & -3l \\ 3l & l^2 & -3l & 2l^2 \end{bmatrix} \begin{Bmatrix} u_1 \\ v'_1 \\ u_2 \\ v'_2 \end{Bmatrix}$$

equation 4.3

$$\begin{Bmatrix} F_{w1} \\ F_{w2} \end{Bmatrix} = \frac{EA}{l} \begin{bmatrix} 1 & -1 \\ -1 & 1 \end{bmatrix} \begin{Bmatrix} w_1 \\ w_2 \end{Bmatrix}$$

equation 4.4

- $T_{w1}$  torque acting on node one, orientation  $w$ , etc.
- $F_{w1}$  force acting on node one, direction  $w$ , etc.
- $G$  Modulus of rigidity.
- $I_p$  polar moment of inertia.
- $l$  length of element.
- $I_d$  diametral moment of inertia.
- $E$  modulus of elasticity
- $A$  cross sectional area of element.

### 4.2.2 Mass Matrices for Bar Element

$$\begin{Bmatrix} T_{w1} \\ T_{w2} \end{Bmatrix} = \frac{\rho l p l}{6} \begin{bmatrix} 2 & 1 \\ 1 & 2 \end{bmatrix} \begin{Bmatrix} \ddot{w}'_1 \\ \ddot{w}'_2 \end{Bmatrix}$$

equation 4.5

$$\begin{Bmatrix} F_{v1} \\ T_{u1} \\ F_{v2} \\ T_{u2} \end{Bmatrix} = \frac{\rho A l}{420} \begin{bmatrix} 156 & 22l & 54 & -13l \\ 22l & 4l^2 & 13l & -3l^2 \\ 54 & 13l & 156 & -22l \\ -13l & -3l^2 & -22l & 4l^2 \end{bmatrix} \begin{Bmatrix} \ddot{v}_1 \\ \ddot{u}'_1 \\ \ddot{v}_2 \\ \ddot{u}'_2 \end{Bmatrix}$$

equation 4.6

$$\begin{Bmatrix} F_{u1} \\ T_{v1} \\ F_{u2} \\ T_{v2} \end{Bmatrix} = \frac{\rho A l}{420} \begin{bmatrix} 156 & -22l & 54 & 13l \\ -22l & 4l^2 & -13l & -3l^2 \\ 54 & -13l & 156 & 22l \\ 13l & -3l^2 & 22l & 4l^2 \end{bmatrix} \begin{Bmatrix} \ddot{u}_1 \\ \ddot{v}'_1 \\ \ddot{u}_2 \\ \ddot{v}'_2 \end{Bmatrix}$$

equation 4.7

$$\begin{Bmatrix} F_{w1} \\ F_{w2} \end{Bmatrix} = \frac{\rho A l}{6} \begin{bmatrix} 2 & 1 \\ 1 & 2 \end{bmatrix} \begin{Bmatrix} \ddot{w}_1 \\ \ddot{w}_2 \end{Bmatrix}$$

equation 4.8

$\rho$  mass density  
 $\ddot{w}$  acceleration in direction w. etc.

### 4.2.3 Element Mass Matrix for Discs

Each disc in the system is assumed to be rigid. Only the disc's mass and inertia affects the system. See diagram 4.3

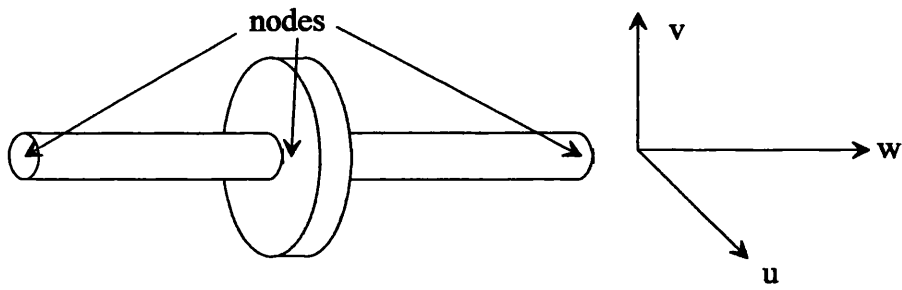


diagram 4.3

$$\begin{Bmatrix} F_u \\ F_v \\ F_w \\ T_u \\ T_v \\ T_w \end{Bmatrix} = \begin{bmatrix} m_d & & & & & \\ & m_d & & & & \\ & & m_d & & & \\ & & & I_d & & \\ & & & & I_d & \\ & & & & & I_p \end{bmatrix} \begin{Bmatrix} \ddot{u} \\ \ddot{v} \\ \ddot{w} \\ \dot{u}' \\ \dot{v}' \\ \dot{w}' \end{Bmatrix}$$

equation 4.9

- $m_d$  mass of disc
- $I_d$  diametral moment of inertia
- $I_p$  polar moment of inertia

#### 4.2.4 Simple Model of Bearing

Bearings and seals are assumed to connect a node to ground, via generalised stiffness and damping matrices. See diagram 4.4.

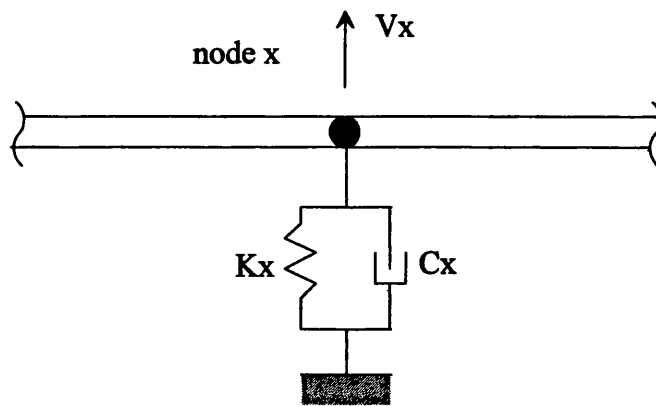
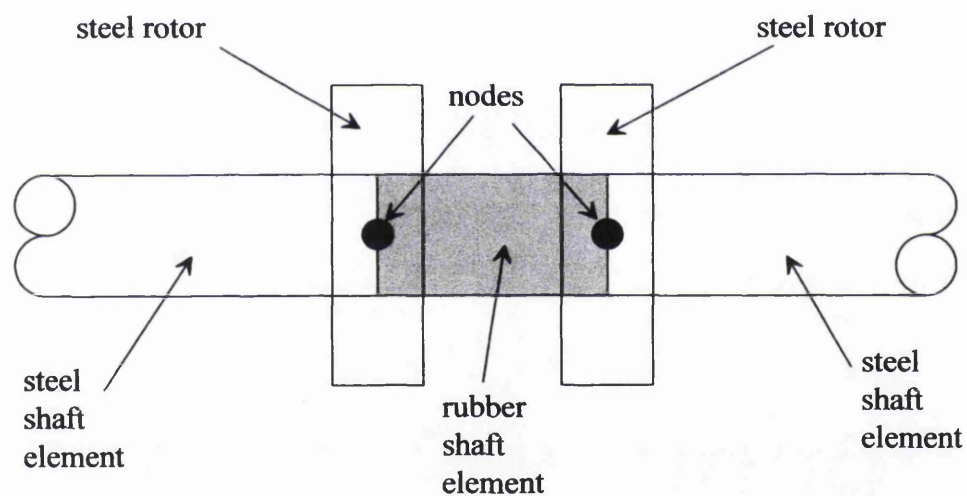


diagram 4.4

Diagram 4.4 shows the effect of placing a bearing of stiffness  $K_x$  and damping  $C_x$  on node  $x$ , in the vertical direction. The value of  $K_x$  and  $C_x$  was chosen such that the FEA model would resonate at the same frequency as the test-rig at that point. Initially  $C_x$  was assumed to be one percent of critical viscous damping.

#### 4.2.5 The Rubber Couplings

The couplings connect the shafts together, reduce the transmission of lateral vibrations, damp torsional vibrations and reduce the effect of misalignment. The type of coupling used on the test-rig were three-jaw Essex couplings, with a rubber torsion disc. They were modelled by inserting a rubber shaft element, as in diagram 4.5.



**diagram 4.5**

The modulus of rigidity of the rubber shaft element was found by performing a simple experiment, in which a known torque was applied to one shaft while the other shaft was clamped in place. The displacement angle was measured and the modulus of rigidity obtained. The rotational damping of the rubber shaft element was found by releasing the torque and measuring how far the disc had returned to its original position in a set time. The equations of motion yielded the damping coefficient. The Young's modulus of the rubber shaft element was taken to be zero, for the purposes

of mathematical modelling. This gave the rubber element zero bending stiffness', but a finite torsional stiffness. Zero bending stiffness was required as there was a small amount of play between the rubber coupling and the discs.

#### ***4.2.6 Eigenvalues and Eigenvectors***

Once the stiffness matrix 'K', mass matrix 'M' and damping matrix 'C', were determined the eigenvalues (natural frequencies) and normalised eigenvectors (mode shapes) were evaluated using the Matlab m-file 'eig.m'.

#### ***4.2.7 Validation***

The equations for natural frequencies of bar and rotor combinations are well known [38]. By constructing several of these simple systems, it was possible to show that the FEA models agreed with the theory, for beams in bending, torsion and extension. The natural frequencies of the models were slightly higher than theory would suggest, but this is to be expected as the number of elements was finite. The more elements that were added to the FEA models the closer the natural frequencies approached the theoretical prediction [36]. This simple test was used to ensure that the program had been debugged correctly and was calculating sensible answers.

#### ***4.2.8 The Model of the Test-rig***

The test-rig consists of an input and an output shaft. This was modelled by creating two shafts of bar elements, as described, and then rotating the input shaft through 90° using a translation matrix. See diagram 4.6.



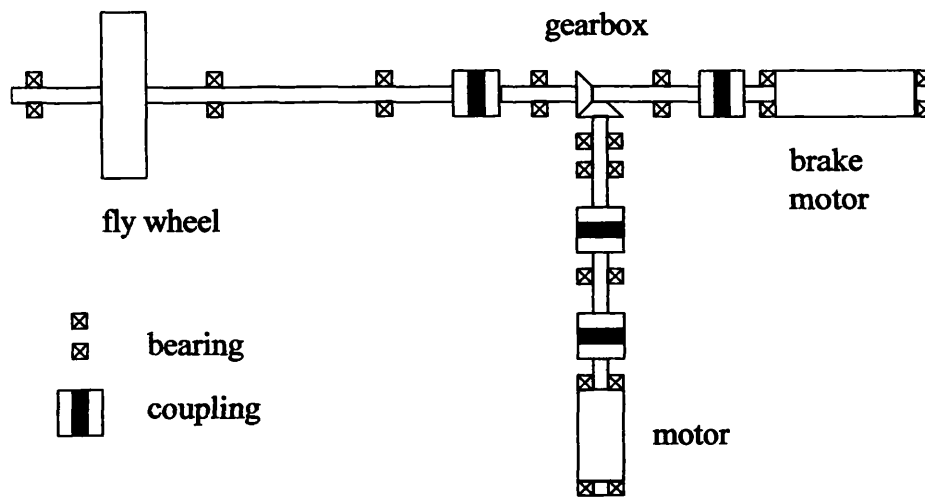


diagram 4.6

#### 4.2.9 Bearing Stiffness

The resonant frequency of the system is determined by the mass and stiffness of the shafts and rotors, and the bearing pedestal stiffness. For example, with near infinite bearing stiffness, the critical frequency of the system, in which the FEA flywheel experienced maximum amplitude, was 105 Hz, in both the horizontal and vertical directions. A simple hammer test was performed by placing an accelerometer, with a magnetic mount, on to the bottom of the stationary flywheel of the real test-rig. The flywheel was then struck with a rubber mallet. The accelerometer signal showed a resonance at just under 100 Hz. The vertical bearing stiffness of the model was lowered from near infinity until the FEA model's critical frequency matched the experimental results. This test was repeated for the horizontal direction. The simple hammer test was used to obtain the axial, horizontal and vertical resonances of all the bearing pedestals on the test-rig. This was done by placing the accelerometer in the position to be measured, and striking the rig with the mallet close by.

The results showed that the response of the model did not match the response curves of the hammer tests. The majority of the bearings exhibited at least two resonant frequencies. The lower resonant frequency was of the whole rig moving axially, horizontally and vertically (w.r.t. the output shaft), on its support structure (the table

- see plate 1 in the appendix). The second higher frequency was of the individual bearing pedestals themselves. An extra element was added to the model to represent the rig structure. The stiffness value 'K' of the rig was then added to ground. Each of the individual bearing pedestals stiffness' were then connected to this new 'table' node. The mass of the table node was adjusted so that the response curve of the FEA model fitted the hammer test response curve.

One more element was required to achieve the correct response from the model. Diagram 4.6, depicting the rig, shows that the input and output shaft of the gearbox may move independently of one another. This was not the case in reality. In reality the gearbox casing was very stiff in comparison to the box section that supported it (see plate 2 & 3). Previous experiments had shown that the gearbox itself moved as one rigid body, supported by a softer base.

The final element was added to model the gearbox casing. Figure 61 depicts the FEA model. The bar, beam and rotor elements are red, the bearings yellow and the two extra nodes blue. It should be noted that the typical bearing pedestal stiffness in the model is of the order of  $10^6$  N/m. The stiffness of the bearings within the gearbox, supporting the shafts, was set at  $10^9$  N/m to represent infinite stiffness and to allow the gearbox to move as a rigid body.

#### ***4.2.10 Coupling the Gearwheels***

The final adjustment made to the model was to couple the gearwheels together. If this is not done, the gearwheels may move independently of one another. The gearwheels must be coupled so that if one turns the other must turn. This motion was also coupled so that if one gearwheel moved up or down the other must also move up or down, etc.

The form of coupling used allows the teeth to separate. To allow separation each gearwheel must retain it's own individual node. In the real test-rig the tooth was not entirely removed from the input shaft, leaving a gap, rather it was mostly removed

using a small angle grinder. As the broken tooth enters the mesh it is less capable of transmitting the load through the gearbox, compared to the rest of the teeth. When the next healthy tooth enters the mesh it impacts on the gear teeth of the output shaft. This impact excites lateral and torsional vibrations throughout the rig.

#### 4.2.11 Modelling a Partially Broken Tooth

If a unit force,  $F(t)$ , is placed on the first gearwheel's tooth, an equal and opposite reaction force is placed on the tooth of the second gearwheel. The unit force  $F(t)$ , placed on the tooth, can be resolved into a torque around the shaft centre, and a lateral force through the shaft centre - see diagram 4.7 and equation 4.2.

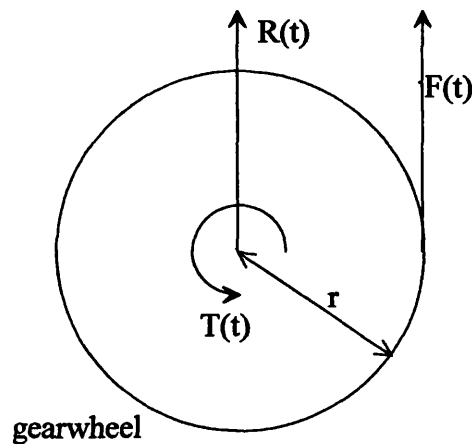


diagram 4.7

t	time (seconds)
$F(t)$	unit force on tooth (N)
$R(t)$	resolved lateral force through shaft centre (N)
$T(t)$	resolved torque around shaft centre (Nm)
r	radius of gearwheel (m)

$$R(t) = F(t)$$

$$T(t) = rF(t)$$

equation 4.12

The equal and opposite force placed on the second gearwheel's tooth is treated in a similar manner. It should be noted that this is a 2:1 reduction ratio gearbox, so that the torque on the output shaft is double that of the first.  $F(t)$  is an oscillating force according to equation 4.13

$$F(t) = \Re e^{2\pi i f t}$$

**equation 4.13**

f                      frequency (Hz)

This oscillating unit force may excite the natural vibrations of the model in both lateral and torsional modes, once resolved. The impact of the next healthy tooth, following the broken tooth, uses the method above in the following manner. The input shaft has a rotational time period of 'T' seconds. An impact occurs every 'T' seconds, as shown in diagram 4.8.

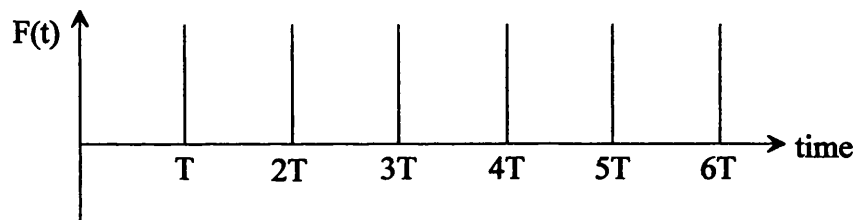


**diagram 4.8**

T                      time period of one rotation of the input shaft (with broken tooth) = 1/speed.

This force is transformed into the frequency domain by Fourier transform, as shown in diagram 4.9.

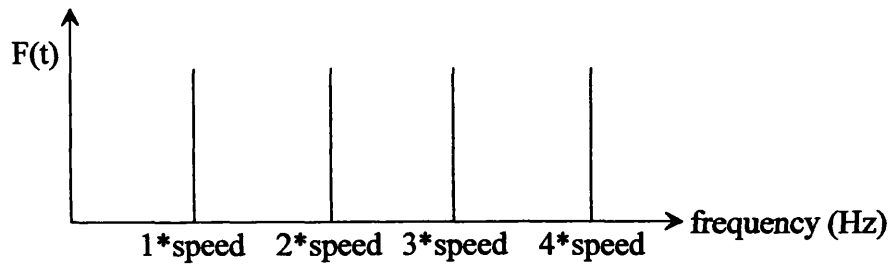


**diagram 4.9**

This force is placed on the input shaft's gearwheel tooth (resolved into force through shaft centre and torque) and it's equal and opposite force placed on the output shaft's gearwheel. This represents an impacting force that attempts to push the gear teeth apart. The impacts cause lateral and torsional vibrations which are passed through the rig.

### **4.3 Results of FEA Model**

Figure 61 is a graphical representation of the test-rig. The shafts and rotors are red, the bearings yellow and the two extra nodes representing the test-rig table and gearbox casing are blue. It should be noted that the bearings connecting the shafts of the gearbox to the gearbox case are approximately one thousand times stiffer than the other bearings. This allows the gearbox to move as a single near rigid body.

Figure 62 shows the response curves for the gearbox, in the axial, vertical, and horizontal directions (w.r.t. the output shaft). These response curves were generated by placing an accelerometer onto the gearbox, in the horizontal, axial and vertical directions. The exact placement was on the output shaft bearing, closest to the flywheel. The point was then struck with a rubber mallet. It should be noted that both experimental and theoretical data have been normalised to allow direct comparison.

The vertical FEA response curve fits the data well, except at the lowest frequencies and two points at approximately 32 and 55 Hz.

The horizontal response curve is far more complex. The damping of the first resonance peak at 23 Hz appears to be insufficient, while the peaks between 50 and 150 Hz are an approximate match only. The axial response fits the experimental data reasonably well, except for the peak at 42 Hz.

Figures 63 to 69 are the modeshapes of the model at the various frequencies of interest highlighted in the response curves.

A note of explanation is required to understand these modeshape plots. The input and output shafts of the test-rig are depicted as straight blue lines. The bearings are shown as small blue circles. The input and output shaft join together at the gearbox (compare figure 63 with diagram 4.6). The red lines represent the amplitude and direction of the modeshape for each individual node, while the green lines represent phase.

Figure 63 shows the vertical resonant frequency of 12.3 Hz of the gearbox. The gearbox is a rigid body mounted on a soft base. A peak can be seen on the vertical response curve (figure 62) at 12.3 Hz. The horizontal response curve shows resonant peaks at 26.3, 104, 114 and 116 Hz. The modeshapes relating to these figures is depicted in figures 64 to 67. The first two mode shapes, figures 64 and 65, is of the whole rig moving together on the support table at resonant frequencies of 26.3 and 104 Hz, respectively. Figures 66 and 67 show the principle resonant frequency of the brake motor at 114 Hz and a resonant frequency of the gearbox at 116 Hz.

Figure 68 shows the axial motion (with respect to the output shaft) of the whole rig moving at 13.4 Hz. Figure 69 is a modeshape of the rig at 45 Hz in the axial direction. This can be seen on the response curve of figure 62 axial, but it does not match the experimental data. The experimental data shows that this modeshape does not exist.

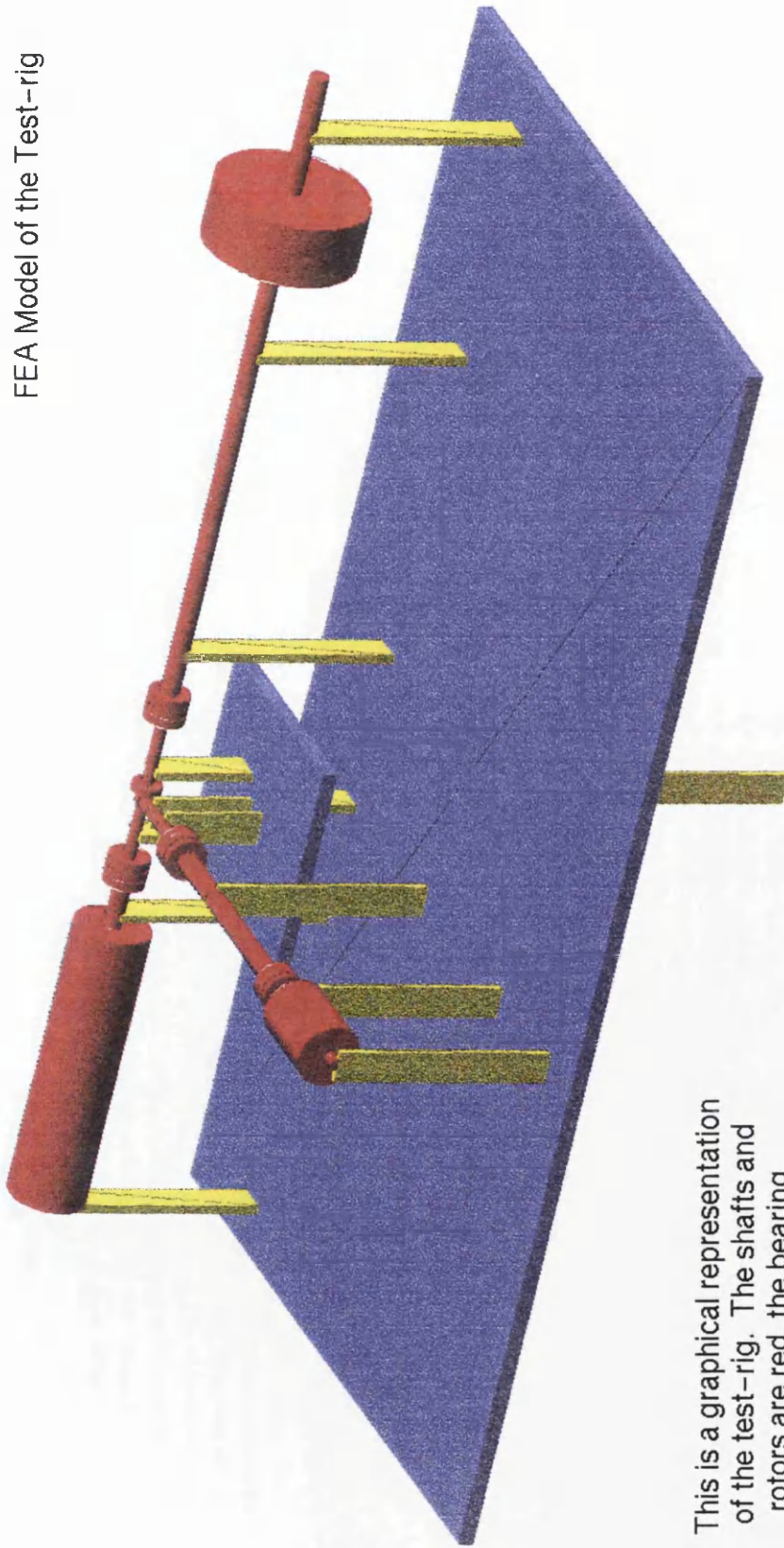
Figure 70 is a close up of the flexible coupling to the left of the gearbox. These figures show torsional displacement. The radius of the red circles represent the

amplitude of the torsional response of the nodes they encircle. Again, the green lines represent phase. There is a  $180^\circ$  phase shift at the flexible coupling as expected, as all the torsional damping occurs within this element.

Figure 71 shows the torsional displacement of the flywheel. The flexing continues past the input shaft unhindered. Again, the  $180^\circ$  phase shift may be observed at the flexible coupling.

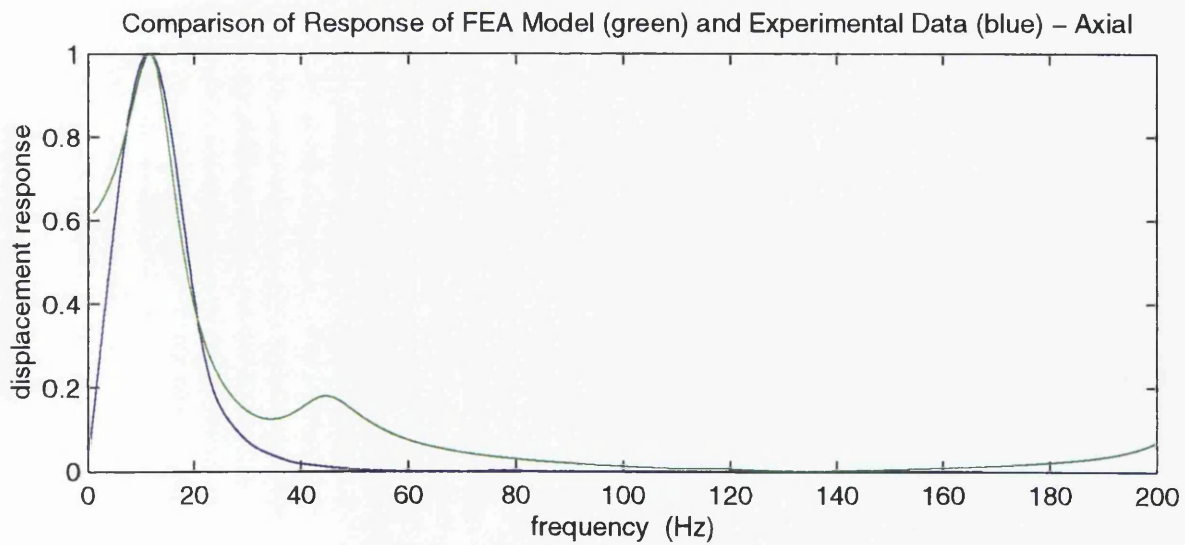
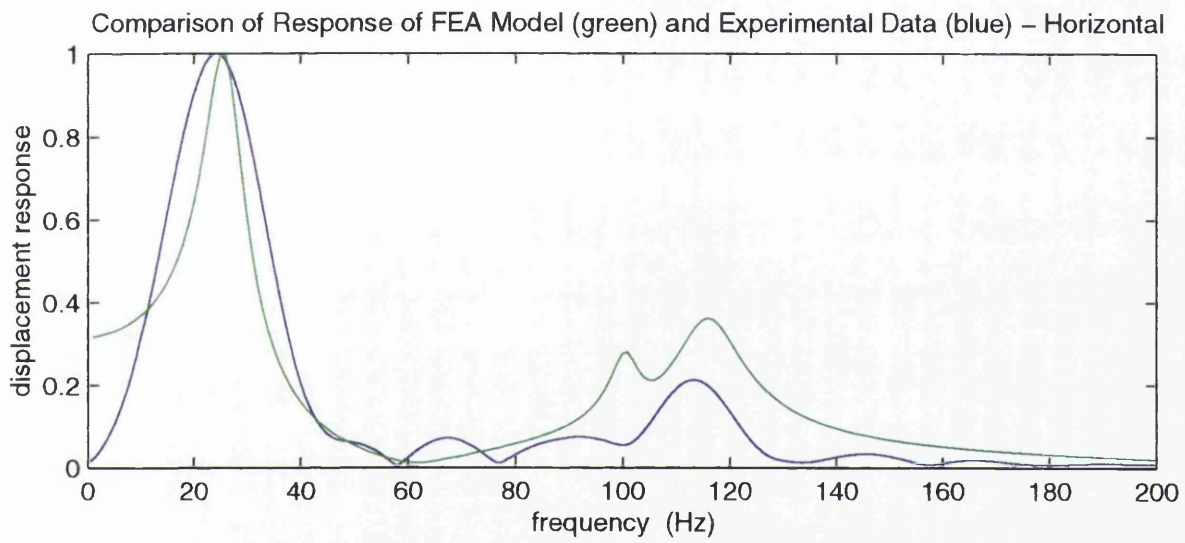
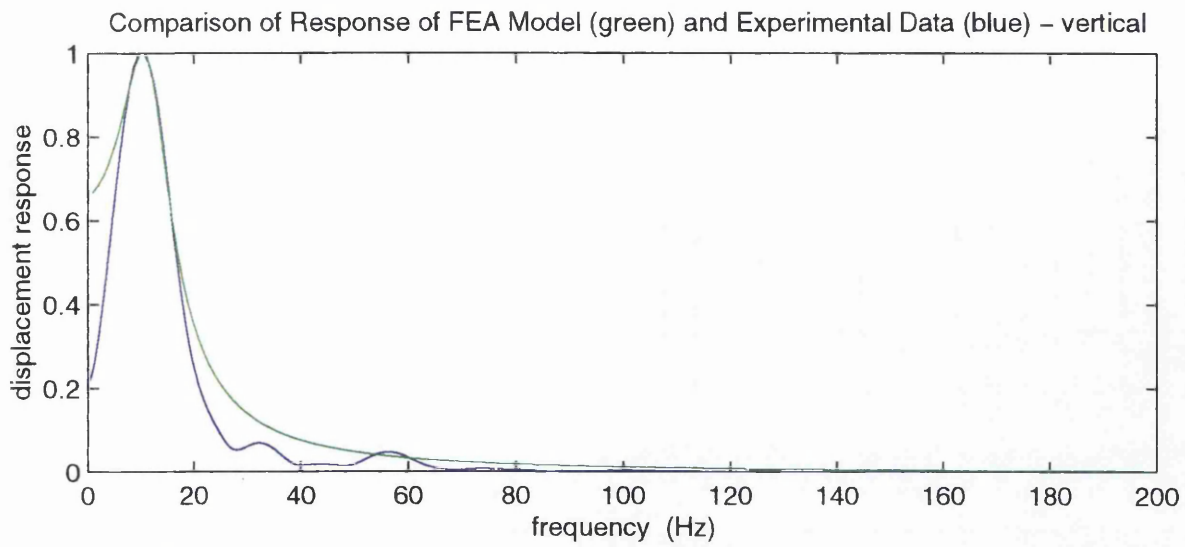
Figure 72 shows the experimental and theoretical results for the broken tooth. The experimental results (blue) showed a series of shaft orders of the output shaft (33 cps) and the input shaft (16.5 cps, as it is a 2:1 reduction ratio gearbox). The shaft orders in the 0 to 200 Hz region are caused by imbalance, misalignment and other faults not modelled by the FEA model. The theoretical results show shaft orders of the output shaft (33 cps) with the broken tooth. A resonance exists at around 400 Hz. This resonance cannot be seen in either the experimental response curves or the theoretical response curves, and yet both the model and the experimental results show that this resonance exists. This will be explained in the discussion. It should be noted that the input shaft has 12 teeth, giving a tooth passing frequency of 396 Hz at 33 cps. The FEA model does not model the tooth passing frequencies or side bands, only the impacts of the broken tooth.

Figure 73 is the lateral displacement of the test-rig caused by the broken tooth while figure 74 is the torsional deflection of the test-rig caused by the impacting tooth.

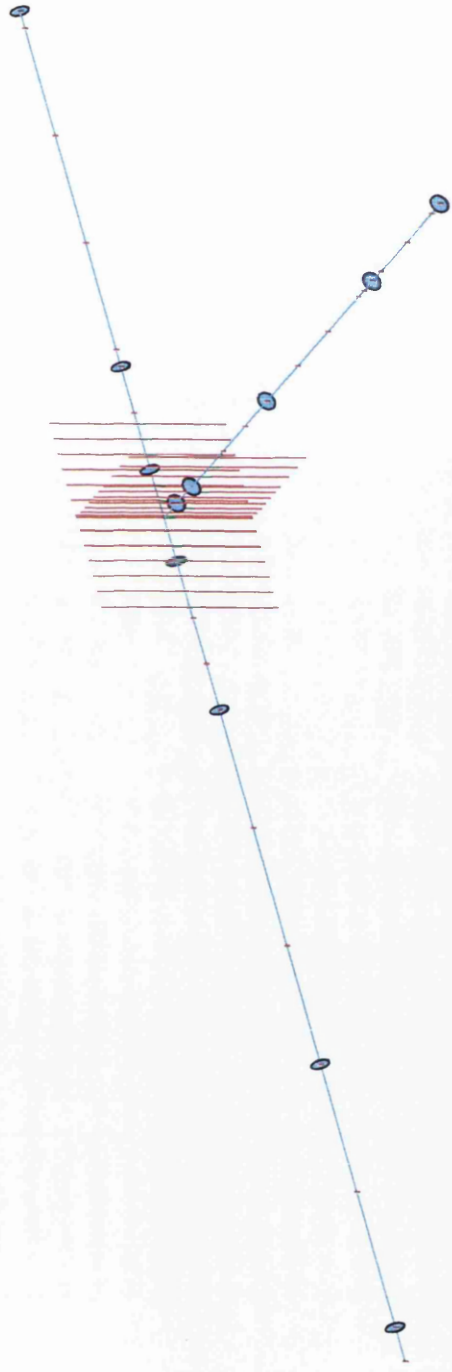


This is a graphical representation of the test-rig. The shafts and rotors are red, the bearing pedestals yellow and the table & gearbox case nodes are blue



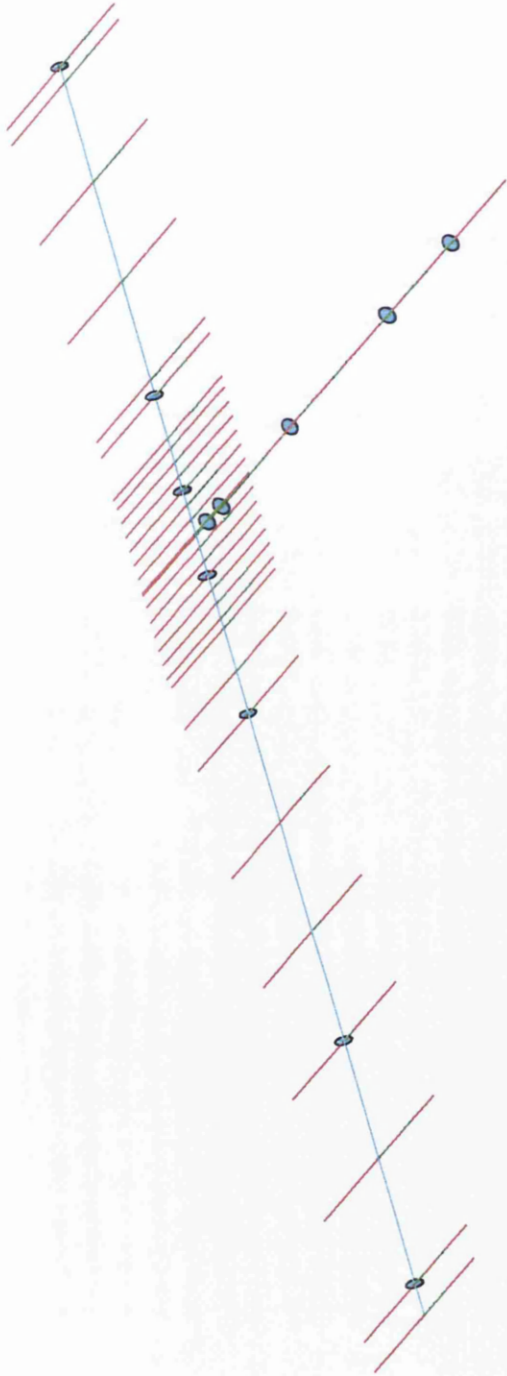


Vertical Resonance of Gearbox – 12.31 Hz



This is the modeshape of the gearbox resonating in the vertical direction at a frequency of 12.31 Hz

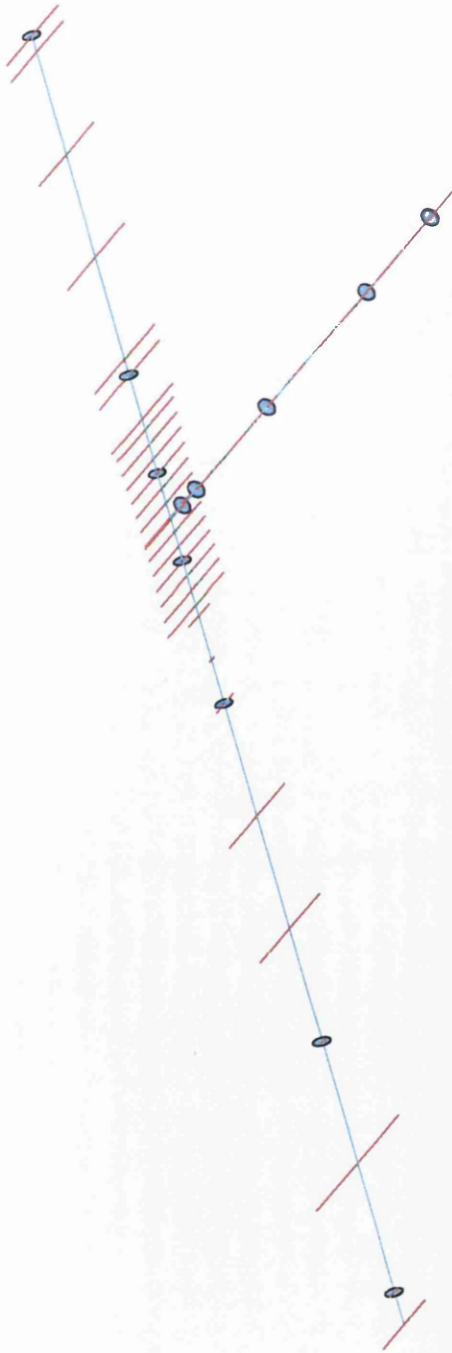
Horizontal Resonance of Test-rig – 26.32 Hz



This is the modeshape of the whole rig resonating in the horizontal direction at a frequency of 26.32 Hz

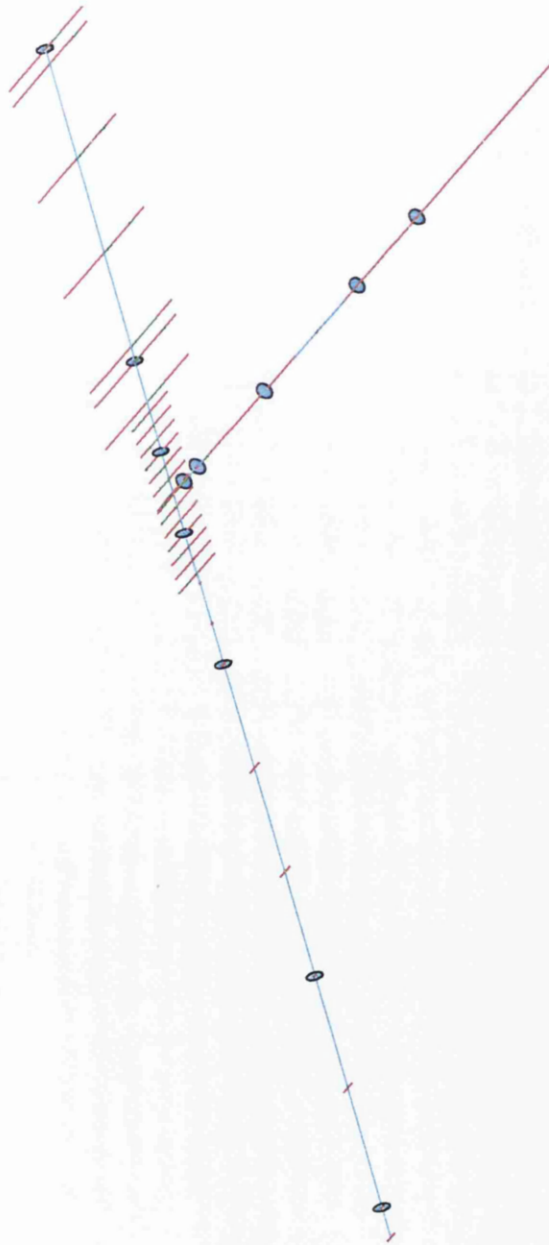
figure 64

Horizontal Resonance of Test-rig – 103.19 Hz



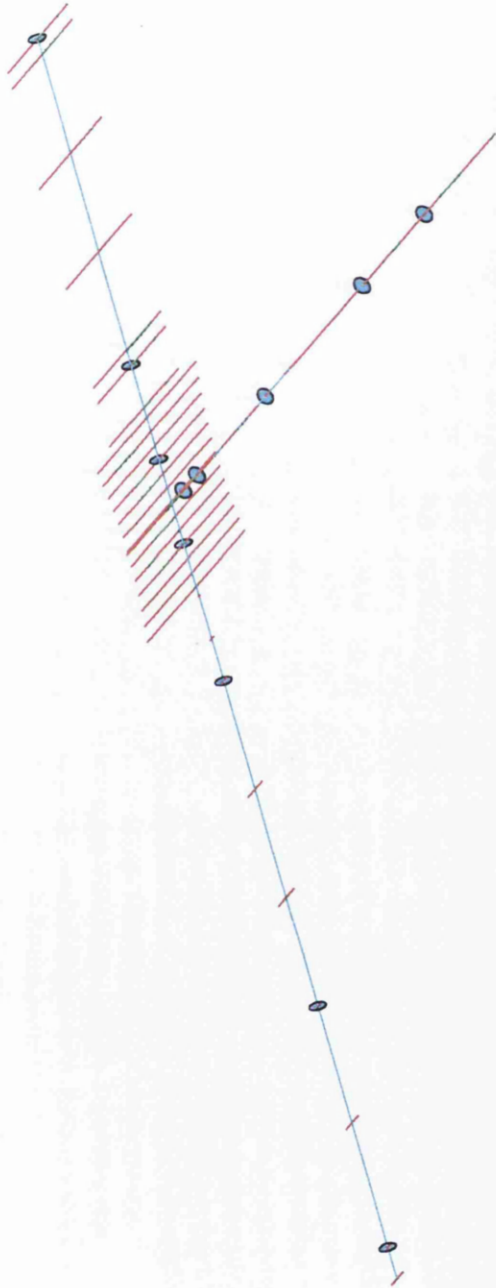
This is the modeshape of the whole rig resonating in the horizontal direction at a frequency of 103.19 Hz

Horizontal Resonance of Test-rig – 113.74 Hz



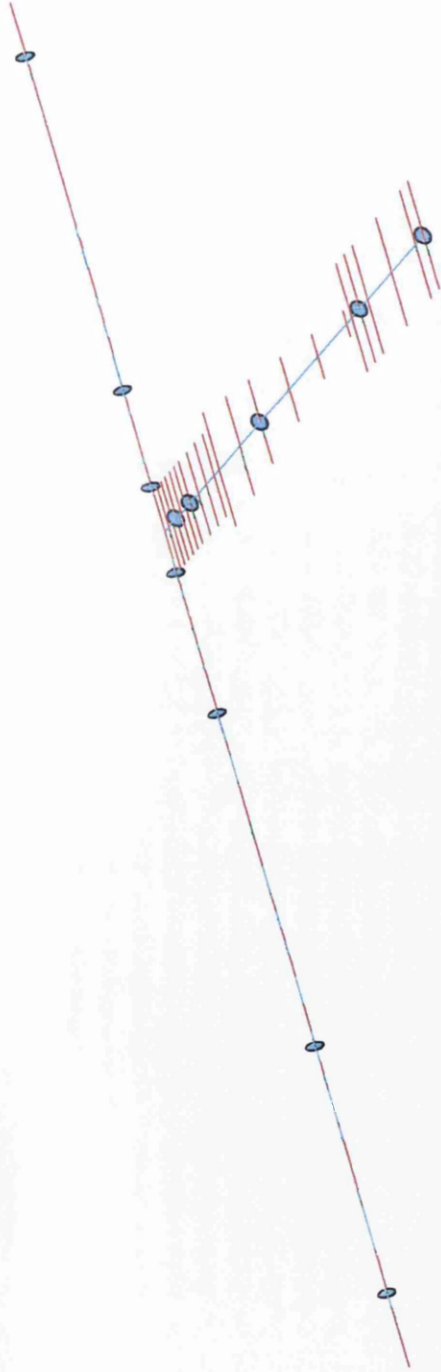
This is the modeshape of the test-rig resonating in the horizontal direction at a frequency of 113.74 Hz

Horizontal Resonance of Test-rig – 116.19 Hz



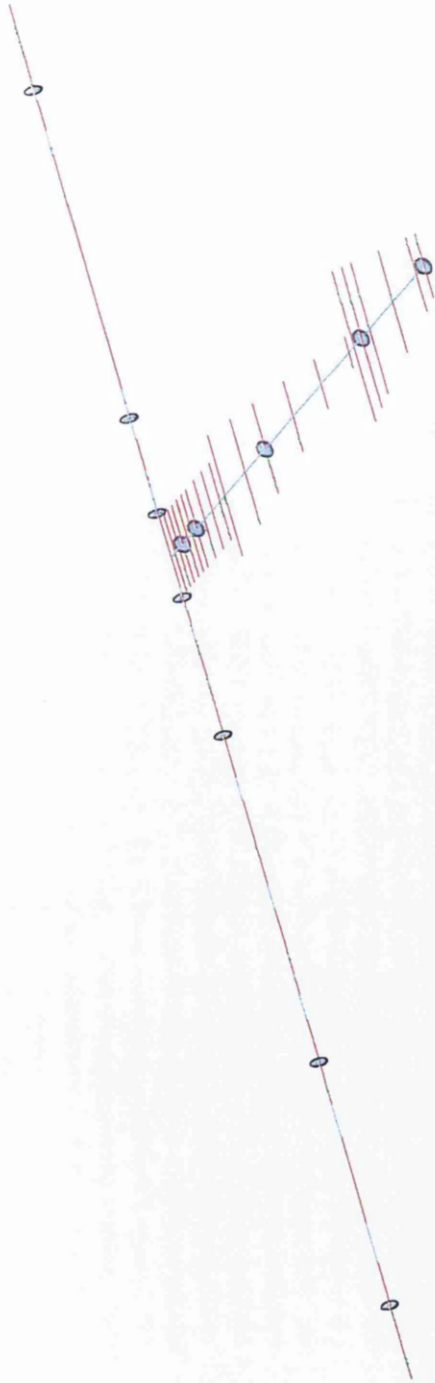
This is the modeshape of the test-rig resonating in the horizontal direction at a frequency of 116.19 Hz

Axial Resonance of Test-rig – 13.44 Hz



This is the modeshape of the test-rig resonating in the axial direction at a frequency of 13.44 Hz

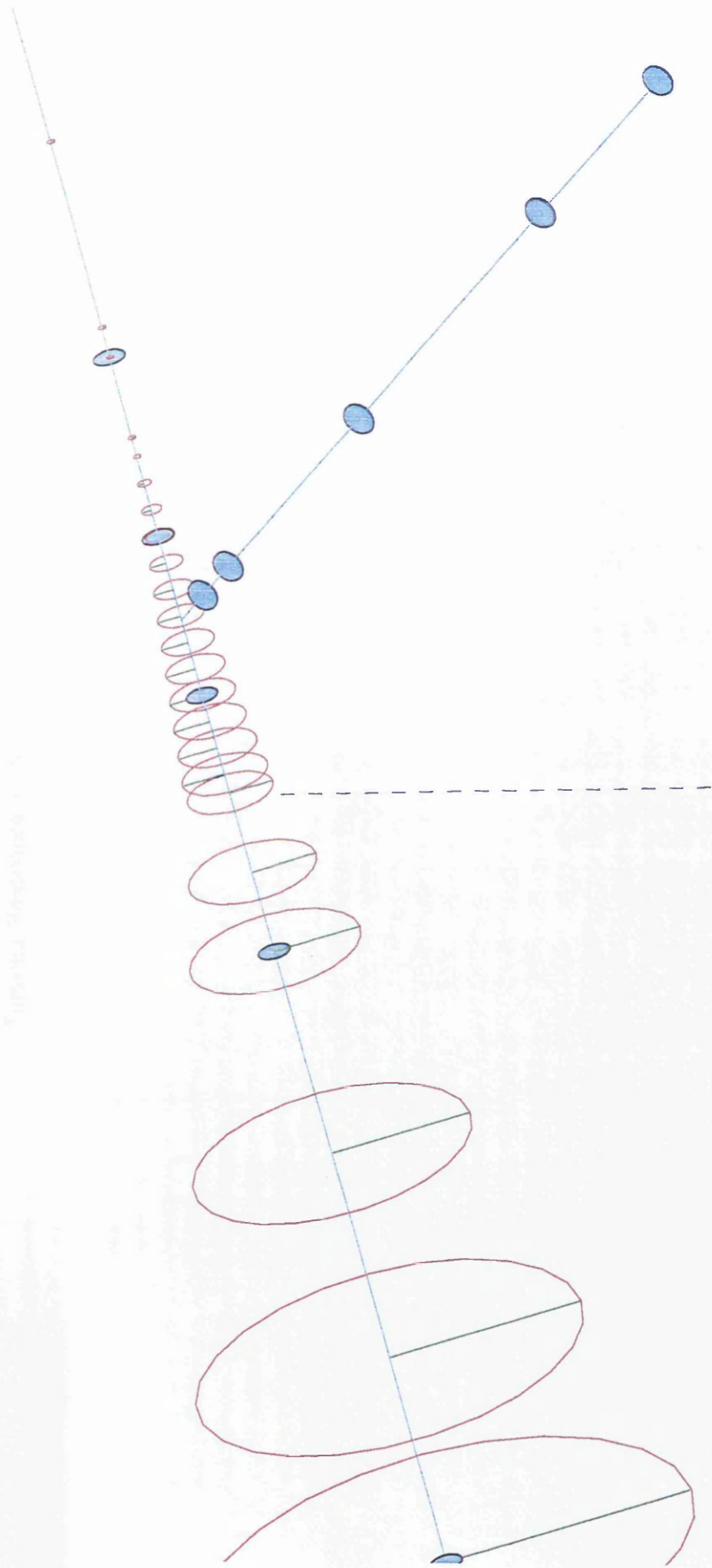
Axial Resonance of Test-rig – 45.0 Hz



This is the modeshape of the test-rig resonating in the axial direction at a frequency of 45.0 Hz

figure 69

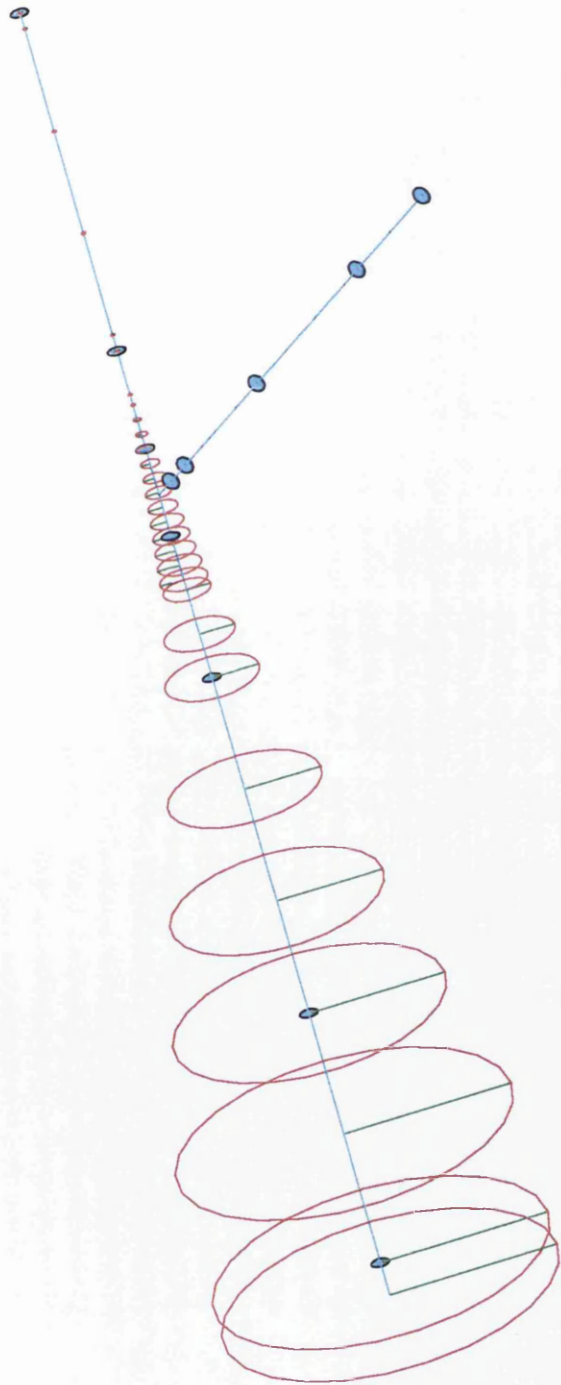




Phase shift of 180 degrees at the flexible coupling

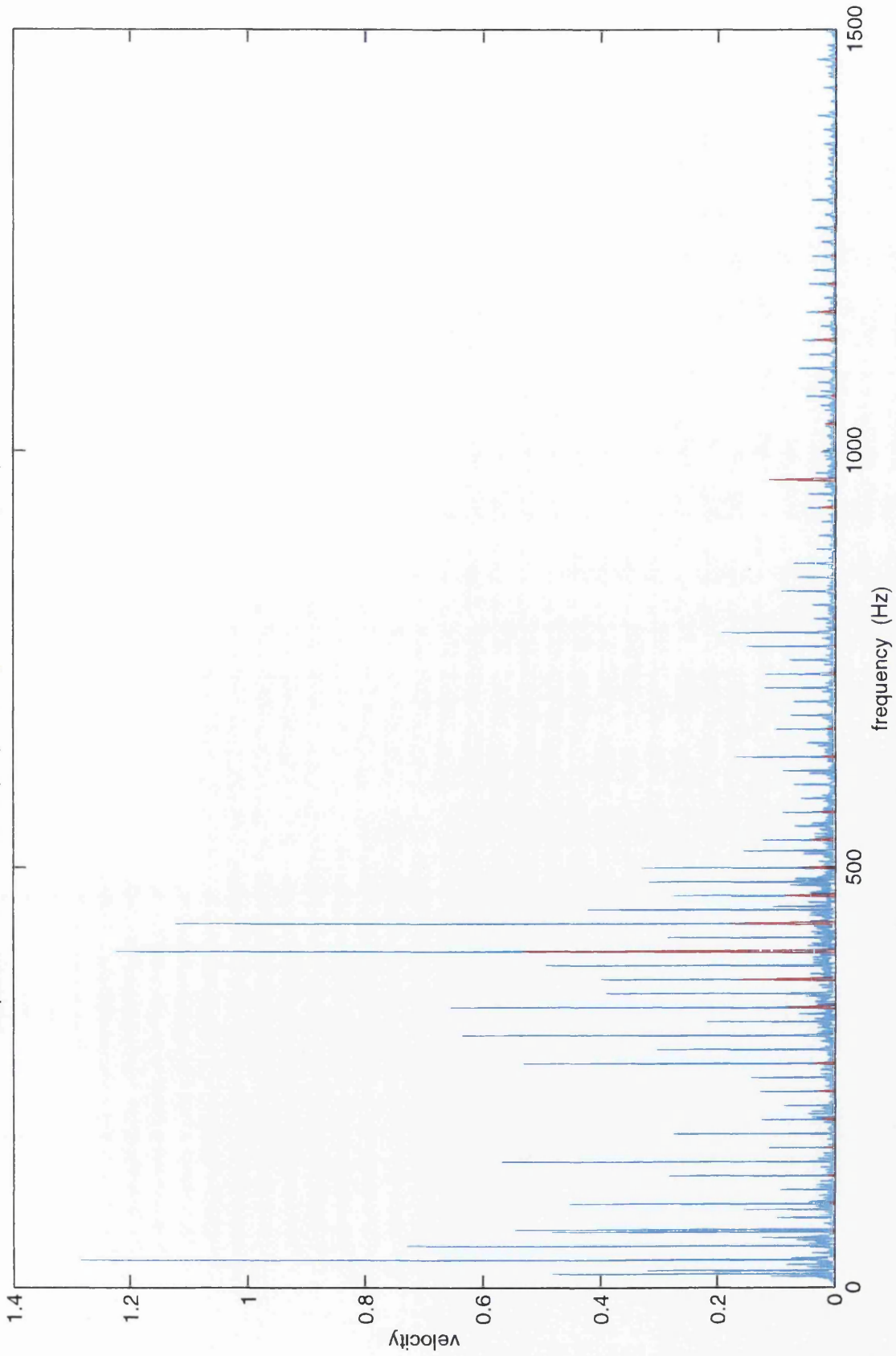
figure 70

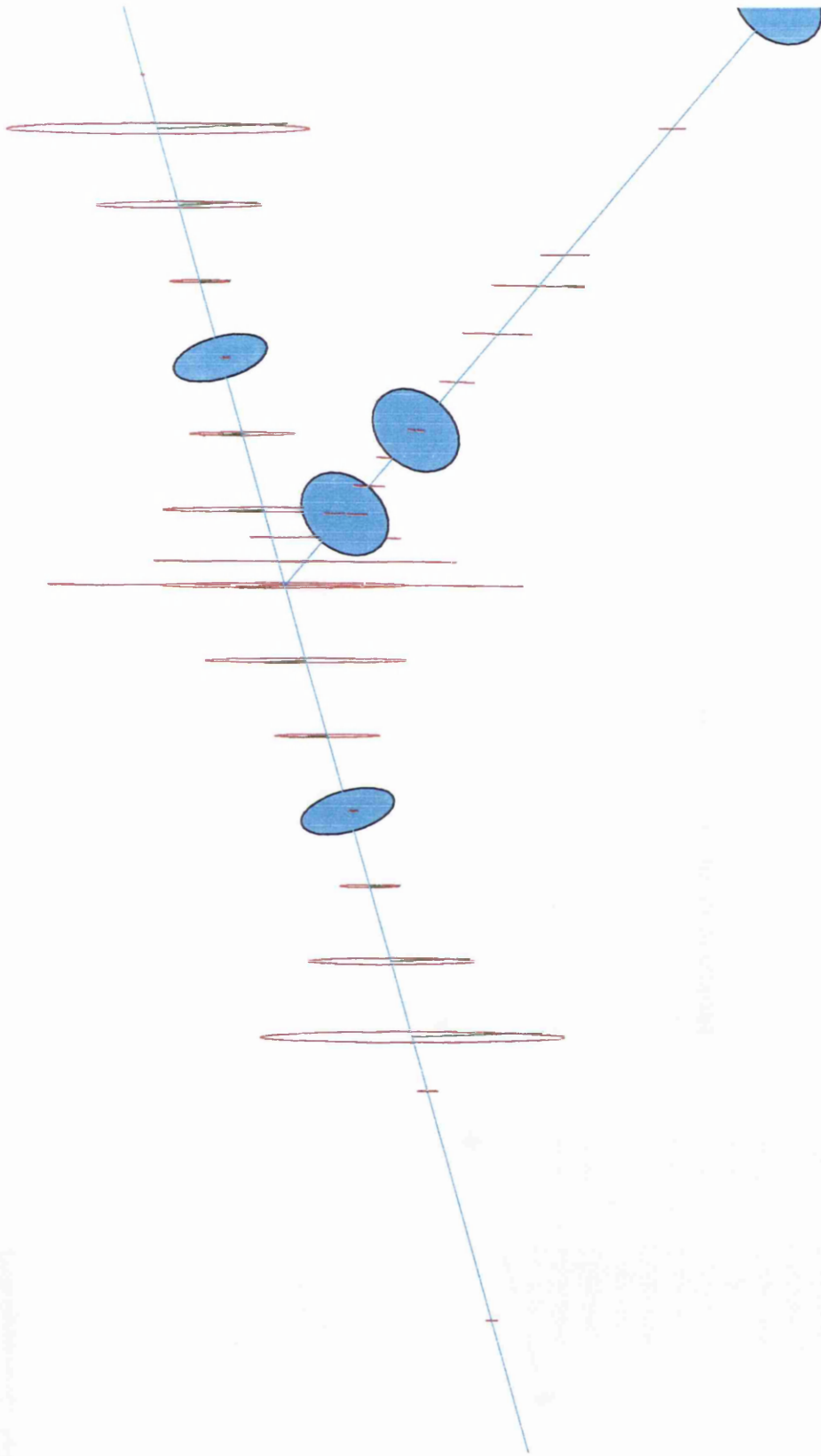
Torsional Resonance of Flywheel – 31.8 Hz



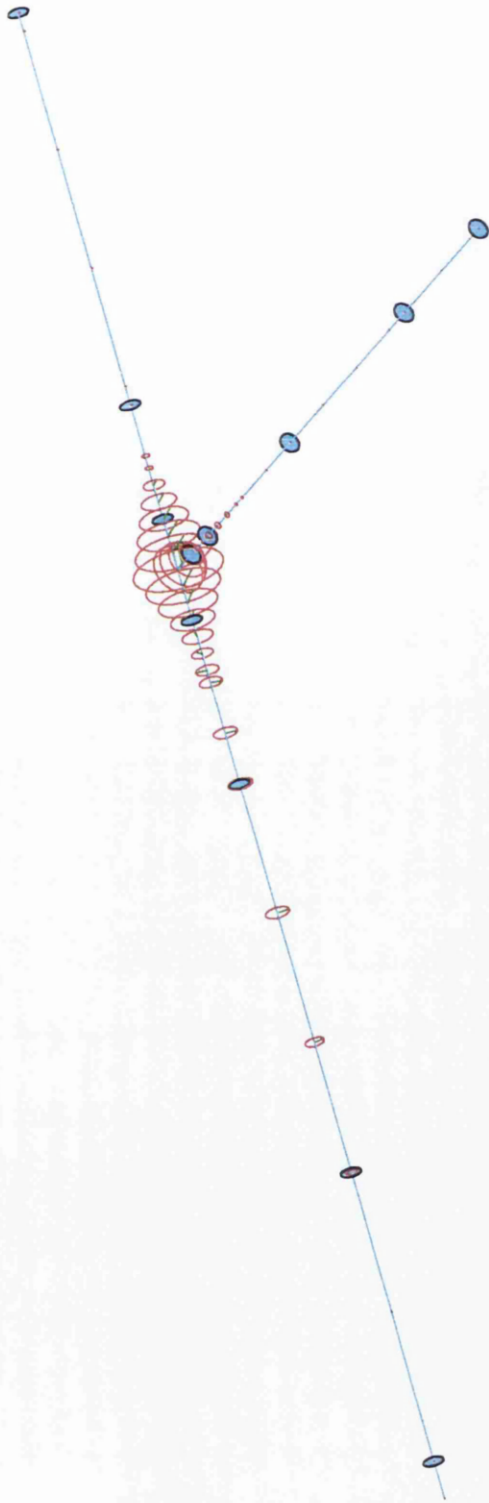
This is a modeplot showing the torsional resonance of the flywheel, with the shafts disconnected

Comparison of FEA Result (red) and Experimental Data (blue) for the Broken Tooth





Broken tooth result – the gearbox shafts  
resonate at 400 Hz when struck



Broken tooth result – the torsional effect upon the shafts

## 5 *Discussion*

The discussion and conclusion have been split into two. The first part of each deals with the mathematical model, and its relation to the experimental work. The second part relates solely to the experimental work.

### 5.1 **Discussion of Mathematical Modelling**

The 400 Hz modeshape is shown in figure 73, it is caused by the bowing of the output shaft within the gearbox. This is not shown in the theoretical or experimental response curves, as the *casing* of the gearbox was struck with the mallet, and not the gearbox *shaft*. The impact from the mallet blow would have been transferred directly through the gearbox casing and into the table. This impact would *not* set the output shaft resonating as the gearbox casing acts a rigid body. The FEA model *also* allows the gearbox casing to act as a rigid body. This explains why both the theoretical and experimental response curves fail to reveal this 400 Hz resonance. A study of the waterfall plots in the sound and vibration section of this thesis, such as in figure 4, also shows a 400 Hz resonance. This result highlights the advantage of using an FEA model in this kind of work. It may reveal additional information that would not normally be found in experimental work alone.

The biggest problem in creating the FEA model was determining the correct resonant frequency of the bearing pedestals. The test-rig is quite unusual as a machine, most machines of this kind would be bolted to a concrete foundation to provide correct mechanical grounding. This machine was bolted to a purpose built table, to allow ease of access for the operator. This unusual design caused several problems, both with the FEA work and the experimental work. In principle with a machine bolted to the floor, with flexible couplings, there is little transmission of vibration from one component of the machine to the others. With the machine bolted to a table, acting as a soft base, the transmission of vibration was very high, despite the flexible coupling. This made analysis of the experimental data unusually difficult. For

example, the motor, driving the rig, had an electrical fault which produced vibration at 100 Hz. The resonant frequency of the flywheel was also approximately 100 Hz. This electrical fault vibration would travel through the table and excite the flywheel resonance. This would not happen if the rig was bolted to the floor.

The problem of the rig table also severely hampered the FEA modelling. At first the problem was ignored, and the individual resonances of the bearing pedestals were set so that they would resonate according to the response curves. Unfortunately the results did not match the experimental results, as the components of the rig lacked the single body motion shown in figures 64, 65 and 68. It also led to the creation of non-existent eigenfrequencies and eigenmodes.

The addition of another node to represent the test-rig table solved this problem to a greater extent, but there were still several resonant frequencies missing from the model. For example, figure 62, the vertical response curve, shows peaks at approximately 33 and 55 Hz. These peaks could not be modelled; they are almost certainly due to the rig table surface acting as a vibrating plate rather than a simple beam elements in extension. In this respect the model is overly simplistic. However, the principle resonant frequencies were correctly modelled.

The original plan, regarding the model, was to add two extra degrees of freedom to the original FEA model, to allow extension and rotation of the shafts. The basic rotors and shafts would then be created, and bearing stiffness added. Once the basic model was complete, 'fault subroutines' were to be added to model *all* of the faults in the experimental section of the thesis.

The complexity of the rig structure and the additional modelling required, meant that only the broken tooth fault subroutine was investigated due to lack of time.

Modal analysis of the test-rig would have been more appropriate in determining the correct stiffness of the bearing pedestals. The simple rubber mallet tests provided the correct resonant frequencies, but could not determine the stiffness, mass and

damping in the same manner as modal analysis. Unfortunately, this procedure was not available due to budget constraints.

The final FEA model, presented in this thesis, worked well, however, there are some notable successes, that explained many of the vibrational aspects of the rig that were not explained by experimental work alone. The importance of the gearbox, moving as a rigid body was not fully appreciated before modelling. The effect of the rig structure and low frequency resonances was highlighted by the model. Torsional resonances were studied in greater detail. The 100 Hz electrical fault and its affect on the flywheel was not understood before modelling.

The FEA model's most important contribution was in determining the source of the 400 Hz resonance of the gearbox output shaft, as shown in figure 73. This resonance dramatically increased machine vibration when excited by the tooth passing frequency, and impact harmonics of the broken tooth. The source of this resonance was not identified until the FEA model was completed. This success highlights the benefit of vibrational FEA models in general. Modern gearbox manufactures use such FEA models to reduce sound and vibration of their products - avoiding costly trial and error experimentation.



## 5.2 Discussion of Experimental Work

The experiments have proven that the microphone is capable of detecting many of the faults associated with condition monitoring. It was particularly effective at picking up the sounds of faults whose fault frequency is higher than the low frequency resonances of cabinet's and guards. High frequency impacts, such as those created by tooth impacts, were particularly easy to detect. Low frequency faults such as misalignment and bearing faults were harder to diagnose.

Time synchronous averaging was essential when diagnosing faults in a noisy environment. This technique increases the signal to noise ratio dramatically, but can only be used with faults whose fault frequencies are synchronous with the shaft speed.

It is reported that time synchronous averaging can be used to detect bearing faults [9] but these experiments have failed to validate this. Bearings rarely run with 0% slip, making the bearing defect frequencies approximations only. The *exact* slip frequency must be known to perform this kind of diagnosis. Without this knowledge, a precise time period for each revolution cannot be obtained, and time synchronous averaging cannot be used. Time synchronous averaging of the microphone signal was particularly useful in diagnosing faults regarding gearbox tooth errors, as the gearbox is often the loudest component of a machine.

Time synchronous averaging suffers from another problem. Most evaluation of time synchronous averaged signals is done either in the time domain or the time/frequency domain, displayed in the spectrogram or wavelet. It is difficult to analyse time synchronous averaged signals in the frequency domain alone, as the averaged signal is short and provides poor resolution in the frequency domain [23]. This makes shaft order analysis and amplitude demodulation very difficult. The fact that a shaft encoder, or other device is required often limits it's use. The use of the microphone also has several problems. Low frequency resonance can hamper diagnosis in the

low frequency regions as mentioned previously. Reverberation time can also decrease the resolution in the time domain.

The objective of this project was to develop a technique, using microphones, to screen large areas of plant for faults. The use of a microphone can achieve this especially if the faults in question arise in the gearbox or if the faults affect the normal operation of the gearbox, such as the case with the partial rotor rub. The fault in question must be synchronous with the shaft speed; this will cause problems when dealing with non synchronous faults such as 2 x line frequency motor faults.

Other faults that produce synchronous impacts include ball and socket wear of axial piston pumps, cartridge wear of vane pumps and other compressor/pump type machines. These machines are typically arranged in 'banks' with several machines in a row. The techniques developed in this project may be ideal for monitoring these kinds of machines, cutting the cost of monitoring dramatically.

Crestfactor and Kurtosis can give a single parameter that increases with machine damage, but must be used in conjunction with a high pass filter, and a microphone with a reasonably high frequency range to capture data with frequencies higher than the tooth passing frequency harmonics. Once a fault has been detected via crestfactor and Kurtosis, the spectrogram can be employed to provide a more detailed picture of the fault. Time synchronous averaging is not required if the machine in question is much louder than its neighbours. In this instance the microphone can be employed to detect possible faults. Without time synchronous averaging, however, correct vibration analysis must be employed as the microphone gives misleading information as seen in the tooth lubrication experiment. It may also be inaccurate when trending, as atmospheric properties and building audio acoustic properties may change between successive readings.

## 6 *Conclusion*

The FEA model was used to study the effect of the broken tooth in detail. The model showed that the impacting tooth excited a 400 Hz resonance in the gearbox's output shaft. The effect of this 400 Hz resonance can be clearly seen in the waterfall plots of sound and vibration in the experimental section of this thesis, such as in figure 4, but the source of the resonance was not identified until the FEA model was used. The 400 Hz resonance is a major source of sound and vibration energy.

The results of the workshop experiments showed that the time synchronous averaged microphone signal could be used to detect synchronous impacting faults such as gearbox tooth problems, or faults which affected the loading of the gearbox. This was possible even with a signal to noise ratio of -15 dB. The time synchronous averaged microphone signal was less successful, compared to an accelerometer signal, at detecting faults whose fault frequencies were low, did not generate high frequency impact harmonics, or whose faults were not synchronous with the shaft speed such as bearing faults. In the case of the lower fault frequencies the fault sound was masked by sound generated by lightly damped plates, which acted as loud speakers. In the case of non synchronous impacting faults, such as bearing faults, the time synchronous averaging technique could not be used, as the precise time period of the faulty component could not be determined due to slipping.

Crestfactor and Kurtosis, in conjunction with a high pass filter, are typically used to identify and measure faults involving impacts. Their ability to do this was confirmed by the experiments. As the time synchronous averaged microphone signal was proven to be able to isolate synchronous impacts, Crestfactor and Kurtosis were chosen as the parameters that would increase with machine damage.

It was found that double differentiation of the time synchronous averaged sound signal could be used to emphasise the higher frequency impact harmonics. Further diagnosis could then be performed by employing the spectrogram.

It was shown that the time synchronous averaging was not always necessary. If the machine in question created a greater sound pressure level than the machines around it, and the fault frequencies are known, then a non differentiated sound signal could be used to assess condition. This was demonstrated by comparing the relative sound pressure level of fault frequency harmonics of the descaling fluid pump's gearbox tooth passing frequencies. It should be noted that this technique is not as accurate as vibration analysis, and should be used as a guide only. Vibration analysis should be used to confirm diagnosis before committing to expensive remedial action and maintenance.

The objectives of this project were to develop a system, using a microphone, that could be used to assess the condition of non critical machines, and to find parameters that would increase with machine damage. It was proven that time synchronous averaging of a double differentiated microphone signal could be used to isolate synchronous impacts, and that crestfactor or Kurtosis, in conjunction with a high pass filter, increased with machine damage as required. This technique was particularly suited to identify impacting faults, such as gearbox tooth faults, but was not suitable for identifying faults whose fault frequency was low, such as misalignment or unbalance.

## 7 *References*

1. DE Johnson, GJ Trmal. *Use of noise as an inspection tool*, International symposium of automotive technology and automation, 20th conference. 1989.
2. A Middleton, A Rumble. *Measurement of noise from geared transmission*, Noise and vibration worldwide, November 1991.
3. ANJ Van Roosmalen. *Noise generation mechanisms of gear transmissions*, IMechE 2nd international conference on gearbox noise vibration and diagnostics, 1995.
4. J Sumita, H Takada, Y Konya, S Muroyama. *New visual and sound monitoring system for emergency engine generators*, IEEE proceedings of the 20th international telecom energy conference, 1998.
5. S Takata, JH Ahn, M Miki, T Sata. *Sound monitoring system for fault detection of machine and machining states*, Annals of the CIRP vol. 35/1/1986, 1986.
6. RA Collacott. *Condition monitoring by sound analysis*, Non destructive testing, October 1975.
7. T Sata, F Kimura, K Matsushima, S Takata, J Otsuka. *Identification of machine and machining states by use of pattern recognition techniques*, 16th CIRP International seminar on manufacturing systems, Tokyo. 1984.
8. MNM Badi, DJ Dell, AE Fellows. *Alternative methods for diagnosing gearbox faults*, Profitable condition monitoring, 1992.
9. RBW Heng, MJ Mohd Nor. *Condition monitoring using acoustic signals*, Profitable condition monitoring, 1996.
10. MNM Badi, TH Breckell. *Condition monitoring of wet and dry gears using noise, sws and accelerometer signals*, Proceedings of the 2nd Biennial European joint conference on engineering system design and analysis 1994.
11. *Measuring sound*, Brüel and Kjær, September 1994.

12. KP Maynard. *Interstitial processing: the application of noise processing to gear fault detection*, International conference on condition monitoring, University of Wales - Swansea, April 1999.
13. GAW Setford. *Bearing condition monitoring, condition measurement, and condition control*, 4th int. conf. on Profitable condition monitoring, 1993.
14. A Barkov, N Barkov. *Condition assessment and life prediction of rolling element bearings - part one*, Sound and vibration, June 1995.
15. CM Harris, *Shock and Vibration Handbook*, 3rd edition McGraw - Hill, 1988.
16. JE Nicks, G Krishnappa. *Gear fault detection using modulation analysis*. IMechE 2nd international conference on gearbox noise, vibration and diagnostics, 1995.
17. PD McFadden. *Application of the wavelet transform to early detection of gear failure by vibration analysis*. International conference on condition monitoring, University of Wales - Swansea, March 1994.
18. ST Lin, PD McFadden. *Vibration analysis of gearboxes by the linear wavelet transform*, IMechE 2nd international conference on gearbox noise, vibration and diagnostics, 1995.
19. WJ Wang, PD McFadden. *Application of wavelets to gearbox vibration signals for fault detection*, Academic Press Ltd, 1996.
20. RB Randall. *Cepstrum analysis and gearbox fault diagnosis*, maintenance management international 3 pages 183 - 208, 1982.
21. RB Randall. *Advances in the application of Cepstrum analysis to gearbox diagnosis*, IMechE proceedings of the 2nd international conference in vibration in rotating machinery, March 1980.
22. RB Randall. *Separating excitation and structural response effects in gearboxes*. IMechE 3rd international conference on vibrations in rotating machinery, 1984.
23. SJ Orfanidis. *Introduction to signal processing*, Prentice - Hall, USA, 1996.
24. *Sound Intensity*, Brüel and Kjær, September 1993
25. RM Jones. *A guide to the interpretation of machinery vibration measurement - part one*, Sound and vibration, May 1994.

26. N Williams. *Condition monitoring at British Steel Llanwern*, Steel times, October 1995.
27. RB Randall. *Computer aided vibration spectrum trend analysis for condition monitoring*, Maintenance management international 5, 1985.
28. J MacIntyre, P Smith et al. *Comprehensive condition monitoring of the Babcock 10E coal mill*, International conference on condition monitoring, University of Wales - Swansea, 1994.
29. J MacIntyre, J Tait et al. *Neural networks application in condition monitoring*. Artificial intelligence in engineering, 1995.
30. T Dawn. *Condition monitoring experts add neural nets to seek out the unknown*, Noise and vibration worldwide, 1994.
31. PD McFadden. *Low frequency vibrations generated by gear tooth impacts*, NDT international vol. 18 no. 5, 1985.
32. TJ Holroyd, N Randall. *Applying acoustic emission to industrial machine monitoring*, Intentional conference on condition monitoring, University of Wales - Swansea, March 1994.
33. AC McCormick, AK Nandi. *Cyclostationarity in rotating machine vibrations*, Mechanical systems and signal processing, 1998.
34. DN Futter. *Vibration monitoring of industrial gearboxes using time domain averaging*, IMechE 2nd int. conf. on gearbox noise, vibration and diagnostics, 1995.
35. FP Wardle, SY Poon. *Rolling bearing noise - cause and cure*, CME, July/August 1983.
36. DJ Dawe. *Matrix and finite element displacement analysis of structures*. Oxford engineering sciences series.
37. B Nath. *Fundamentals of finite elements for engineers*. Athlone press, University of London, 1974.
38. M Geradin, D Dixon, *Mechanical vibrations, theory and application to structural dynamics*, 2nd edition, John Wiley & Sons, 1996.





## 8.1 Plates

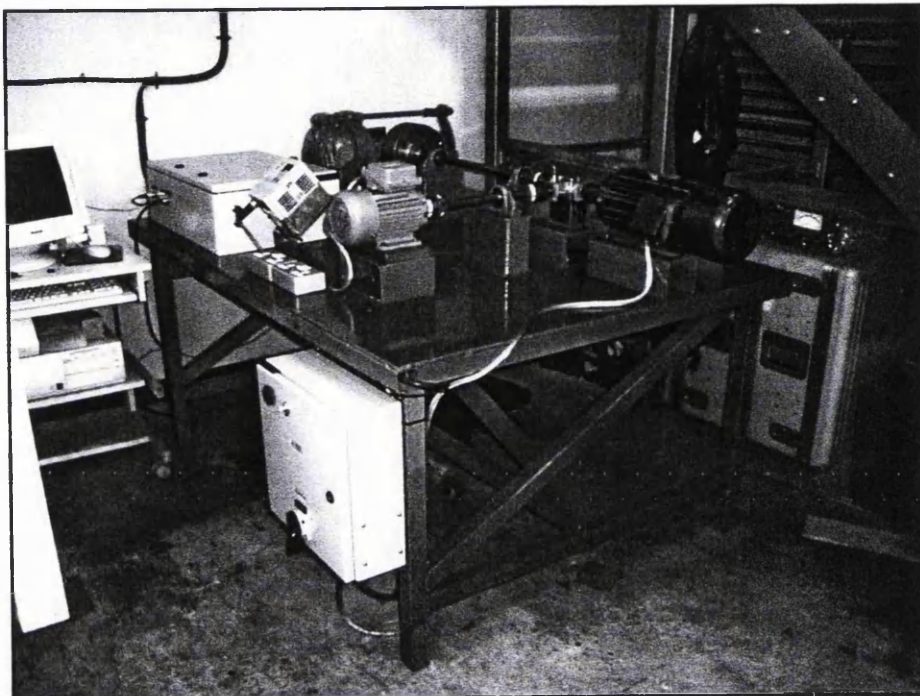


plate 1

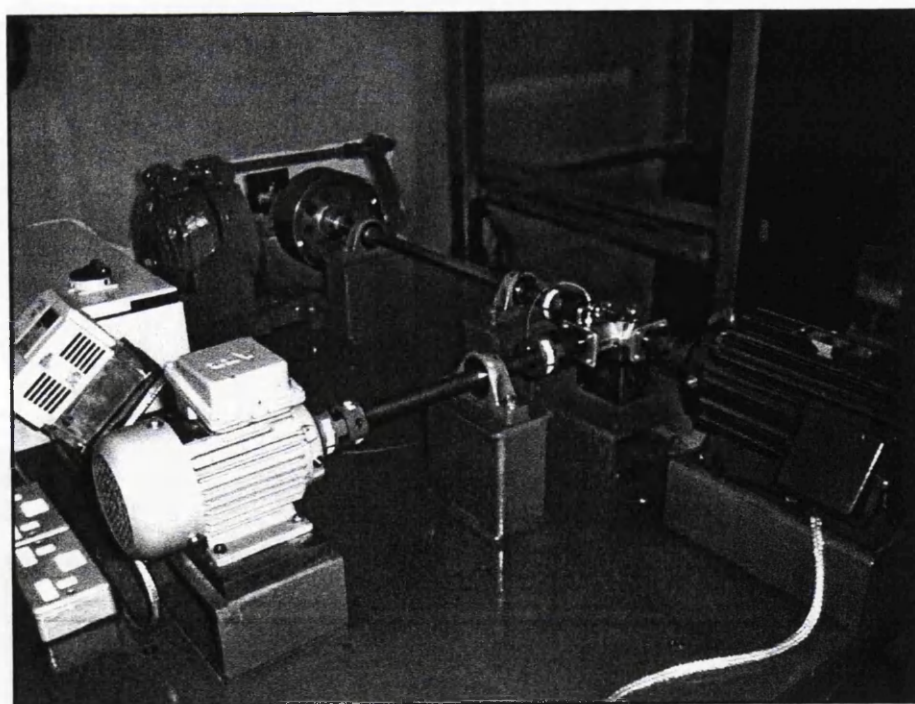
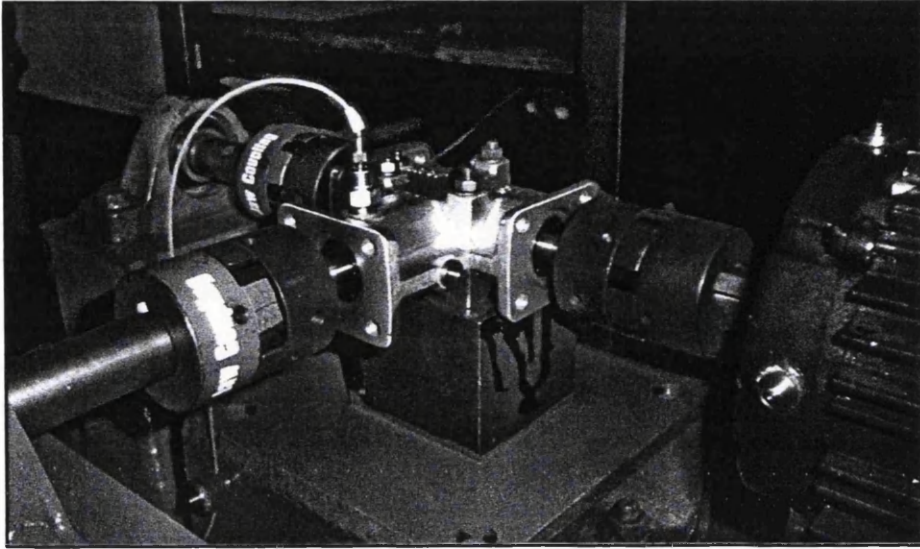
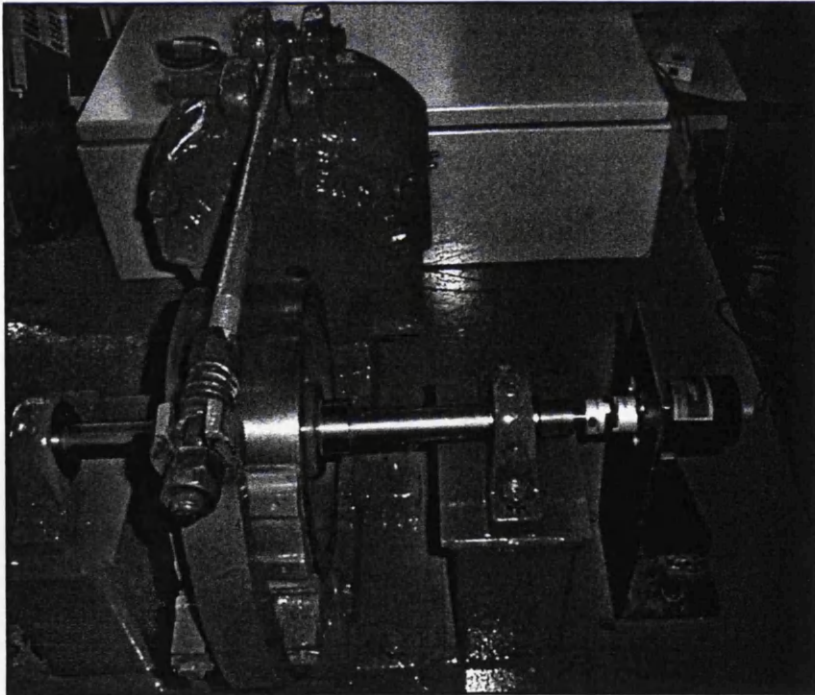


plate 2



**plate 3**



**plate 4**

## 8.2 Spectrograms

Analysis of sound and vibration signals can be conducted in the time domain or the frequency domain. However, it is often useful to view the signal in both the time and frequency domain simultaneously. This is particularly useful when the frequency content of the signal is not constant in time. For example, if a tooth is broken there will be a short time transient impact once per revolution of the shaft. This impact will contain high frequencies, but will only last for a short length of time. The accepted way of simultaneously viewing signals in the time and frequency domain is the 'wavelet'. Unfortunately, this tool was not available for the project. Instead, Matlab's 'Specgram' program was used to generate a spectrogram view of the signal. This divides the signal up into small sections in the time domain, with each small section overlapping the next section. See diagram 8.1.

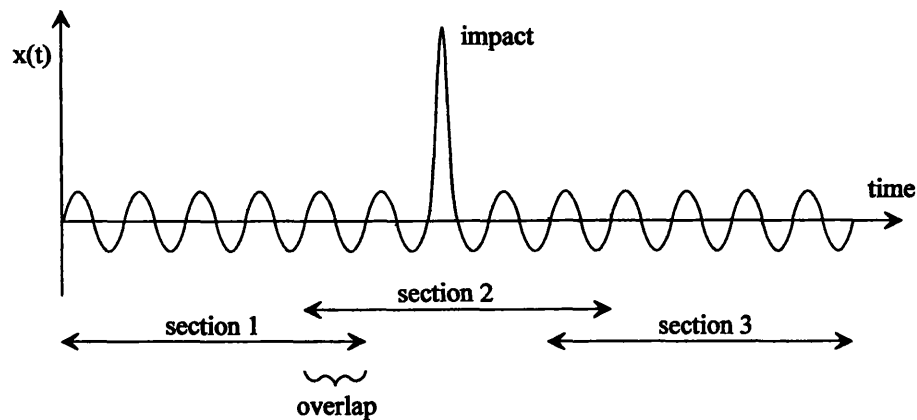


**diagram 8.1**

An FFT of each section is then calculated with a Hanning window. See diagram 8.2.

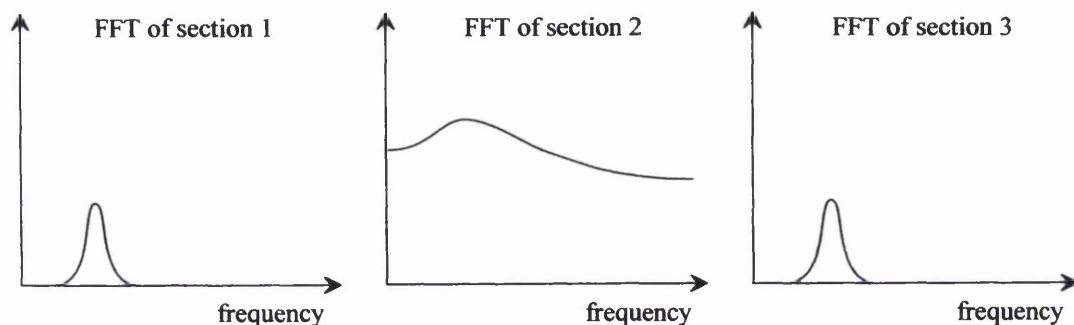


**diagram 8.2**

The FFT vectors are placed into a vertical column of numbers, typically 1000 long. A matrix is formed with the successive FFTs along the rows. This matrix is then used to form an 8 bit grey scale bitmap. Diagram 8.3 represents a spectrogram of a signal split into the three sections. A normal spectrogram would typically split the signal into 400 sections, rather than just three. The impact in section 2 forms a vertical line in the spectrogram, whilst the pure tones form horizontal lines.

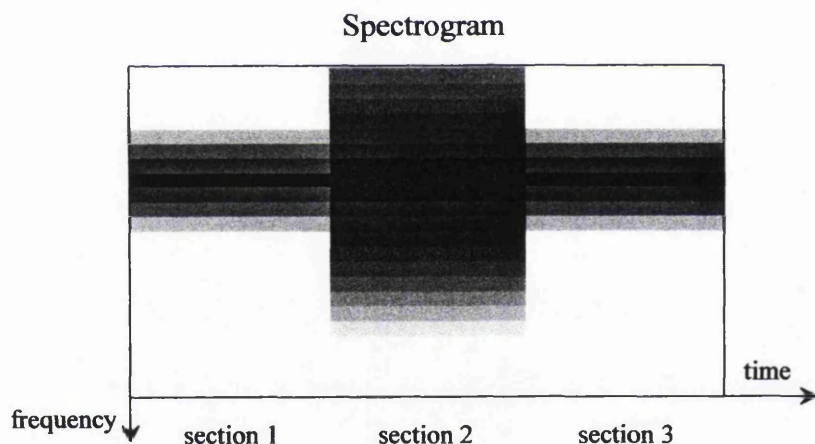


**diagram 8.3**

Spectrograms have been used extensively in this project to identify small impacts in the higher frequency range. They have also been used to identify resonances to a lesser degree; resonances form broad horizontal dark bands across the spectrogram. The frequency of these horizontal bands remain constant regardless of the speed of rotation.

## **8.3 EPSRC - Engineering Doctorate Programme**

### **Steel Technology**

#### **Record of Training - Bruce Blakeley**

##### ***Project Aim***

The aim of this work was to develop a system of microphones capable of monitoring the condition of rotating machinery.

##### ***Objectives***

- To build a test-rig, consisting of motor, gearbox and load. Faults, such as misalignment, were then introduced and the effect on sound and vibration noted.
- To develop a method of increasing the signal to noise ratio using time synchronous averaging (TSA).
- Investigate the possibility of reducing the data down to a single parameter that increases with machine damage.
- Test the method in an industrial environment.
- Create an FEA model to increase the understanding of the vibrational behaviour of the test-rig.

##### ***Deliverables***

A system of microphones capable of screening more than one rotating machine for faults. All objectives and deliverables have been successfully completed.

### ***Formal Industrial Experience***

- A category one safety certificate was obtained to allow the author to conduct research, unaided, on Corus' Port Talbot plant.
- Training within Corus' FMMS department. This department is responsible for plant condition monitoring (PCM) within Corus.
- Quarterly presentations to senior management on technology issues regarding PCM within Corus UK.

### ***EngD Training (October 1996 - September 2000)***

- Technical, professional and management modules normally found in a modern MBA. Formal record of courses is appended.
- Safety training to allow the author to work unsupervised on plant.

### ***Progress Monitoring***

The completion of formal procedures used for progress monitoring against predefined targets and objectives have included:-

- Presentations at four-monthly Theme Group meetings, chaired by a senior industrialist (with academic and industrial supervisors, customer/supplier representatives, academic and industrial EngD co-ordinators, as well as other research engineers present).
- Frequent meetings with academic and industrial supervisors (as necessary throughout the four year period).
- Annual appraisals (using the corporate Corus appraisal system) involving both academic and industrial supervisors.
- Poster presentations.
- EngD presentations at the annual EngD seminar (1999).

### ***Professional Development***

Professional development has been carried out according to the Institute of Mechanical Engineers guidelines, including: -

- Regular meetings with senior industrial manager acting as the professional development mentor.
- Maintenance of a professional log book.
- Associate membership of the institute of Mechanical Engineers (AMIMechE).
- Full chartered status (CEng) is expected in 2001.

### ***Conference Presentation / Publications***

Blakeley B., Lees A., Lewis B., '*Audio Acoustic Monitoring of a spiral bevel gearbox*'. Conf proc Modern Practices in stress and vibration. Nottingham University - Sept. 2000.

Blakeley B., Lees A., Lewis B., '*Audio Acoustic PCM*'. Ironmaking and steelmaking 2001, Vol. 28, No. 3.

### ***Poster Presentations***

Poster presentations titled 'Audio acoustic PCM' at the annual EngD seminars 1997, 1998 and 2000.

## 8.4 Table of Course Results

During the four year engineering doctorate scheme a series of compulsory courses were held. The purpose of these courses was to promote the understanding of the steel industry, improve the communication and business skills of the participants and to provide knowledge of common engineering skills.

<i>Module</i>	<i>Score</i>
Steel process evolution	61
Refractories/steel structures	87
Steel processing	58
Coated products	65
Engineering applications	67
Environmental issues I	77
Steel product development	59
Investment appraisal	72
Numerical/computer methods	65
Finite element	80
Statistical design of experiments	66
Communication skills	pass
Professional skills	pass
Leadership skills	pass
Business process engineering	70
Graduate management	pass
Project planning	
Effective management	60
Employee relations	64
Financial awareness	90
Business awareness	58
Health and safety	68